ISSN 0021-9673

PUBLISHED WEEKLY

VOL. 264 NO. 2 JULY 15, 1983

JOURNAL OF CHROMATOGRAPHY

INTERNATIONAL JOURNAL ON CHROMATOGRAPHY, ELECTROPHORESIS AND RELATED METHODS

ELSEVIER

JOURNAL OF CHROMATOGRAPHY

Scope. The *Journal of Chromatography* publishes papers on all aspects of chromatography, electrophoresis and related methods. Contributions consist mainly of research papers dealing with chromatographic theory, instrumental development and their applications. The section *Biomedical Applications,* which is under separate editorship, deals with the following aspects: developments in and applications of chromatographic and electrophoretic techniques related to clinical diagnosis (including the publication of normal values); screening and profiling procedures with special reference to metabolic disorders; results from basic medical research with direct consequences in clinical practice; combinations of chromatographic and electrophoretic methods with other physicochemical techniques such as mass spectrometry. In *Chromatographic Reviews,* reviews on all aspects of chromatography, electrophoresis and related methods are published.

Submission of Papers. Papers in English, French and German may be submitted, in three copies. Manuscripts should be submitted to: The Editor of *Journal of Chromatography,* P.O. Box 681, 1000 AR Amsterdam, The Netherlands, or to: The Editor of *Journal of Chromatography, Biomedical Applications,* P.O. Box 681, 1000 AR Amsterdam, The Netherlands. Review articles are invited or proposed by letter to the Editors and will appear in *Chromatographic Reviews* or *Biomedical Applications.* An outline of the proposed review should first be forwarded to the Editors for preliminary discussion prior to preparation. Submission of an article is understood to imply that the article is original and unpublished and is not being considered for publication elsewhere. For copyright regulations, see below.

Subscription Orders. Subscription orders should be sent to: Elsevier Science Publishers B.V., P.O. Box 211, 1000 AE Amsterdam, The Netherlands. The *Journal of Chromatography* and the *Biomedical Applications* section can be subscribed to separately.

Publication. The *Journal of Chromatography* (incl. *Biomedical Applications, Chromatographic Reviews* and *Cumulative Author and Subject Indexes, Vols. 251-260* and *261-270*) has 27 volumes in 1983. The subscription prices for 1983 are:

J. Chromatogr. (incl. *Chromatogr. Rev.* and *Cum. Indexes Vols. 251-260* and *261-270*) + *Biomed. Appl.* (Vols. 252-278):
Dfl. 4185.00 plus Dfl. 540.00 (postage) (total *ca.* US$ 1890.00)

J. Chromatogr. (incl. *Chromatogr. Rev.* and *Cum. Indexes Vols. 251-260* and *261-270*) only (Vols. 252-271):
Dfl. 3400.00 plus Dfl. 400.00 (postage) (total *ca.* US$ 1520.00)

Biomed. Appl. only (Vols. 272-278):
Dfl. 1120.00 plus Dfl. 140.00 (postage) (total *ca.* US$ 504.00).

Journals are automatically sent by airmail to the U.S.A. and Canada at no extra costs, and to Japan, Australia and New Zealand, with a small additional postal charge. Back volumes of the *Journal of Chromatography* (Vols. 1 through 251) are available at Dfl. 173.00 (plus postage). Claims for issues not received should be made within three months of publication of the issue. If not, they cannot be honoured free of charge. For customers in the U.S.A. and Canada, wishing additional bibliography information on this and other Elsevier journals, please contact Elsevier Science Publishing Company Inc., Journal Information Center, 52 Vanderbilt Avenue, New York, NY 10017. Tel: (212) 867-9040.

Abstracts/Contents Lists published in Analytical Abstracts, Biochemical Abstracts, Biological Abstracts, Chemical Abstracts, Chemical Titles, Current Contents/Physical, Chemical & Earth Sciences, Current Contents/Life Sciences, Index Medicus, Mass Spectrometry Bulletin, and Science Citation Index.

See page 3 of cover for Publication Schedule, Information for Authors, and information on the News Section and Advertisements.

0021-9673/83/$03.00

Printed in The Netherlands

CONTENTS

(Abstracts/Contents Lists published in Analytical Abstracts, Biochemical Abstracts, Biological Abstracts, Chemical Abstracts, Chemical Titles, Current Contents/Physical, Chemical & Earth Sciences, Current Contents/Life Sciences, Index Medicus, Mass Spectrometry Bulletin and Science Citation Index)

(Continued overleaf)

CHROMATOGRAPHY OF ALKALOIDS

Part A: Thin-Layer Chromatography

by A. BAERHEIM SVENDSEN *and* R. VERPOORTE,
Department of Pharmacognosy, State University of Leiden, Leiden, The Netherlands

JOURNAL OF CHROMATOGRAPHY LIBRARY, VOL. 23A

In the analysis of alkaloids, thin-layer chromatography (TLC) has been applied more than any other chromatographic technique so far. This volume is a thorough and complete review of research carried out and conclusions reached on the widespread use of this most important technique.

It presents the most effective methods in the separation and detection of alkaloids occurring in plant material, biological material (toxicological and pharmacological analysis), pharmaceutical preparations and drugs of abuse. Both traditional TLC techniques and newly developed systems are covered; a selection of TLC separation systems which have proved best for solving specific analytical problems are clearly presented and sample preparation techniques are described in a separate section for each group of alkaloids.

1983 xiv + 536 pages
US $104.25 (In USA & Canada); Dfl. 245.00 (Rest of World)
ISBN 0-444-42145-9

ELSEVIER

P.O. Box 211, 1000 AE Amsterdam, The Netherlands.

52 Vanderbilt Ave., New York. N.Y. 10017.

The Dutch guilder price is definitive. US $ prices are subject to exchange rate fluctuations.

Journal of Chromatography, 264 (1983) 183–196
Elsevier Science Publishers B.V., Amsterdam – Printed in The Netherlands

CHROM. 15,745

APPLICATIONS OF A MICROPROCESSOR-CONTROLLED VALVE-SWITCHING UNIT FOR AUTOMATED SAMPLE CLEANUP AND TRACE ENRICHMENT IN HIGH-PERFORMANCE LIQUID CHROMATOGRAPHY*

C.J. LITTLE*, D.J. TOMPKINS and O. STAHEL
Kontron Electrolab Ltd., Unit 16 Shield Road, Ashford, Middlesex, TW15 1A4 (Great Britain)
and
R.W. FREI and C.E. WERKHOVEN-GOEWIE
Department of Analytical Chemistry, Free University, De Boelelaan 1083, 1081 HV Amsterdam (The Netherlands)

(First received June 7th, 1982; revised manuscript received February 4th, 1983)

SUMMARY

Various methods and principles of column switching are described with particular emphasis being given to their use in automated sample cleanup and trace enrichment. Commercial equipment is defined which enables all the methods described to be carried out automatically using microprocessor control.

INTRODUCTION

Conventional chromatographic methods now comprise a wide range of techniques including adsorption (normal-phase), reversed-phase, ion-suppression, ion-pairing, ion-exchange, partition, size-exclusion and several other popular forms of chromatography.

There are potential advantages in combining several of these methods[1–4]. For example, adsorption or size exclusion is often used to cleanup a sample prior to chromatographic analysis or other analytical methods. Prior chromatography is sometimes used to separate a complex mixture into different groups of compounds, followed by more specific analysis.

In some complex mixtures, it is necessary to carry out two separations using different methods such as adsorption followed by ion pairing or size exclusion followed by reversed phase or many other combinations of methods. In high-performance liquid chromatography (HPLC) this combination of methods is often referred to as multidimensional HPLC.

The principles just described, form the basis of sample cleanup using valve

* Presented at the *VIth International Symposium on Column Liquid Chromatography, Cherry Hill, NJ. June 6–11, 1982.* The majority of the papers presented at this symposium have been published in *J. Chromatogr.*, Vol. 255 (1983).

0021-9673/83/$03.00

TABLE I

METHODS OF VALVE SWITCHING

1	Sample cleanup
2	Trace enrichment
3	Method development
4	Sample identification
5	Boxcar chromatography
6	Multi-column chromatography
7	Incremental gradient elution

switching methods. Here valves re-route the chromatographic eluent flow from one column to another. Other valves change the solvents. Both operations must be carried out precisely and accurately.

In trace enrichment, dilute aqueous samples are selected and routed through small reversed-phase pre-columns. Concentration of the solute arises from non-elution from the pre-column and only when the solvent is changed by re-routing the pre-column in-line with an analytical column, will the enriched solute species be eluted from the pre-column. This approach enables very low levels of pollutants to be determined.

In addition to these methods, there are several others which benefit from a valve-switching approach, as indicated in Table I.

DESCRIPTION OF VALVE SWITCHING

In order to carry out the methods indicated in the introduction it is necessary to utilize several valve-switching techniques. A list of these techniques is given in Table II, some of which will be described in greater detail.

Principles of valve switching

There are two types of valve used in the Kontron valve-switching unit. These are Rheodyne 6-port, 2-way valves (Model 7000) which operate at high pressure and Rheodyne 6-way selector valves (Model 5012) which operate at low pressure.

TABLE II

USES OF SWITCHING

1	Column selection
2	Column switching
3	Solvent switching
4	Solvent selection
5	Zone cutting
6	Auxilliary pump on/off
7	Trap solute in detector
8	Recycle
9	Fraction collection
10	Sample injection
11	Detector selection

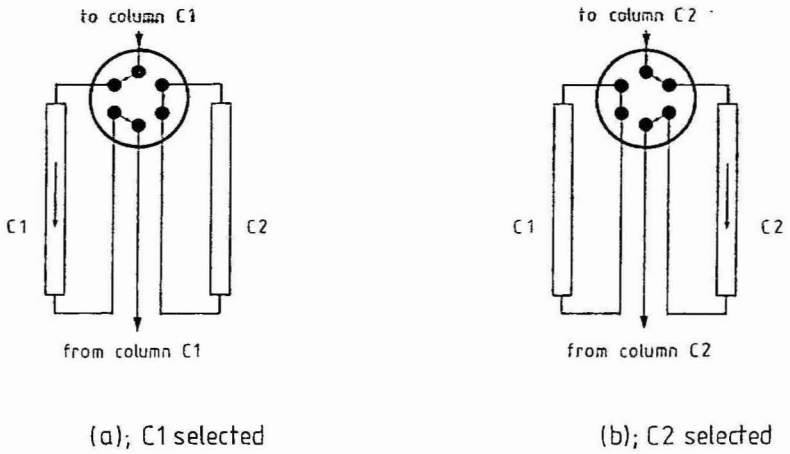

Fig. 1. Description of column selection using a 6-port, 2-way valve.

Essentially, the 2-way valves (Model 7000) have two internal pathways connecting ports 1 and 2, 3 and 4, 5 and 6, in the non-switched position, and in the switched position, ports 2 and 3, 4 and 5, 6 and 1 are connected. Depending on the valve position, different external connections to the valve are selected.

The 6-way valves, however, do not return directly to their starting position but step sequentially through ports 1 to 6, thus enabling the selection of different samples for trace enrichment and when connected in reverse order, for the collection of fractions from semi-preparative seperations.

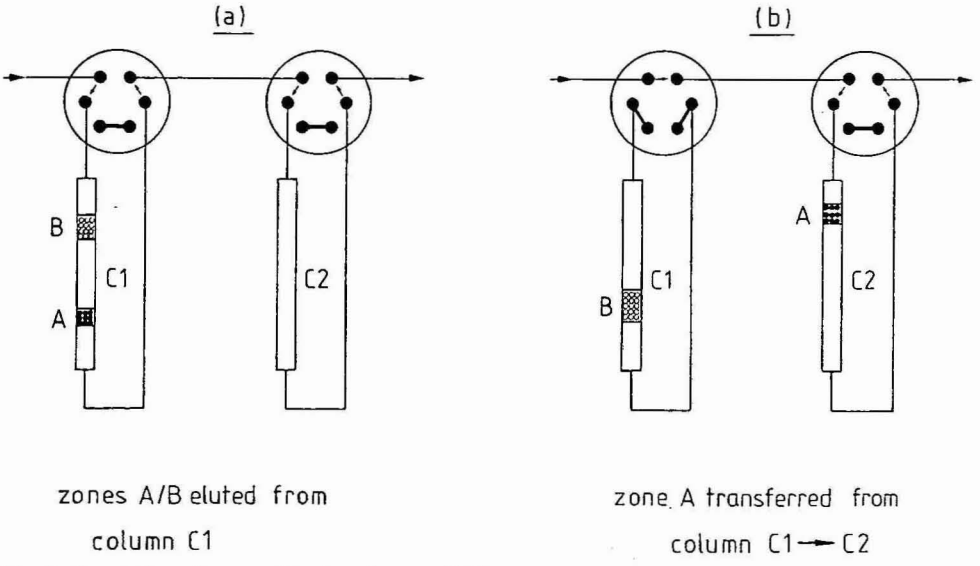

Fig. 2. Description of zone cutting by column switching.

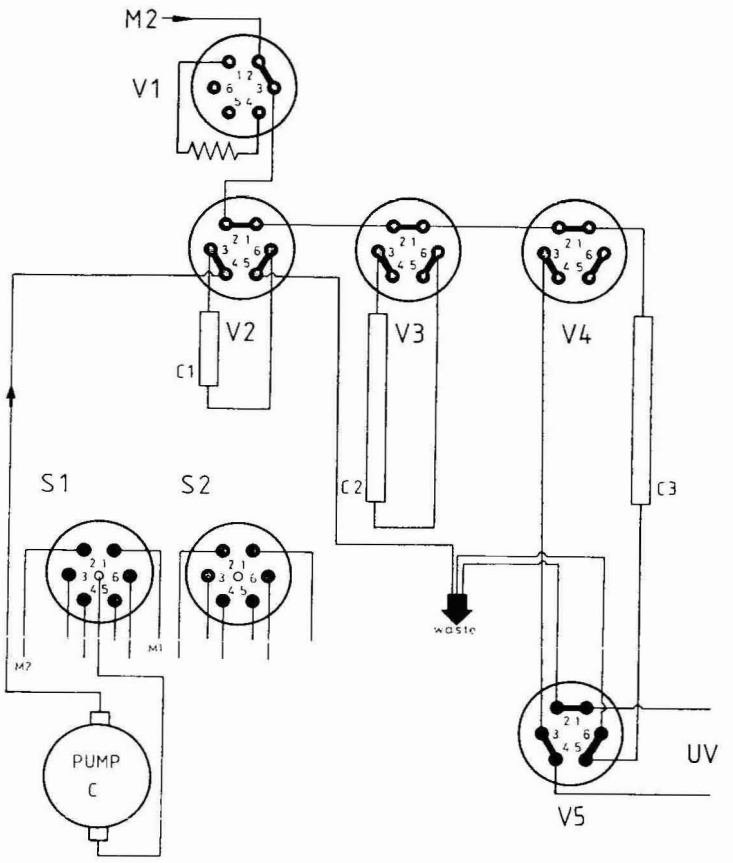

Fig. 3. Kontron MCS 670 Tracer configuration suitable for sample cleanup using zone cutting methods and automatic solvent change for regeneration of pre-columns.

Column selection

Fig. 1 shows how a 2-way valve can be used to select one of two columns. The procedure is used in this paper for valve V4 in order to select the detector flow cell. Switching V5 when a solute is passing trough the detector enables the trapping of the solute for wavelength scanning etc. (see Fig. 3).

Column switching

Fig. 2 indicates how the eluent can be re-routed from one column to another. This procedure is very important and is used to:

(a) Carry out zone transfer and zone cutting.
(b) Optimise analysis time.
(c) Change the selectivity of the system.
(d) Increase column length.

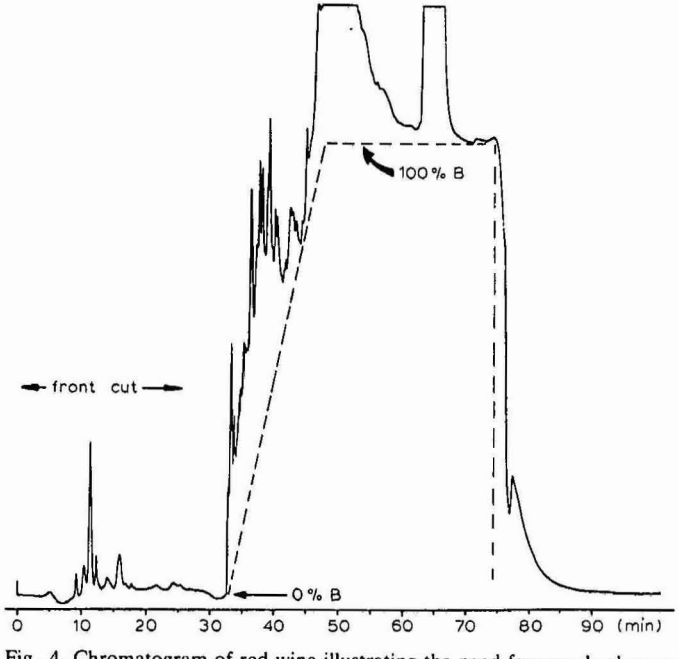

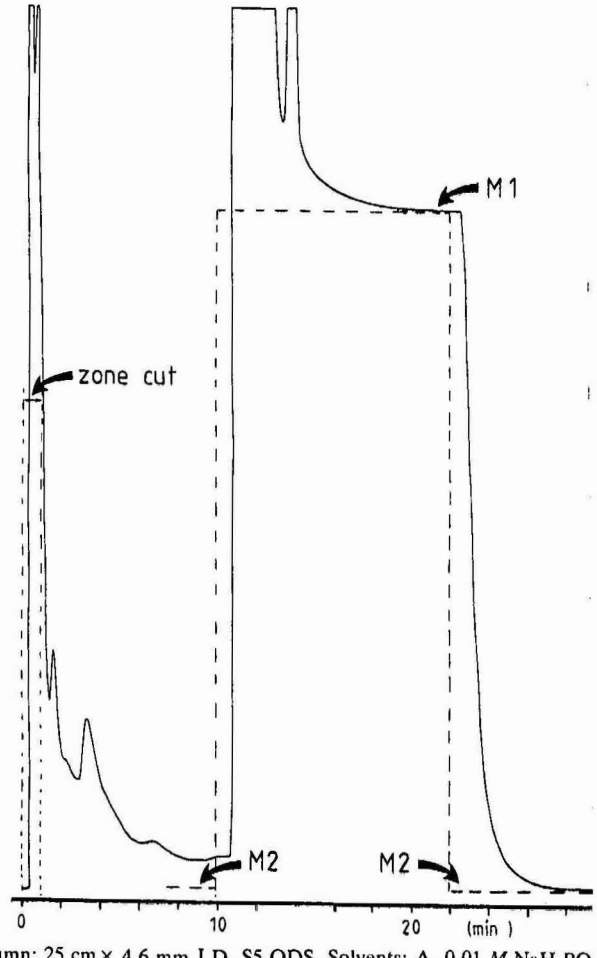

Fig. 4. Chromatogram of red wine illustrating the need for sample cleanup by zone cutting. Column: 25 cm × 4.6 mm I.D. S5 ODS. Solvents: A, 0.01 *M* NaH_2PO_4, pH 2.4; B, methanol. Detection: UV at 214 nm.

Fig. 5. Chromatogram of red wine on Brownlee pre-column illustrating timing of the front cut taken and the cleaning and re-equilibration requirements.

Zone transfer and zone cutting

Zone transfer is illustrated in Fig. 2 and represents the basic principles of column switching, where a zone is allowed to elute from one column to another. To minimise extra column band broadening, the tubing connecting the column to the valve should be made from the finest bore capillary tube (*e.g.* 0.007 in. I.D. tube).

Zone cutting is an extension of this principle and is probably the most useful and versatile of all the column switching techniques. The figure shows how a heart cut can be taken from column C1 and transferred to column C2. Once the cut has been made, C1 can be isolated from the system. If further zones are required, C1 can be used to store the remainder of the chromatogram until elution from C2 is complete. Further zone cuts can be made in the same way as the first.

Column C1 can be isolated from the analytical system and regenerated by means of a secondary pumping system. This is the principle used to carry out sample cleanup and is one of the most useful and versatile techniques of column switching.

Solvent selection

Selector valves S1 and S2 (Fig. 3) enable solvent changes to be made either sequentially or arbitrarily. If the common outlet is connected to a pump, several applications arise.

(a) Solvent change for column cleaning and re-equilibration, as used in the examples of sample cleanup.

(b) Incremental gradient elution necessitates a series of mobile phases of in-

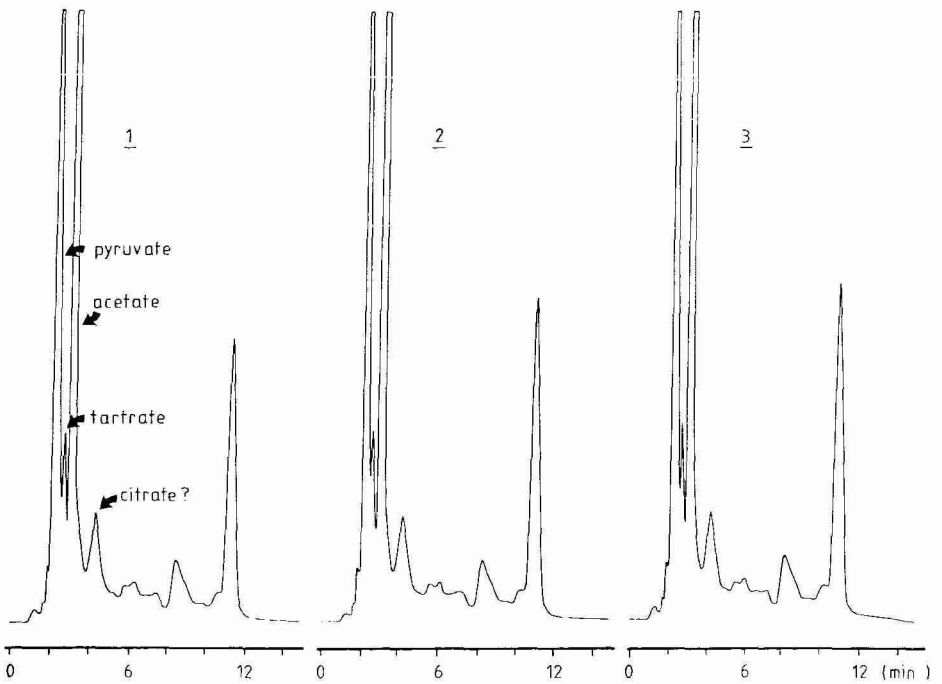

Fig. 6. Chromatogram of organic acids in red wine using automatic sample cleanup by zone cutting. 1, 2 and 3 are replicates.

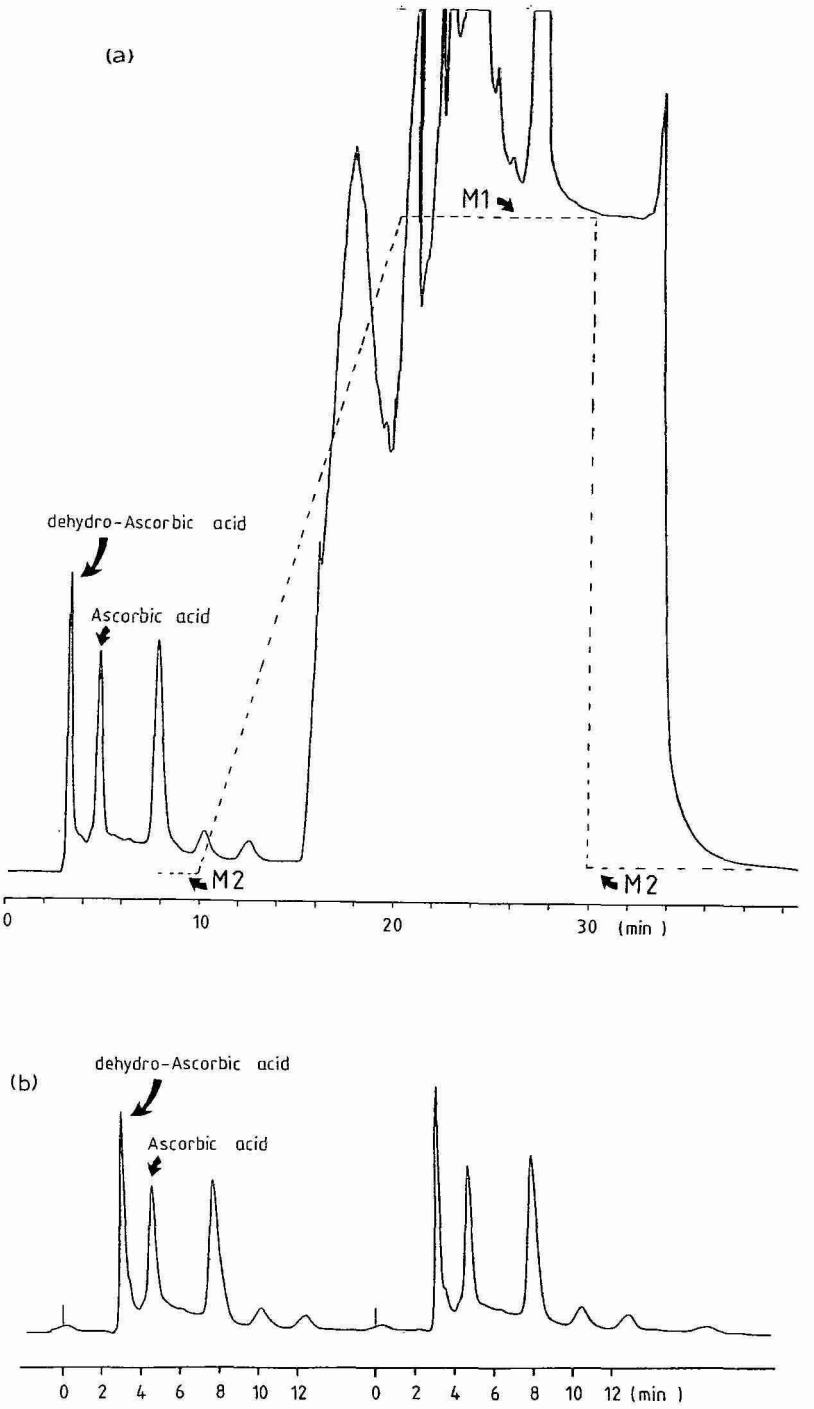

Fig. 7. Chromatogram showing the separation of blackcurrant syrup without (a) and with (b) sample cleanup.

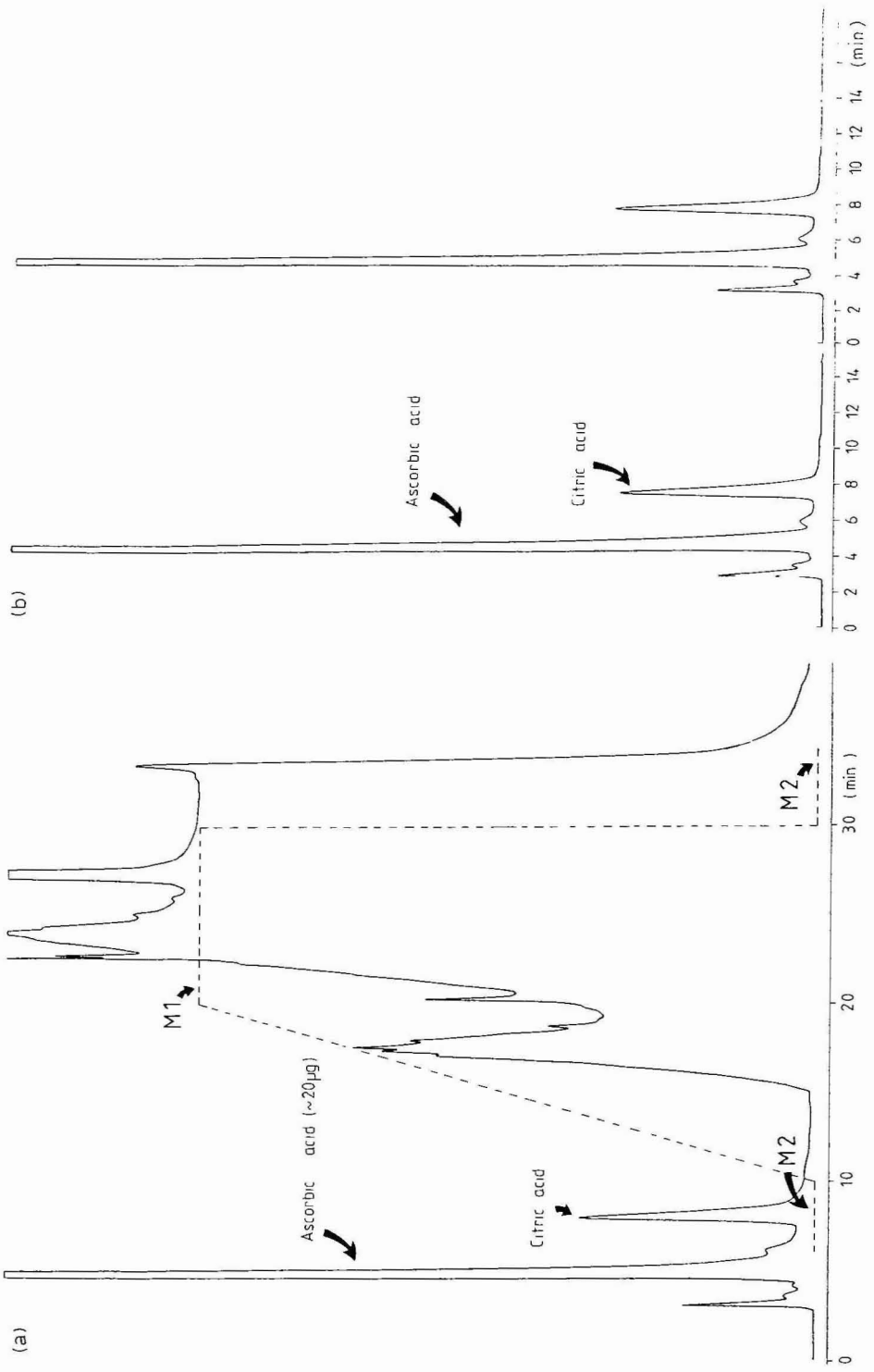

Fig. 8. Chromatogram showing the separation of rose hip syrup without (a) and with (b) sample cleanup.

creasing eluting power. As changes are made sequentially it is obvious that solvents adjacent in the series, must be mutually miscible.

(c) Arbitrary solvent selection for different methodologies is possible. As the Tracer recognizes position No. 1 it is best the reset to position 1 and switch the valve x times to select the required solvent; *i.e.* switch twice to select position No. 3.

Sample selection

Each outlet can be connected to a dilute aqueous sample. After selection, the sample can be pumped through a pre-column for trace enrichment.

Fraction collection

By reversing the connections so that the common outlet is connected to the column end; up to six fractions can be collected of any volume per fraction. This is useful in semi-preparative chromatography, particularly when multiple runs are envisaged.

EXPERIMENTAL

Apparatus

A Kontron Model 640 gradient elution chromatograph with automatic sampler, Kontron MCS 670, "Tracer", valve-switching unit, and Uvikon 720 LC detector (Kontron) were used. All units were controlled through the Kontron Model 200 or 205 programmer. The Model 205 programmer has dedicated keys for valve switching, detector control and autosampler control and is therefore the easiest method for control; however, other methods of control include (a) manual switching, (b) Model 210 Tracer Timer unit and (c) computer control via built-in RS232 interface.

Reagents

All solvents were HPLC grade (Rathburn) and water was freshly double-distilled. Sodium dihydrogen orthophosphate and phosphoric acid were of AnalaR grade (BDH).

Columns

Kontron Spherisorb S5 ODS column and Brownlee S5 ODS pre-columns were used throughout.

RESULTS

Two areas of application were considered in this paper: (a) sample cleanup, and (b) trace enrichment.

Automatic sample cleanup

The fundamental concept of valve switching which relates to sample cleanup is "zone cutting" and has previously been described. The configuration shown in Fig. 3 is extremely versatile and flexible, allowing two successive zone cuts prior to final analysis. In the following applications column C1 is used as the pre-column where the cleanup takes place. In each application, a single zone cut is sufficient to allow subsequent high resolution analysis. Once the zone cut has been made, C1 is then cleaned and

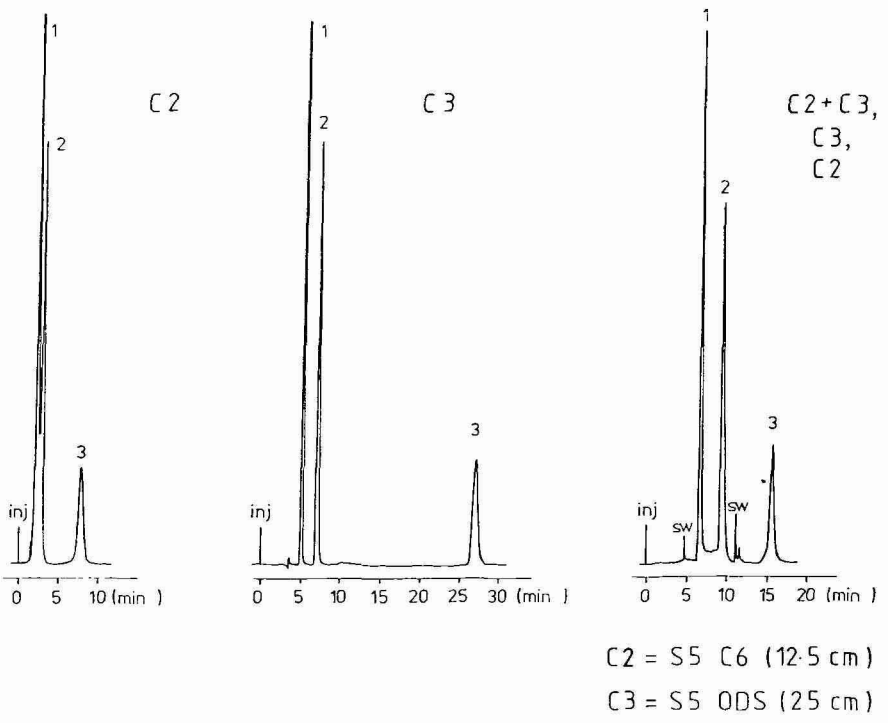

Fig. 9. Application of muticolumn chromatography to the optimization of the chromatogram. Peaks: 1 = acetone; 2 = methyl ethyl ketone; 3 = octaphenone. Detection, UV at 254 nm, 0.05 a.u.f.s., flow-rate, 1 ml/min.

re-equilibrated through the second flow path through the system, driven by pump C. Cleaning is generally made in the foreflush mode to protect the column lifetime and the mobile phase changes are made by selector valve S1.

Acids in wine, fruit juices, beverages, etc.

Organic acids in wine are important for quality control purposes for the control of the fermentation processes. Vitamin C control of fruit juices and extracts is also of significance.

Fig. 4 shows a chromatogram of red wine injected directly onto the analytical column C3. The compounds of interest elute in the front cut shown. The principle of sample cleanup is further demonstrated in Fig. 5, where the same sample is eluted from C1. The zone containing the acids of interest is a tight band eluting at the front of the chromatogram. Subsequent cleaning with methanol (Ml) and re-equilibration with buffer (M2) establishes the necessary times for regeneration. Consequently, C1 and C3 are switched in-line at the start of the analysis such that the zone cut is transferred to C3. At the point, C1 is switched out of line and is regenerated as described. Analysis proceeds on C3 as shown in Fig. 6.

Under similar conditions, but where C3 is a 20-cm Hypersil-5 ODS column, similar applications are shown for the direct analysis of (a) vitamin C in blackcurrant syrup (Fig. 7) without and with cleanup by column switching; (b) vitamin C in rose hip syrup (Fig. 8) without and with cleaning by column switching.

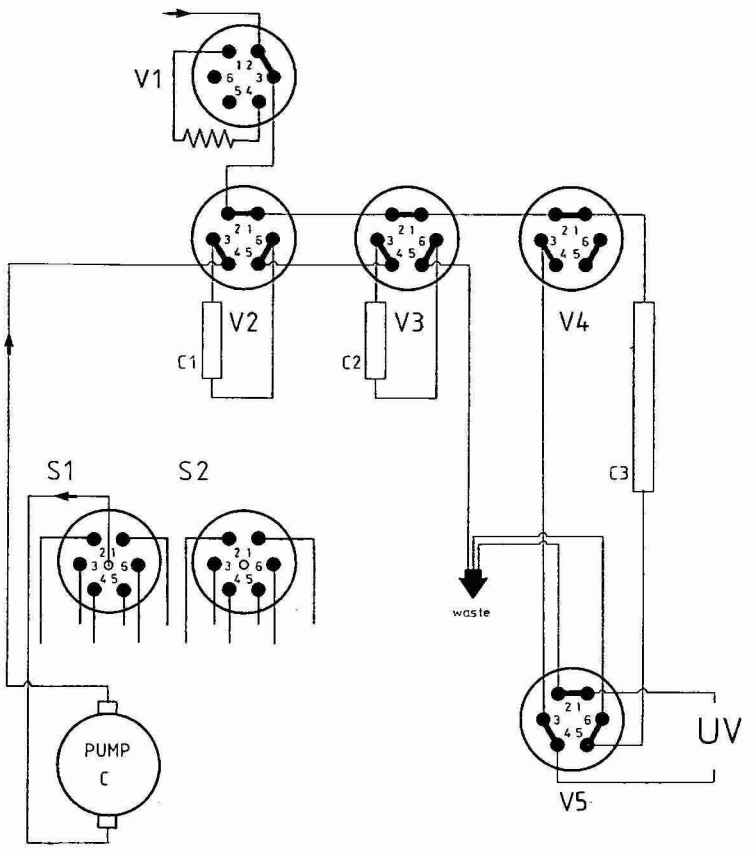

Fig. 10. Kontron MCS 670 Tracer configuration suitable for the trace enrichment. Alternative loading of pre-columns eliminates much lost time.

Multicolumn optimisation of resolution

A further aspect of column switching which is pertinent to sample cleanup is illustrated by Fig. 9.

After the primary zone cut has been made for cleanup, the zone of interest may chromatograph as shown on columns C2 and C3 (C2, C3 as indicated on Fig. 9). In order to optimise this separation, columns C2 and C3 are placed "in-line" to allow peaks 1 and 2 to elute from C2 onto C3. Then C2 is switched "off-line" while higher resolution of peaks 1 and 2 occurs on C3. After elution from column C3, column C3 is switched "off-line" and C2 switched "in-line" allowing elution of peak 3. This is a powerful approach to optimization of chromatographic elution. The example given is for a mixture of ketones.

Automatic trace enrichment

The simplest forms of trace enrichment have been described in the introduction. This instrument (Tracer) facilitates the automation of this process as shown in Fig. 10.

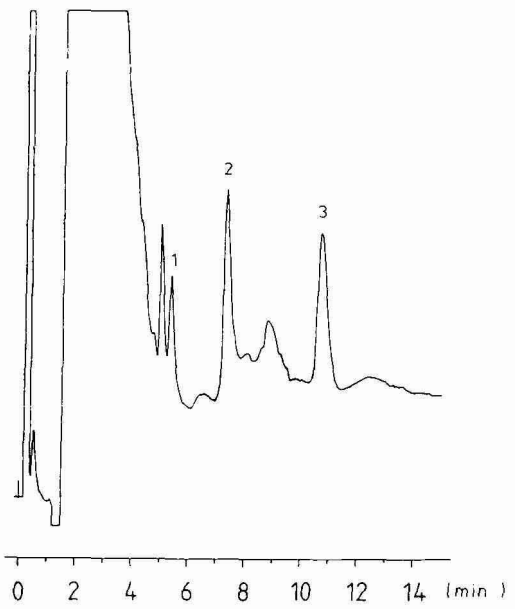

Fig. 11. Application of trace enrichment to chlorophenols in tapwater. Volume concentrated (50 ml water acidified to pH 2.4). Pre-column: Brownlee RP18 cartridge (3 cm). Analytical column: 25 cm × 4.6 mm I.D. S5 ODS (Kontron). Eluent; methanol–$10^{-3}M$ H_3PO_4 (75:25). Flow-rate: 2 ml/min. Detection: UV at 220 nm, 0.01 a.u.f.s.. Peaks: 1 = 3,4,5-trichlorophenol (0.4 ppb); 2 = 2,3,4,5-tetrachlorophenol (0.4 ppb); 3 = pentachlorophenol (0.3 ppb).

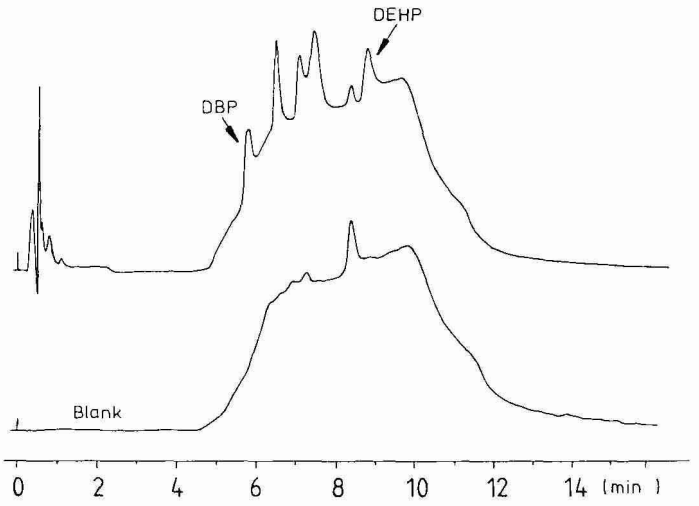

Fig. 12. Application of trace enrichment to plasticisers in aqueous extracts (Evian mineral water). Volume concentrated (50 ml at 10 ml/min). Pre-column: Brownlee RP18 cartridge (3 cm). Column: 10 cm, RP18, 10 mm (Kontron). Flow-rate: 4 ml/min. Eluent: methanol–water gradient (65–100 % methanol gradient over 2-min period, starting at time 4 min, then isocratic for 4 min and then 2-min gradient back to 65% methanol. Detection: UV at 224 nm. DBP = dibutyl phthalate (0.11 ppb); DEHP = diethylhexylphthalate (0.13 ppb).

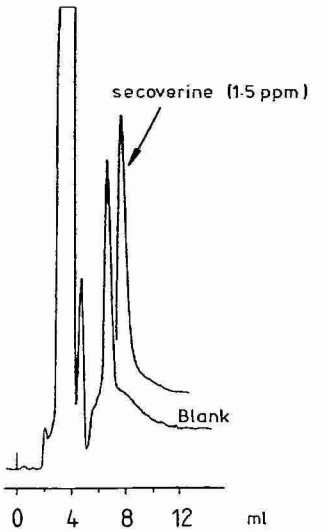

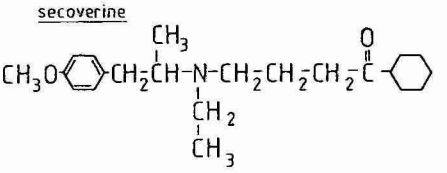

Fig. 13. Trace enrichment of secoverine from deproteinised serum. Volume concentrated; 1 ml serum. Pre-column: 2.2 mm × 4.6 mm I.D., Polygosil-CN (10 μm). Column: 25 cm × 4.6 mm I.D., Sil 60-D5-CN. Eluent: dioxan–0.1 *M* aqueous phosphate pH 3.2 (15:85). Detection: UV at 274.5 nm.

Sample loading occurs through pump C which is directly connected to selector valve S1 or S2 or S1 + S2 (connected together).

The selector valves enable selection of the required dilute aqueous sample which is then routed through one of the pre-columns (*e.g.* C1) typically 50 ml of the sample is pumped through the column. While this is taking place column C2 is "in-line" with the analytical column C3. The appropriate mobile phase (*e.g.*, methanol–water, 75:25) elutes the enriched species (and impurities) from C2 onto C3. After elution, solvent change to water is necessary in order to equilibrate C2. While this re-equilibration is taking place, C3 has been by-passed to preserve stable isocratic conditions. The next stage of the automated process is to switch C2 "off-line" and C1 "in-line". The procedure continues only this time C2 is being loaded while C1 is being eluted.

Chlorophenols in tapwater. Control of phenolic species in tapwater is critically important for environmental control[5–7]. The application of the Tracer to these compounds is very well demonstrated in Fig. 11. The power of trace enrichment is emphasized by the very low levels that can be determined by this method.

Plasticisers. We live in a plastic world which is constantly contributing to environmental pollution by the liberation of toxic plasticisers. The application shown (Fig. 12) indicates that many of the plastic bottles containing beverages, contaminate that beverage with plasticisers such as dibutyl phthalate and diethylhexyl phthalate.

Deproteinated serum. Many drugs can be determined from deproteinated serum but occur at levels too low for easy determination. Enrichment similar so that previously described allows detection at low levels. In these applications shown in Fig. 13, 1 ml deproteinated serum was concentrated on a pre-column and eluted as described previously. However, the loading took place via an autosampler set to load 1 ml samples. Using this method, secoverine at a concentration of 1.5 ppm in plasma was determined.

CONCLUSIONS

The enormous power of valve switching has been indicated and demonstrated for automatic sample cleanup and trace enrichment. It is obious that in trace enrichment, impurities are also concentrated, thus limiting the degree of concentration possible. The Kontron "Tracer" has been shown to be able to carry out all the requirements of this methodology with precision and accuracy. It is versatile, flexible and indicates the way in which much of the future chromatography will be carried out.

REFERENCES

1 R.E. Majors, *J. Chromatogr. Sci.*, 18 (1980) 571.
2 F. Erni, H. P. Keller, C. Morin and M. Schmitt, *J. Chromatogr.*, 204 (1981) 65.
3 J.F.K. Huber, R. van der Linden, E. Ecker and M. Oreans, *J. Chromatogr.*, 83 (1973) 267.
4 F.W. Willmott, I. Mackenzie and R.J. Dolphin, *J. Chromatogr.*, 167 (1978) 31.
5 H.P.M. van Vliet, Th.C. Bootsman, R.W. Frei and U.A.Th. Brinkman, *J. Chromatogr.*, 185 (1979) 483.
6 P.O. Realini, *J. Chromatogr. Sci.*, 19 (1981) 124.
7 L. Renberg and K. Lindström, *J. Chromatogr.*, 214 (1981) 327.

Journal of Chromatography, 264 (1983) 197–213
Elsevier Science Publishers B.V., Amsterdam — Printed in the Netherlands

CHROM. 15,852

CHARACTERIZATION OF CHEMICALLY MODIFIED SILICA GELS BY ^{29}Si AND ^{13}C CROSS-POLARIZATION AND MAGIC ANGLE SPINNING NUCLEAR MAGNETIC RESONANCE

ERNST BAYER*, KLAUS ALBERT, JÜRGEN REINERS and MICHAEL NIEDER
Institut für Organische Chemie, Universität Tübingen, Auf der Morgenstelle 18, D-7400 Tübingen (G.F.R.)
and
DETLEF MÜLLER
Bruker Analytische Messtechnik GmbH, Silberstreifen, D-7512 Rheinstetten (G.F.R.)
(Received March 9th, 1983)

SUMMARY

Chemically modified silica gels were prepared and examined by use of solid-state ^{13}C and ^{29}Si cross-polarization and magic angle spinning nuclear magnetic resonance spectroscopy. By this method, one can not only distinguish between various structural elements in the surface region, but also differentiate according to their mode of preparation. The results of the original manufacturing procedures for reversed-phase high-performance liquid chromatography materials and their subsequent treatment with trimethylsilylating reagents can be investigated. It is also possible to decide whether the solvents (*e.g.*, methanol) used in the preparation remain adsorbed at the surface or are completely removed by heat treatment. Further developments of this method of investigation may reveal the molecular mechanism of chromatographic separations.

INTRODUCTION

A wide variety of silica adsorbents with a narrow distribution of particle diameter, definite pore volume and reproducible specific surface area are commercially available. The applicability of such materials is strongly dependent on their surface properties. Chemical modification of the surface is usually achieved by bonding an appropriate organosilicon compound via the stable Si–O–Si–C moiety. These chemically bonded stationary phases have stimulated more recent development in the field of reversed-phase high-performance liquid chromatography (RP-HPLC). Especially organosilanes with terminal functional groups have been successfully used for chemical modifications.

A wide variety of specific functional groups can be introduced on to silica surfaces. The technique of surface modification developed for silica gels has also been applied to such different fields of chemistry as catalysis by supported metal complexes[1], photochemistry[2], electrochemistry[3] and triphase catalysis[4]. There is not yet a

0021-9673/83/$03.00

method available that gives an exact and detailed picture of the chemical species formed on the surface. Therefore, reproducible batches of preparations of reversed-phase materials are difficult to obtain, and the observed variations of retention and selectivity during the use of reversed phases often cannot be explained.

Only limited information about the bonded species is available from the use of infrared (IR), far infrared (FIR) and difference techniques of IR spectroscopy[5–8]. Other methods used for the characterization of chemically modified silica gels are thermogravimetry, *e.g.*, in combination with differential thermal analysis, and pyrolysis gas chromatography–mass spectrometry. Another possibility is the hydrolytic cleavage of the Si–C bonds. These methods have the disadvantage that they are accompanied by the destruction of the chemically bonded material.

More powerful methods for the characterization of chemisorbed compounds are those in the field of solid-state nuclear magnetic resonance (NMR) spectroscopy. In the solid state, the line width is increased owing to dipole–dipole interactions and the anisotropy of the chemical shift tensor. Dipolar decoupling[9] in combination with magic angle spinning (MAS)[10], however, results in spectra that show resolutions comparable to those of high-resolution spectra. The long relaxation time of ^{13}C and ^{29}Si nuclei in the solid state is reduced by the recently introduced cross polarization (CP)[11,12]. Because CP efficiency is dependent on the Si–H distance, internal Si atoms do not contribute to the CP–MAS spectrum.

Up to the present, ^{13}C NMR spectroscopy with cross-polarization and magic angle spinning (^{13}C CP–MAS NMR) has been mainly used for the investigation of fossil fuels[13] and polymers[14]. Only a few data have been reported for ^{13}C NMR[15–17] and ^{29}Si NMR measurements[18–20] on silica gels modified with organosilanes. For further improvement of our recent investigation of on-line coupling of HPLC and NMR[21], we have prepared silica samples modified with a variety of organofunctional silanes and studied these phases by means of NMR spectroscopy. Both ^{13}C and ^{29}Si NMR spectroscopy[22] seemed very promising for obtaining information on different structural elements of the surface. The results obtained from measurements of modified silica gels prepared in our laboratory[23,24] were also used to characterize a number of commercial reversed-phase HPLC materials.

EXPERIMENTAL

The ^{29}Si and ^{13}C NMR spectra were obtained on a Bruker CXP-300 Fourier transform NMR spectrometer. Samples of 100–200 mg were measured in 6.3 mm I.D. rotors made of boron nitride (for ^{13}C spectra) or of Delrin (for ^{29}Si spectra). CP–MAS was used with alternative inversion of the 90° pulse phase. The proton 90° pulse length was 4.5 μsec. In the case of ^{29}Si contact times of 5 msec and repetition times of 4–6 sec were used. For ^{13}C, the contact times were 3 msec and repetition times 4–6 sec. The spinning speed was between 3.5 and 5 kHz; hence side bands do not appear for those compounds with a rather low anisotropic chemical shift tensor.

The variation of the magic angle was checked with glycine between the experiments; the line width of the carbonyl signal never exceeded 30 Hz. For ^{13}C experiments the chemical shifts were referenced to tetramethylsilane by using the carbonyl signal of glycine as a secondary standard (170.09 ppm). For ^{29}Si data, the referencing of Engelhardt *et al.*[18] was adopted. No magic angle check for ^{29}Si was

necessary, as the broad-band probe tuned between deuterium and ^{13}C without modification.

The inherent stability of cryomagnets allows measurements without lock or internal reference standard.

Materials

The silica gels used for surface modifications are commercially available. LiChroprep Si60 (BET surface area, $S_{BET} = 500\ m^2/g$; particle diameter, $d_p = 15–25\ \mu m$) and Si 60 H ($S_{BET} = 500\ m^2/g$, $d_p = 15\ \mu m$) were purchased from Merck (Darmstadt, G.F.R.). Polygosil 60 ($S_{BET} = 500\ m^2/g$, $d_p = 5–20\ \mu m$) was obtained from Macherey, Nagel & Co. (Düren, G.F.R.).

The sources of other reagents were as follows: butyllithium (as a 15% solution in *n*-hexane), Metallgesellschaft (Frankfurt, G.F.R.); trichlorosilane, Fluka (Buchs, Switzerland); dimethylchlorosilane and 3-aminopropyltriethoxysilane, EGA (Steinheim/Albuch, G.F.R.); and dimethyldichlorosilane, trimethylchlorosilane and hexamethyldisilazane, Merck. 10-Undecenyl-1-dimethylchlorosilane was prepared from 11-chloroundecene-1 and dichlorodimethylsilane by Grignard cross-coupling; *n*-butyl-1-dimethylchlorosilane was prepared by reaction of *n*-butyllithium with dichlorodimethylsilane. The silanes bearing an ester group as precursor for a hydroxyl group were obtained by homogeneously catalysed hydrosilylation (H_2PtCl_6–2-propanol) of the corresponding olefins with trichlorosilane or chlorodimethylsilane.

The following commercial reversed-phase materials were investigated: RP-18, 10 μm (Merck); Nucleosil 5 C_{18} and 5 C_8 (Macherey, Nagel & Co.); ODS-Hypersil (Shandon, Runcorn, Great Britain); and Spherisorb ODS 2 (Phase Separations, Queensferry, Great Britain).

The silica samples were dried before the modification in high vacuum at 170°C for 48 h. After this pre-treatment the adsorbents were stored under an argon atmosphere in Schlenk tubes. If not otherwise noted, all subsequent operations were carried out under argon using the Schlenk technique to avoid any contact with impurities and moisture from the air. The solvents were purified according to known procedures and distilled in an inert gas atmosphere.

Procedures

n-Butyl-1-dimethylsilylsilica (1), 10-undecenyl-1-dimethylsilylsilica (2), 11-acetoxyundecyl-1-dimethylsilylsilica (3), 10-carbomethoxydecyl-1-dimethylsilylsilica (4) and 11-acetoxyundecyl-1-silylsilica (8) were prepared according to the following general procedure. A 10-g sample of silica gel Si 60 H was suspended in 150 ml of toluene and 30 mmol of the corresponding halogenosilane was slowly added to the suspension. The mixture was stirred at 80°C for 24 h while a slight stream of nitrogen was passed through. The silica derivative was filtered off and the excess of silane was extracted with toluene. Residual silanol groups were capped with an excess of TMCS–HMDS (molar ratio 1:2) according to known procedures[25].

The derivatives 1, 2, 3 and 8 and the trimethylsilylated compounds 3-TMS, 4-TMS and 8-TMS were additionally washed with methanol, whereas sample 4 was extracted only with toluene.

The silica derivatives were heated under high vacuum at the temperatures given in the table of elemental analyses (Table I).

TABLE I

PROPERTIES OF SAMPLES 1–4 AND 8

Sample No.	*Carbon content (% C)*	*Surface coverage (mmol/g)*	*Drying temperature (°C)*
1	3.04	0.42	120
2	7.26	0.47	20
3	10.52	0.58	120
3-TMS	12.56		120
4	11.61	0.64	120
4-TMS	13.31		120
8	9.91	0.55	120
8-TMS	11.45		20

A: PREPARATION OF REVERSED-PHASE SILICA GELS

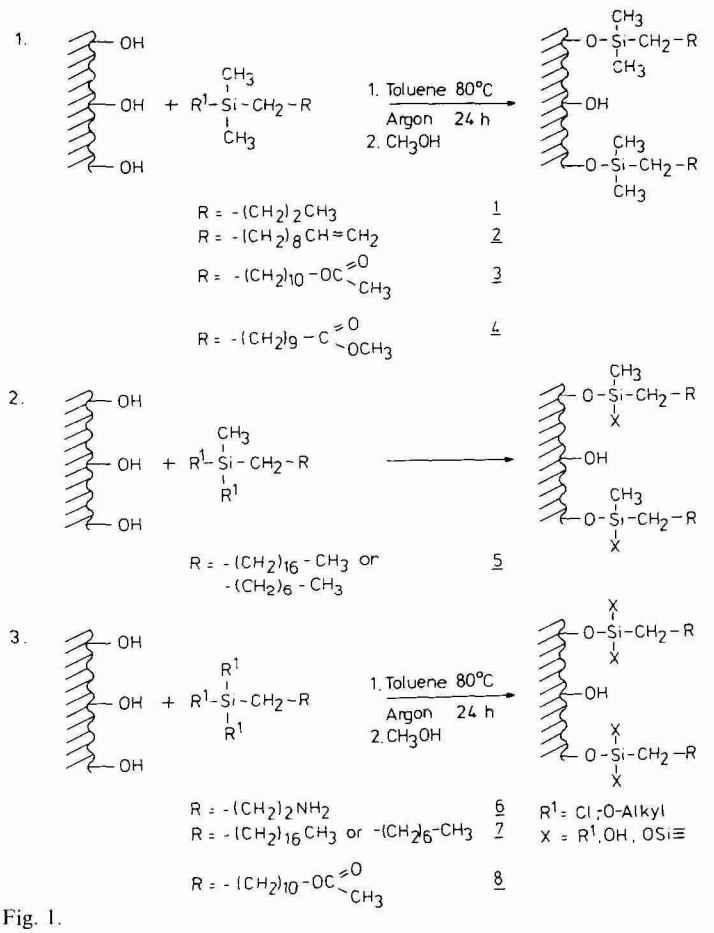

Fig. 1.

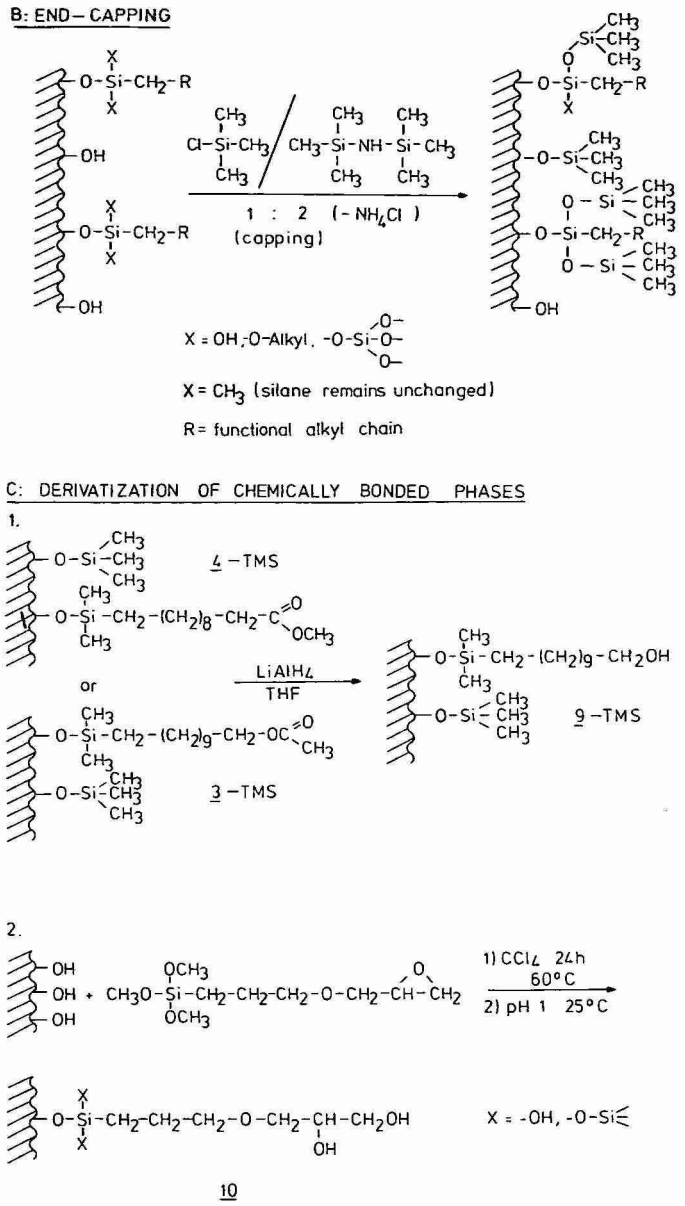

Fig. 1. Reaction scheme for the preparation of chemically modified silica gels.

11-Hydroxyundecyl-1-dimethylsilylsilica (9) (capped 9-TMS) was prepared as follows. A 300-mg amount of lithium tetrahydridoaluminate were suspended in 30 ml of tetrahydrofuran (THF). The filtrate of this suspension was added dropwise at 10°C to 7 g of 3-TMS or 4-TMS suspended in 75 ml of THF. After complete addition the mixture was stirred for 1 h at 20°C. The silica was separated from excess of reducing reagent and washed with THF. After decomposition of the aluminium alco-

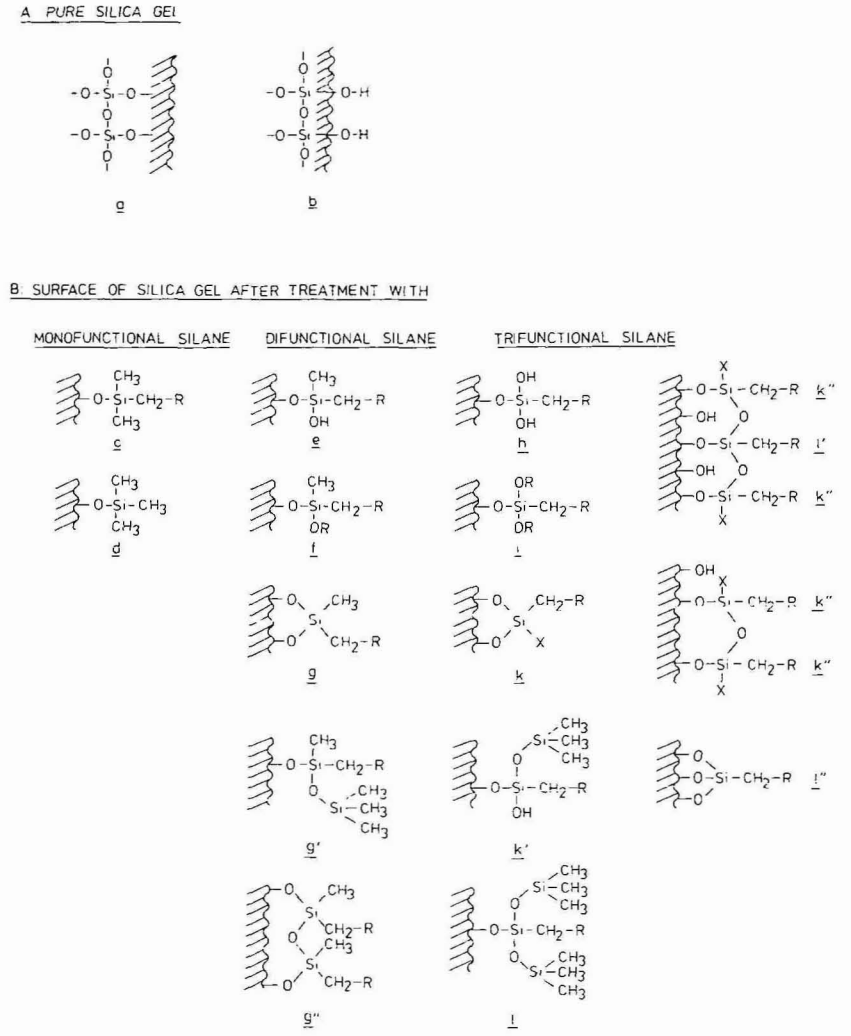

Fig. 2. Structural elements at the surface of bonded stationary phases.

holate in THF by careful addition of 10^{-2} *N* hydrochloric acid, the silica sample was washed repeatedly with water (until the filtrate was free from chloride) and finally with methanol. The reduced silica gel was treated at 150°C under high vacuum for 20 h. The IR spectrum showed no absorption in the C=O region.

The elemental analysis was as follows: 11.78% C (reduction of 3-TMS) and 10.70% C (reduction of 4-TMS).

3-Aminopropyl-1-silylsilica (6) and 1,2-dihydroxypropoxy-3-propyl-1-silylsilica (10) were prepared according to known procedures[26]. Their elemental analyses were as follows: (6) 2.5% C, 0.7% N, specific coverage 0.69 mmol/g; (10) 6.4% C, specific coverage 0.89 mmol/g.

RESULTS AND DISCUSSION

The different types of surface modifications described are shown in Fig. 1. The corresponding structural elements that are possible at the surface of silica gel after silanization are depicted in Fig. 2.

In the ^{29}Si CP–MAS NMR spectrum of pure silica gel Si 60 (Merck) we observed two resonances, at -100 and -110 ppm, which correspond to tetraoxo-coordinated framework silicon (structure a) and surface silanol groups (structure b)[27] as shown in Fig. 2. Sindorf and Maciel[20] interpreted the shoulder at -90 ppm in terms of geminal silanol groups. However, we are not able to confirm their result. A peak due to these geminal silanol groups, if at all present and then in only very low concentration, was not detectable in our measurements.

The data obtained for samples prepared by ourselves are summarized in Tables II and III. First we consider the reaction of monofunctional silanes with silica gel (reaction 1 in Fig. 1). The ^{29}Si CP–MAS NMR spectrum of *n*-butyldimethylsilylsilica (1) is shown in Fig. 3. Compared with pure silica gel, a new resonance of the silicon atom attached to the surface appears at +12.3 ppm. This indicates the existence of structural element c (Fig. 2). The structure of the alkyl chain is obtained from the ^{13}C CP–MAS NMR spectrum shown in Fig. 4.

The assignment for the solid-state spectrum of this silica derivative is based on the proton-coupled ^{13}C NMR spectrum of the silane recorded in solution at 100.62 MHz. Carbons 2 and 3 are distinguishable by their different coupling patterns: C-2 exhibits a triplet of triplets (^1J = 125.4 Hz; ^2J = 3.6 Hz) whereas C-3 shows a triplet of quartets (^1J = 126.4 Hz; ^2J = 5.4 Hz). Comparing the ^{13}C chemical shifts of compound 1 in the solid state and that of the silane we have to consider the chemical environment of the silicon atom due to the attachment of silicon to one chlorine atom in $ClSi(CH_3)_2(CH_2)_3CH_3$ (Table II) and to a surface silicon group. The difference of carbon 1 ($Si–CH_2$) chemical shifts is about 3 ppm. The chemical shifts of carbons 2 and 3 are not severely affected. However, the methyl resonance (C-4) is shifted to higher field by about 3 ppm.

The assignments of the ^{13}C CP–MAS NMR spectra of the other silica gels modified with monofunctional long-chain alkylsilanes are based on the considerations mentioned above. For instance, the $Si–CH_2$ carbon absorbs between 17 and 18.5 ppm (in the corresponding halogenosilane this carbon atom appears at 19–22 ppm). The other carbon atoms of the alkyl chain are only slightly affected by variation of the environment at the silicon atom [this is demonstrated in the spectrum of trimethylsilylated 11-hydroxyundecyl-1-dimethylsilylsilica (9-TMS) in Fig. 5].

TABLE II

CP-MAS NMR DATA FOR SILICA GEL PHASES

A = Structural elements shown in Fig. 2.

X = -OH, -O-Si(=O)-O-, -O-Si(=O)-CH$_2$-, -OR. (Si) ≡ SiO_2 surface.

Compound	*^{13}C CP-MAS NMR data (ppm)*
1	(Si)-O-Si(A', CH_3)(CH_3)-CH_2-CH_2-CH_2-CH_3 (-OCH_3) -3.4 16.0 25.4 24.1 10.6 44.0/50.0
2	(Si)-O-Si(A'', CH_3)(CH_3)-CH_2-CH_2-CH_2-$(CH_2)_5$-CH_2-CH=CH_2 (-OCH_3) -1.5 18.1 23.0 33.1 30.0 33.1 137.1 114.4 44.3/50.1
9-TMS	(Si)-O-Si(A-A'', CH_3)(CH_3)-CH_2-CH_2-CH_2-$(CH_2)_5$-CH_2-CH_2-CH_2-OH * -0.5 17.9 23.1 32.9 28.9 25.6 32.9 62.3
	(Si)-O-Si(A'', CH_3)(CH_3)-CH_2-CH_2-CH_2-$(CH_2)_5$-CH_2-CH_2-CH_2-O-C(=O)-CH_3 -0.5 17.0 22.6 33.0 28.7 25.7 30.0 65.1 20.3
8-TMS	(Si)-O-Si(A-A''', X)(X)-CH_2-CH_2-CH_2-$(CH_2)_5$-CH_2-CH_2-CH_2-O-C(=O)-CH_3* (-OCH_3) -1.0 13.4 22.6 33.0 28.9 25.4 31.7 63.6 19.4 44.5/50.2
4	(Si)-O-Si(A'', CH_3)(CH_3)-CH_2-CH_2-CH_2-$(CH_2)_5$-CH_2-CH_2-C(=O)-O-CH_3 -1.7 16.6 22.3 32.6 28.3 23.5 32.6 50.7
10	(Si)-O-Si(A''', X)(X)-CH_2-CH_2-CH_2-O-CH_2-CH(OH)-CH_2-OH 9.6 22.3 71.2 71.2 71.2 63.1
6	(Si)-O-Si(A''', X)(X)-CH_2-CH_2-CH_2-NH_2 10.0 26.9 43.9

^{29}Si CP-MAS NMR data (ppm)

Samples 1 and 3	*Sample 6*	*Sample 10*
+13.2 *d*	−56.6 *k* + *k''*	−48.0 *h*
−100.8 *b*	−100.2 *b*	−53.2 *k* + *k''*
−100.5 *a*	−109.9 *a*	−66.2 *l'*
		−100.2 *b*
		−108.9 *a*

* Samples containing trimethylsilyl groups attached to the surface.

TABLE III

^{13}C CHEMICAL SHIFTS (ppm) OF ORGANOFUNCTIONAL SILANES, WHICH WERE USED IN THE SURFACE MODIFICATION (FIG. 1)

The assignments are based on proton coupled spectra.

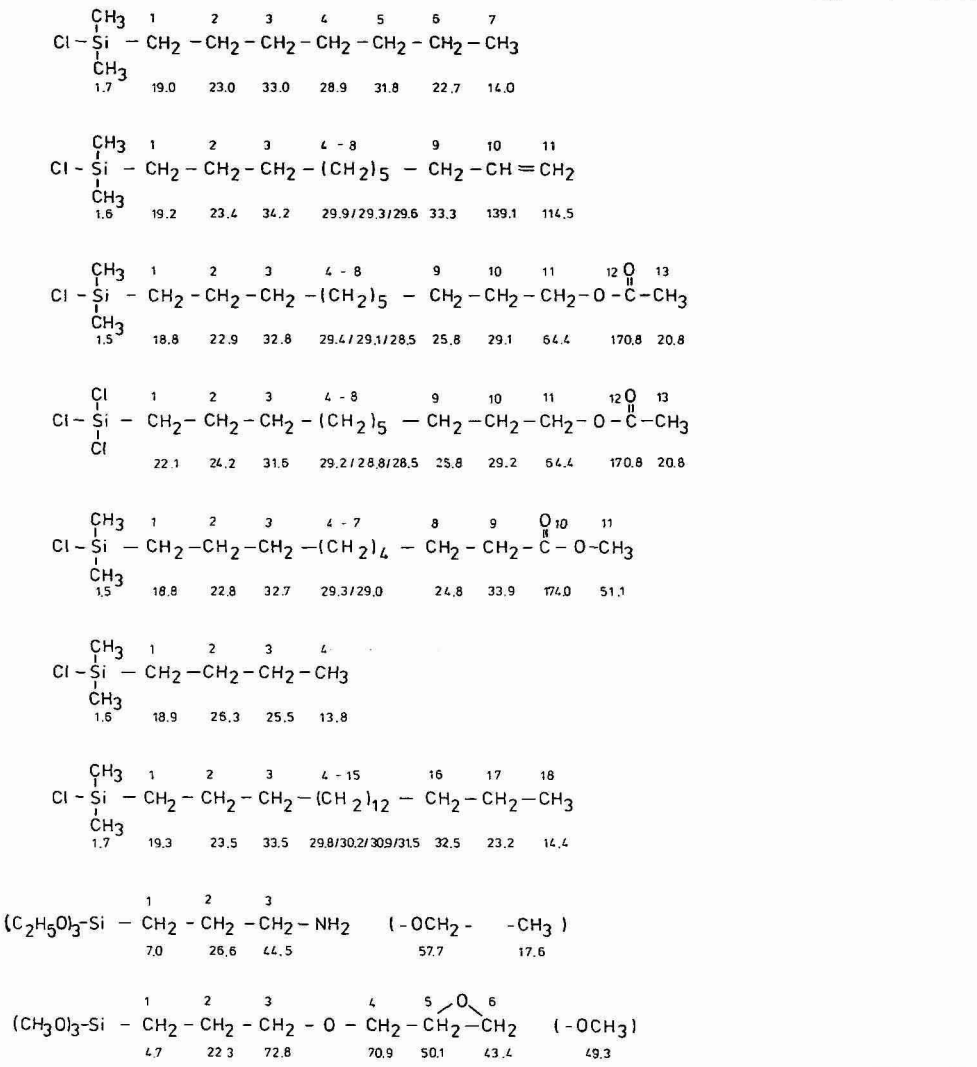

Further, the resonance of a terminal methyl group is shifted to higher fields by reducing the chain length from 17 to 3 methylene units. Thus the chemical shift of the methyl group in octadecylsilica gels is 12.5 $\pm$ 0.4 ppm, in octylsilica gels it appears at 11.9 ppm and in butylsilica gel at 10.6 ppm. This additional shielding may be due to an increased steric interaction between the methyl group and the silica surface with decreasing chain length.

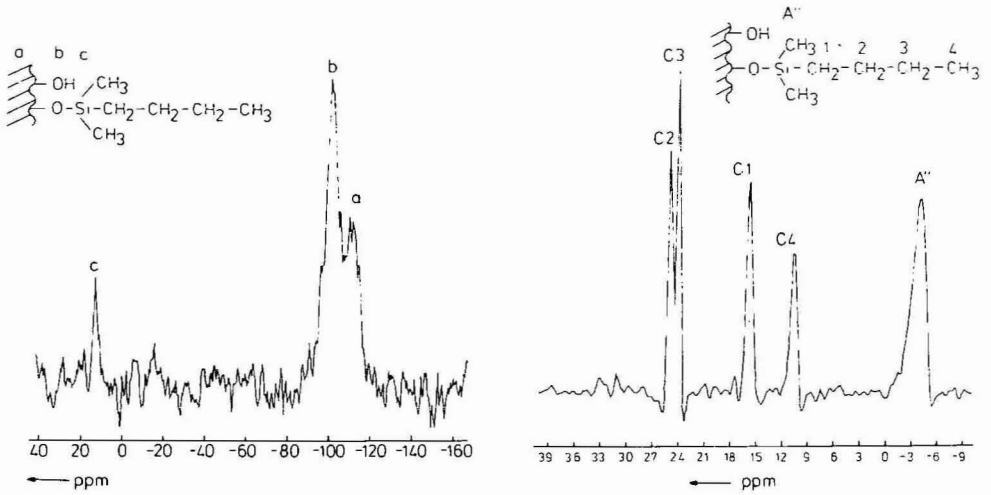

Fig. 3. 59.61 MHz ^{29}Si CP–MAS NMR spectrum of the reaction product of *n*-butyldimethylchlorosilane with silica gel (1).

Fig. 4. 75.46 MHz ^{13}C CP–MAS NMR spectrum of the reaction product of *n*-butyldimethylchlorosilane with silica gel (1).

In general, monofunctional silanes are easily identified by the absorption of the Si–CH_3 group between – 3.4 and 0.5 ppm which is absent in samples modified with trifunctional silanes. It should be noted that the ^{13}C CP–MAS NMR absorptions due to trimethylsilyl and alkyldimethylsilyl groups cannot be resolved. This difficulty also exists in ^{29}Si CP–MAS NMR spectroscopy. The presence of trimethylsilyl groups after end-capping is recognized qualitatively from the difference between the intensities of the ^{13}C signal of about 0 ppm of capped and uncapped material. The ^{13}C resonance of the Si–CH_3 group in a bonded monofunctional silane is found at 2 ppm higher field than for the corresponding halogenosilane in the liquid state.

By use of ^{13}C NMR spectroscopy it is possible to distinguish between the different types of surface bonding, which are dependent on the functionality of the silane used in the modification. For example, the ^{13}C CP–MAS NMR spectrum of end-capped 11-acetoxyundecyl-1-silylsilica (8-TMS) [this sample is readily obtained from reaction of silica gel with $Cl_3Si(CH_2)_{11}OCOCH_3$ and subsequent treatment with TMCS–HMDS (for details see experimental)] is depicted in Fig. 6. The carbon atom directly attached to the silicon atom gives rise to an absorption at 13.4 ppm (22.1 ppm in the trichlorosilane). The chemical shift of carbon 1 is found at 4 ppm lower field in a bonded monofunctional than in a trifunctional silane. A much better distinction of the various binding sites is possible by use of ^{29}Si NMR spectroscopy.

In the ^{29}Si CP–MAS NMR spectra of compounds 6 and 10 additional resonances compared with pure silica gel are observed at -56.6 and -53.2 ppm. This corresponds to the new silicon atom, introduced to the surface by reaction of silica gel with the trialkoxysilane. According to the literature[18,27], the chemical shift values found in the solid state are in good agreement with those measured in solution. Therefore, the position of the new resonance is indicative of a predominant coupling of the silane as a bidentate ligand. We conclude that the structural elements *i*, *k* and *l'*

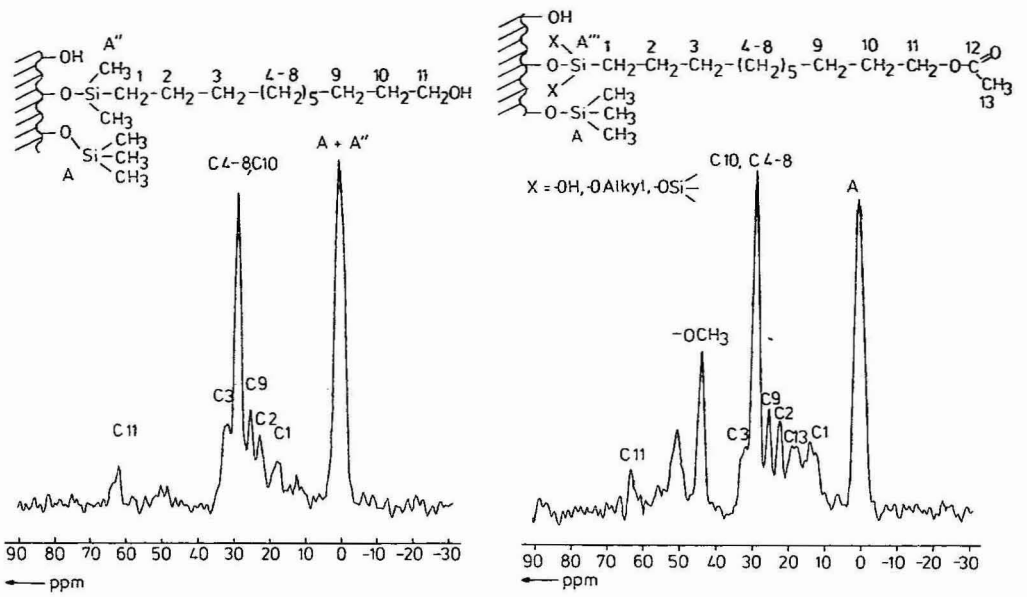

Fig. 5. 75.46 MHz ^{13}C CP–MAS NMR spectrum of the reaction product of 11-acetoxyundecyl-1-dimethylchlorosilane with silica gel, after end-capping and reduction with lithium tetrahydridoaluminate (9-TMS).

Fig. 6. 75.46 MHz ^{13}C CP–MAS NMR spectrum of the reaction product of 11-acetoxyundecyl-1-trichlorosilane with silica gel, after end-capping (8-TMS).

(Fig. 2) are present at the surface. The main peak at -53.2 ppm is assigned to element *k*. This is consistent with the reaction of *two* Si–OR groups with the surface. The weaker peak at -46 ppm is due to reaction of *one* Si–OR group and the peak at -66 ppm is consistent with poly- or oligolayer formation. Also the coupling of adjacent modifier units by Si–O–Si linkages cannot be excluded. This interpretation was also proposed by Sindorf and Maciel[20], who studied the reaction of Cl_3SiCH_3 with silica gel and followed the hydrolysis of unreacted Cl–Si groups by use of ^{29}Si NMR spectroscopy.

Further information about the structure of the alkyl chain after coupling at the surface is obtained from the ^{13}C CP–MAS NMR spectrum of 10 (Fig. 7). Owing to the absence of an absorption at 50 ppm we conclude that the silica derivative does not contain a methoxy group.

The data for 6 indicate that no alkoxy groups remain after the reaction of silica gel with 3-aminopropyltriethoxysilane. It can be seen from Fig. 7 that the oxirane ring of the glycidylsilica is completely hydrolysed (see Table III). The resonance of C-1 in silica samples 6 and 10 prepared by use of trifunctional short-chain silanes appears at about 10 ppm. These results demonstrate that the resonances of C-1 and of the silicon atom of the chemically bonded silane are sensitive indicators for the type of the structural elements present in the surface region. If, in addition, the other resonances of the organic residue are measured, the structure of bonded phases is easily elucidated.

In the same way, we have used the combination of ^{29}Si and ^{13}C NMR spectroscopy to obtain insight into structural details of commercial reversed-phase materials. The RP-8 and RP-18 materials can be distinguished by means of ^{13}C NMR spectroscopy. The functionality of the silane is obtained from the ^{29}Si NMR shift values. The structural elements which can be built up during the chemical modification are shown in Fig. 2. The ^{29}Si and ^{13}C NMR spectra of some commercial reversed phases are presented in Figs. 8–10. The chemical shift values are given in Tables IV and V.

From the data obtained we have drawn the following conclusions. Most of the

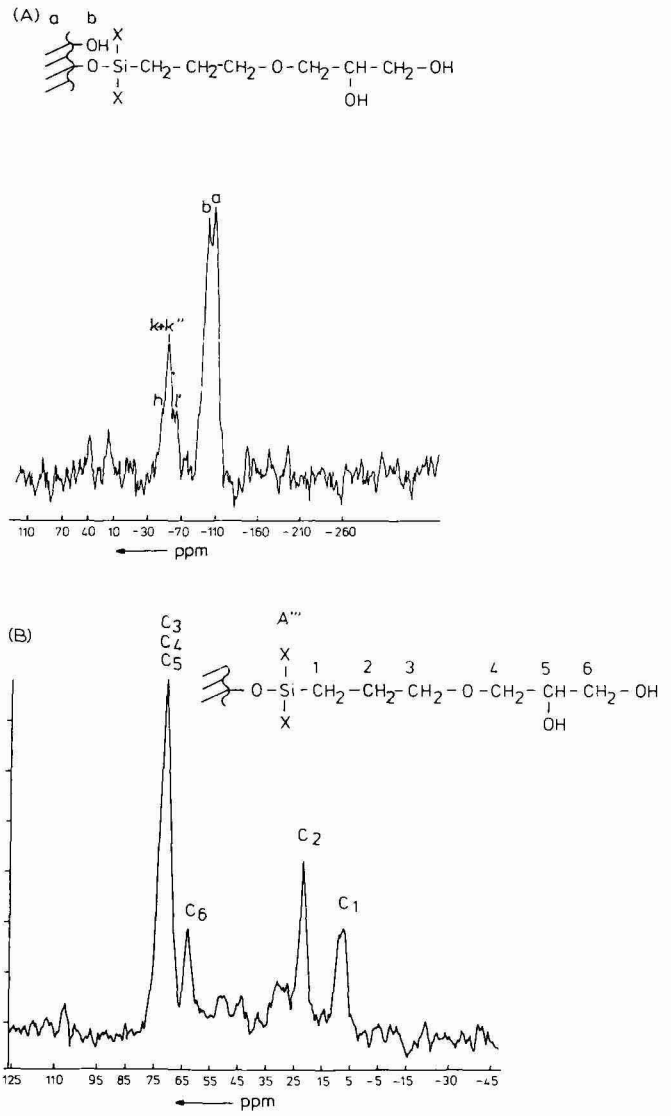

Fig. 7. (A) 59.61 MHz ^{29}Si CP–MAS NMR spectrum of the reaction product of 1,2-epoxy-3-propoxypropyltrimethoxysilane with silica gel (10). (B) 75.46 MHz ^{13}C CP–MAS NMR spectrum of the reaction product of 1,2-epoxy-3-propoxypropyltrimethoxysilane with silica gel (10).

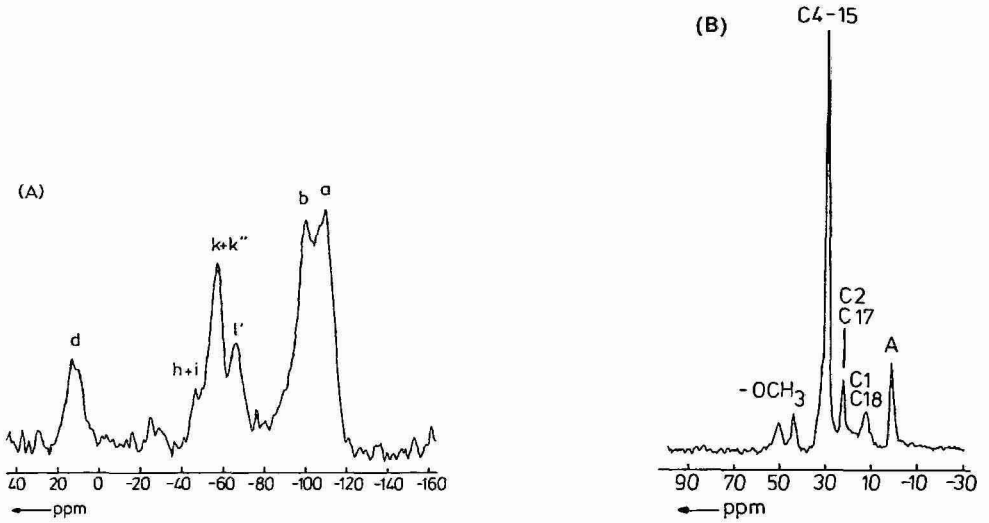

Fig. 8. (A) 59.61 MHz ^{29}Si CP–MAS NMR spectrum of Spherisorb ODS 2 (Phase Separations). (B) 75.46 MHz ^{13}C CP–MAS NMR spectrum of Spherisorb ODS 2 (Phase Separations).

materials investigated in this work were prepared by reaction of silica gel with trialkoxyalkylsilanes. The use of trichloroalkylsilanes would have the disadvantage of decreasing the specific surface area. This effect is attributed to the cleavage of siloxane linkages by hydrogen chloride which is evolved during the modification. In general, the following structural elements (Fig. 2) are detectable in reversed phases derived from trifunctional alkylsilanes: *i* (−48 ppm), *k* and *k′/k″* (−57 ppm) and *l′* (−66 ppm).

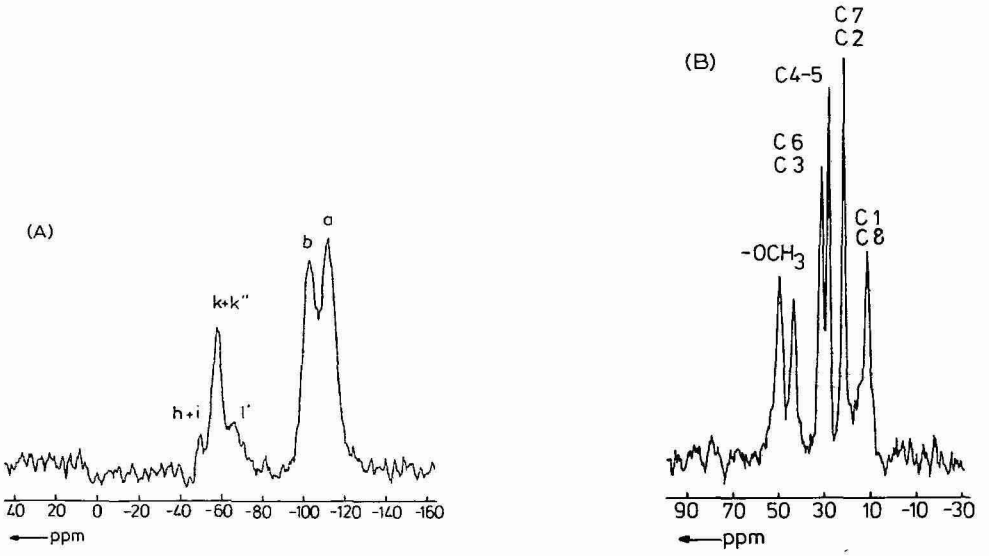

Fig. 9. (A) 59.61 MHz ^{29}Si CP–MAS NMR spectrum of Nucleosil 5 C_8 (Macherey, Nagel & Co.). (B) 75.46 MHz ^{13}C CP–MAS NMR spectrum of Nucleosil 5 C_8 (Macherey, Nagel & Co.).

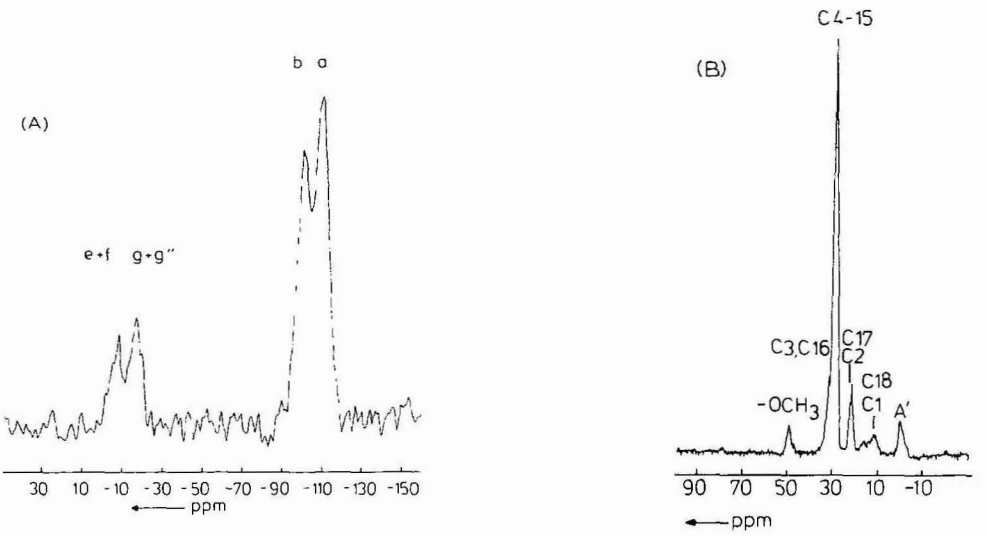

Fig. 10. (A) 59.61 MHz ^{29}Si CP–MAS NMR spectrum of RP-18, 10 μm (Merck). (B) 75.46 MHz ^{13}C CP–MAS NMR spectrum of RP-18, 10 μm (Merck).

Elements designated by the same letter are not resolved in the spectra. Thus we are not able to distinguish between dimers at the surface and an oligolayer. However, we can clearly separate monolayers from condensed silane units. A subsequent treatment with trimethylsilylating reagents is indicated by an additional ^{29}Si resonance at +12.0–13.0 ppm. Thus we find that the RP-18 materials obtained from Phase Separations (Spherisorb ODS 2), Shandon (ODS-Hypersil) and Macherey, Nagel & Co. (Nucleosil C_{18}) are subjected to end-capping. The Macherey, Nagel & Co. phase Nucleosil C_8, however, was not trimethylsilylated. In contrast to these phases, Merck uses difunctional silanes, *e.g.*, dimethoxy- or diethoxymethyloctadecylsilane, for the manufacture of reversed phases (reaction 2, Fig. 1). The structural elements expected for this type of silane are *e*, *f* (−9.9 ppm) and *g*, *g''* (−18.2 ppm). The element *g'* is excluded because of the absence of an absorption at 12 ppm due to an $Si(CH_3)_3$ group. However, it is possible that further silanization was achieved by a dialkoxydimethylsilane, which results in a polylayer with each silicon atom at the surface attached to two organic groups. As described above for the ^{13}C resonance of the $SiCH_3$ group, no shift difference between a $SiCH_3$ group and a $SiCH_2R$ moiety is found in the ^{29}Si data. The coalescence of the signal should also be true for methylalkyldialkoxysilanes.

In the ^{13}C CP–MAS NMR spectra of commercial RP materials, we found two additional resonances at 50 and about 44 ppm. Because methoxy groups in silanes absorb at about 49 ppm (Table III), we assign the resonance at 50 ppm to Si–OCH_3 groups which could be derived from the starting silane. They also could have been generated by slow hydrolysis during storage and by adsorption of methanol used in the washing procedure. We conclude that the resonance at 44 ppm is the result of an adsorption of methanol through hydrogen bonds (Fig. 11). In the silica gel derivatives which we have prepared by modification with a monofunctional silane we detect also

TABLE IV

^{13}C CP–MAS NMR DATA FOR COMMERCIAL RP-SILICA GELS

A = Structural elements shown in Fig. 2.

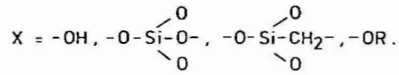

Silica gel	*NMR data (ppm)*								
	A+A‴	1	2	3	4 - 15	16	17	18	
Macherey, Nagel & Co. Nucleosil 5 C_{18}	-0,1*	12,2	22,3	32,0	28,5	32,0	22,3	12,2	(-OCH_3) 49,2
	A+A‴	1	2	3	4 - 15	16	17	18	
Spherisorb ODS 2	1,6*	12,9	22,6	32	29,9	32	22,6	12,9	(-OCH_3) 50,5/44,3
	A'	1	2	3	4 - 15	16	17	18	
Merck RP-18	0,7	14,0	22,4	32,4	29,7	32,4	22,4	12,2	(-OCH_3) 51,1
	A‴	1	2	3	4/5	6	7	8	
Macherey, Nagel & Co. Nucleosil 5 C_8		11,9	22,2	31,9	29,0	31,9	22,2	11,9	(-OCH_3) 50,1/44,0

* Absorption due to trimethylsilyl groups.

two signals due to OCH_3 groups. A possible explanation of the peak at 50 ppm is an equilibrium reaction of free silanol groups with methanol:

$$Si\text{–}OH + CH_3OH \rightleftharpoons Si\text{–}OCH_3 + H_2O$$

Our results are confirmed by the finding that both peaks disappear on prolonged heating of the silica gel phase above 120°C under high vacuum. Thus the assignment given by Leyden *et al.*[16] for silica gel silanized with chloromethylphenyltrimethoxy-silane, assigning the absorptions at 43 and 50 ppm to the benzylic carbon atom, must be incorrect. Using the above assignments of NMR spectra, changes of chemically bondes phases, until now only detectable by the chromatographic behaviour, can be understood and improvements achieved.

It can be expected that in the future solid-state NMR spectroscopy will also give information on the molecular mechanism of the interaction between stationary

TABLE V

^{29}SI CP-MAS NMR DATA OF COMMERCIAL RP-SILICA GELS

Silica gel	*Chemical shift value (ppm)*	*Assignment*
Shandon ODS-Hypersil	+12.1	*d*
	−55.8	*k* + (*k'*) + *k''*
	−66.8	*l'*
	−100.2	*b*
	−109.9	*a*
Macherey, Nagel & Co. Nucleosil 5 C_{18}	+12.7	*d*
	−49.5	*i*
	−57.1	*k* + (*k'*) + *k''*
	−66.4	*l'*
	−100.1	*b*
	−110.3	*a*
Macherey, Nagel & Co. Nucleosil 5 C_8	−49.5	*i*
	−56.9	*k* + *k''*
	−66.2	*l'*
	−101.9	*b*
	−110.8	*a*
Merck RP-18	−9.9/−8.4	*e* + *f*
	−18.2/−17.1	*g* + *g''*
	−101.5/−100.6	*b*
	−110.5/−109.8	*a*
Merck RP-8	−7.9	*e* + *f*
	−16.0	*g* + *g''*
	−100.8	*b*
	−110.0	*a*
Spherisorb ODS 2	+12.9/9.9	*d*
	−25 (weak)	
	−48.2	*i*
	−57.1	*k* + (*k'*) + *k''*
	−66.4	*l'*
	−100	*b*
	−109.1	*a*

phases and both the mobile phases and solutes. Investigations of the conformation of the organic groups bound to the silica matrix are also possible. This certainly will contribute to the further development of columns in liquid chromatography.

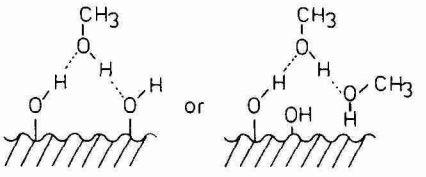

Fig. 11. Schematic representation of physisorbed methanol.

REFERENCES

1 L. Horner and F. Schumacher, *Justus Liebigs Ann. Chem.*, (1976) 633.
2 R. R. Hautala, R. B. King, E. M. Sweet, J. L. Little and A. W. Shields, *J. Organomet. Chem.*, 216 (1981) 281.
3 R. W. Murray, *Acc. Chem. Res.*, 13 (1980) 135.
4 S. L. Regen, *Angew. Chem.*, 91 (1979) 464.
5 A. V. Kiselev and V. J. Lignin, *Infrared Spectra of Surface Compounds*, Wiley-Interscience, New York, 1975.
6 K. K. Unger, *Porous Silica*, Elsevier, Amsterdam, 1979.
7 M. L. Hair, *Infrared Spectroscopy in Surface Chemistry*, Marcel Dekker, New York, 1967.
8 H. Ishida and J. L. Koenig, *J. Colloid Interface Sci.*, 64 (1978) 555.
9 J. Schaefer and E. O. Stejskal, *Top. Carbon NMR Spectrosc.*, 3 (1979) 283.
10 J. Schaefer and E. O. Stejskal, *J. Amer. Chem. Soc.*, 98 (1976) 1031.
11 S. R. Hartmann and E. L. Hahn, *Phys. Rev.*, 128 (1962) 2042.
12 A. Pines, M. G. Gibby and J. S. Waugh, *J. Chem. Phys.*, 59 (1973) 569.
13 H. L. Retkofsky and D. L. van der Hart, *Fuel*, 57 (1978) 421.
14 E. O. Stejskal, J. Schaefer, M. D. Sefcik, G. S. Jacob and R. A. McKay, *Pure Appl. Chem.*, 54 (1982) 461.
15 W. H. Dawson, S. W. Kaiser, P. D. Ellis and R. R. Inners, *J. Amer. Chem. Soc.*, 103 (1981) 6780.
16 D. E. Leyden, D. S. Kendall and T. G. Waddell, *Anal. Chim. Acta*, 126 (1981) 207.
17 C.-H. Chiang, N. Liu and J. L. Koenig, *J. Colloid Interface Sci.*, 86 (1982) 26.
18 G. Engelhardt, H. Jancke, E. Lippmaa and A. Samoson, *J. Organomet. Chem.*, 210 (1981) 295.
19 G. A. Maciel and D. W. Sindorf, *J. Amer. Chem. Soc.*, 102 (1980) 7606.
20 D. W. Sindorf and G. E. Maciel, *J. Amer. Chem. Soc.*, 103 (1981) 4263.
21 E. Bayer, K. Albert, M. Nieder, E. Grom, G. Wolff and M. Rindlisbacher, *Anal. Chem.*, 54 (1982) 1747.
22 G. E. Maciel, D. W. Sindorf and V. J. Bartuska, *J. Chromatogr.*, 205 (1981) 438.
23 J. Reiners, *Dissertation*, Universität Tübingen, Tübingen, 1982.
24 M. Nieder, *Dissertation*, Universität Tübingen, Tübingen, 1982.
25 C. J. Little, A. D. Dale and J. A. Whatley, *J. Chromatogr.*, 171 (1979) 431.
26 K. K. Unger, N. Becker and P. Roumeliotis, *J. Chromatogr.*, 125 (1978) 115.
27 H. C. Marsmann, *Z. Naturforsch. B*, 29 (1974) 495.

Journal of Chromatography, 264 (1983) 215–222
Elsevier Science Publishers B.V., Amsterdam — Printed in The Netherlands

CHROM. 15,856

SACCHARIDE SEPARATIONS IN REVERSED-PHASE HIGH-PERFORMANCE LIQUID CHROMATOGRAPHY USING *n*-ALKYL AMINE MOBILE PHASE ADDITIVES

C. H. LOCHMÜLLER* and W. B. HILL, Jr.
P. M. Gross Chemical laboratory, Duke University, Durham, NC 27706 (U.S.A.)
(Received March 7th, 1983)

SUMMARY

A high-performance liquid chromatography method is described for the separation of mono-, di- and trisaccharides on reversed-phase columns using *n*-alkyl amine mobile-phase additives. Saccharide capacity is dependent on solvent conditions and on the amount of adsorbed modifier. When compared with results from an amino column, the additive system requires weaker solvent conditions for the effective resolution of saccharide mixtures. The reproducibility and stability of this modified reversed-phase system is also demonstrated.

INTRODUCTION

Because of their relative abundance and their widespread importance in biology, medicine, agriculture and the food industry, the analysis of carbohydrate mixtures is an area of high interest. Traditionally, paper, ion-exchange, thin-layer and gel filtration chromatography have been used to separate these mixtures[1,2]. For analysis by gas chromatography and mass spectroscopy, trimethylsilane[3,4] butylboronic acid[5,6] and a variety of substituted benzeneboronic acid[7] derivatives of saccharides have been prepared. Sugar separations using high-performance liquid chromatography (HPLC) combining refractive index detection and microparticulate amine phases have been developed[8–11]. Amine mobile-phase additives have also been effective in separating saccharides on silica gel columns[12–15] and on cation-exchange resins[16]. In order to enhance the detection sensitivity of these separation techniques, several ultraviolet (UV) post-column reagents have been introduced[17–20]. Saccharides have also been derivatized with both UV and fluorescent labels prior to separation on silica gel to enhance the detection sensitivity[21–23]. Recently, reversed-phase HPLC has been used to separate classes of oligosaccharides according to their degree of polymerization[24,25].

Due to the stability of reversed-phase columns, several mobile-phase additives have been developed to achieve other difficult separations. Enantiomeric separations of amino acids in modified reversed-phase systems have been achieved using chiral, metal complexes[26–28]. Using its charge-transfer properties, Lochmüller and Jensen

0021-9673/83/$03.00

used a chiral, non-ionic mobile modifier [N-(2,4-dinitrophenyl)-L-alanine-*n*-dodecyl ester] to separate enantiomers of 1-aza-hexahelicene on reversed-phase columns[29]. Enhanced separations of aromatic amines and pyridine derivatives hve also been achieved using a coordinatively unsaturated nickel complex [bis(2,2,6,6-tetramethyl-heptane-3,5-dionate)nickel(II)] [Ni(DPM)] with reversed-phase systems[30]. The present study reports on the utility of *n*-alkyl amine mobile-phase additives in reversed-phase systems in effectively retaining and separating mono-, di- and trisaccharides. These modifiers provide both capacity and selectivity for these saccharides not normally provided by reversed-phase systems. The approach also minimizes the effect of rapid deterioration and spoiling observed when separating saccharides using amine or carbohydrate columns since the amine modifier may be reproducibility removed and replaced with minimal time and expense and, for some, eliminates the need for an amine column for an occasional saccharide separation. Furthermore, the performance differences between the amine column and the amine additives contribute to a more complete understanding of both systems.

EXPERIMENTAL

Apparatus

The chromatographic system incoporated a Varian (Walnut Creek, CA, U.S.A.) Model 8500 solvent delivery system, a Valco (Houston, TX, U.S.A.) Model CV-6-UHPa-N60 7000 p.s.i.g. injection valve fitted with a 10-μl injection loop, a laboratory Data Control (Riviera Beach, FL, U.S.A.) RefractoMonitor Model 1107 and 0.177 mm I.D. stainless-steel tubing. A DuPont (Wilmington, DE, U.S.A.) 25 cm × 4.6 mm I.D. Zorbax-NH_2 column was used to analyze selected saccharides. A 25 cm × 4.6 mm I.D. reversed-phase column was prepared with Partisil 10 (Whatman, Clifton, NJ, U.S.A.) and dichloromethyloctadecylsilane (Petrarch Systems, Bristol, PA, U.S.A.) according to the procedure of Evans *et al.*[31] and upward slurry packed with methanol at 8000 p.s.i.g. The average efficiency for the reversed-phase column was calculated from the mean values of multiple injections of mixtures of benzene, naphthalene and biphenyl with an acetonitrile–water (70:30) mobile phase at 1.0 ml/min using a Varian Vari-Chrom UV VIS detector Model VUV-10 with an 8-μl flow cell at 254 nm. The column efficiency initially was 3300 and fell to 2517 after eight months of continual use. The average efficiency for the additive system was 650 as calculated from the mean values of multiple injections of mixtures of D-(+)-ribose, fructose and sorbitol with an acetonitrile–water (89:11) mobile phase with 0.150 g of *n*-tetradecylamine adsorbed at 1.0 ml/min using the refractive index detector.

Materials

The *n*-alkyl amines were obtained from Aldrich (Milwaukee, WI, U.S.A.) and were recrystallized twice from water prior to use. The saccharides were also purchased from Aldrich and used without further purification. Acetonitrile and water were Omnisolv-HPLC grade from MCB (Cincinnati, OH, U.S.A.).

Chromatographic measurements

Mobile phases with the *n*-alkyl amine additives were prepared by dissolving the appropriate amount of additive in acetonitrile and diluting with water. All mobile

phases were filtered and degassed before use. The columns were equilibrated by pumping the mobile phase until constant $\Delta k'$ values were obtained for glucose and fructose. All chromatographic measurements were taken at 25°C and at a flow-rate of 1.0 ml/min.

RESULTS AND DISCUSSION

Table I summarizes the capacity factors (k') of selected mono- and disaccharides on a Zorbax-NH_2 column. The elution order for these saccharides is identical to that found in previous studies with amine bonded phases[8–11]. The observed normal-phase behavior agrees with the proposed retention mechanism of a competitive interaction between water and the saccharides[32–34]. The limitation of primary amine columns is their reactivity with reducing saccharides to form Schiff bases[35] which limits the use of amine columns for common mono- and disccharides such as ribose, arabinose, xylose, mannose, galactose, glucose, fructose and sorbitol[36]. Since secondary amines are less reactive toward reducing saccharides[37], columns incorporating secondary amines (such as Partisil-10-PAC) are recommended when separating reducing saccharides. In this study, *n*-dodecylamine and *n*-tetradecylamine were used as mobile-phase additives since *n*-alkyl amines with less than ten carbons did not retain saccharides even at high concentrations and the low solubility of *n*-hexadecylamine in acetonitrile–water mixtures prevented its use. All these amines could be removed from the column after use, allowing reproducible capacity factors to be maintained.

Table II shows the changes in saccharide capacity ($\Delta k'$) using the dodecylamine additive under various mobile-phase conditions. For mobile-phase compositions greater than or equal to 90% acetonitrile, the retention order is identical to that on the Zorbax-NH_2 column at lower acetonitrile concentrations. As the percentage of acetonitrile increases, the solubility of the saccharides decreases and the reactivity of the reducing sugars with the amines increases.

Table III shows the changes in saccharide capacity ($\Delta k'$) when using the tetradecylamine additive under various mobile-phase conditions. The elution order for

TABLE I

SACCHARIDE CAPACITY FACTORS (k') ON AN AMINE COLUMN*

Saccharide	*Acetonitrile (%)*			
	65	*70*	*75*	*80*
D-(+)-Xylose	0.90	1.24	1.74	2.38
Fructose	1.14	1.67	2.41	3.44
D-Glucose	1.20	1.86	2.63	4.16
Sorbitol	1.29	2.01	2.94	4.60
D-(+)-Galactose	1.33	2.03	2.99	4.74
Sucrose	1.50	2.46	3.94	7.09
D-(+)-Maltose	1.68	2.87	4.66	8.69
Inositol	1.89	3.14	4.87	9.28
Lactose	1.95	3.22	5.59	11.70

* Capacity factors obtained on a Zorbax-NH_2 column at 1.0 ml/min.

TABLE II

n-DODECYLAMINE ADDITIVE DATA

Acetonitrile (%)	*Concn. (10^3 M)*	q_{ads} *(g)*	$\Delta k'$				
			Fructose	D-*Glucose*	D-*Galactose*	*Sucrose*	*Maltose*
80	11.8	0.243	0.20	0.19	0.20	0.00	0.05
85	6.78	0.165	0.38	0.44	0.42	0.30	0.32
90	14.8	0.211	0.97	1.04	1.10	1.15	1.58
90	17.3	0.229	1.02	1.26	1.42	1.54	1.93
95	6.28	0.118	1.21	1.47	1.80	1.80	n.s.*
95	15.1	0.185	1.81	2.43	9.97	2.78	n.s.*

* n.s. = Not seen.

the reversed-phase column modified with tetradecylamine is identical to the Zorbax-NH_2 results except for sorbitol and D-galactose. A plot of $\Delta k'$ *vs.* the amount of adsorbed modifier (q_{ads}) for *n*-tetradecylamine additive at 89:11 acetonitrile–water displays a linear relationship between $\Delta k'$ and q_{ads}. When the acetonitrile–water concentrations are varied, $\Delta k'$ is not proportional to q_{ads} nor to the amine concentration in solution. A linear relationship is found with q_{ads} only when identical acetonitrile–water conditions are used. Once the system reached equilibrium, the capacity factors for these saccharides remained unchanged over several days of continual use. This stability allows changes in the acetonitrile–water percentages to enhance a particular saccharide separation with only minimal equilibration times. Fig. 1 shows a typical saccharide separation with $2.10 \cdot 10^{-3}$ *M* *n*-tetradecylamine in acetonitrile–water (89:11) (q_{ads} = 0.150 g) in this reversed-phase system.

The reproducibility of the *n*-alkyl amine additive system was investigated using a $2.24 \cdot 10^{-3}$ *M* solution of *n*-tetradecylamine in 90:10 acetonitrile–water. After the system reached equilibrium (q_{ads} = 0.165 g), three injections of each saccharide were made. The column was then washed with 1 l of methanol to remove the amine modifier. The system was re-equilibrated with the same *n*-tetradecylamine solution (q_{ads} = 0.165 g), and three injections of each saccharide were made. Table IV lists the results which demonstrate that this approach to saccharide separations is reproducible within the margin of experimental error even though the capacity factors increased slightly between the two trials.

The primary distinction between the results obtained with the amino column and the amine additive is the acetonitrile–water concentration required for adequate retention and resolution of saccharides. The results in Fig. 1 show that an acetonitrile–water (90:10) (with q_{ads} = 0.165 g) mobile phase was required to obtain capacities similar to those obtained on the Zorbax-NH_2 column an acetonitrile–water (70:30) mobile phase. Although some differences in capacity (comparing $\Delta k'$ and k') could be the result of amine concentration, the major difference in mobile-phase conditions resulted from the increased hydrophobicity in the additive system. The hydrocarboneous character of the reversed-phase material as well as the added reversed-phase character of the *n*-alkyl amine chains decreased saccharide capacity requiring the use of weaker solvent conditions. This difference could not be the result

TABLE III

n-TETRADECYLAMINE ADDITIVE DATA

Acetonitrile (%)	*Concn. (10^3 M)*	q_{ads} *(g)*	$\Delta k'$																	
			D-(+)-*Xylose*	D-(−)-*Ribose*	L-(−)-*Fucose*	L-(+)-*Arabinose*	*Fructose*	D-(+)-*Mannose*	D-*Glucose*	D-(+)-*Galactose*	*Sorbitol*	*Dulcitol*	*Sucrose*	D-(+)-*Maltose*	D-*Cellobiose*	*Inositol*	*Lactose*	*Maltotriose*	α-D-*Melibiose*	D-*Raffinose*
80	2.24	0.167	0.406	0.472	0.506	0.541	0.497	0.453	0.444	0.493	0.565	0.565	0.328	0.387	0.384	0.722	0.384	0.412	0.522	0.437
83	2.25	0.166	0.412	0.467	0.589	0.641	0.613	0.585	0.610	0.689	0.763	0.799	0.570	0.677	0.668	1.17	0.872	0.802	0.982	0.891
87	2.24	0.165	0.538	0.557	0.798	0.889	0.881	0.900	0.987	1.09	1.20	1.27	1.07	1.33	1.34	2.13	1.78	1.87	2.19	2.14
89	2.21	0.165	0.886	0.873	1.28	1.41	1.61	1.76	1.83	2.19	2.48	2.57	2.70	3.39	3.53	4.56	4.69	6.52	6.45	8.05
89	0.480	0.0152	–	–	–	–	1.08	–	1.31	1.51	–	–	1.90	2.61	–	–	–	–	–	–
89	1.40	0.136	–	–	–	–	1.47	–	1.81	2.04	–	–	2.25	2.99	–	–	–	–	–	–
89	15.6	0.351	–	–	–	–	1.80	–	2.49	2.85	–	–	3.21	3.47	–	–	–	–	–	–
90	2.23	0.165	0.965	–	–	–	1.78	–	2.10	2.37	2.82	–	3.48	4.11	–	5.59	5.86	–	–	–
93	2.25	0.162	1.55	1.38	2.13	2.37	3.03	–	3.81	–	–	–	–	–	–	–	–	–	–	–

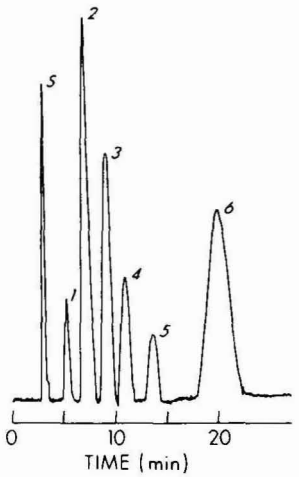

Fig. 1. Separation of saccharides on an octadecyl column with the *n*-tetradecylamine additive (q_{ads} = 0.150 g); mobile phase, acetonitrile–water (89:11); flow-rate, 1.0 ml/min. Peaks: S = water; 1 = D-(+)-xylose; 2 = fructose; 3 = sorbitol; 4 = D-(+)-maltose; 5 = lactose; 6 = D-raffinose.

of a difference in basicity between the *n*-propylamine on the bonded phase and the *n*-tetradecylamine modifier since their pK_a values are nearly equivalent (see Table V).

Another factor influencing this capacity loss in the additive system could be the result of an increase in the effective pore size. Due to the length of both the bound and adsorbed aliphatic chains, the additive system may result in the amine functionality being further from the pore surface than for the amino bonded phase which effectively increased the average pore size. This increase may limit the effectiveness of the amine to buffer the pore environment (because the amine chains are more accessible to solvent) and thus reduce the strength of interaction between the solute and the adsorbed molecule.

TABLE IV

SYSTEM REPRODUCIBILITY TEST*

Solute	*Δk'*			
	Trial 1	*Trial 2*	*Average*	*Increase (%)***
D-(+)-Xylose	0.929 (±0.006)	1.00 (±0.3)	0.97 (±0.5)	+7.9
Fructose	1.76 (±0.4)	1.80 (±0.04)	1.78 (±0.2)	+2.2
D-Glucose	2.03 (±0.1)	2.16 (±0.3)	2.10 (±0.8)	+6.4
D-(+)-Galactose	2.26 (±0.4)	2.47 (±0.1)	2.37 (±1.0)	+9.0
Sorbitol	2.70 (±0.4)	2.93 (±0.1)	2.82 (±1.5)	+8.5
Sucrose	3.32 (±1.9)	3.63 (±0.1)	3.48 (±1.9)	+9.1
D-Maltose	4.04 (±0.6)	4.18 (±1.1)	4.11 (±0.9)	+3.5
Inositol	5.54 (±1.6)	5.63 (±1.1)	5.59 (±0.5)	+1.5
Lactose	5.76 (±0.9)	5.95 (±0.9)	5.86 (±0.7)	+3.2

* For each solute, three injections were made. The variance in the parenthesis was computed at 95% confidence limits.

** The percentage increase is computed as $\frac{(\text{trial 2} - \text{trial 1})}{\text{trial 1}} \times 100$.

TABLE V

pK_a VALUES OF *n*-ALKYL AMINES

Carbon No.	*Name*	pK_a	*Ref.*
1	Methylamine	10.62	38
2	Ethylamine	10.63	38
3	Propylamine	10.53	38
4	Butylamine	10.59	38
5	Pentylamine	10.63	39
6	Hexylamine	10.56	39
7	Heptylamine	10.66	39
8	Octylamine	10.65	39
8	Octylamine	10.65	40
9	Nonylamine	10.64	39
14	Tetradecylamine	10.62	39
16	Hexadecylamine	10.61	40

ACKNOWLEDGEMENT

This work was supported, in part, by the National Science Foundation under grant CHE-8119600 (to C.H.L.).

REFERENCES

1 P. Jandera and J. Churáček, *J. Chromatogr.*, 98 (1974) 55.
2 M. D'Amboise, D. Noel and T. Hanai, *J. Liquid Chromatogr.*, 2 (1979) 1325.
3 C. C. Sweeley, R. Bentley, M. Makita and W. W. Wells, *J. Amer. Chem. Soc.*, 85 (1968) 2497.
4 P. J. Wood and I. R. Siddiqui, *Carbohydr. Res.*, 19 (1971) 283.
5 C. J. W. Brooks and I. Maclean, *J. Chromatogr. Sci.* 9 (1971) 18.
6 F. Eisenberg, Jr., *Carbohydr. Res.*, 19 (1971) 135.
7 C. F. Poole, S. Singhawangcha and A. Zlatkis, *J. Chromatogr.*, 158 (1978) 33.
8 J. C. Linden and C. L. Lawhead, *J. Chromatogr.*, 105 (1975) 125.
9 R. Schwarzenbach, *J. Chromatogr.*, 117 (1976) 206.
10 K. Kainuma, T. Nakakuki and T. Ogawa, *J. Chromatogr.*, 212 (1981) 126.
11 M. T. Yang, L. P. Milligan and G. W. Mathison, *J. Chromatogr., 209* (1981) 316.
12 K. Aitzetmüller, *J. Chromatogr.*, 156 (1978) 354.
13 K. Aitzetmüller, M. Bohrs and E. Arzberger, *J. High Resolut. Chromatogr. Chromatogr. Commun.*, 2 (1979) 589.
14 K. Aitzetmüller, *Chromatographia*, 13 (1980) 432.
15 B. B. Wheals and P. C. White, *J. Chromatogr.*, 176 (1979) 421.
16 L. A. Th. Verhaar and B. F. M. Kuster, *J. Chromatogr.*, 210 (1981) 279.
17 M. Sinner and J. Puls, *J. Chromatogr.*, 156 (1978) 197.
18 S. Honda, Y. Matsuda, M. Takahashi, K. Kakehi and S. Ganno, *Anal. Chem.*, 52 (1980) 1079.
19 S. Honda, K. Kakimoto, K. Kakehi and K. Takiura, *Anal. Chim. Acta*, 64 (1973) 310.
20 K. Mopper, R. Dawson, G. Liebezeit and H. P. Hansen, *Anal. Chem.*, 52 (1980) 2018.
21 F. Nachtmann, H. Spitzy and R. W. Frei, *Anal. Chem.*, 48 (1976) 1576.
22 J. Lehrfeld, *J. Chromatogr.*, 120 (1976) 141.
23 C. F. Poole, S. Singhawangcha, A. Zlatkis and E. D. Morgan, *J. High Resolut. Chromatogr. Chromatogr. Comm.*, 1 (1978) 96.
24 N. W. H. Cheetham, P. Sirimanne and W. R. Day, *J. Chromatogr.*, 207 (1981) 439.
25 F. P. B. van der Maeden, M. E. F. Biemond and P. C. G. M. Janssen, *J. Chromatogr.*, 149 (1978) 539.
26 Y. Tapuhi, N. Miller and B. L. Karger, *J. Chromatogr.*, 205 (1981) 325.

27 C. Gilon, R. Leshan and E. Grushka, *Anal. Chem.*, 52 (1980) 1206.
28 V. A. Davankov, A. S. Bochkov, A. A. Kurganov, P. Roumeliotis and K. K. Unger, *Chromatographia*, 13 (1980) 677.
29 C. H. Lochmüller and E. C. Jensen, *J. Chromatogr.*, 216 (1981) 333.
30 C. H. Lochmüller and H. H. Hangac, *J. Chromatogr. Sci.*, 20 (1982) 171.
31 M. B. Evans, A. D. Dale and C. J. Little, *Chromatographia*, 13 (1980) 5.
32 R. E. Majors, *J. Chromatogr. Sci.*, 18 (1980) 488.
33 F. M. Rabel, A. G. Caputo and E. T. Butts, *J. Chromatogr.*, 126 (1976) 731.
34 J. Hettinger and R. E. Majors, *Varian Instruments Appl.*, 10 (1976) 6.
35 G. P. Ellis and J. Honeyman, *Advan. Carbohydr. Chem.*, 10 (1955) 95.
36 S. R. Abbott, *J. Chromatogr. Sci.*, 18 (1980) 540.
37 J. K. Haken and D. K. M. Ho, *J. Chromatogr.*, 112 (1975) 135.
38 J. Hall, *J. Amer. Chem. Soc.*, 79 (1957) 5441.
39 D. D. Perrin, *Dissociation Constants of Organic Bases in Aqueous Solutions*, Butterworths, London, 1965.
40 A. Albert, *Ionization Constants of Acids and Bases*, Methuen, London, 1962.

Journal of Chromatography, 264 (1983) 223–229
Elsevier Science Publishers B.V., Amsterdam — Printed in the Netherlands

CHROM. 15,833

COMPARISON OF REVERSED-PHASE AND WEAK ANION-EXCHANGE HIGH-PERFORMANCE LIQUID CHROMATOGRAPHIC METHODS FOR PEPTIDE SEPARATIONS

MIRAL DIZDAROGLU*
Department of Chemistry, University of Maryland Baltimore County, Catonsville, MD 21228 (U.S.A.)
and
HENRY C. KRUTZSCH
Laboratory of Carcinogen Metabolism, National Cancer Institute, National Institutes of Health, Bethesda, MD 20205 (U.S.A.)

(Received March 7th, 1983)

SUMMARY

Weak anion-exchange and reversed-phase high-performance liquid chromatographic methods for peptide separations were compared using a tryptic digest of "rat small myelin basic protein". In these experiments, a number of tryptic peptides that were not resolved on the reversed-phase column could be separated on the weak anion-exchange column, and in other instances, as might be expected, reversed-phase chromatography provided better resolution of certain peptides than did the weak anion-exchange method. The results obtained strongly suggest that the combined use of these two methods of separation, which utilize different selectivities, can provide an excellent improvement in resolving power for a number of peptide separations.

INTRODUCTION

During the past decade, high-performance liquid chromatography (HPLC) has emerged as a powerful tool for peptide separations. The reversed-phase mode of HPLC (RP-HPLC) has become the most popular and broadly used technique for many separation problems in peptide chemistry[1–13]. Ion-exchange HPLC has also been employed for peptide separations, although to a lesser extent[14–18].

We recently reported a method for peptide separations using anion-exchange HPLC (AE-HPLC) on a weak AE bonded phase with mixtures of acetonitrile and triethylammonium acetate (TEAA) buffer as the eluent[19–23]. In the present work, we compare this method and a standard RP-HPLC method for peptide separations using a tryptic digest of "rat small myelin basic protein" (RSMBP) isolated from rat brain.

0021-9673/83/$03.00

EXPERIMENTAL

Apparatus

A Model 1084B liquid chromatograph (Hewlett-Packard, Avondale, PA, U.S.A.) equipped with a microprocessor, an automatic injector and a variable-wavelength detector was used. AE separations were carried out on a 30 × 0.4 cm MicroPak AX-10 column (Varian, Walnut Creek, CA, U.S.A.). A 15 × 0.46 cm Supelcosil LC-8-DB column (Supelco, Bellefonte, PA, U.S.A.) was used for RP separations. Specific conditions for all separations are given in the Figures.

Materials

RSMBP was a gift of Gladys Diebler and Marion Kies of the National Institutes of Health. Triethylamine was purchased from Eastman-Kodak (Rochester, NY, U.S.A.) and purified by distillation from phthalic anhydride. TEAA buffer solutions were prepared by titrating 0.01 *M* acetic acid solutions with triethylamine to pH 6.0. Glass-distilled acetonitrile was purchased from Burdick & Jackson Labs. (Muskegon, MI, U.S.A.). Trifluoroacetic acid (TFA) was obtained from Sigma (St. Louis, MO, U.S.A.). Water purified through a Millipore system (Millipore, Bedford, MA, U.S.A.) was used for all purposes. Aqueous solvents were filtered prior to use. Trypsin was purchased from Worthington Biochemicals (Freehold, NJ, U.S.A.).

Tryptic digestion

Two milligrams of RSMBP were incubated at 37°C for 24 h in 1 ml of 0.1 *M* ammonium bicarbonate buffer (pH 8.2) with a peptide–enzyme ratio of 50:1 (w/w). After incubation, the sample was freeze-dried and then taken up in 0.5 ml of water for injections.

Amino acid analysis

Eluted peptides were dried *in vacuo* and hydrolyzed with constant-boiling HCl in evacuated and sealed tubes at 110°C for 24 h. The hydrolyzates were analyzed on a Durrum D-500 amino acid analyzer.

RESULTS AND DISCUSSION

RSMBP contains 127 amino acid residues[24] and is expected to yield twenty-one peptide fragments and two arginine molecules upon digestion with trypsin. The tryptic digest of this protein was analyzed by weak AE-HPLC as previously described[19–23] and by RP-HPLC using a solvent system containing 0.1% TFA in water and acetonitrile[12]. For peak assignments, in both systems, eluted peptides were collected and then subjected to amino acid analysis, and structural assignments were made by referring to tryptic peptides expected from the known sequence of RSMBP.

Fig. 1 shows the separation of the tryptic digest of RSMBP by weak AE-HPLC, where a resolution of sixteen peaks was observed. Amino acid sequences of the corresponding peptides and their positions in the total sequence are given in Table I. Peaks 7, 9, 11 and 13 each contain two peptides, which were not resolved from each other, whereas peaks 2–6, 8, 10, 12 and 14–16 correspond to single peptides. Peak 1 contains the two expected dipeptides and two free arginine molecules. Inspection of Table I shows that the identified peptides cover the total sequence of RSMBP.

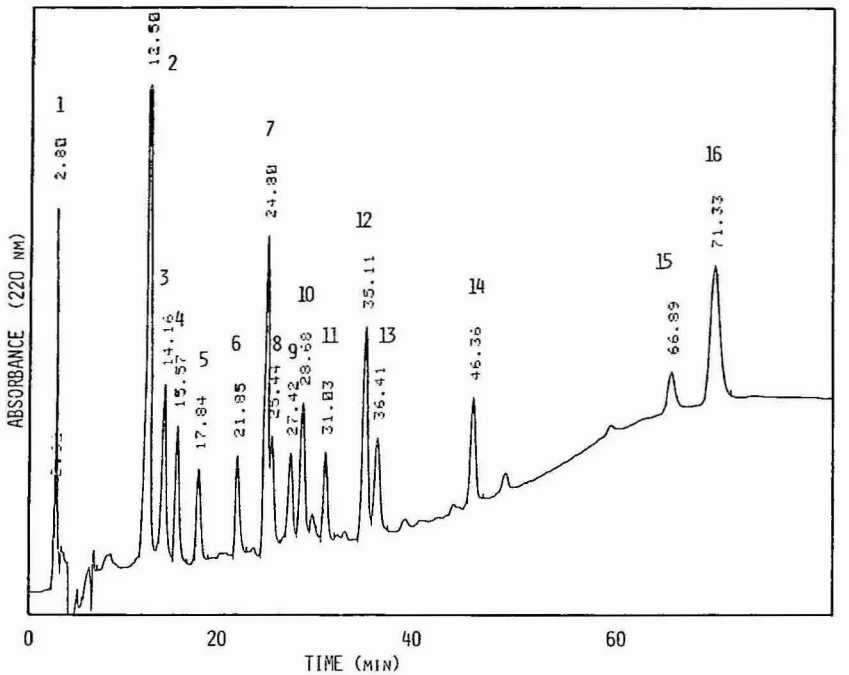

Fig. 1. Separation of a tryptic digest of RSMBP by weak AE-HPLC. Column: MicroPak AX-10 (10 μm), 30 × 0.4 cm. Temperature: 40°C. Eluents: A, acetonitrile; B, 0.01 *M* TEAA buffer (pH 6.0). Gradient program: linear starting from 23% B with a rate of 0.7% B/min for 40 min then 1% B/min to 100% B. Flow-rate: 1 ml/min. Peak identification and sequences are given in Table I. a.u.f.s. = 0.2 at 220 nm.

TABLE I

PEAK IDENTIFICATION AND SEQUENCES IN FIG. 1

Peak	*Sequence*	*Position in sequence*
1	His-Arg	32–33
	Gly-Arg	103–104
	2 Arg	54, 127
2	Phe-Ser-Trp-Gly-Gly-Arg	111–116
3	His-Gly-Phe-Leu-Pro-Arg	26–31
4	Asn-Ile-Val-Thr-Pro-Arg	89–94
5	Gly-Leu-Ser-Leu-Ser-Arg	105–110
6	Ser-Gly-Ser-Pro-Met-Ala-Arg	120–126
7	Arg-Pro-Ser-Gln-Arg	5–9
	Thr-Thr-His-Tyr-Gly-Ser-Leu-Pro-Gln-Lys	64–73
8	Ser-Gln-Arg	74–76
9	Ac-Ala-Ser-Gln-Lys	1–4
	Gly-Ala-Pro-Lys	50–53
10	Thr-Pro-Pro-Pro-Ser-Gln-Gly-Lys	95–102
11	His-Gly-Ser-Lys	10–13
	Gly-Ser-Gly-Lys	55–58
12	Tyr-Leu-Ala-Thr-Ala-Ser-Thr-Met-Asp-His-Ala-Arg	14–25
13	Phe-Phe-Ser-Gly-Asp-Arg	44–49
	Asp-Ser-Arg	117–119
14	Asp-Ser-His-Thr-Arg	59–63
15	Asp-Thr-Gly-Ile-Leu-Asp-Ser-Ile-Gly-Arg	34–43
16	Thr-Gln-Asp-Glu-Asn-Pro-Val-Val-His-Phe-Phe-Lys	77–88

Fig. 2 shows the separation by RP-HPLC of another aliquot of the same sample. An accumulation of several peaks near the void volume (designated as 1) and resolution of twelve peaks were observed. The amino acid sequences of the peptides and their positions in the total sequence are given in Table II. By deduction from the known sequence of RSMBP[24], the number of peptides accumulated near the void volume should total nine, including the two dipeptides, because peaks 2–13 contain the remaining twelve tryptic peptides contained in RSMBP (compare Tables I and II).

Comparison of the results obtained by the two methods applied here shows that all of the tryptic peptides, except for the two dipeptides, were strongly retained on the weak AE column, whereas some additional peptides had little or no retention on the RP column and were eluted without being resolved from one another. As a demonstration of the different selectivities of these two separation principles, peptides eluting near the void volume of the RP column (designated as peak 1 in Fig. 2) were collected and, after removal of the volatile solvent, injected onto the weak AE column. Six peaks were resolved (Fig. 3), and the amino acid sequences of the peptides contained in them are given in Table III. Peak I corresponds to the two dipeptides and two free arginine molecules. Peaks 3 and 4 each represent two peptides, which were not separated from each other, whereas peaks 2, 5 and 6 correspond to single peptides. This means that these peptides, except for the two dipeptides, were strongly retained on the weak AE column in contrast to the RP column, and three of them

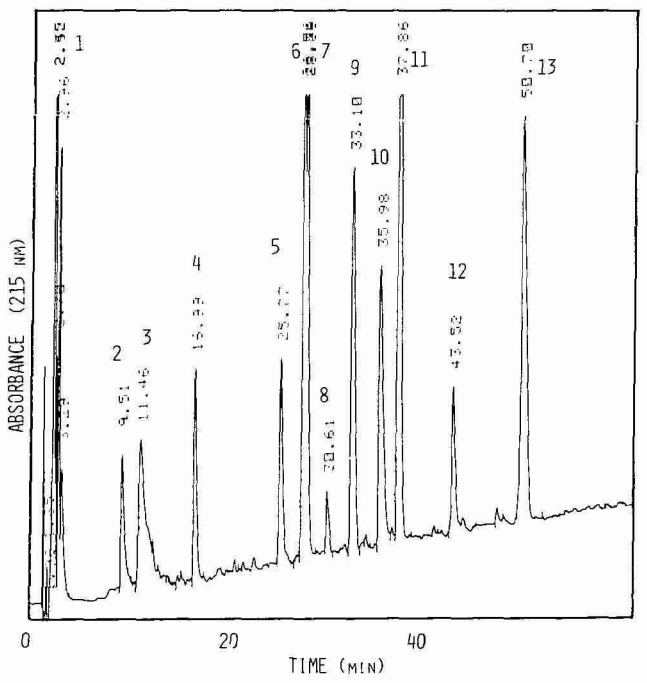

Fig. 2. Separation of a tryptic digest of RSMBP by RP-HPLC. Column: Supelcosil LC-8-DB (5 μm), 15 × 0.46 cm. Temperature: 30 °C. Eluents: A, 0.1% TFA in water; B, 0.1% TFA in acetonitrile. Gradient program: linear starting from 0% B with a rate of 0.5% B/min. Flow-rate: 1.2 ml/min. Peak identification and sequences are given in Table II. a.u.f.s. = 0.4 at 215 nm.

TABLE II

PEAK IDENTIFICATION AND SEQUENCES IN FIG. 2

Peak	*Sequence*	*Position in sequence*
1	Ac-Ala-Ser-Gly-Lys	1–4
	His-Gly-Ser-Lys	10–13
	His-Arg	32–33
	Gly-Ala-Pro-Lys	50–53
	2 Arg	54, 127
	Gly-Ser-Gly-Lys	55–58
	Asp-Ser-His-Thr-Arg	59–63
	Ser-Gln-Arg	74–76
	Gly-Arg	103–104
	Asp-Ser-Arg	117–119
2	Arg-Pro-Ser-Gln-Arg	5–9
3	Thr-Pro-Pro-Pro-Ser-Gln-Gly-Lys	95–102
4	Ser-Gly-Ser-Pro-Met-Ala-Arg	120–126
5	Asn-Ile-Val-Thr-Pro-Arg	89–94
6	Thr-Thr-His-Tyr-Gly-Ser-Leu-Pro-Gln-Lys	64–73
7	Phe-Phe-Ser-Gly-Asp-Arg	44–49
8	Gly-Leu-Ser-Leu-Ser-Arg	105–110
9	Tyr-Leu-Ala-Thr-Ala-Ser-Thr-Met-Asp-His-Ala-Arg	14–25
10	His-Gly-Phe-Leu-Pro-Arg	26–31
11	Phe-Ser-Trp-Gly-Gly-Arg	111–116
12	Asp-Thr-Gly-Ile-Leu-Asp-Ser-Ile-Gly-Arg	34–43
13	Thr-Gln-Asp-Glu-Asn-Pro-Val-Val-His-Phe-Phe-Lys	77–88

could be obtained in pure form. Another instance of the advantage of weak AE-HPLC over RP-HPLC in this particular application was the separation of two peptides by weak AE-HPLC (peaks 7 and 13 in Fig. 1) that were only slightly resolved on the RP column (peaks 6 and 7 in Fig. 2 and Table II). To illustrate this more clearly, the peptides from the RP column were collected and, after removal of the volatile solvent, injected onto the weak AE column. Fig. 4 shows their complete separation by weak AE-HPLC, and peaks 1 and 2 correspond, respectively, to the peptides represented by peaks 6 and 7 in Fig. 2. These two examples are also excellent demonstrations of the combined use of RP- and weak AE-HPLC methods for isolation of peptides, which were not resolved on the RP column (peaks 6 and 7 in Fig. 2).

In another instance of the combined use of the two methods, RP-HPLC could be used as a second separation step for four peptides which eluted as two pairs on the weak AE column (peaks 7 and 13 in Fig. 1 and Table I). As Fig. 2 shows, these two pairs were completely separated from each other on the RP column (peaks 2 and 6, and 1 and 7). However, in this case, the peptide of residues 117–119 was coeluted with other peptides in peak 1 and the peptides represented by peaks 6 and 7 were also coeluted (Fig. 2 and Table II); RP-HPLC would also function as a second separation step in this instance. Only the peptide of residues 5–9 could be obtained in pure form (peak 2 in Fig. 2) when the whole tryptic digest was injected onto the RP column. The peptide of residues 117–119 could also be isolated in pure form by first applying RP-HPLC to the tryptic mixture and then weak AE-HPLC (peak 5 in Fig. 3). Two pairs of peptides containing residues 1–4 and 50–53 (peak 9 in Fig. 1 and peak 1 in Fig. 2),

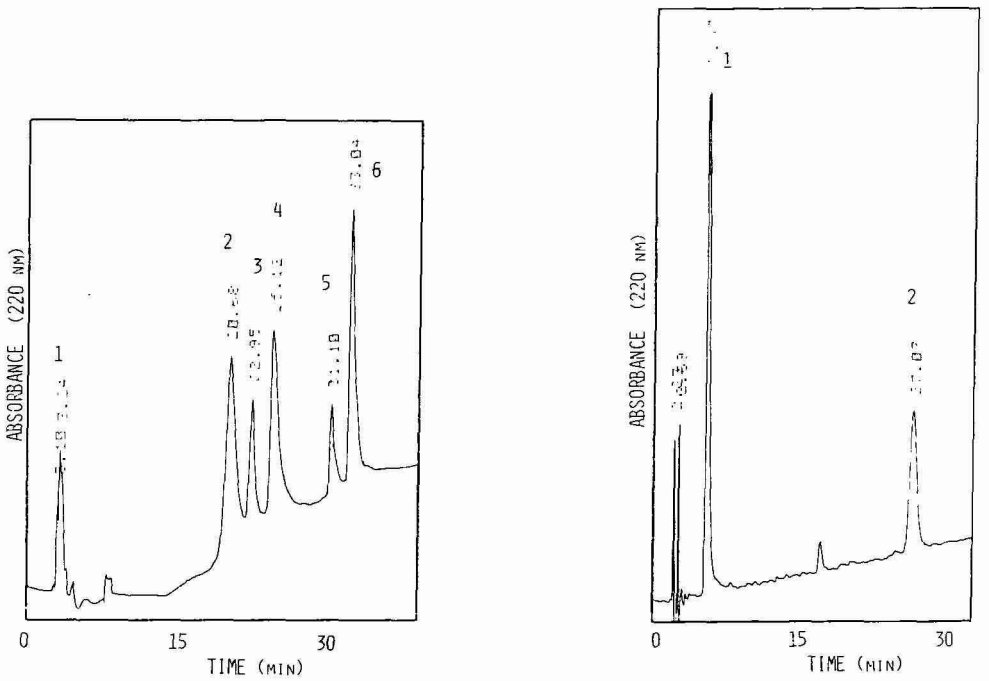

Fig. 3. Separation of peptides eluted from RP column (designated as I in Fig. 2) by weak AE-HPLC. Column details as in Fig. 1 except for temperature (50°C) and gradient program: isocratic with 26% B for 10 min then 1.5% B/min. Peak identification and sequences are given in Table III.

Fig. 4. Separation of peptides eluted from RP column (peaks 6 and 7 in Fig. 2) by weak AE-HPLC. Column details as in Fig. 1 except for gradient program: starting from 45% B with a rate of 0.5% B/min. Peaks 1 and 2 correspond to peaks 6 and 7 in Fig. 2, respectively. a.u.f.s. = 0.1 at 220 nm.

TABLE III

PEAK IDENTIFICATION AND SEQUENCES IN FIG. 3

Peak	*Sequence*	*Position in sequence*
1	His-Arg	32–33
	Gly-Arg	103–104
	2 Arg	54, 127
2	Ser-Gln-Arg	74–76
3	Ac-Ala-Ser-Gln-Lys	1–4
	Gly-Ala-Pro-Lys	50–53
4	His-Gly-Ser-Lys	10–13
	Gly-Ser-Gly-Lys	55–58
5	Asp-Ser-Arg	117–119
6	Asp-Ser-His-Thr-Arg	59–63

and 10–13 and 55–58 (peak 11 in Fig. 1 and peak 1 in Fig. 2), were the only pairs that could not be obtained in pure form by the combined use of RP-HPLC and weak AE-HPLC.

CONCLUSIONS

The results obtained clearly demonstrate the usefulness of the different selectivities of RP- and weak AE-HPLC methods for peptide separations. It is also apparent that the combined application of these two different separation principles can provide even more resolving power and thus yield a higher probability for the complete separation of a given mixture of peptides into its components.

ACKNOWLEDGEMENTS

We appreciate the gift of RSMBP from Mrs. Gladys Diebler and Dr. Marion Kies of National Institutes of Health.

REFERENCES

1 K. Krummen and R. W. Frei, *J. Chromatogr.*, 132 (1977) 27.
2 J. J. Hansen, T. Greibrokk, B. L. Currie, K. N.-G. Johansson and K. Folkers, *J. Chromatogr.*, 135 (1977) 155.
3 E. J. Kikta, Jr. and E. Grushka, *J. Chromatogr.*, 135 (1977) 367.
4 I. Molnár and Cs. Horváth, *J. Chromatogr.*, 142 (1977) 623.
5 H. P. J. Bennett, A. M. Hudson, C. McMartin and G. E. Purdon, *Biochem. J.*, 168 (1977) 9.
6 J. E. Rivier, *J. Liquid Chromatogr.*, 1 (1978) 343.
7 J. A. Feldman, M. L. Cohn and D. Blair, *J. Liquid Chromatogr.*, 174 (1979) 833.
8 W. S. Hancock, C. A. Bishop, R. L. Prestidge, D. R. K. Harding and M. T. W. Hearn, *J. Chromatogr.*, 153 (1978) 391.
9 M. T. W. Hearn and W. S. Hancock, *Trends Biochem. Sci.*, 4 (1979) N58.
10 M. J. O'Hare and E. C. Nice, *J. Chromatogr.*, 171 (1979) 209.
11 W. A. Schroeder, J. B. Shelton, J. R. Shelton and D. Powars, *J. Chromatogr.*, 174 (1979) 385.
12 W. C. Mahony and M. A. Hermodson, *J. Biol. Chem.*, 255 (1980) 11199.
13 M. Schöneshöfer and A. Fenner, *J. Chromatogr.*, 224 (1981) 472.
14 A. N. Radhakrishnan, S. Stein, A. Licht, K. A. Gruber and S. Udenfriend, *J. Chromatogr.*, 132 (1977) 552.
15 J. A. Smith and R. A. McWilliams, *Amer. Lab.*, 12 (1980) 25.
16 N. Takahashi, T. Isobe, H. Kasai, K. Seta and T. Okuyama, *Anal. Biochem.*, 115 (1981) 181.
17 T. Isobe, N. Isioko and T. Okuyama, *Biochem. Biophys. Res. Commun.*, 102 (1981) 279.
18 T. Isobe, T. Takayasu, N. Takai and T. Okuyama, *Anal. Biochem.*, 122 (1982) 417.
19 M. Dizdaroglu and M. G. Simic, *J. Chromatogr.*, 195 (1980) 119.
20 M. Dizdaroglu, H. C. Krutzsch and M. G. Simic, *J. Chromatogr.*, 237 (1982) 417.
21 M. Dizdaroglu, H. C. Krutzsch and M. G. Simic, *Anal. Biochem.*, 123 (1982) 190.
22 M. Dizdaroglu, M. G. Simic, F. Rioux and S. St.-Pierre, *J. Chromatogr.*, 245 (1982) 158.
23 M. Dizdaroglu, in W. S. Hancock (Editor), *Handbook of the Use of HPLC for the Separation of Amino Acids, Peptides and Proteins*, CRC Press, Boca Raton, FL, 1983, in press.
24 P. R. Dunkley and P. R. Carnegie, *Biochem. J.*, 141 (1974) 243.

Journal of Chromatography, 264 (1983) 231–239
Elsevier Science Publishers B.V., Amsterdam — Printed in the Netherlands

CHROM. 15,827

QUANTITATION OF 1-NITROPYRENE IN DIESEL EXHAUST PARTICULATES BY CAPILLARY GAS CHROMATOGRAPHY–MASS SPECTROMETRY AND CAPILLARY GAS CHROMATOGRAPHY

H. Y. TONG, J. A. SWEETMAN and F. W. KARASEK*
Department of Chemistry, University of Waterloo, Waterloo, Ontario N2L 3G1 (Canada)
(Received March 3rd, 1983)

SUMMARY

Obtaining accurate quantitation of 1-nitropyrene in a complex mixture is difficult because of variable decomposition occurring in the analytical system at the low 10–100 ng quantities involved. The procedure described here involves pre-separation of the extract by high-performance liquid chromatography and analysis by both capillary gas chromatography and capillary gas chromatography–mass spectrometry. A modified cool on-column injection technique and bonded phase fused silica capillary columns were used to minimize the decomposition and improve the precision for the quantitative analysis. The method is demonstrated using four different diesel particulate extracts containing 1-nitropyrene in the 10–100 ng/μl range.

INTRODUCTION

Nitroaromatics have been found in some environmental samples such as airborne and diesel exhaust particulate matter[1–4]. Those identified nitroaromatics include nitronaphthalene, nitroanthracene or nitrophenanthracene, nitromethylanthracene or phenanthrene, 6-nitrobenzo[*a*]pyrene, 9-nitroanthrancene, 3-nitrofluoranthene and 1-nitropyrene. The identification and quantitation of those compounds have recently received increasing attention because some of them are believed to be direct-acting mutagens (Ames *Salmonella typhimurium* assay without activation, TA98-S). Several investigators have indicated that a small amount of 1-nitropyrene (1-NP) accounts for about 30% of direct-acting mutagenicity of total extract of the diesel particulate matter[1] and accounts for about 20% of the direct-acting mutagenicity exhibited by the total dichloromethane extract of diesel exhaust particulates[5]. Chemical quantitation of 1-NP and other nitroarmatics has been required in order to assess their behaviour as mutagens. The method of choice for quantitation of such compounds is to fractionate the sample using techniques such as high-performance liquid chromatography (HPLC) or column chromatography[1,2], followed by gas chromatographic (GC)–mass spectrometric (MS) analysis. MS–MS techniques have also been used for quantitation of 1-NP[6]. However, the decomposition of 1-NP has been shown to occur during GC–MS analysis[1,6,7]. This decomposition greatly limits

0021-9673/83/$03.00

the accuracy, precision and sensitivity obtainable in quantitation of 1-NP at low 10–100-ng quantities.

In this study, the 1-NP content in four different samples of diesel exhaust particulate extract has been determined by capillary GC and capillary GC–MS analyses following HPLC fractionation. It has been found that the decomposition of 1-NP during analysis appears to be a catalyzed thermal decomposition and that the quantitation result of 1-NP critically depends on the cleanliness of the analytical system used. A modified cool on-column injection technique and bonded phase fused silica capillary column were used to minimize the decomposition of sample and improve the precision for the quantitative analysis. The four diesel exhaust particulate extracts show a 1-nitropyrene content in the 10–100 ng/μl range. The quantitative results obtained from GC and GC–MS are consistent.

EXPERIMENTAL

Sample collection and extraction

Four dichloromethane extracts of the diesel particulate matter collected from the in-use diesel automobiles were received from the New York State Department of Environmental Conservation. The vehicle testing, sample collection and filter extraction procedure for those in-use diesel automobiles have been reported previously[8,9]. These samples came from different testing vehicles, driving cycles, fuel and lubricant combinations. Table I lists the sample name, vehicle type and their values of the soluble organic fraction (SOF) of particulate matter.

TABLE I

DIESEL PARTICULATE EXTRACT

Sample	*Vehicle type*	*SOF (%)*
VW-1	Volkswagen	11.1
VW-2	Volkswagen	14.1
VW-3	Volkswagen	12.1
VW-4	Volkswagen	21.2

Solvent and standard

All solvents were "distilled in glass", UV grade from Caledon Labs. (Georgetown, Canada). A 1-nitropyrene and a [$^2H_9$]1-nitropyrene standard were received from Ford Motor Company (Dearborn, MI, U.S.A.).

HPLC pre-separation

Each dry sample received was dissolved in dichloromethane–acetone (3:1) at a concentration of about 20 mg/ml. A modified HPLC procedure previously described by Schuetzle *et al.*[1] was used to separate these complex diesel particulate extracts into six fractions according to the polarity of the component in the extract. The instrument consisted of a Spectra-Physics SP-8000 liquid chromatograph equipped with a SP-8400 UV–VIS detector and SP-4100 integrator. The monitoring wavelength was 254 nm. A 10-μm, semipreparative Spherisorb silica column (250 × 9.4 mm; Terochem, Toronto, Canada) was employed with a 140-μl sample loop. Each sample was frac-

tionated four times and the corresponding fractions were composited. The sample VW-3 was subjected to the HPLC fractionation procedure in duplicate in order to test the reproducibility of HPLC pre-separation. The solvent of all fractions was reduced to dryness. Based on previous works, fraction 3 contains all the 1-NP and its residual was finally dissolved in 100 μl of a mixture of dichloromethane and benzene (70%) for GC and GC–MS analyses.

Capillary GC analysis

GC analysis was done on a Hewlett-Packard HP-5880 A gas chromatograph equipped with a flame ionization detector and cool on-column injection. A 30 m × 0.32 mm I.D. Durabond DB-5 fused silica capillary column (J & W Scientific, Rancho Cardova, CA, U.S.A.) was mainly used. The GC conditions were: injection port < 50°C; column temperature programmed from 80°C for 1 min to 300°C at a rate of 3°C/min; detector temperature 320°C; and helium carrier gas flow-rate measured at 200°C, 1.5 ml/min.

Capillary GC–MS analysis

GC–MS analyses were performed on a Hewlett-Packard HP-5992 quadrupole gas chromatograph–mass spectrometer equipped with HP-59916A glass capillary effluent splitter interface and on-column injection. Two bonded-phase fused-silica capillary columns, 50 m × 0.32 mm I.D. SE-54 cross-linked column (Hewlett-Packard, Avondale, PA, U.S.A.) and 30-m DB-5 column described under *Capillary GC analysis* were used. The GC condition was similar to that described therein. The helium carrier gas flow-rate was 3 ml/min at room temperature. The capillary effluent splitter allowed approximately 0.5 ml/min to enter the MS analyzer. Electron impact ionization with 70 eV was used in GC–MS.

On-column injection at low temperature

A modified injection technique was used for on-column injection at room temperature in both GC and GC–MS analyses. For the Hamilton 701 RN 10-μl microsyringe with a fused-silica needle (0.18 mm O.D., *ca.* 0.5-μl needle dead volume; Hewlett-Packard), the syringe filling sequence is: pure solvent (*ca.* 0.8 μl) followed by an air space (*ca.* 0.8 μl), then a desired volume of sample solution (0.5–5 μl) to be taken. The sample solution is pulled into the syringe barrel and an empty needle is left. An accurate reading of sample solution in the syringe barrel is taken. This read amount of sample solution can be exactly delivered onto the column when the syringe needle is inserted into the column, then the syringe bar is pushed all the way in.

RESULTS AND DISCUSSION

The presence of 1-nitropyrene in these four diesel particulate extracts was indicated by carefully comparing the retention time in the gas chromatogram of HPLC fraction 3 for each sample with that of 1-nitropyrene external standard. Fig. 1 shows this comparison and a good agreement in retention time between 1-NP in sample and 1-NP standard is observed. Small deviations in retention time (±0.05 min) were caused by the deviation of injection time from sample to sample. This

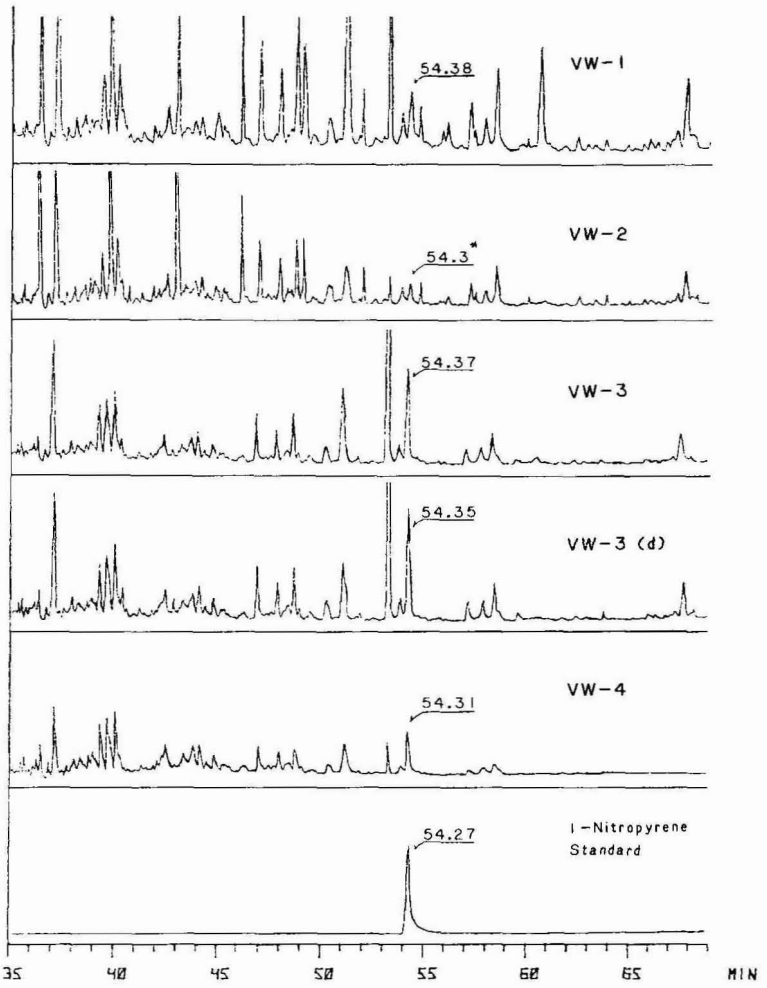

Fig. 1. Gas chromatograms of 1-nitropyrene standard and HPLC fraction 3 of four diesel particulate extracts (sample VW-3 in duplication). *GC conditions:* 30 m × 0.32 mm I.D. DB-5 fused-silica capillary column; flame ionization detector; cool on-column injection operated at room temperature; temperature 80°C for 1 min, programmed to 300°C at 3°C/min; 66-ng injection for 1-nitropyrene standard and 0.6-μl injection for HPLC fraction 3. *Estimated retention time due to failure in terminal print.

presence of 1-nitropyrene in the sample determined was further confirmed by GC–MS analysis based on the matching in mass spectrum and retention time obtained from the sample to that obtained from the 1-NP standard which was injected separately. Fig. 2 shows the mass spectrum obtained from sample VW-3 compared to the mass spectrum of 1-nitropyrene standard. Slight difference in the minor fragment ion peak may be caused by the impurities. Owing to operation under similar column and temperature programming conditions, the injected samples gave quite similar patterns of gas chromatogram and total ion current trace of GC–MS. It was easy to identify correctly the peak representing 1-NP in the sample GC chromatogram by comparison of two traces.

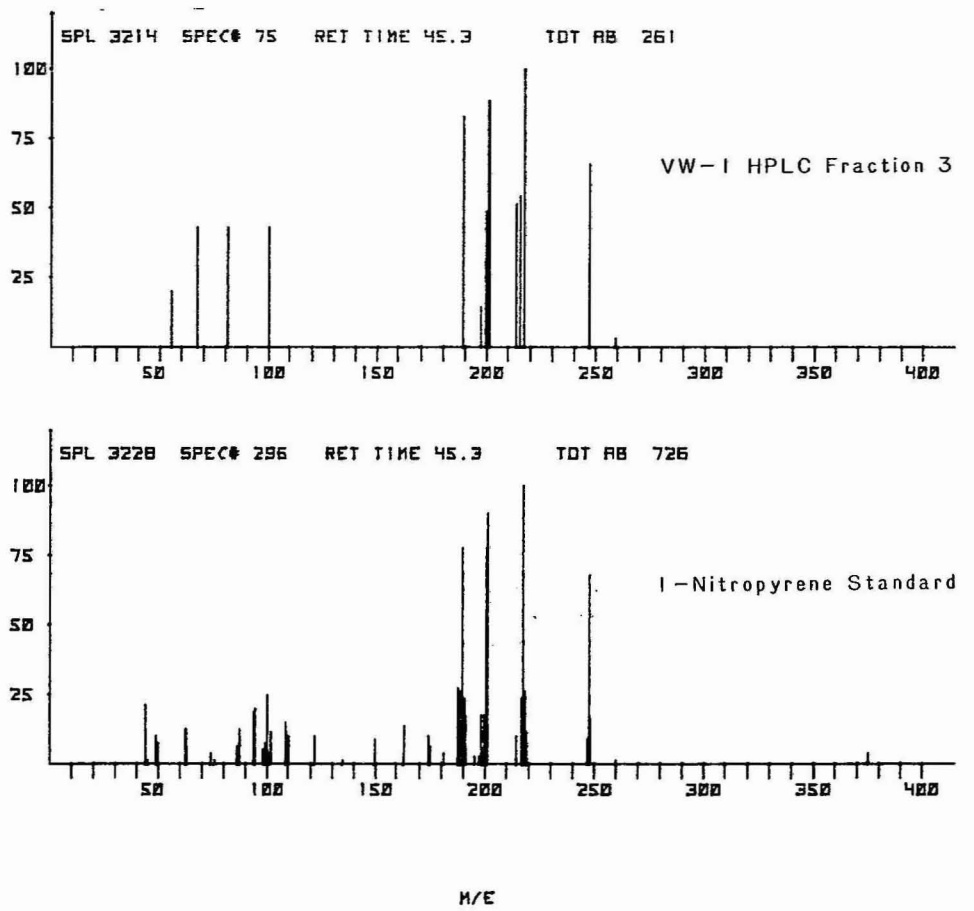

Fig. 2. Mass spectra of 1-nitropyrene obtained from HPLC fraction 3 of diesel particulate extract and from standard.

As shown in Fig. 1, the GC-peak of 1-NP in these complex matrices has been reasonably separated from the adjacent peaks with a high-resolution capillary column. This separation makes a correct integration of GC peak area of 1-NP possible. The baseline of the peak was constructed between the two adjacent valleys and the integrated area of 1-NP peak was automatically printed on the HP-5880A terminal. Quantitation of 1-NP in the sample determined by GC was based on the comparison of integrated peak area of 1-NP obtained from the samples with that obtained from an external standard of 1-NP. The calibration curve of 1-NP standard showed good linearity in the analysis range. The GC result of 1-NP in HPLC fraction 3 is listed in Table II.

In cases where other components interfere with the GC peak of 1-NP and especially when low concentrations are involved, the data obtained solely from GC are not enough for positive quantitation. This has been encountered in the analysis of samples VW-1 and VW-2. From the GC trace of sample VW-1 in Fig. 1, a relatively large error in the integrated peak area of 1-NP was expected because the 1-NP peak

TABLE II

1-NITROPYRENE CONCENYTRATION IN HLPC FRACTION 3 OF DIESEL PARTICULATE EXTRACT DETERMINED BY CAPILLARY GC

Sample	*No. of injections*	*Concentration (μg/μl)*	*Standard error*
VW-1	2	46.9	2.1
VW-2	3	13.3	0.9
VW-3	2	81.6	2.3
VW-3 (duplicate)	2	90.3	1.8
VW-4	5	36.7	1.0

was not well-separated from the neighboring peaks. In the GC analysis of sample VW-2, the value of integrated peak area of 1-NP was very close to the integration threshold set in the instrument. Two of the values of integrated peak area of 1-NP in three GC injections were estimated from the values given by the neighboring peaks because the instrument failed to print out the peak value of 1-NP peak. GC–MS with selected ion monitoring (SIM) was employed to cross-check the result obtained from the GC analysis. [$^2H_9$]1-nitropyrene (1-NP-d_9) standard was used as an internal standard in GC–MS–SIM analysis. Three characteristics ions of 1-NP and 1-NP-d_9, $(M)^+$, $(M - NO)^+$ and $(M - NO_2)^+$, were selectivity monitored. Fig. 3 shows a GC–MS–SIM trace of an injection of 1-NP standard and 1-NP-d_9 internal standard.

The quantitation of 1-NP by GC–MS–SIM was carried out by comparison of the ion current response of $(M)^+$ (m/z 247.1 and m/z 256.1) of 1-NP in samples and 1-NP-d_9 internal standard with a known concentration. The heights of ion current response were used for the quantitative comparison. By doing so the empirical baseline could be easily constructed for the ion of m/z 256.1 which was contaminated by some other component in some samples. A typical GC–MS–SIM trace from the sample VW-1 and 1-NP-d_9 internal standard is shown in Fig. 4. The ions at m/z 217.1, 226.1, 201.1 and 210.1 were used to confirm the position of 1-NP in each SIM trace and also served as the reference to construct the baseline for the ion current response of $(M)^+$. These four ions were not used for the purpose of quantitation because they contained interference in some samples and showed less regular behavior in GC–MS. In previous studies, it has been found that the relative abundance among the $(M)^+$, $(M - NO)^+$ and $(M - NO_2)^+$ ions of 1-NP depends on the amount of 1-NP injected at low quantity level[1,7]. This concentration dependence of relative abundance can be observed by comparison of Figs. 3 and 4, and thus creates a difficulty in quantitation work. It is important to match the injected amount between the sample and internal standard for obtaining a reliable result.

The degradation of 1-NP during GC and GC–MS analyses appears to be a catalyzed thermal decomposition. It has been found that the result of 1-NP determination critically depends on the cleanliness of the analytical system. A column contaminated after a certain number of injections of complex samples or a hot glass injection port easily lead to an irregular behavior of 1-NP occurring in GC and GC–MS analyses, such as a tailing peak of 1-NP in GC analysis or an unexpected change in relative abundance of fragment ions of 1-NP in GC–MS analysis. Those phenom-

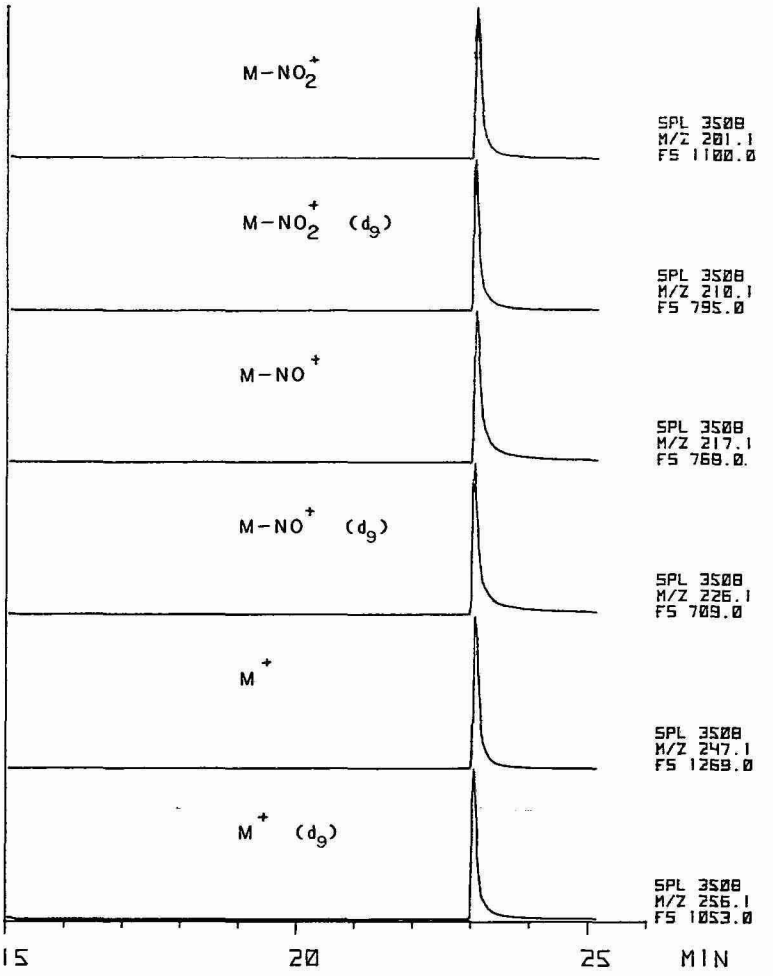

Fig. 3. SIM data for a co-injection of 1-nitropyrene (53 ng) and 1-NP-d_9 (43 ng), monitoring $(M)^+$, $(M - NO)^+$ and $(M - NO_2)^+$. Conditions: 30 m × 0.32 mm I.D. DB-5 fused-silica capillary column; on-column injection at room temperature; temperature 50°C programmed to 300°C at 10°C/min. Subscript (d_9) indicates ions of 1-NP-d_9. FS = Full-scale value.

ena make the quantitation of 1-NP impossible. On-column injection at low temperature and clean system greatly prevent the decomposition of sample by minimizing the contact of 1-NP with the hot surface of metal or glass. A more predictable behavior of 1-NP can be observed in GC and GC–MS analyses. However, the decomposition of 1-NP is more serious in the GC–MS because it can occur at both the glass interface and the ionization chamber of the mass analyzer even when cool on-column injection has been used. Generally, a more reliable result of quantitation of 1-NP is more easily obtained by high resolution GC.

In on-column injection at low temperature, the solvent injected may strip the coated stationary phase and leave an active surface at the front of some conventional capillary columns (non-bonded). This is important to some compounds such as 1-NP which is sensitive to adsorption and decomposition. A peak-broadening of 1-NP has been observed in GC analysis after certain numbers of on-column injection on

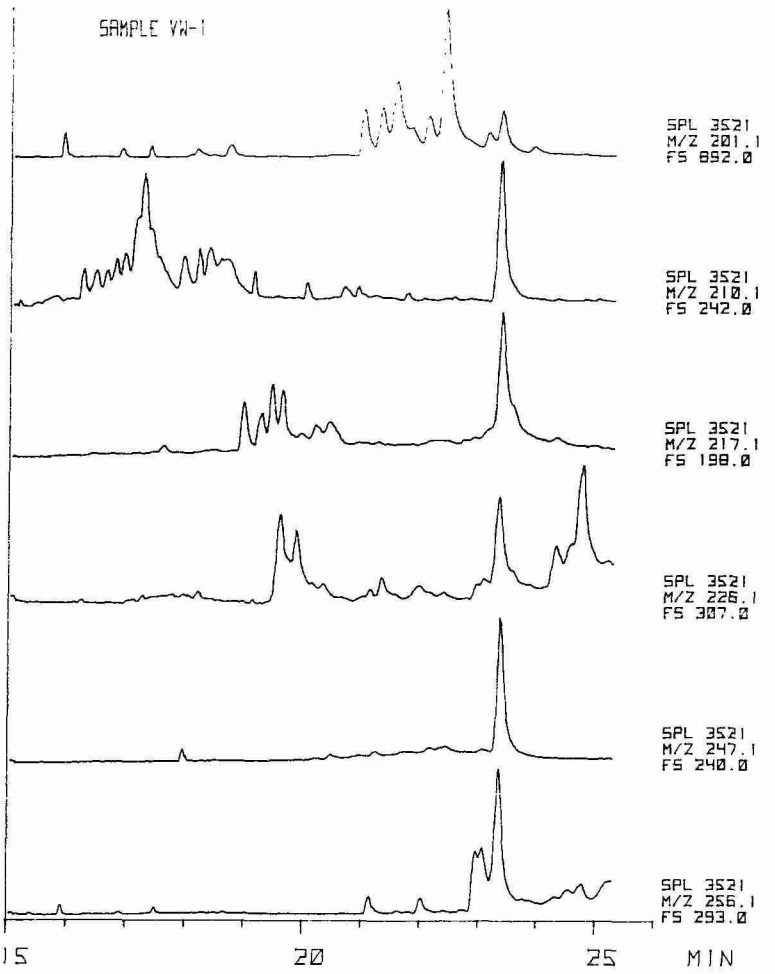

Fig. 4. SIM data for a co-injection of HPLC fraction 3 of diesel particulate extract and 1-NP-d_9 standard. Conditions as in Fig. 2.

a conventional fused-silica capillary column. The use of a bonded-phase fused-silica capillary column overcomes this problem.

For quantitative capillary GC analysis, an accurate delivery of a small volume sample is required. Most conventional injection techniques[10,11] are less satisfactory for the cool on-column injection in terms of controlling the injected amount and reproducibility. In our modified injection technique described in the Experimental section, the empty needle prevents the pre-evaporation of sample solution in the extremely fine needle of the syringe before injection is made. The air space left between the sample solution and the pure solvent plug prevents the sample solution from diffusing into the solvent plug which will exhibit an incomplete evaporation in cool on-column injection. A desired amount of sample solution can be easily taken and accurately read. Using this technique, a controlled small volume of sample so-

TABLE III

1-NITROPYRENE CONTENT IN DIESEL PARTICULATE MATTER

Sample	*No. of injections*	*1-NP content (ng/mg)*	*Standard error*
By capillary GC			
VW-1	2	49.9	2.3
VW-2	3	17.8	1.1
VW-3	2	92.2	2.6
VW-3 (duplicate)	2	102.0	2.1
VW-4	5	67.2	1.9
By capillary GC–MS			
VW-1	2	42.7	0.5
VW-2	2	22.4	0.3
VW-3 (duplicate)	2	103.2	0.6
VW-4	2	64.9	4.5

lution can be introduced upon the capillary column at low temperature with high reproducibility.

The recovery of 1-NP in the pre-separation procedure was determined in duplicate to be 105%. After taking account the SOF value given in Table I, the content of 1-NP determined in the four diesel exhaust particulate matter is listed in Table III. The results from GC and GC–MS analyses are reasonably consistent.

ACKNOWLEDGEMENTS

We thank Dr. R. Gibbs and his colleagues of the New York State Department of Environmental Conservation for supplying the diesel particulate extracts and the related data.

REFERENCES

1 D. Schuetzle, F. S.-C. Lee and T. J. Prater, *Int. J. Environ. Anal. Chem.*, 9 (1981) 93.
2 M.-L. Yu and R. A. Hites, *Anal. Chem.*, 53 (1981) 951.
3 D. L. Newton, M. D. Erickson, K. B. Tomer, E. D. Pellizzari, P. Gentry and R. B. Zweidinger, *Environ. Sci. Technol.*, 16 (1982) 206.
4 R. G. Becher and A. Bjørseth, *Environ. Sci. Technol.*, 16 (1982) 861.
5 J. N. Pitts, Jr., D. M. Lokensgard, W. Harger, T. S. Fisher, V. Mejia, J. J. Schuler, G. M. Scorziell and Y. A. Katzenstein, *Mutat. Res.*, 103 (1982) 241.
6 D. Schuetzle, T. L. Riley, T. J. Prater, T. M. Harvey and D. F. Hunt, *Anal. Chem.*, 54 (1982) 265.
7 J. A. Sweetman, F. W. Karasek and D. Schuetzle, *J. Chromatogr.*, 247 (1982) 245.
8 R. E. Gibbs, J. D. Hyde and S. M. Byer, Paper 801372 presented at *SAE Fuels and Lubricants Meeting, Baltimore, MD, October 1980*, Report EPA/J-80-209.
9 *Federal Register*, 40CFR86, March 5, 1980, p. 14496.
10 K. Grob and G. Grob, *J. Chromatogr. Sci.*, 7 (1969) 584.
11 K. Grob and K. Grob, Jr., *J. Chromatogr.*, 151 (1978) 311.

Journal of Chromatography, 264 (1983) 241–248
Elsevier Science Publishers B.V., Amsterdam — Printed in the Netherlands

CHROM. 15,822

LIQUID CHROMATOGRAPHIC DETERMINATION OF LINCOMYCIN IN FERMENTATION BEERS

PAUL A. ASMUS* and JOHN B. LANDIS
The Upjohn Company, Kalamazoo, MI 49001 (U.S.A.)
and
CARLOS L. VILA
The Upjohn Manufacturing Company, Barceloneta (Puerto Rico)
(Received March 1st, 1983)

SUMMARY

A reversed-phase ion-pairing liquid chromatographic method with UV detection at 214 nm is described for the determination of lincomycin A and lincomycin B in fermentation beers. The chromatographic system consists of a microparticulate octylsilica column and a mobile phase composed of 10 m*M* sodium dodecyl sulfate in ammonium phosphate-buffered aqueous acetonitrile (pH 6). Thermostating the column at 45°C improves the symmetry of the lincomycin peaks by eliminating fronting. The sample is diluted with phosphate buffer, centrifuged and the supernatant injected on the chromatographic column. The ion-pairing reagent causes lincomycin A and lincomycin B to be separated from each other and from all other substances present in raw fermentation beers. Precision of the assay for lincomycin A was 1.2% relative standard deviation. Recovery of spiked lincomycin A and lincomycin B from a fermentation beer sample was quantitative. A comparison of this high-performance liquid chromatographic (HPLC) method to a standard automated wet chemical method shows the HPLC method is more precise, specific and accurate, while being as simple to accomplish.

INTRODUCTION

Lincomycin is a medium spectrum antibiotic which is produced by fermentation as a mixture of the compounds lincomycin A and lincomycin B. The structures of these compounds are shown in Fig. 1. Lincomycin B shows only 25% the activity of lincomycin A, and typically represents less than 5% of the total lincomycin concentration in the bulk drug[1].

The lincomycin fermentation beer is a complex, heterogeneous mixture, whose composition changes as the fermentation progresses. The lincomycin fermentation is a directed fermentation in which the formation of side reaction products, such as lincomycin B, is suppressed. In order to monitor and direct the fermentation, the concentration of both lincomycin A and lincomycin B are monitored as the fermentation progresses.

0021-9673/83/$03.00

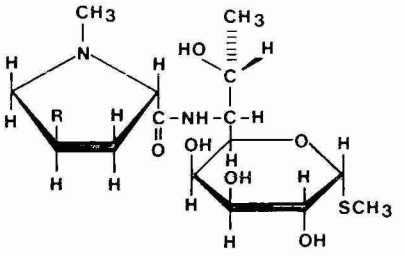

LINCOMYCIN A: R= $CH_2CH_2CH_3$

LINCOMYCIN B: R= CH_2CH_3

Fig. 1. Chemical structure of lincomycin A and lincomycin B.

A wet chemical method developed by Prescott[2] is the method most used for the determination of lincomycin in fermentation beers. The method is based on the reaction of 5,5′-dithiobis(2-nitrobenzoic acid) with the methanethiol generated by acid hydrolysis of the methylthioglycosido group of the antibiotic molecule. The colored product is then measured spectrophotometrically. Automation of the method with an AutoAnalyzer™ makes possible 150 assays per day, with an assay precision of 6% R.S.D. The AutoAnalyzer method is not specific for lincomycin A and measures all compounds having a hydrolyzable thio group, such as for example, lincomycin B. In addition, a positive bias is obtained from certain components, in the fermentation media[2]. Other assay methods which solve the AutoAnalyzer's methods specificity problem are a gas chromatographic procedure[3] and a gas chromatographic–mass spectrometric assay[4]. These methods, however, require derivatization of the lincomycin to form a volatile analyte, and are not rapid enough for routine monitoring of fermentation beers.

Our intention in developing a process assay for lincomycin was to replace the AutoAnalyzer method with one having a simple sample preparation, better specificity for lincomycin A and an analysis time comparable to the AutoAnalyzer method. The assay method developed and described below is an isocratic high-performance liquid chromatographic (HPLC) method using reversed-phase ion-pairing chromatography with UV detection at 214 nm. Sample preparation is very similar to the AutoAnalyzer method sample preparation, except in this chromatographic assay samples are diluted with pH 3 phosphate buffer solution instead of water. Chromatographic resolution and quantitation of both lincomycin A and lincomycin B within 15 min provides very useful information on the progress of the fermentation. The utility of the method was demonstrated by analyzing several samples of fermentation beers and comparing the analytical results obtained to the results from the AutoAnalyzer method.

EXPERIMENTAL

Chromatography

Experiments were conducted on a modular liquid chromatograph consisting of a Model 110A pump (Altex, Berkeley, CA, U.S.A.), an autosampler containing an injection valve with a 50-μl loop, (Valco, Austin, TX, U.S.A.), a RP-8 guard column

(Brownlee Labs., Santa Clara, CA, U.S.A.) and a Model 1203 detector with a zinc source (214 nm) (LDC, St. Petersbery, FL, U.S.A.) and a recorder (Sargent-Welch, Skokie, IL, U.S.A.). For quantitation, the data was collected and processed by a PDP 11 digital computer (Digital Equipment, Maynard, MA, U.S.A.).

The analytical column, a Zorbax C_8 (25 cm × 4.6 mm) (DuPont, Wilmington, DE, U.S.A.) was operated at a flow-rate of 2 ml/min. The use of a guard column in this assay method is very important due to the large amount of particulate matter and very hydrophobic impurities in raw fermentation beers. Changing the guard column when poor peak shape is observed will, in most cases, restore the separation to initial conditions. Both columns were thermostated at 45°C. The mobile phase was prepared by dissolving 2.9 g of sodium dodecyl sulfate and 10 ml of concentrated (85%) phosphoric acid in 660 ml distilled water and then adding 330 ml of HPLC grade acetonitrile (Burdick & Jackson Labs., Muskegon, MI, U.S.A.). The solution is titrated to an apparent pH of 6.0 with concentrated ammonium hydroxide and then filtered. Using these chromatographic conditions, the retention times of lincomycin A and lincomycin B are approximately 11 and 6 min, respectively.

Procedure

Before sampling, the fermentation beer is thoroughly mixed by shaking and inverting the sample container to obtain a homogeneous mixture. An accurately weighed aliquot of the sample is diluted with a phosphate buffer solution to obtain a

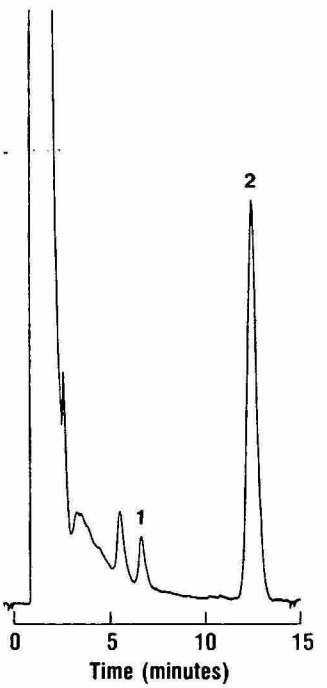

Fig. 2. Chromatogram of lincomycin fermentation beer sample preparation. Conditions: mobile phase, 10 m*M* sodium dodecyl sulfate and 150 m*M* ammonium phosphate in 33% acetonitrile, pH 6.0; flow-rate, 2.0 ml/min; temperature, 45°C. Peaks: 1 = lincomycin B; 2 = lincomycin A.

lincomycin A concentration of 20–400 μg/ml. The phosphate buffer is prepared by dissolving 7 ml of concentrated phosphoric acid in 1000 ml of distilled water and adjusting to pH 3.0 with concentrated ammonium hydroxide. The sample is shaken for 1 min and an aliquot of the diluted sample centrifuged for at least 10 min at a minimum of 2000 *g*. A 25–100-μl volume of the clear supernatant is analyzed by LC. The concentration of lincomycin A and B in the sample preparations is then determined by a comparison to standard curves over the range of 20–400 μg/ml lincomycin A and 2–40 μg/ml lincomycin B.

RESULTS AND DISCUSSION

A typical chromatogram of a lincomycin fermentation beer sample is shown in Fig. 2. The lincomycin A and lincomycin B peaks are sharp and well resolved from each other and from the rest of the sample constituents. The only sample preparation is dilution of the beer with phosphate buffer and centrifugation. The addition of the dodecyl sulfate ion to the mobile phase enables the separation of the lincomycin peaks from the many other compounds in this very complex matrix without any sample "clean up". Without dodecyl sulfate as an ion-pairing reagent, these drug peaks are lost in a "forest" of constituent peaks.

Dodecyl sulfate was chosen as the ion-pairing reagent after several other alkyl sulfate and sulfonates were tried. In general, we found that the more hydrophobic the ion-pairing reagent, the greater was the retention of lincomycin and the greater the selecitivity. As the dodecyl sulfate concentration was increased retention was increased. Both of these observations agree with well known reversed-phase ion-pairing behavior. The use of dodecyl sulfate imparted enough selectivity to the system in order to separate lincomycin A and lincomycin B from the rest of the UV-absorbing constituents in this sample, while still being soluble in the mobile phase. The dodecyl sulfate concentration was arbitrarily set at 10 m*M* to allow fairly rapid loading on the column, so that stable retention times would be obtained within 2 h. With this concentration of dodecyl sulfate, the acetonitrile concentration of 33% gives a lincomycin A retention time of approximately 11 min. In addition to controlling selec-

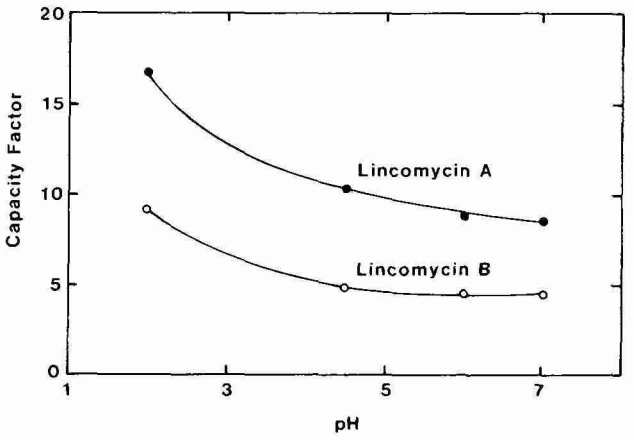

Fig. 3. Effect of mobile phase pH on retention. Conditions as in Fig. 2.

tivity, the sodium dodecyl sulfate helps reduce tailing of the lincomycin peak on the silica based reversed-phase packing material. Addition of ion-pairing reagents to the mobile phase has previously been shown, in some cases, to reduce tailing of nitrogen-containing compounds[5].

The pH of the mobile phase was used as a further means of altering the selectivity of the separation between lincomycin and interfering compounds. Fig. 3 illustrates the dependence of lincomycin retention on the pH of the mobile phase. With decreasing pH, the retention of lincomycin increases. This is attributed to greater protonation of the pyrrolidine nitrogen atom at lower pH, the pK_a of which is 7.6[6]. With an increase in the concentration of the positively charged lincomycin, more ion interaction occurs and therefore greater retention. The beer samples contain other compounds which are also more retained as the pH of the mobile phase is lowered. However, by raising the mobile phase pH to 6, the selectivity between the drug and other beer constituents is greatly enhanced so that adequate resolution is obtained.

Another problem encountered with the development of this separation was a "fronting" lincomycin peak when the assay was attempted at room temperature. Thermostating the analytical column and guard column at 45°C dramatically improves peak shape over that observed at room temperature by elimination of the peak front (Fig. 4). The reason for this improvement in peak shape has not been investigated in detail. However, the addition of the competing amine, N,N-dimethyloctylamine, to the mobile phase did not affect the fronting phenomenon. Since competing amines have been shown to reduce solute interaction with residual

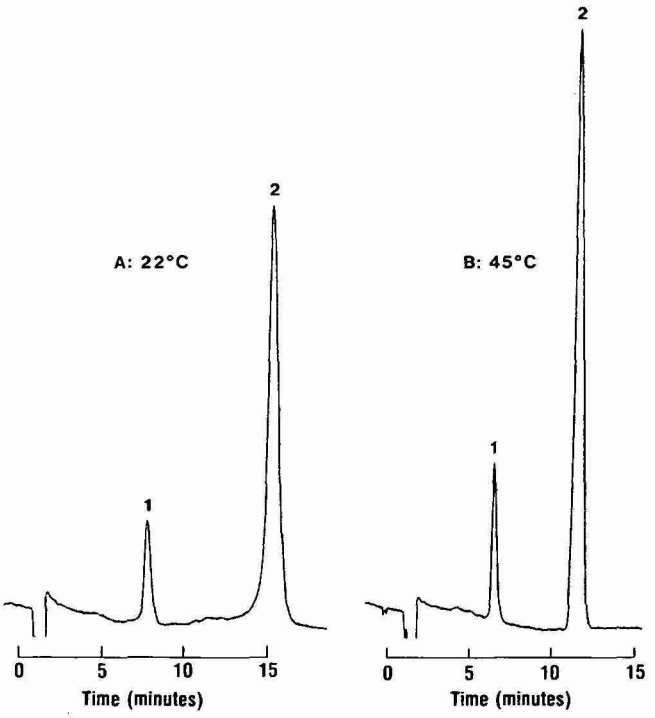

Fig. 4. Chromatograms of lincomycin standards: A, 22°C and B, 45°C. Conditions as in Fig. 2.

TABLE I

STANDARD ADDITION TO LINCOMYCIN BEER SAMPLE

Lincomycin A (mg)		*Lincomycin B (mg)*	
Added	*Found*	*Added*	*Found*
0	0.86	0	0.05
1.763	2.62	0.291	0.36
3.525	4.58	0.582	0.63
5.288	6.41	0.873	0.90
8.813	9.76	1.455	1.53
Slope	1.016		1.007
Intercept	0.904		0.050
Corr. coeff.	0.9995		0.9995
E.S.D.* slope	0.018		0.019
E.S.D. intercept	0.087		0.016

* Estimated standard deviation.

silanol groups[7], these results indicate that the disturbing effect is not an ion-exchange or adsorption retention mechanism.

Linearity of the method was determined over the concentration range of 1.76–35.2 μg/ml and 0.29–5.82 μg/ml for lincomycin A and lincomycin B respectively. The resulting standard curve for lincomycin A is described by the following regression equation:

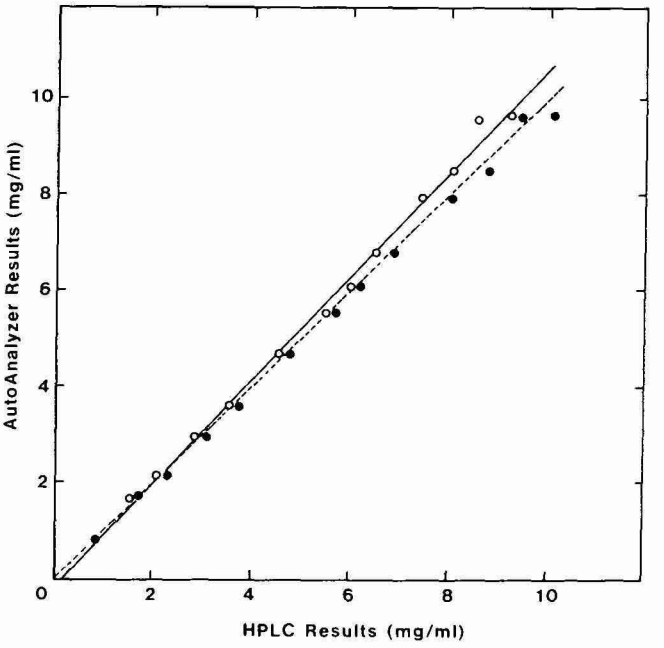

Fig. 5. Correlation of HPLC and AutoAnalyzer results. Regression equation for lincomycin A (solid line): $y = 1.093\ (\pm\ 0.001)x - 0.188\ (\pm\ 0.123)$; $r = 0.998$. Dashed line = theoretical curve.

peak area ratio = 0.343 × concentration (mg/ml) + 0.070

For lincomycin B the regression equation was:

peak area ratio = 0.344 × concentration (mg/ml) + 0.004

The correlation coefficients of the regression were 0.9998 and 0.9991 for lincomycin A and B, respectively.

Precision of the assay method was tested by preparing and analyzing a typical beer sample five times. The relative standard deviations obtained were 1.2% and 6.6% for lincomycin A and B, respectively.

A standard addition experiment was performed by spiking 1-ml aliquots of a young beer sample with various amounts of lincomycin and analyzing the resulting samples. The results of this study are shown in Table I. The linear regression equations obtained show that lincomycin is not being adsorbed by components in the beer sample. The slopes of the lines are not significantly different from the theoretical value of 1.000 ($p = 0.05$), and the correlation coefficients of the regression are greater than 0.999. The intercepts give a very accurate measurement of the lincomycin A and B concentrations in the original sample.

To compare the HPLC procedure for lincomycin with the AutoAnalyzer

TABLE II

COMPARISON OF LINCOMYCIN ASSAY RESULTS OBTAINED BY HPLC AND AUTOANALYZER METHODS (mg/ml)

Sample	*Time of sampling**	*AutoAnalyzer Total lincomycin*	*HPLC*		
			Lincomycin A	*Lincomycin B*	*Total*
A	0.25	0.74	0.81	<0.03	0.81
A	0.30	1.67	1.54	0.16	1.70
A	0.36	2.15	2.06	0.21	2.27
A	0.42	2.96	2.85	0.24	3.09
A	0.48	3.59	3.56	0.20	3.76
A	0.54	4.65	4.54	0.19	4.73
A	0.60	5.53	5.48	0.21	5.69
A	0.66	6.08	5.95	0.21	6.17
A	0.72	6.81	6.44	0.39	6.83
A	0.84	7.96	7.38	0.63	8.01
A	0.89	8.54	8.01	0.71	8.73
A	0.95	9.57	8.49	0.84	9.33
A	1.00	9.65	9.14	0.88	10.02
B	0.18	0.33	0.23	0.03	0.26
C	0.73	6.14	5.95	0.15	6.11
D	0.32	1.53	1.57	0.10	1.66
D	0.52	4.33	3.84	0.18	4.02
E	0.20	0.35	0.34	<0.03	0.34
F	0.37	2.21	2.21	0.18	2.39

* Normalized to the end of the fermentation.

method one lot of fermentation beer sampled at various times during the course of the fermentation, as well as different beer samples, were assayed by both methods (Table II). As shown in Fig. 5, close agreement between the methods is obtained when a comparison of the AutoAnalyzer result and the sum of the lincomycin A and B concentrations by HPLC is made. The regression equation for the line (not shown) is $y = 0.999\ (\pm\ 0.014)x - 0.089\ (\pm\ 0.084)$. However, when the lincomycin A concentration only by HPLC is plotted against the AutoAnalyzer results (solid line in Fig. 5), we see a statistically significant deviation ($p = 0.05$) between the two methods; with the AutoAnalyzer method giving the higher result. The reason for the deviation is clearly the lincomycin B concentration.

REFERENCES

1 D. J. Mason and C. Lewis, in J. C. Sylvester (Editor), *Antimicrobial Agents and Chemotherapy, Proc. Interscience Conf. Antimicrobial Agents and Chemotherapy, New York, NY, October 26–28, 1964*, Am. Soc. for Microbio., 1965.
2 G. C. Prescott, *J. Pharm. Sci.*, 55 (1966) 423.
3 R. L. Houtman, D. G. Kaiser and A. J. Taraszka, *J. Pharm. Sci.*, 57 (1968) 643.
4 R. L. Niewoonder, personal communication.
5 H. F. Proeless, H. J. Lohmann and D. G. Miles, *Clin. Chem.*, 24 (1978) 1948.
6 R. R. Herr and G. Slomp, *J. Amer. Chem. Soc.*, 89 (1967) 2444.
7 A. Sokolowski and K.-G. Wahlund, *J. Chromatogr.*, 189 (1980) 299

Journal of Chromatography, 264 (1983) 249–257
Elsevier Science Publishers B.V., Amsterdam — Printed in the Netherlands

CHROM. 15,851

RAPID SEPARATION AND MEASUREMENT OF RAT URINARY KALLIKREIN BY HIGH-PERFORMANCE LIQUID CHROMATOGRAPHY WITH A CONTINUOUS FLOW ENZYME DETECTOR

YOSHIHIKO FUNAE*
Laboratory of Chemistry, Osaka City University Medical School, Asahi-machi, Abeno-ku, Osaka 545 (Japan)
HIROKO AKIYAMA
Osaka College of Pharmacy, 2-10-65 Kawai, Matsubara, Osaka 580 (Japan)
SUSUMU IMAOKA
Laboratory of Chemistry, Osaka City University Medical School, Asahi-machi, Abeno-ku, Osaka 545 (Japan)
and
MASANORI TAKAOKA and SHIRO MORIMOTO
Osaka College of Pharmacy, 2-10-65 Kawai, Matsubara, Osaka 580 (Japan)
(Received March 10th, 1983)

SUMMARY

Rat urinary kallikrein was separated by high-performance liquid chromatography (HPLC) using an ion-exchange or gel-permeation column. Kallikrein activity was monitored continuously with peptidase or esterase activity using a post-reactor system directly adapted to HPLC. A PTFE helically coiled tube served as the enzyme reactor vessel. Four and three peaks with peptidase and esterase activity, respectively, were detected on application of normal rat urine.

INTRODUCTION

Rat urinary kallikrein is heterogeneous and DEAE-cellulose chromatography is routinely used to separate the related kallikrein-like substances[1–3]. In chromatography, kallikrein activity is measured not continuously but rather by assessment of each fraction using synthetic substrates. Conventional ion-exchange chromatography requires a long separation time and its resolution is poor.

High-performance liquid chromatographic (HPLC) methods using gel-permeation or ion-exchange types of column have been developed to separate proteins[4–9]. The advantages of HPLC are high speed, resolution and reproducibility and automatic control over the chromatography and detection system. This method has been used to separate isoenzymes related to enzyme activity by a post-reactor system[10–14].

We now report a rapid and complete separation and a simple method of measurement of rat urinary kallikrein by continuously monitoring the peptidase and

0021-9673/83/$03.00

esterase activity using a post-reactor system. Peptidase and esterase activities were detected with prolylphenylalanylarginine-4-methylcoumaryl-7-amide (MCA) and N-α-tosyl-L-arginine methyl ester (TAME) as the enzyme substrate, respectively.

EXPERIMENTAL

Materials

MCA was obtained from the Protein Research Foundation (Minoh, Osaka, Japan) and TAME and aprotinin from Sigma (St. Louis, MO, U.S.A.). Other chemicals were of analytical-reagent grade and were used as received.

Urine samples and partially purified urinary kallikrein. Male Wistar rats weighing 210–240 g were kept in stainless-steel metabolic cages and were provided water but no solid food during urine collection. Urine was centrifuged at 3000 rpm for 30 min and dialysed at 4°C against deionized water for 24 h and lyophilized. The concentrations of protein, MCA peptidase and TAME esterase activities in the resulting urine sample were 33 mg/ml, 1314 peptidase unit (PU)/ml and 7.7 esterase unit (EU)/ml, respectively. Partially purified urinary kallikrein was prepared by DEAE-cellulose chromatography according to the method of Chao and Margolius[3]. MCA peptidase activity of the preparation was 1254 PU/mg protein. MCA peptidase and TAME esterase activities were measured as reported previously[15]. Protein was determined by the method of Lowry *et al.*[16] using bovine serum albumin as the standard.

Columns

Anion-exchange HPLC was performed on a 300 × 4 mm I.D. column of IEX-540 DEAE SIL (particle size 5 ± 1 μm) provided by Toyo Soda (Tokyo, Japan). Two columns of TSK-GEL G3000SW (Toyo Soda) which were directly connected were used on a gel-permeation HPLC system.

Apparatus

The HPLC instrument (Toyo Soda Model SP-8700) was equipped with a spectrophotometer (UV-8 model) fitted with an 8-μl flow cell. An RF-530 (Shimadzu, Tokyo, Japan) fitted with a 12-μl flow cell was used to detect fluorescence, a Model 4MD-3G four-channel (Ch-1, -2, -3 and -4) constamatic pump (Gasukuro Kogyo, Tokyo, Japan) was used for the post-reactor system and a Shimadzu C-R1A data processor served for calculation of peak areas.

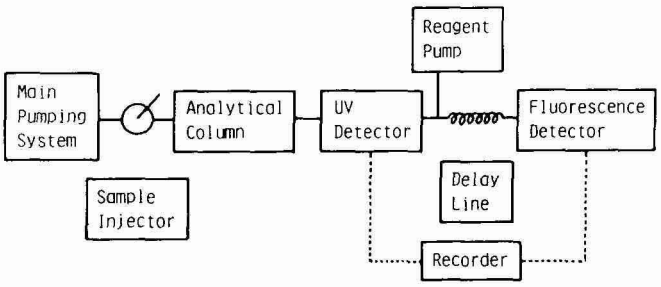

Fig. 1. Diagram of the HPLC system with continuous flow detector.

HPLC

Ion-exchange chromatography was carried out at a flow-rate of 0.7 ml/min with a linear salt gradient made by controlling buffer A (0.02 *M* Tris–acetate, pH 7.5) and buffer B (1.0 *M* sodium acetate added to buffer A, pH 7.5) using a solvent programmer, at 20–25°C. The mobile phase for gel-permeation chromatography was 0.05 *M* sodium phosphate buffer (pH 7.5) containing 0.1 *M* sodium chloride. The flow-rate was 0.5 ml/min and chromatography was carried out at 20–25°C. Bovine serum albumin (MW 68,000), ovalbumin (45,000), α-chymotrypsinogen (24,500) and cytochrome *c* (12,500) were used as standards for calculation of molecular weight.

Post-reactor system

The HPLC system with the continuous post-reactor is shown schematically in Fig. 1.

Peptidase activity. The principle of assay was according to Kato *et al.*[17]. The assay solution for the post-reactor detection of peptidase activities was 0.05 *M* Tris–HCl (pH 8.2) containing 5 μ*M* MCA. Aprotinin was added to the assay solution in the studies on inhibition. The assay solution was allowed to flow through a three-diagonal mixing joint made of PTFE, at a flow-rate of 0.75 ml/min just after the UV detector equipped for detection of the protein, using a constamatic reagent pump. Enzymatic reaction was carried out in a 20-m helically coiled PTFE capillary tube (0.25 mm I.D., 1.5 mm O.D.) at 40°C using a water-bath. The 7-amino-4-methylcoumarin generated was monitored fluorimetrically at 460 nm with excitation at 380 nm and the peak area was calculated using a data processor.

Esterase activity. The principle of the assay was according to Matsuda *et al.*[18]. The substrate solution of 0.1 *M* sodium phosphate buffer (pH 8.0) containing 10 m*M* TAME was combined with the eluate using pump Ch-1 at a flow-rate of 0.24 ml/min. The enzymatic reaction was carried out in a 20-m helically coiled PTFE capillary tube (0.25 mm I.D., 1.5 mm O.D.) at 40°C using a water-bath. Next, a mixed solution (1:2) of 0.1% potassium permanganate and 10% perchloric acid was added to the stream of reaction mixture using pump Ch-2 at a flow-rate of 0.5 ml/min, at 20–25°C to oxidize the generated methanol to formaldehyde. The length and inner diameter of this PTFE delay line tube were 20 m and 0.5 mm, respectively. To neutralize the reaction mixture, 0.1% hydroxylamine hydrochloride was added to the stream of reaction mixture at a flow-rate of 0.32 ml/min using pump Ch-3, at 20–25°C. The length and inner diameter of this PTFE tube were 20 m and 0.5 mm, respectively. Finally, to form a fluorescent compound, 2 *M* ammonium acetate containing 0.2% acetylacetone and 0.3% acetic acid was added to the stream using pump Ch-4 at a flow-rate 0.76 ml/min. The reaction was carried out at 80°C in a 10-m PTFE capillary tube (0.5 mm I.D., 1.5 mm O.D.) and the resulting fluorescence was measured at 510 nm with excitation at 410 nm.

RESULTS

Peptidase activity

The elution profiles of urine protein and MCA peptidase activity are shown in Fig. 2. Proteins were clearly separated into more than ten peaks, and this profile was similar to that seen with plasma in previous work[9]. The highest peak in the centre of

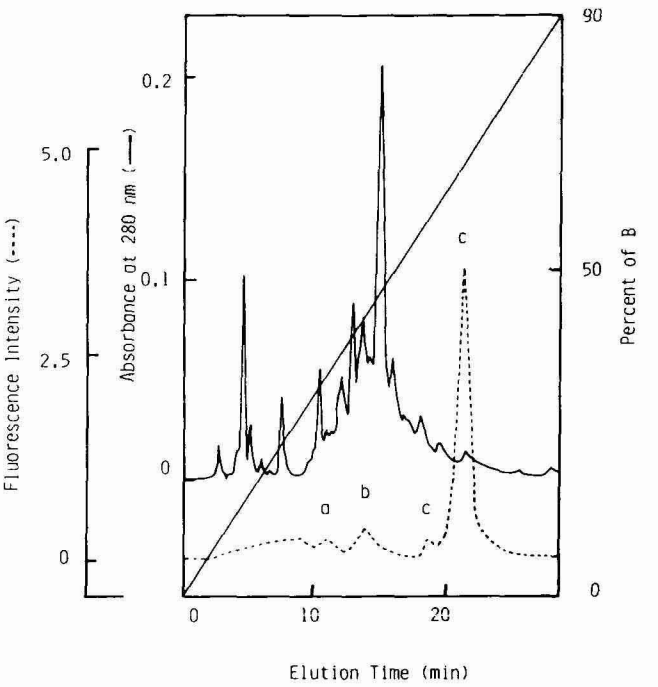

Fig. 2. Elution profile of rat urinary MCA peptidases. The urine sample (10 μl) was directly chromatographed on a DEAE-type of column with a linear gradient (0–1 *M* sodium acetate) at a flow-rate of 0.7 ml/min. The MCA solution (5 μM) was added at 0.75 ml/min. The delay line (0.25 mm I.D.) was 20 m long and the post-reactor temperature was 40°C. Percent of B indicates the percentage of buffer B.

the chromatogram of protein was assumed to be albumin. Three small peaks (peaks a, b and c') and a large peak (c) with peptidase activity were apparent. Peak c was identified as urinary kallikrein, based on the following evidence. The elution profile of MCA peptidases of partially purified urinary kallikrein is shown in Fig. 3. Only one peak was detected. The retention time of this peak (22.6 min) was the same as that of peak c (Fig. 2). The molecular weight of MCA peptidases was measured by gel-permeation HPLC and the elution profile is shown in Fig. 4. One large peak and two small MCA peptidase peaks were detected and the molecular weights were calculated to be 38,000, 35,000 and 34,000, respectively. The major peak (molecular weight 38,000) was considered to correspond to peak c, and two small peaks seemed to relate to peak a or b, because of the intensity of fluorescence.

The fluorescence sensitivity (peak area) of the peaks of peptidase activity was influenced by the sample volume, concentration of substrate (MCA), reaction time, length of the PTFE tube and incubation temperature. The effect of the sample volume on the area of peak c is shown in Fig. 5. The relationship between the peak area computed by a data processor and the volume of sample was linear in the range 2.5–10 μl, under the conditions of the post-reactor described in Fig. 5. These results indicate that this method should facilitate quantitative studies of kallikrein. A 2.5-μl volume of sample contained 82 μg of protein and the peptidase and esterase activities were 3.3 PU and 0.02 EU, respectively. When 5 μl of dialysed normal rat urine

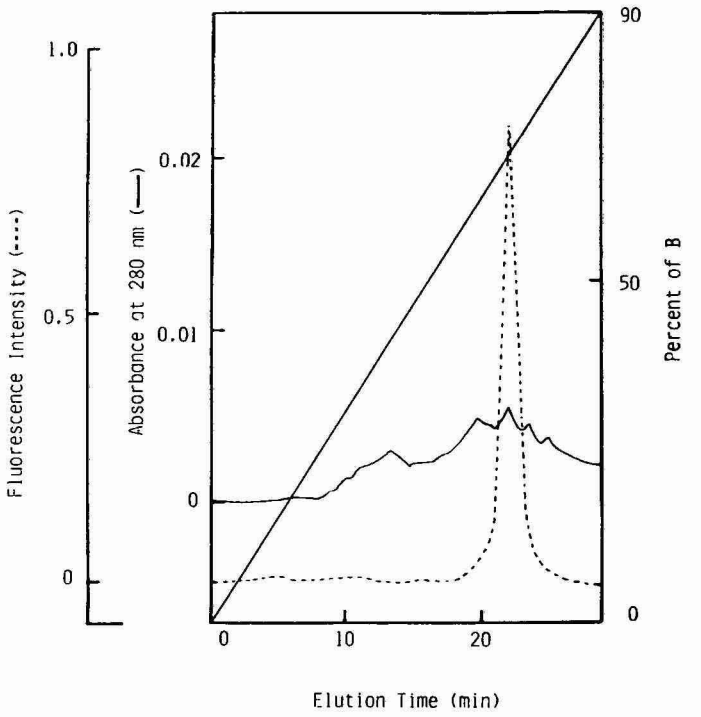

Fig. 3. Elution profile of partially purified urinary kallikrein. Conditions as in Fig. 2. Sample volume, 50 μl.

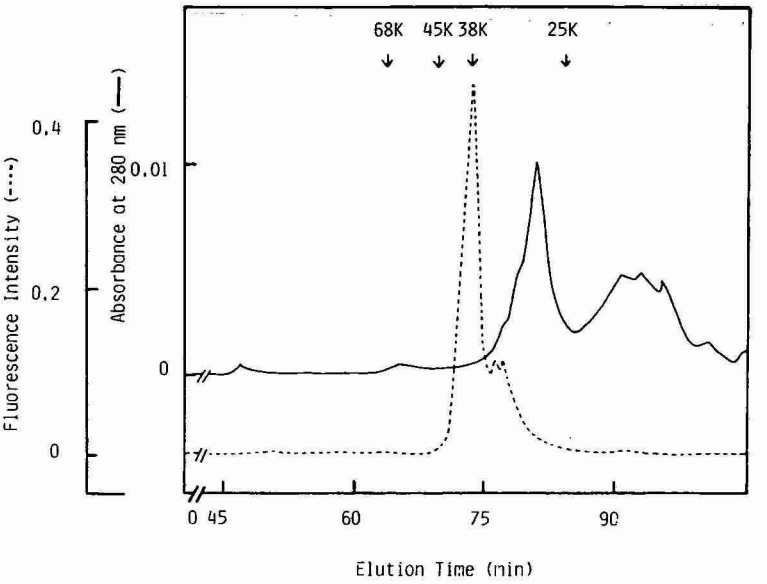

Fig. 4. Elution profile of urinary MCA peptidases on gel-permeation HPLC. A urine sample (10 μl) was chromatographed on a TSK G-3000 SW (60 cm × 2) column with 0.05 *M* phosphate buffer (pH 7.5) containing 0.1 *M* sodium chloride at a flow-rate 0.5 ml/min. Conditions of post-reactor system as in Fig. 2. K = kilodalton.

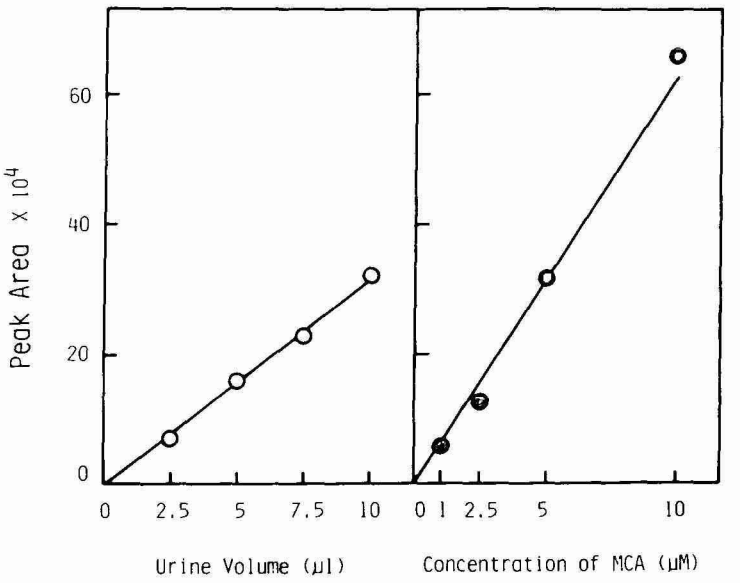

Fig. 5. Correlation of sample volume and the concentration of MCA with area of peak c. Sample volumes were 2.5, 5.0, 7.5 and 10.0 μl. Concentrations of MCA were 1.0, 2.5, 5.0 and 10.0 μ*M*. Other conditions of HPLC and post-reactor as in Fig. 2.

were injected on to the column under the same conditions as for Fig. 2, MCA peptidase activity was clearly detected.

The effect of the concentration of substrate (MCA) on the area of peak c is shown in Fig. 5. This area increased with increase in the concentration of MCA. The enzyme reaction time could be controlled by the length of the PTFE tube in the post-reactor system. When 10- and 20-m lengths of PTFE tube were used, the areas of peak c were $15.6 \cdot 10^4$ and $31.4 \cdot 10^4$ μV · sec, respectively. The peak area also increased with increasing incubation time. When HPLC was carried out under the conditions described in Fig. 2, the incubation time of the enzyme reaction was 40 sec and here the temperature affected the peak area. The peak area at 40°C ($31.4 \cdot 10^4$ μV · sec) was larger than that at 25°C ($14.6 \cdot 10^4$ μV · sec).

Esterase activity

The elution profiles of urine protein and TAME esterase activity are shown in Fig. 6. The elution profile of protein was slightly different from that of the assay of peptidase activity because the flow-rate of the column and the volume of sample differed with the assay system. Three peaks (I, II and III) with esterase activity were detected. As the sensitivity of the esterase activity detection system was lower than that of peptidase activity detection system, ten times the volume of sample was injected. The flow-rate of the ion-exchange chromatography was reduced to 0.5 ml/min as the back-pressure was high with four reactor pumps, the total flow-rate of which was 1.82 ml/min. The post-reactor system for detection of the esterase activity was more complicated than that for the peptidase activity, as four different reagent pumps were required. In the first step, substrate solution (TAME) flowed to generate meth-

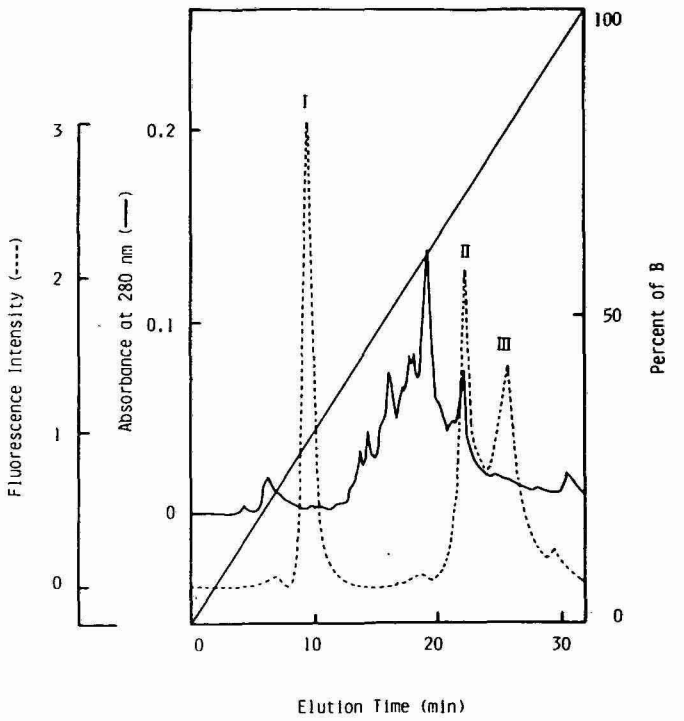

Fig. 6. Elution profile of TAME esterase. A urine sample (10 μl) was chromatographed on a DEAE-type of column at a flow-rate of 0.5 ml/min. Conditions of the post-reactor system as described in the text.

anol using pump Ch-1 at a flow-rate of 0.24 ml/min. The conditions (delay line and incubation temperature) of the enzyme reaction were the same as for detection of the peptidase activity. In the second step, acetic acid was used instead of perchloric acid for pump protection but the sensitivity was poor. In this step, potassium permanganate was reduced to manganese dioxide, which dissolved only slightly in the mobile phase. The resulting microparticles sometimes plugged the 0.25 mm I.D. PTFE tube. PTFE tubing of 0.5 mm I.D. was therefore used. At an incubation temperature of 60°C, good results were not always obtained. This step is critical in this post-reactor system. The final step producing the fluorescent compound by reaction with acetylacetone was fairly easy to control. A high concentration of acetylacetone (0.6%) and a longer delay line (20 m) did not affect the peak area.

Inhibition studies with aprotinin

To elucidate which peaks were for kallikrein, we investigated the peaks that decreased with aprotinin treatment. In the assay for peptidase activity, peak c (Fig. 2) decreased as a function of concentration whereas the other peaks remained unchanged. The percentage inhibition of peak c by aprotinin is shown in Table I. When the concentration of aprotinin was high (over 1000 kallikrein inhibitor units (KIU) per ml under these experimental conditions), peak c was completely inhibited. In the assay system for esterase activity, only peak III was inhibited by aprotinin.

TABLE I

INHIBITION OF MCA PEPTIDASE WITH APROTININ

Percentage inhibition of peak c shown in Fig. 2 by four different concentrations of aprotinin is shown. Peak area was computed by data processor. Conditions of HPLC and post-reactor system as in Fig. 2. Aprotinin was added to MCA solution.

Concentration of aprotinin (KIU/ml)	*Peak area ($\times 10^3$) ($\mu V \cdot sec$)*	*Inhibition (%)*
0	314.0	0
10	225.6	28.2
100	54.7	82.6
1000	6.4	97.9

DISCUSSION

The most commonly used technique for the separation of enzymes is ion-exchange chromatography. However, the slow flow-rates make it unsuitable for routine analytical work. Manual methods are extremely tedious and, because only a given eluate fraction is subsequently measured, one cannot be sure of the resolution of one fraction from another. An ion-exchange type of HPLC column for the separation of proteins and a continuous flow detector of enzyme activity have been developed[10–14]. Our approach differs in that a PTFE tube is used as the enzyme reactor vessel. Schroeder *et al.*[11] used a stainless-steel tube as an enzyme reactor, but PTFE is probably better as there is no problem with corrosion. Schlabach *et al.*[12] and Huber *et al.*[13] found that a packed-column reactor was more efficient than a capillary tube. However, in our post-reactor system, band spreading did not occur to a measurable extent because the width of the peaks of enzyme activity did not spread as seen with the proteins. PTFE tubing as an enzyme reactor facilitates easy control of the incubation time by appropriate selection of the tube length and the incubation temperature for the reaction.

The detection of peptidase activity was superior to that of esterase activity with regard to sensitivity of the enzyme activity, probably because with the system used to determine the esterase activity it was necessary to drive the four reactor pumps concomitantly. Thus, it is difficult to regulate each step for optimal conditions (flow-rate, reaction temperature and concentration of carrier solution). Another reason is that oxidation of the generated methanol with potassium permanganate does not completely terminate in formaldehyde but proceeds partially to formic acid. As potassium permanganate oxidizes not only methanol but also tris(hydroxymethyl)aminomethane, it is difficult to control this step with optimal conditions.

Synthetic substrates (MCA and TAME) were used to detect kallikrein activity; however, these substrates are not specific for kallikrein, but rather are substrates showing peptidase or esterase activity. We identified the kallikrein peak in the following way. Peaks c and III were identified as kallikrein peaks and both were considered to be the same enzyme. Although the retention times of peaks c and III differed because the flow-rates in HPLC were different, the eluted postions of peaks c and III

seemed to be the same in comparison with the protein elution profile. Kallikrein is inhibited by aprotinin[19]. Only the two peaks c and III were inhibited by aprotinin, other peaks being little affected. The molecular weight (38,000) of the peak c enzyme was compatible with that of urinary kallikrein reported by other workers[1,3], indicating that peak c was urinary kallikrein. The retention time (Fig. 3) of partially purified urinary kallikrein which had biological kallikrein activity was the same as that of peak c, and therefore peak c is undoubtedly urinary kallikrein.

The activity of kallikrein is usually measured using a synthetic substrate nonspecific for kallikrein because it is tedious to measure the biological and kinin-forming activities. With our new technique, urinary kallikrein can be readily separated, identified and measured.

ACKNOWLEDGEMENTS

We thank Toyo Soda Manufacturing Co. (Tokyo) for providing the TSK gel and M. Ohara for critical reading of the manuscript.

REFERENCES

1 C. P. Mcpartland, D. L. Sustarsic and J. P. Rapp, *Endocrinology*, 108 (1981) 1634.
2 K. Nustad and J. V. Pierce, *Biochemistry*, 13 (1974) 2312.
3 J. Chao and H. S. Margolius, *Biochem. Pharmacol.*, 28 (1979) 2071.
4 S. H. Chang, K. M. Gooding and F. E. Regnier, *J. Chromatogr.*, 125 (1976) 103.
5 F. E. Regnier and K. M. Gooding, *Anal. Biochem.*, 103 (1980) 1.
6 G. Vanecek and F. E. Regnier, *Anal. Biochem.*, 121 (1982) 156.
7 K. Buchholz, B. Gödelmann and I. Molnar, *J. Chromatogr.*, 238 (1982) 193.
8 A. N. Kotake and Y. Funae, *Proc. Nat. Acad. Sci. U.S.*, 77 (1980) 6473.
9 Y. Funae, R. Seo and S. Morimoto, *Jap. J. Clin. Chem.*, 11 (1982) 342.
10 T. D. Schlabach, A. J. Alpert and F. E. Regnier, *Clin. Chem.*, 24 (1978) 1351.
11 R. R. Schroeder, P. J. Kudirka and E. C. Toren, Jr., *J. Chromatogr.*, 134 (1977) 83.
12 T. D. Schlabach, S. H. Chang, K. M. Gooding and F. E. Regnier, *J. Chromatogr.*, 134 (1977) 91.
13 J. F. K. Huber, K. M. Jonker and H. Poppe, *Anal. Chem.*, 52 (1980) 2.
14 D. N. Vacik and E. C. Toren, Jr., *J. Chromatogr.*, 228 (1982) 1.
15 M. Nakajima, A. Fukuhara and S. Morimoto, *Chem. Pharm. Bull.*, 30 (1982) 3328.
16 O. H. Lowry, N. J. Rosebrough, A. L. Farr and R. J. Randall, *J. Biol. Chem.*, 193 (1951) 265.
17 H. Kato, N. Adachi, S. Iwanaga, K. Abe, K. Takada, T. Kimura and S. Sakakibara, *J. Biochem. (Tokyo)*, 87 (1980) 1127.
18 Y. Matsuda, H. Moriya, C. Moriwaki, Y. Fujimoto and M. Matsuda, *J. Biochem. (Tokyo)*, 79 (1976) 1197.
19 K. Nustad, *Brit. J. Pharmacol.*, 39 (1970) 73.

Journal of Chromatography, 264 (1983) 258–263
Elsevier Science Publishers B.V., Amsterdam — Printed in The Netherlands

CHROM. 15,844

Note

Effect on column efficiency of packing capillary columns with inert spheres for use in liquid chromatography

HERNAN J. CORTES
The Dow Chemical Company, Analytical Laboratories, Midland, MI (U.S.A.)
(Received March 8th, 1983)

The limiting theoretical efficiency in liquid chromatography (LC) was defined by Giddings[1] as

$$N_{\text{lim}} = \frac{d_p^2 \, \Delta P}{4 \, \psi \, \gamma \, \eta \, D_m} \tag{1}$$

Where d_p = particle size, ΔP = pressure drop, ψ and γ = geometrical constants, η = viscosity and D_m = diffusional coefficient in the mobile phase.

Recent trends intended to increase theoretical plate count and speed of analysis in LC have centered on reducing particle size to a few micrometers[2], reducing column diameter in what are termed microbore columns[3,4] and using open tubular columns, analogous to capillary gas chromatography[5–7]. Due to high pressure drops encountered with a decrease in particle size, it is unlikely that significant advances can be made by reducing particle size below 3 μm.

Microbore columns have found utility; however, the limit in efficiency is determined by the eddy diffusion found in microparticulate packed columns. Open tubular columns offer an alternative to packed column liquid chromatography, and as shown by the Taylor equation[8] for an unretained component:

$$\frac{H}{\mu} = \frac{r^2}{24 \, D_m} \tag{2}$$

where H = theoretical plate height and μ = linear velocity.

It is evident that a decrease in capillary radius (r), and/or an increase in the diffusion coefficient in the mobile phase (D_m) should lead to a higher theoretical plate count. For capillary LC to compete with packed-column LC, Yang[9] indicated that

$$(h/v)_c \, d_c^2 < (h/v)_p \, d_p^2 \tag{3}$$

where h = reduced plate height, v = reduced velocity and d_c = capillary diameter.

Thus, capillaries of 10 μm or less are apparently necessary. The problems encountered with extra-column effects in the injector, detector and connections become considerable with such small columns.

0021-9673/83/$03.00

Various approaches have been taken in the attempt to utilize relatively large (100–250 μm) capillary columns, such as the introduction of secondary flow (radial redistribution of components across a capillary) by tightly coiling a column[10] or using geometrically deformed open tubes[11]. The present work describes the effect of packing 250-μm I.D. capillary columns with 175-μm glass beads. Such an approach proved effective in reducing band spreading in hollow fiber suppressors for ion chromatography[12].

EXPERIMENTAL

Chemicals

Chemicals used were reagent grade, available from Aldrich (Milwaukee, WI, U.S.A.). Solvents used were distilled in glass, available from Burdick & Jackson Labs. (Muskegon, MI, U.S.A.).

Liquid chromatography

The LC system consisted of a Jasco UVIDEC 100-II detector equipped with a modified cell[13], whose volume was calculated as 48 nl from the capillary diameter and the slit size. Wavelength used was 235 nm at 0.005 a.u.f.s.

A Valco injector was used in the split injection mode, where the tip of the capillary column was used as the splitter, and a needle valve controlled the flow into the columns. The pump used was a Waters Assoc. Model M-6000, at a flow-rate of 1.0 ml/min. The eluent throughout this work was hexane with 0.07% methanol.

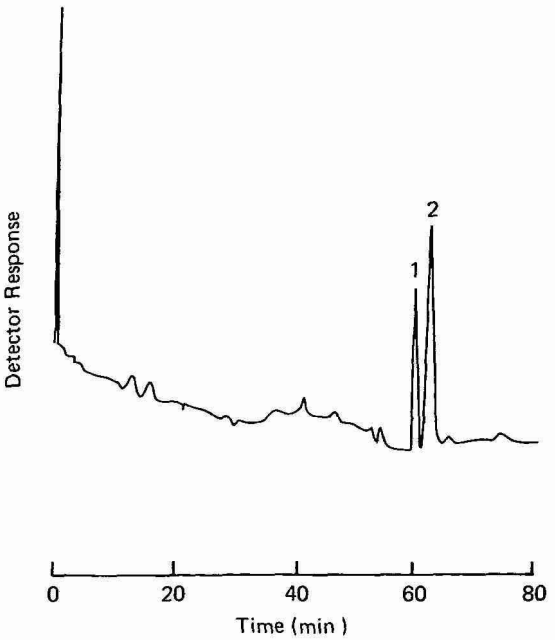

Fig. 1. Separation of nitrobenzene (1) and acetophenone (2) on a 5 m × 250 μm I.D. column. Eluent, hexane–methanol (99.93:0.07); flow-rate, 1.2 μl/min; detector, Jasco Uvidec 100-II at 235 nm; split ratio, 1000:1. Injected components were prepared to give concentrations of 1000 μg/ml.

Columns

Columns were prepared from soft glass by drawing 0.25 in. O.D. × 1 mm I.D. tubes in a glass-drawing machine. Column dimensions were 0.25 mm I.D. × 0.80 mm O.D. after drawing. The surface of the capillary was treated with 1 *N* sodium hydroxide solution for 48 h at 30°C, as reported by Ishii *et al.*[14], and then washed with methanol and methanol–hexane.

The column was packed with 175-μm glass beads available from Duke Scientific (Palo Alto, CA, U.S.A.), by applying vacuum and drawing the beads while the column was immersed in an ultrasonic bath.

RESULTS AND DISCUSSION

A 5-m sodium hydroxide-treated column was evaluated by injecting a mixture of nitrobenzene and acetophenone. A separation was obtained at the conditions listed in Fig. 1. Plate heights obtained as a function of linear velocity for nitrobenzene, the unretained component, are plotted in Fig. 2. The theoretical plate heights calculated from the Taylor equation were also plotted and are included for comparison, indicating an acceptable agreement. The same column was then packed with 175-μm glass beads as described in the Experimental section and evaluated in a similar manner (Fig. 3).

Comparing Figs. 1 and 3, it is evident that both the unretained and retained components are sharper in Fig. 1, the unpacked capillary. We expected to obtain sharper peaks in the packed capillary due to the introduction of secondary flow caused by the packing.

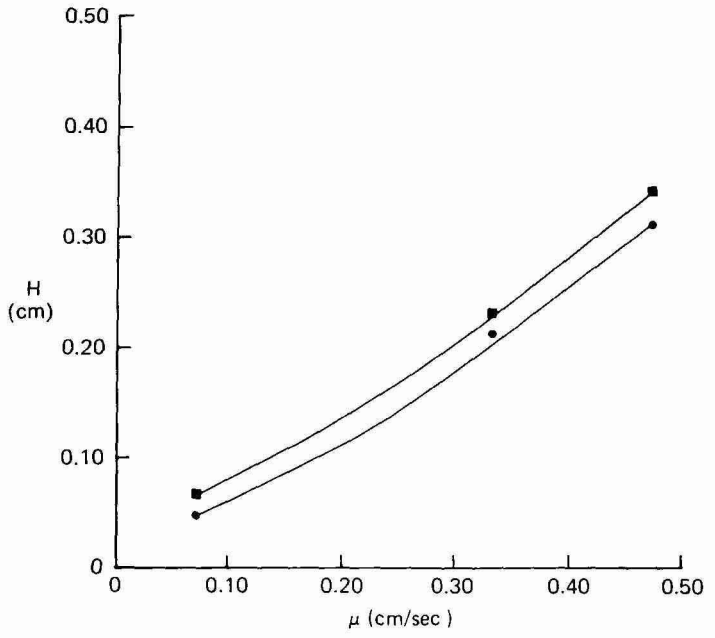

Fig. 2. Plot of plate height *vs.* linear velocity for open tubular 250-μm I.D. column; ● = theoretical; ■ = experimental.

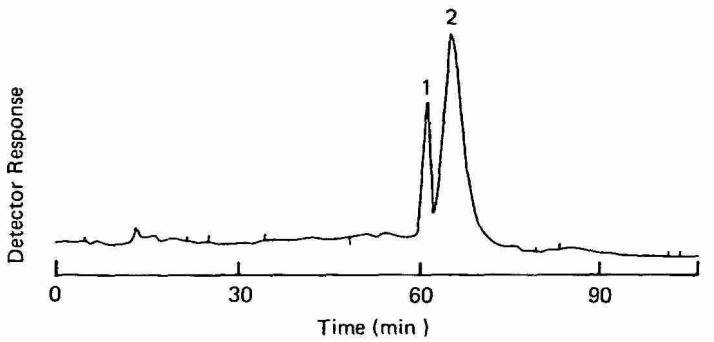

Fig. 3. Separation of nitrobenzene (1) and acetophenone (2) on 5 m × 250 μm I.D. column packed with 175-μm spheres. Conditions as in Fig. 1.

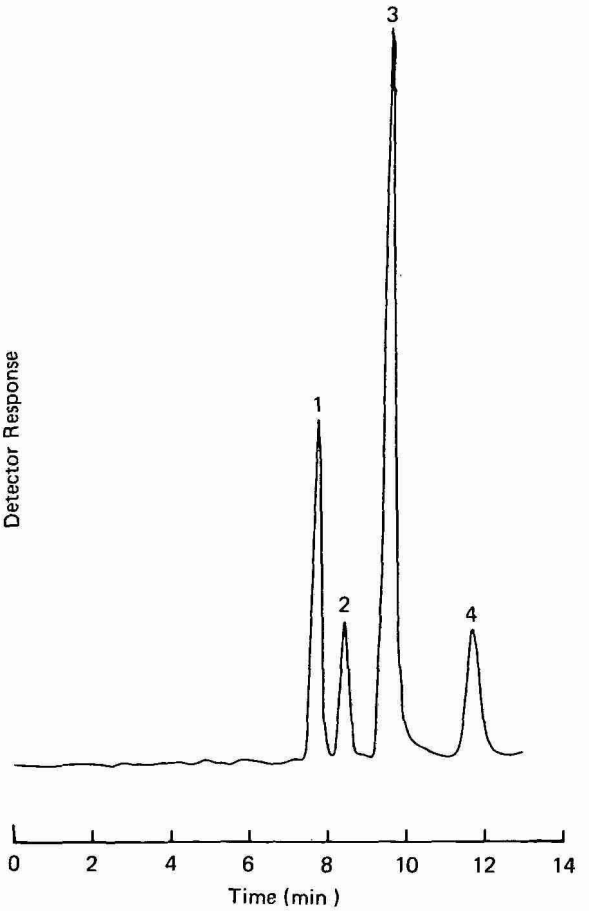

Fig. 4. Separation of pentamethylbenzene (1), nitrobenzene (2), benzaldehyde (3), and acetophenone (4) on 325 cm × 50 μm I.D. column. Conditions as in Fig. 1, except flow-rate, 0.83 μl/min.

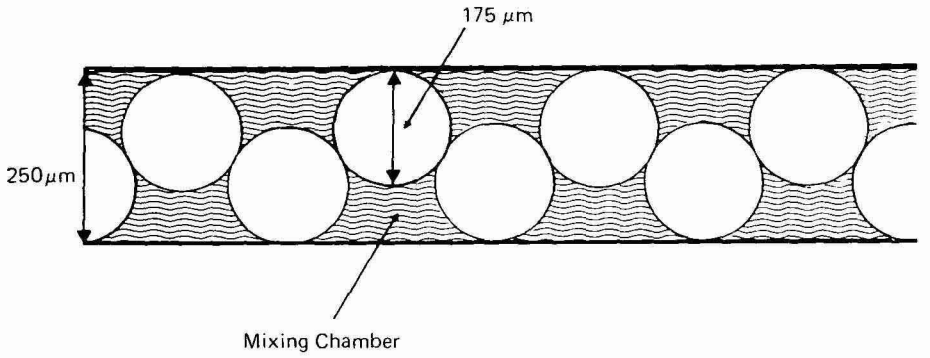

Fig. 5. Expanded view of capillary column packed with spheres.

Hofmann and Halász[11] reported a sharpening of unretained peaks and a broadening of retained peaks for geometrically deformed capillary columns. They attributed the phenomena to lack of a satisfactory method of coating a stationary phase on the capillary surface. In order to determine if that was the case in our system, a 50-μm I.D. column was treated as previously described and evaluated by injecting a mixture of pentamethylbenzene, nitrobenzene, benzaldehyde, and acetophenone (Fig. 4). The 2–10-fold decrease in efficiency of retained peaks described[11] was not observed, indicating a satisfactory coating technique.

We offer an alternate hypothesis: the flow velocity profile across an ideal capillary operated under laminar flow conditions is a parabola, and results in band broadening of eluting peaks. Creating secondary flow, *i.e.* radial mixing in a capillary, should reduce band broadening by radially redistributing the components across the capillary; however, in a system with inert spheres of *ca.* 0.7 capillary diameter size, voids exist between the stationary phase surface and the contact point of the bead (Fig. 5). At the linear velocities used, these voids can act as mixing chambers, described as the "tanks in series model"[15] by

$$c = \frac{1}{t'}\left(\frac{t}{t'}\right)^{N-1}\frac{1}{(N-1)!}e^{-t/t'} \tag{4}$$

where c = observed concentration, t' = mean residence time, N = number of mixing chambers, t = injection time. Thus, at large values of N, the variance observed on an eluting peak can be described as

$$\sigma^2 = Nt'^2 \tag{5}$$

explaining the results obtained.

CONCLUSIONS

The use of inert beads to induce secondary flow in capillary liquid chromatography does not increase theoretical plate count due to mixing chamber effects.

Both retained and unretained components experienced band-broadening when injected into 250-μm capillaries packed with 175-μm spheres. Although an improvement is seen on large-bore tubes[12], at smaller diameters open tubes appear to be more efficient.

ACKNOWLEDGEMENTS

The author thanks T. Stevens and G. Jewett for their helpful discussions.

REFERENCES

1 J. Giddings, *Anal. Chem.*, 36 (1964) 1890.
2 J. DiCesare, M. Dong and L. Ettre, *Chromatographia*, 14 (1981) 257.
3 R. P. W. Scott and P. Kucera, *J. Chromatogr.*, 169 (1979) 51.
4 R. P. W. Scott, P. Kucera and M. Munroe, *J. Chromatogr.*, 186 (1979) 475.
5 T. Tsuda and M. Novotny, *Anal. Chem.*, 50 (1978) 271.
6 T. Tsuda, K. Hibi, T. Nakanishi, T. Takeuchi and D. Ishii, *J. Chromatogr.*, 158 (1978) 227.
7 K. Hibi, T. Tsuda, T. Takeuchi, T. Nakanishi and D. Ishii, *J. Chromatogr.*, 175 (1979) 105.
8 G. Taylor, *Proc. Roy. Soc. London, Ser. A*, 219 (1953) 183.
9 F. J. Yang, *J. Chromatogr. Sci.*, 20 (1982) 241.
10 R. Tijssen, *J. Separ. Sci. Technol.*, 13 (1978) 681.
11 K. Hofmann and I. Halász, *J. Chromatogr.*, 199 (1980) 3.
12 T. Stevens, G. Jewett and R. Bredeweg, *Anal. Chem.*, 54 (1982) 1206.
13 F. Yang, *J. Chromatogr.*, 236 (1982) 265.
14 D. Ishii, T. Tsuda and T. Takeuchi, *J. Chromatogr.*, 185 (1979) 73.
15 J. Ruzicka and E. Hansen, *Flow Injection Analysis*, Wiley, New York, 1981.

Journal of Chromatography, 264 (1983) 264–271
Elsevier Science Publishers B.V., Amsterdam — Printed in The Netherlands

CHROM. 15,841

Note

Reversed-phase high-performance liquid chromatographic separation for pilocarpine and isopilocarpine using radial compression columns

DANNY L. DUNN*
Analytical Chemistry, Alcon Laboratories, Inc., 6201 South Freeway, Fort Worth, TX 76134 (U.S.A.)
and
RICHARD E. THOMPSON
Department of Chemistry, North Texas State University, Denton, TX 76203, and Texas College of Osteopathic Medicine, Fort Worth, TX 76107 (U.S.A.)
(Received March 8th, 1983)

The alkaloid pilocarpine is frequently used in ophthalmology to treat glaucoma because of its ability to lower intraocular pressure. In aqueous formulations pilocarpine has been observed to isomerize at the α-carbon to form isopilocarpine (Fig. 1). The rate of this isomerization is dependent upon pH and temperature[1]. Since isopilocarpine is pharmacologically inactive[2,3], a specific analysis for pilocarpine in the presence of isopilocarpine is highly desirable.

Because of a high separation capability and ease of use, several high-performance liquid chromatographic (HPLC) procedures have been reported. Originally, a separation for pilocarpine and isopilocarpine was described using Aminex A-7 cation-exchange resin with peak detection at 217 nm in the ultraviolet (UV)[4]. Later this system was reported to produce erratic results[2]. Khalil[5] used a μBondapak C_{18} column in series with a μBondapak CN column using detection at 254 nm to analyze for pilocarpine. Later investigators noted that the borate buffer (pH 9.2)–tetrahydrofuran (70:30) mobile phase gradually dissolved the column packing material[6].

More recently, several HPLC systems have been described that provide adequate separation between pilocarpine and isopilocarpine, and in addition, were used for the analysis of actual ophthalmic samples. Noordam and co-workers[7,8] and

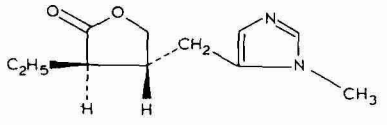

I

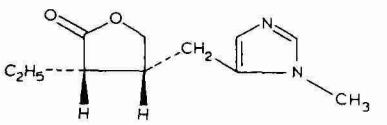

II

Fig. 1. The structures of pilocarpine (I) and isopilocarpine (II).

0021-9673/83/$03.00

O'Donnell and co-workers[9,10] have published essentially the same reversed-phase procedure which uses a water–methanol (97:3) mobile phase containing 5% monobasic potassium phosphate at pH 2.5 with a 10-μm RP-18 column. At first, refractive index detection was used, but finally both groups used UV detection at 215–216 nm. Dunn *et al.*[11] developed a normal-phase system using a mobile phase of 70:30 hexane–2% ammonium hydroxide in 2-propanol with a 5-μm Si60 column. Peak detection was at 220 nm. Finally Kennedy and McNamara[6] reported a reversed-phase procedure using a mobile phase of 5% aqueous monobasic potassium phosphate at pH 2.5 on a 10-μm μBondapak Phenyl column. Peak detection was at 215 nm.

Unfortunately, all these procedures either produce only a minimal resolution (R_s) between pilocarpine and isopilocarpine or require a lengthy elution time. We report here a reversed-phase HPLC separation for pilocarpine–isopilocarpine which produces a resolution (R_s) of 1.38 in an elution time of 6.9 min. A 5-μm C_{18} radial compression cartridge was used with a mobile phase of 8.7% 2-aminopropane, 14.6% methanol, 22.0% 2 *M* phosphoric acid, and 54.7% 0.15 *M* aqueous sodium sulfate at a flow-rate of 3.2 ml/min. Because of the complexity of the mobile phase and the numerous factors which could potentially effect the separation (*i.e.*, pH, ionic strength, polarity, column modification, etc.), a Simplex optimization program was utilized to find a statisfactory mobile phase composition and flow-rate.

EXPERIMENTAL

Materials

Isopilocarpine hydrochloride was purchased from Inland Alkaloid (Tipton, IN, U.S.A.). Analysis of this material by normal-phase HPLC[11] showed it to be a 42:58 mixture of pilocarpine hydrochloride and isopilocarpine hydrochloride. A 2.5 mg/ml solution of this sample was used without further purification as a convenient mixture to demonstrate separation of the two alkaloids. Pure USP-grade pilocarpine hydrochloride (Quimitra S.A., Merck) was used to establish the elution order. 2-Aminopropane was purchased from Aldrich (Milwaukee, WI., U.S.A.) and methanol was HPLC grade from Baker (Phillipsburg, NJ, U.S.A.). All other chemicals were reagent grade.

Chromatography

Separations were performed on a Waters Assoc. (Milford, MA, U.S.A.) radial compression module, Model RCM-100, using a 10 cm × 8 mm 5-μm Radial-Pak C_{18} cartridge. A Waters liquid chromatograph was equipped with a M6000A pump, a U6K syringe injector, and a Model 450 variable-wavelength UV detector. A Sargent (Dallas, TX, U.S.A.) Model SR strip-chart recorder was used. Injections of 5 μl were made and the detection wavelength was 220 nm.

Simplex algorithm

The Simplex method of optimization was first presented by Spendley *et al.*[12] and later modified by Nelder and Mead[13]. Our version of the Simplex algorithm provides for quadratic interpolations as suggested by Routh *et al.*[14], when (a) a successful reflection is followed by an unsuccessful expansion or (b) an unsuccessful

reflection is followed by a successful contraction. If the interpolation point is within a predefined narrow range of the centroid, it is rejected to avoid a collapse of the Simplex.

A general form of the objective function is shown in eqn. 1 and contains both resolution and time penalty components. The separation is considered to be optimized when maximum resolution is obtained in a minimum elution time. The specific objective function minimized is defined by eqn. 2.

$$F_{obj} = F_{sep} + F_{time} \tag{1}$$

where F_{sep} = chromatographic resolution function; F_{time} = time penalty function; and

$$F_{obj} = \sum_{i=1}^{N} 100\, e^{(1.5 - R_{s_i})} + (T_p - T_L)^3 \tag{2}$$

where N = number of peaks -1; R_{s_i} = resolution of the ith pair of peaks as conventionally defined[15]; T_p = elution time at which the penalty is to begin; and T_L = elution time for the last peak.

The time penalty is set to zero when $T_L < T_p$. It is added to the separation function in order to force selection of variables which tend toward shorter elution times. The free parameters for the optimization were as follows:

$$\alpha_1 = f_1 \tag{3}$$

$$\alpha_2 = \frac{f_2}{1 - f_1} \tag{4}$$

$$\alpha_3 = \frac{f_3}{1 - f_1 - f_2} \tag{5}$$

$$\alpha_4 = \text{flow-rate} \tag{6}$$

where f_1 was the mobile-phase fraction of 2-aminopropane, f_2 was the fraction of methanol, f_3 was the fraction of 2 M phosphoric acid (aqueous), and the fourth component of the mobile phase was 0.15 M sodium sulfate (aqueous) defined by:

$$f_4 = 1 - f_1 - f_2 - f_3 \tag{7}$$

Parameter constraints were defined as follows:

$$0 \leqslant f_1 \leqslant 0.15 \tag{8}$$

$$0 \leqslant f_2 \leqslant 1.00 \tag{9}$$

$$0 \leqslant f_3 \leqslant 0.30 \tag{10}$$

$$0.5 \leqslant \text{flow-rate} \leqslant 5.00 \text{ ml/min} \quad (11)$$

The time penalty was set to begin at times greater than 5 min.

RESULTS AND DISCUSSION

Radially compressed HPLC columns were chosen to produce an assay which required a minimal amount of time per injection. The excellent efficiency and low back-pressures exhibited by radially compressed columns supported this objective. Because free silanol groups are not completely end-capped on Waters Radial-Pak C_{18} columns, a column modifier was added to the mobile phase to eliminate peak broadening. When 2-aminopropane was used as a column modifier, an initial separation of pilocarpine and isopilocarpine was readily obtained using a phosphate buffer–methanol mobile phase.

Because of the many factors effecting the separation, a Simplex optimization program was used to find a satisfactory mobile phase composition and flow-rate. The Simplex algorithm described in the Experimental section has been used previously to optimize a number of HPLC separations[16–18]. The mobile phase consisted of four variable components, each representing key factors which control the separation. The mobile phase components were: (1) 2-aminopropane (to control the degree of column modification); (2) methanol (to vary polarity); (3) 2 *M* phosphoric acid (to vary pH); (4) 0.15 *M* sodium sulfate (to vary ionic strength). In addition, the flow-rate was also varied.

The objective function (F_{obj}) minimized in eqn. 2 consisted of two parts, chromatographic resolution (F_{sep}) and the time required for separation (F_{time}). The resolution factor (F_{sep}) was designed to vary exponentially so that no baseline resolution (*i.e.*, $R_s < 1.5$) would be penalized more severely than baseline resolution (*i.e.*, $R_s > 1.5$). Baseline resolutions give values less than 100. A time penalty function [$F_{time} = (T_p - T_L)^3$] was added in an attempt to obtain an acceptable resolution in a realistic time. If the time penalty was not added, the separation could have been obtained solely by increasing the polarity of the mobile phase causing broad peaks

TABLE I

SUMMARY OF EXPERIMENTS PERFORMED DURING OPTIMIZATION

Decimal numbers under each of the mobile phase components indicate volume fractional composition.

Point	*2-Aminopropane*	*Methanol*	*2 M Phosphoric acid*	*0.15 M Sodium sulfate*	*Flow-rate (ml/min)*
1	0.050	0.150	0.125	0.675	4.5
2	0.100	0.180	0.150	0.570	1.0
3	0.100	0.100	0.200	0.600	2.5
4	0.093	0.110	0.073	0.724	2.6
5	0.025	0.125	0.250	0.600	1.5
6	0.097	0.120	0.175	0.608	3.3
7	0.107	0.106	0.213	0.573	4.0
8	0.087	0.146	0.220	0.547	3.2

TABLE II

SUMMARY OF RESULTS OF EACH OF THE EXPERIMENTS PERFORMED DURING THE OPTIMIZATION UNDER CONDITIONS LISTED IN TABLE I

R_s, F_{sep}, F_{time} and F_{obj} are defined in the text. $T(1)$ and $W(1)$ are the retention time and width for the isopilocarpine peak, $T(2)$ and $W(2)$ are the retention time and width for the pilocarpine peak.

Point	*T(1) (min)*	*W(1) (min)*	*T(2) (min)*	*W(2) (min)*	R_s	F_{sep}	F_{time}	F_{obj}	*Resulting from*
1	7.95	0.65	9.09	0.71	1.68	84	68	152	Initial
2	8.13	0.51	8.64	0.55	0.96	171	48	219	Initial
3	8.09	0.51	8.80	0.59	1.29	123	55	178	Initial
4	3.11	0.37	3.31	0.49	0.47	282	0	282	Initial
5	7.28	1.61	7.46	1.61	0.11	401	15	416	Initial
6	3.78	0.31	4.13	0.33	1.09	150	0	150	Reflection
7	4.76	0.39	5.26	0.41	1.25	128	0	128	Expansion
8	6.14	0.51	6.87	0.55	1.38	113	7	120	Contraction

and undesirably long retention times. Having selected a relatively short target elution time (T_L = 5 min for this attempt), separation of pilocarpine and isopilocarpine was obtained by exploiting the selectivity factors of the mobile phase and not just polarity.

A summary of the mobile phases and flow-rates evaluated is in Table I. A summary of the objective function values is shown in Table II. The first five points are part of the initial Simplex. Points six, seven and eight were generated by the Simplex algorithm by a reflection, expansion, and a contraction, respectively. Since point. No. 8 achieved an acceptable resolution of 1.38 in 6.9 min., the search was terminated (see Fig. 2). This corresponded to a mobile-phase composition of 8.7% 2-aminopropane, 14.6% methanol, 22.0% 2 *M* phosphoric acid, and 54.7% 0.15 *M* sodium sulfate at a flow-rate of 3.2 ml/min. The resulting chromatogram is shown in Fig. 2.

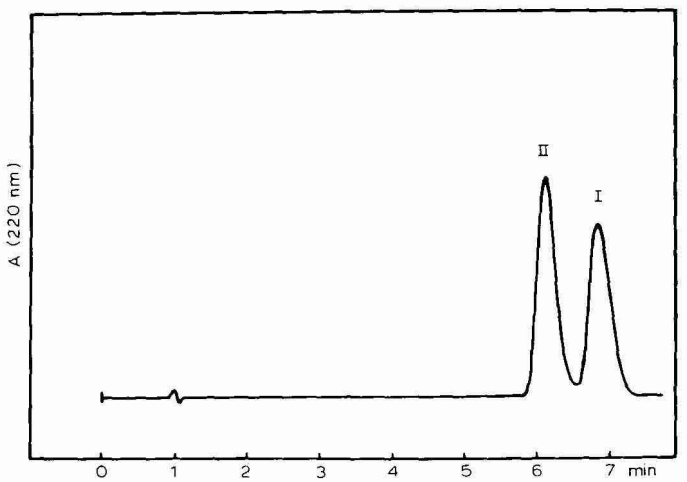

Fig. 2. The separation of pilocarpine (I) from isopilocarpine (II) using a mobile phase consisting of 8.7% 2-aminopropane, 14.6% methanol, 22.0% 2 *M* phosphoric acid, 54.7% 0.15 *M* sodium sulfate at a flow-rate of 3.2 ml/min.

TABLE III

SUMMARY OF PUBLISHED SEPARATIONS OF PILOCARPINE AND ISOPILOCARPINE

Method	*Column*	R_s	*Retention time* (min)*	*Retention time/R_s*	*Ref.*
A	C_{18}	1.10**	15.4 (Pilocarpine)	14.0	7
B	C_{18}	0.95**	11.7 (Pilocarpine)	12.3	9
C	Si 60	2.13	21.9 (Isopilocarpine)	10.3	11
D	Phenyl	0.91**	13.1 (Pilocarpine)	14.3	6
E	Radial-Pak C_{18}	1.38	6.9 (Pilocarpine)	5.0	–

* The retention time of the longest eluting peak of the pilocarpine–isopilocarpine pair.

** R_s values were not reported. They were estimated from measuring the chromatograms given in the references listed.

Because of the many factors involved, prediction that this mobile-phase composition could produce a satisfactory separation would be difficult even for an experienced chromatographer. The presence of 8.7% 2-aminopropane, which is normally considered as a column modifier, is unusual. The Simplex method of optimization thus appears to be an extremely powerful empirical technique which can produce unique and original mobile phase combinations based only on the demands of the separation and not on preconceived ideas.

Table III compares this separation of pilocarpine and isopilocarpine with other separations reported in the literature. Clearly, a higher resolution in a shorter time has been achieved. This is illustrated by a comparison of the ratio of retention time to R_s shown in the fifth column of Table III. Using this criterion, method E is clearly the most satisfactory.

In order to evaluate this HPLC separation as a potential method of analysis for ophthalmic solutions, a commercially available 10% pilocarpine hydrochloride

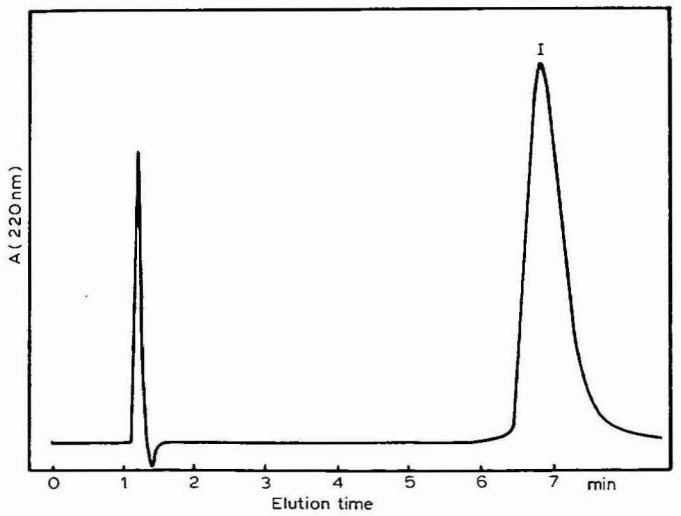

Fig. 3. The elution of pilocarpine (I) from a 10% ophthalmic solution.

solution was diluted to 1.0 mg/ml with water and analyzed using a single-point standard. The chromatogram is shown in Fig. 3 and 102.0% label was obtained. Another degradation product of pilocarpine, pilocarpic acid, was prepared by basic hydrolysis as previously described[6,8]. An injection of this material eluted on the solvent front and did not interfere with either the pilocarpine or isopilocarpine peaks. This is not the situation for other previously reported C_{18} separations[7–10], were pilocarpic acid was found to elute after the pilocarpine and isopilocarpine peaks. This suggests that perhaps a different separation mechanism was involved using this mobile phase and a Radial-Pak C_{18} column.

Because the mobile phase is fairly basic, an extended experiment was devised to check column degradation. The HPLC system was equilibrated and an initial plate count of 6455 plates/m for pilocarpine was calculated. The mobile phase was then pumped through the column for 70 h and another plate count of 6095 plates/m was calculated. This is only a 6% change and it seems that the column should not be greatly degraded with normal day-to-day use. However, the R_s value for pilocarpine and isopilocarpine was noted to vary from column to column, and the mobile phase composition usually needed an adjustment to produce optimal results.

CONCLUSIONS

HPLC separation for pilocarpine and isopilocarpine has been obtained using a Radial-Pak C_{18} column with a mobile phase of 8.7% 2-aminopropane, 14.6% methanol, 22.0% 2 *M* phosphoric acid, and 54.7% 0.15 *M* sodium sulfate at 3.2 ml/min. A resolution of 1.38 was achieved in an elution time of 6.9 min. This is a definite improvement over other reported HPLC separations and represents a potential routine method of analysis for pilocarpine ophthalmic solutions.

In addition, it is also apparent that the Simplex algorithm can provide an efficient search strategy in complex chromatographic systems where the effect of several interdependent variables on the separation are difficult to predict. Furthermore, the use of an elution time penalty with solvent flow-rate as a variable resulted in the identification of conditions consistent with both an acceptable resolution and an acceptable separation time.

ACKNOWLEDGEMENTS

We thank Tyler Tull, Waters Associates, for many helpful discussions and overall support of this project, and also acknowledge support of the project by NTSU Faculty Research.

REFERENCES

1 J. D. Weber, *J. Ass. Offic. Anal. Chem.*, 59 (1976) 1409.
2 R. K. Hill and S. Barcza, *Tetrahedron*, 22 (1966) 2889.
3 T. A. Anderson and J. B. Cowle, *Brit. J. Ophthalmol.*, 52 (1968) 607.
4 T. Urbanyi, A. Piedmont, E. Willis and G. Manning, *J. Pharm. Sci.*, 65 (1976) 257.
5 S. K. W. Khalil, *J. Pharm. Sci.*, 66 (1977) 1625.
6 J. M. Kennedy and P. E. McNamara, *J. Chromatogr.*, 212 (1981) 331.
7 A. Noordam, K. Waliszewski, C. Olieman, L. Maat and H. C. Beyerman, *J. Chromatogr.*, 153 (1978) 271.

8 A. Noordam, L. Maat and H. C. Beyerman, *J. Pharm. Sci.*, 70 (1981) 96.
9 J. J. O'Donnell, R. P. Sandman and M. V. Drake, *J. Pharm. Sci.*, 69 (1980) 1096.
10 M. V. Drake, J. J. O'Donnell and R. P. Sandman, *J. Pharm. Sci.*, 71 (1982) 358.
11 D. L. Dunn, B. S. Scott and E. D. Dorsey, *J. Pharm. Sci.*, 70 (1981) 446.
12 W. Spendley, S. R. Hext and F. R. Himsworth, *Technometrics*, 4 (1962) 441.
13 J. A. Nelder and R. Mead, *Computer J.*, 7 (1965) 308.
14 M. W. Routh, P. A. Swartz and M. B. Denton, *Anal. Chem.*, 49 (1977) 1422.
15 L. R. Snyder and J. J. Kirkland, *Introduction to Modern Liquid Chromatography*, Wiley-Interscience, New York, 2nd ed., 1979, p. 34.
16 M. W. Watson and P. W. Carr, *Anal. Chem.*, 51 (1979) 1835.
17 M. L. Rainey and W. C. Purdy, *Anal. Chim. Acta*, 93 (1977) 211.
18 M. R. Detaevernier, L. Dryon and D. L. Massart, *J. Chromatogr.*, 128 (1976) 204.
19 M. A. Nunes and E. Brochmann-Hanssen, *J. Pharm. Sci.*, 63 (1974) 716.

Journal of Chromatography, 264 (1983) 272–278
Elsevier Science Publishers B.V., Amsterdam — Printed in The Netherlands

CHROM. 15,839

Note

Determination of volatile microimpurities in alkaline polymerizates and neutral propylene oxide polyethers by gas chromatographic headspace analysis

R. N. MOKEYEVA*, Y. A. TSARFIN and W. ERNST
Analytical Laboratory, All-Union Research Institute for Synthetic Resins, Vladimir (U.S.S.R.)
(First received March 15th, 1982; revised manuscript received March 10th, 1983)

Headspace gas chromatography (GC) has been used to determine the level of volatile impurities in propylene oxide alkaline polymerizates[1–3], enabling volatile products to be detected at contents within the range 0.001–0.0001%. Unlike direct chromatography, this procedure does not involve the use of solvent and avoids chromatographic column contamination with polymer moieties, while increasing the analytical sensitivity by two or three orders of magnitude.

The volatiles are determined by continuous gas extraction, resulting from the inert gas flow passing through the sample at a constant rate[4–7]. Two procedures are available:

(1) GC of the headspace over the polymerizate under steady-state conditions, with subsequent determination of the partition coefficient by continuous gas extraction;

(2) Dynamic method for discovering volatiles in the polymerizates based on the exponential decrease in the compound concentration in a vapour phase with gas extraction time, graphical calculation of its initial concentration in the vapour phase.

Both alternatives have been used in this study.

EXPERIMENTAL

Headspace GC and calibration were carried out with a Tsvet-5 chromatograph, flame ionization detector and 3 × 0.03 m glass column packed with 20% bis(2-cyanoethoxy-2-methoxyethyl) ether on Chromosorb W (60–80 mesh), at 55°C and an argon flow-rate of 38 ml/min.

Fig. 1 shows an equilibrium vapour phase chromatogram of propylene oxide polymerizates.

The instrument was calibrated with standard solutions of the analysed components in dichloroethane or propanol within the concentration range of 0.25–0.50%; 1–2 ml of solution were injected into the evaporator.

Peak parameters were calculated from the chromatogram and the amount of compound per 1 cm^2 of peak area was found from

$$T = \frac{V_1 d c}{A \cdot 100} \text{ g/cm}^2 \text{ or g/cm} \quad (1)$$

0021-9673/83/$03.00

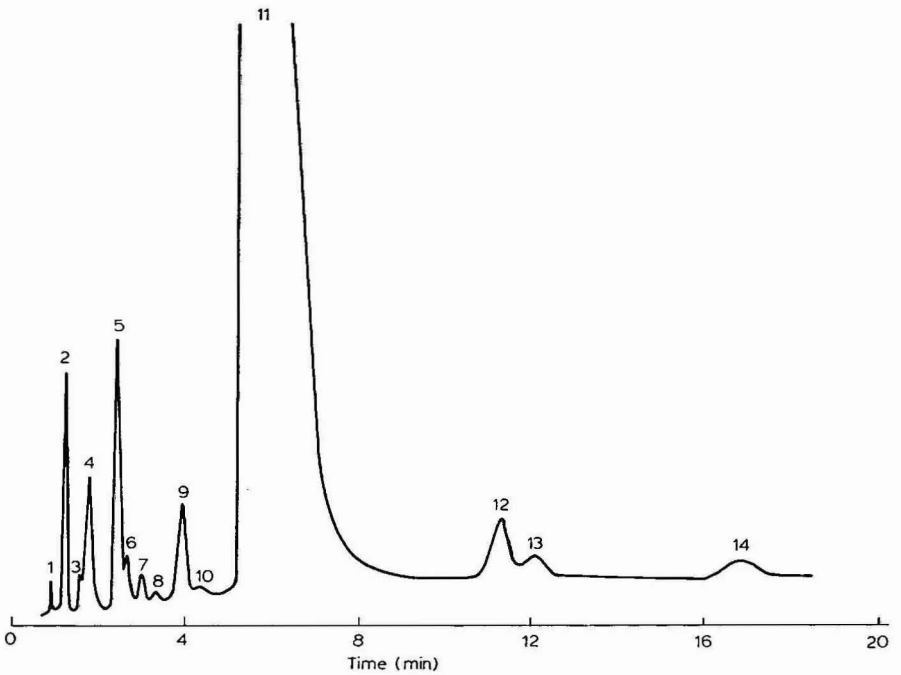

Fig. 1. Poly(propylene oxide) polyol gas phase chromatogram. Peaks: 1 = methane, $4.3 \cdot 10^{-4}$%; 2 = pentane, $3.9 \cdot 10^{-4}$%; 4 = hexane, $5.4 \cdot 10^{-4}$%; 5 = heptane, $6.2 \cdot 10^{-4}$%; 8 = ethylene oxide, $0.2 \cdot 10^{-4}$%; 10 = acetaldehyde, $0.2 \cdot 10^{-4}$%; 11 = propylene oxide, 5%; 12 = acetone, $8.9 \cdot 10^{-4}$%; 14 = isopropanol, $4.3 \cdot 10^{-4}$%. 3,6,7,9,13 = unidentified components.

where V_1 = injected volume (ml) of standard solution, d = solvent-specific gravity (g/ml), c = mass fraction (%) of analysed compound in standard solution, and A = parameter of chromatographic peak, area S (cm^2) or height h (cm), of analysed compound.

In the static procedure (1) the equilibrium vapour phase was injected with a glass medical syringe (PTFE piston) which had been previously conditioned in an oven at 70°C. The determination of the partition coefficient of volatiles in the polymerizate–argon system by continuous gas extraction and in the dynamic procedure (2) was effected by injections into the equilibrium vapour phase using a six-way gas distribution tap with a 1-ml loop. To avoid sorption and condensation of volatiles in the injector, supply lines and loop, the entire injection unit was maintained at 120°C in the chromatograph–detector thermostat (the electron-capture detector having been removed). The apparates for thermostating the samples and continuous gas extraction was supported over the thermostat containing the injection unit. It was closed with a silicone rubber plug and connected to the injector with a stainless-steel welded needle point capillary.

Due to the pronounced effect of temperature on the distribution of compounds between heterogeneous phases, the samples were conditioned in a water thermostat with an accuracy of ± 0.1°C.

The optimal sample thermostatting temperature varies with the nature of the

temperature dependence of the partition coefficient and with the stability of the system to be analyzed. The most suitable temperature for propylene oxide alkaline polymerizates was found to be 50°C at which samples thermostatted for 2–3 h brought about no appreciable change in compound concentration in the equilibrium vapour phase due to possible reactions with the alkaline medium. At 50°C, thermodynamic equilibrium in the polymerizate-argon system is attained within 15–30 min, as evidenced by the constancy of the analyzed compound concentration in the gas phase (see Fig. 2).

To determine volatile microimpurities in the propylene oxide polymerizates by the first procedure (1), up to 4.000 g of sample were placed in a 50-ml water-jacketed sample thermostatting vial which was then closed with a silicone rubber plug connected to a water thermostat and thermostatted at 50°C for 30 min.

The peak areas of the analysed components were calculated from the chromatogram of the equilibrium vapour phase sampled by a medical syringe, V ml, and the compound concentration in the gas phase was determined from:

$$C_g = T\,S/V \text{ g/ml} \qquad (2)$$

The partition coefficients of the components in the propylene oxide polymerizate–argon system were determined by continuous gas extraction using previously prepared compound–polymerizate mixtures within the concentration range of 0.001–0.01%. A 4-g amount of the mixture was placed in a 20-ml water-jacketed gas extraction vessel which then was connected to the water thermostat preheated at 50°C and through a welded metal needle capillary to the injection unit. Gas sampling was started 5 min after gas extraction commenced and was carried on until the peak area had changed two- or three-fold. It was timed to fit the compound retention times and the partition coefficient values.

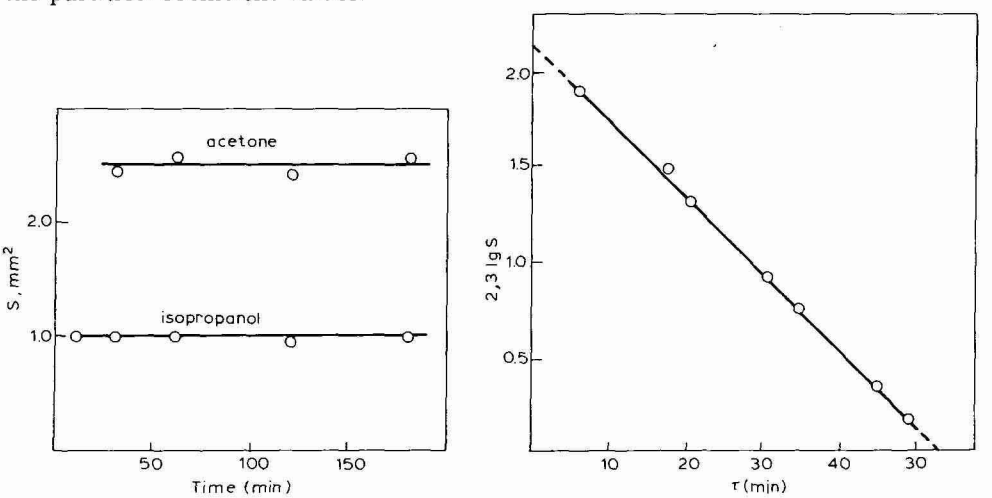

Fig. 2. Stabilization of acetone and isopropanol equilibrium concentrations in the alkaline polymerizate-argon system at 50° C. S = Peak area (mm²).

Fig. 3. Acetone peak area as a function of the duration of argon flow through the propylene oxide polymerizate. Thermostatting temperature: 50°C; v = 16.27 ml/min; V_1 = 4.27 ml.

The partition coefficients, K, were calculated from[8]

$$K = \frac{\tilde{v}\,(t_n - t_1)}{\ln \frac{S_1}{S_n} \cdot V_1} \tag{3}$$

where $\tilde{v}$ = gas flow-rate (ml/min), t_1, t_n = times (min) of the first and nth gas extraction samplings, S_1, S_n = peak areas of analysed compounds in the first and nth samplings and V_1 = volume (ml) of the polymerizate analysed. At least four samples were taken and the average partition coefficient calculated from three parallel equations.

The contents of the compounds in the propylene oxide alkaline polymerizate, C_1^0, was found using the observed values of C_g and K

$$C_1^0 = C_g\,(K + \frac{V_g}{V_1}) \tag{4}$$

where V_g is equilibrium gas phase volume.

In the dynamic approach (2), 4.000 g of the polymerizate were placed in a 20-ml gas extraction vessel maintained at 50°C. As in the case of the partition coefficient determination, sampling was performed 5 min after gas extraction had begun by means of an injector. The time intervals between injections were set in accordance with the retention time of the last peak. At least four gas extract samples were taken. Peak areas were calculated from the chromatograms obtained, and the value corresponding to the concentration of the component in the gas phase, C_g^0, at time τ = 0 min (Fig. 3), found by extrapolating the curve $\ln S = f(\tau)$ onto the y axis.

The content of an analysed compound in a sample was determined from

$$C_1^0 = C_g^0\,\tilde{v}/\beta\,V_1 \tag{5}$$

where β is the slope of the curve $\ln S = f(\tau)$.

RESULTS AND DISCUSSION

Eqn. 5 for the calculation of the content of volatiles in a non-volatile liquid (polymerizate) may be obtained from the relationship describing the decrease in content of volatiles in a solution as a result of an inert gas being passed through it at a constant rate, v (ref. 4)

$$\ln\frac{C_1^0}{C_1} = \frac{V_{gf}}{KV_1} \tag{6}$$

where V_{gf} = volume of gas flow during the time τ. Using the relationships $C_1 = KC_g$, $V_{gf} = \tilde{v}\tau$ and eqn. 2 at $v = 1$, eqn. 6 can be rewritten as:

$$\ln S = \ln \frac{C_1^0}{KT} - \frac{\tilde{v}}{KV_1} \cdot \tau \tag{7}$$

Eqn. 7 is linear and represents the peak area of the compound in the gas phase as a function of the gas extraction time, τ. Its slope $\beta = \tilde{v}/KV_l$, hence:

$$K = \tilde{v}/\beta V_l \tag{8}$$

With $\tau = 0$, eqn. 7 assumes the form:

$$S^0 = C_l^0/KT \tag{9}$$

Eqn. 5 may be inferred from eqns. 8 and 9:

$$C_l^0 = \frac{S^0 T\tilde{v}}{\beta V_l} = \frac{C_g^0 \tilde{v}}{\beta V_l}$$

The results obtained for the determination of the acetone content in alkaline polymerizates using eqn. 5 were compared (Table I) with those calculated from the equation suggested in ref. 4:

$$C_l^0 = C_g \cdot \frac{V_g - V_g^0}{V_l \cdot \ln \frac{A_g^0}{A_g}} \cdot \exp \left[\frac{V_g^0 \cdot \ln \frac{A_g^0}{A_g}}{V_g - V_g^0} \right] \tag{10}$$

It is noteworthy that eqn. 10 describes the continuous gas extraction model where the analysed compound is backflashed under the conditions of thermodynamic equilibrium between phases. In other words, as a gas bubble passes through a liquid layer, instantaneous exchange occurs not only between its volume and solution but also between above-the-liquid-surface volume and solution. Therefore, both the ex-solution bubble and the above-the-solution gas have equal concentrations of analysed compound[5].

The good agreement between the results calculated from eqns. 5 and 10 demonstrates the validity of eqn. 5. It also proves that the backflushing of volatiles from

TABLE I

ACETONE ANALYSIS IN PROPYLENE OXIDE ALKALINE POLYMERIZATES

$C \cdot 10^{-5}$ (g/ml)	
Eqn. 5	*Eqn. 10*
9.37	9.35
29.09	29.49
42.73	42.28
36.08	37.36
23.28	23.40
23.84	23.90

TABLE II

PRODUCT $C_g^i \tilde{v}^i$ FOR ACETONE AS A FUNCTION OF GAS FLOW-RATE IN THE ALKALINE POLYUMERIZATE–ARGON SYSTEM

$\tilde{v}^i$ (ml/min)	15	15.4	20.2	23	26	29.5	33	40.2	51	56
$C_g^i \cdot 10^{-7}$ (g/min)	13	12.5	13.0	12.5	12.7	13.0	12	12.6	13.5	12.5

propylene oxide polymerizates by the inert gas (argon) flow was carried out under thermodynamic equilibrium at all stages.

In this case loss of compound from the solution proceeds exponentially, and the concentration of a compound in the gas phase before the start of gas extraction (at $\tau = 0$) coincides with the maximum compound concentration in the gas phase. It enables the value of ln S^0 (hence C_g^0) to be found by extrapolating ln $S = f(\tau)$ onto the y axis at a preselected gas flow-rate.

According to our experimental data, the range of inert gas flow-rate which ensures maintenance of thermodynamic equilibrium is 15–60 ml/min. In this range the product $C_g^i \tilde{v}^i$ is constant irrespective of gas flow-rate (see Table II). Here C_g^i and $\tilde{v}^i$ are respectively the compound concentration in the gas phase and gas flow-rate at the time i.

The selection of which procedure to adopt depends on the content and qualitative composition of the impurities. When the content of impurities borders on the limit of sensitivity of the method it is useful to follow the first procedure (1), combining equilibrium vapour sampling with the dynamic analysis of partition coefficients in model mixtures of compounds in the polymerizates investigated. Should the amount of compound be sufficient for four gas phase extractions, it is advisable to resort to the second procedure (2), *i.e.*, continuous gas extraction.

Table III gives the results of volatiles analysis in propylene oxide polymerizates as well as the partition coefficients and mean-square errors, S.

The procedures suggested may also be used for analysis of neutral propylene oxide polyethers.

TABLE III

ANALYTICAL DATA FOR PROPYLENE OXIDE ALKALINE POLYMERIZATE AND POLYMERIZATE-ARGON SYSTEM PARTITION COEFFICIENTS AT 50°C

Compound	$C \cdot 10^{-4}$ *(%)*	$S \cdot 10^{-4}$ *($n = 8, r = 0.95$)*	K	S *($n = 10, r = 0.95$)*
Methane	4.3	0.4	5.75	0.10
Pentane	3.9	0.2	47.2	2.6
Hexane	5.4	0.9	78.2	2.3
Heptane	6.2	0.7	159.8	4.6
Ethylene oxide	0.2	0.02	23.8	1.2
Propylene oxide	–	–	61.0	1.4
Acetaldehyde	0.2	0.04	36.8	0.5
Propionaldehyde	–	–	46.6	2.2
Acetone	8.9	0.6	79.9	2.1
Isopropanol	4.3	0.3	60.4	2.6

CONCLUSIONS

To determine the content of methane, pentane, hexane, heptane, ethylene oxide, propylene oxide, acetic and propionic aldehydes, acetone and isopropanol microimpurities in propylene oxide polymerizates, two procedures have been proposed: static head space analysis with determination of partition coefficients by continuous gas extraction and continuous gas extraction analysis. For the latter we have suggested an equation and a method for the determination of the initial equilibrium concentration of the analysed compound in a gas phase by extrapolation of the curve $\ln S = f(\tau)$.

Thermodynamic equilibrium has been shown to be maintained in the gas extraction analysis of microimpurities in propylene oxide alkaline polymerizates within the flow-rate range of 15–60 ml/min.

Partition coefficients have been determined for microimpurities in the polymerizate–argon system.

REFERENCES

1 V. G. Berezkin, V. D. Loshtchilova, A. G. Pankov and V. D. Yagodivsky, *Chromato-distributional method*, Nauka, Moscow, 1976.
2 H. Hachenberg and A. P. Schmidt, *Gas Chromatographic Headspace Analysis*, Mir, Moscow, 1979.
3 A. G. Vittenberg and B. V. Ioffe, *Gas Extraction in Chromatographic Analysis*, Khimia, Leningrad, 1982.
4 A. G. Vittenberg and B. V. Ioffe, *Dokl. Acad. Sci., USSR*, 235 (1977) 1071.
5 A. G. Vittenberg and M. I. Kostkina, *Zh. Anal. Khim.*, 34 (1979) 1800.
6 M. G. Burnett, *Anal. Chem.*, 35 (1963) 1567.
7 I. A. Fowlis and R. P. W. Scott, *J. Chromatogr.*, 11 (1963) 1.
8 A. G. Vittenberg and B. V. Ioffe, *J. Chromatogr.*, 11 (1963) 41.

Journal of Chromatography, 264 (1983) 279–286
Elsevier Science Publishers B.V., Amsterdam — Printed in The Netherlands

CHROM. 15,847

Note

Liquid crystals

IV*. Study of the supercooling effect on laterally substituted liquid crystalline compounds**

D. G. PANSE*, S. M. LIKHITE, B. V. BAPAT and B. B. GHATGE
National Chemical Laboratory, Pune 411 008 (India)
(Received February 8th, 1983)

In earlier papers[1,2] we stated that for some laterally monosubstituted stationary phases, the retention time for any solute molecule decreases with increase in oven temperature. Near the crystal to nematic transition temperature retention times were found not to increase, which is the normal property of any liquid crystalline stationary phase. These phases have shown higher relative retention values for disubstituted aromatic hydrocarbons below the crystal to nematic transition temperature, *i.e.* in the solid state.

Studies of liquid crystalline stationary phases below their crystal to nematic transition temperatures have been carried out by several workers. Wasik and Chesler[3] reported the use of nematic liquid crystalline stationary phases 65°C below the crystal to nematic transition temperature of 181°C. Holzek and Gutwillinger[4] demonstrated the use of liquid crystals as stationary phase up to 65°C, which is 100°C below the crystal to nematic transition temperature. Liquid crystals as stationary phases in gas–liquid chromatography (GLC) have been studied below the crystal to nematic transition temperatures[5–7].

Janini and Ubeid[8] and others[9,10] have studied the effect of the solid support on the chromatographic properties of liquid crystalline stationary phases.

In this work, the objective was to investigate the extent of the supercooling property of laterally mono- and disubstituted liquid crystalline phases, liquid crystals having an azo group linkage in two aromatic rings being employed.

EXPERIMENTAL

The liquid crystals synthesized and used as stationary phases in column packing were of the formula

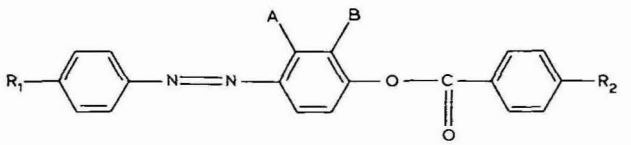

* For Part III, see ref. 12.
** N.C.L. communication No. 3215.

0021-9673/83/$03.00

TABLE I

LIQUID CRYSTALLINE COMPOUNDS AND THEIR NEMATIC RANGES

See formula in text.

Compound No.	R_1	R_2	*A*	*B*	*Transition temperature (°C)*	*Nematic range (°C)*
1	n-C_4H_9	CH_3	Cl	H	88–176	88
2	n-C_4H_9	C_2H_5	Cl	H	90–177	87
3	n-C_4H_9	n-C_4H_9	Cl	H	87–175	88
4	n-C_4H_9	CH_3	CH_3	CH_3	114–215	101
5	n-C_4H_9	n-C_4H_9	CH_3	CH_3	112–216	104
6	C_2H_5	n-C_4H_9	Cl	H	117 172	55

where A = Cl or CH_3, B = CH_3 or H, R_1 = ethyl or n-butyl and R_2 = methyl, ethyl or n-butyl. They were synthesized by the method reported previously[11]. Liquid crystals used to prepare stationary phases were thoroughly purified by repeated crystallization to give constant transition temperatures. Structures and transition temperatures are given in Table I.

The solid supports used were Celite (60–80 mesh), Chromosorb W AW, Chromosorb 750 and Anakrom ABS (60–80 mesh).

The usual method of impregnation is to transfer a solution of a weighed amount of liquid crystal in an appropriate solvent to a weighed solid support. Excess of solvent is removed gently on a water-bath below 60°C and the semi-dried, coated support is dried in an oven at 60–70°C.

To study the supercooling effect of liquid crystals, modified methods of impregnation were employed: (1) physical mixing and (2) impregnation by using a very low-boiling solvent such as diethyl ether.

Method 1

A weighed amount of support was placed in a stoppered bottle and a suitable amount of finely powdered liquid crystal of particle size 300–400 mesh was accurately weighed and added to the support material. The mixture was mixed in a roller mill for 48 h and then packed in a stainless-steel column of 180 cm × 2 mm I.D.

Method 2

The liquid crystalline compound was weighed accurately and dissolved in 25 ml of dry diethyl ether and the solution was poured onto the previously weighed solid support in an evaporating dish. The ether was removed at room temperature and the impregnated material, after having removed almost all of the ether, was kept in a desiccator for 24 h to remove any moisture. The support impregnated with liquid crystalline material was packed in a stainless-steel tube of 180 cm × 2 mm I.D.

The concentrations of all the stationary phases were 5% (w/w). The solutes were *m*- and *p*-xylene and *m*- and *p*-bromotoluene.

Apparatus

Retention times were obtained using a Hewlett-Packard 5730A gas chroma-

TABLE II

RETENTION TIMES OF LIQUID CRYSTALLINE STATIONARY PHASES PREPARED BY PHYSICAL MIXING METHOD

Support: Celite (60–80 mesh).

*Compound No.**	Temperature (°C)	m-Xylene		*m-Bromotoluene*	
		t_{R1} *(min)*	t_{R2} *(min)*	t_{R1} *(min)*	t_{R2} *(min)*
1	40	1.71	8.01	5.12	–
	50	1.27	5.12	3.31	–
	60	1.00	3.65	2.26	18.51
	70	0.81	2.77	1.64	–
	80	0.72	2.29	1.25	8.82
	90	1.68	1.78	6.29	6.41
	100	1.48	1.32	5.68	4.72
	110	1.30	0.95		
2	40	1.05	–	6.51	–
	50	0.89	–	5.63	–
	60	0.78	–	4.83	–
	70	–	3.93	4.71	18.80
	80	0.67	2.32	–	14.32
	90	1.73	1.61	6.82	10.13
	100	1.32	1.04	–	–
6	50	–	–	1.73	6.2
	80	–	–	0.73	5.32
	100	–	–	0.65	4.21
	122	–	–	1.27	3.52
	130	–	–	1.06	3.12

* Crystal to nematic and nematic to isotropic transition temperatures: compound No. 1, 88 and 176°C; compound No. 2, 90 and 177°C; and compound No. 6, 117 and 177°C, respectively.

TABLE III

RETENTION TIMES ON A LATERALLY DISUBSTITUTED LIQUID CRYSTALLINE STATIONARY PHASE

Compound No. 5: nematic range = 104°C.

Oven temperature (°C)	*m-Xylene*	
	t_{R1}(min)	t_{R2}(min)
60	1.326	1.319
70	1.23	1.216
80	1.79	1.76
90	0.65	0.6
100	0.52	0.5
115	1.54	1.523
120	1.4	1.37
125	1.25	1.23
130	1.16	1.14

TABLE IV

RETENTION TIMES OF COMPOUND NO.I ON DIFFERENT SOLID SUPPORTS

Support	*Temperature (°C)*	*m-Xylene*		*m-Bromotoluene*	
		t_{R_1} *(min)*	t_{R_2} *(min)*	t_{R_1} *(min)*	t_{R_2} *(min)*
Chromosorb G AW DMCS	25	2.95	–	14.92	–
	50	1.12	5.08	4.19	–
	60	0.86	–	2.74	–
	70	0.69	2.55	1.93	–
	80	0.58	1.89	1.50	8.84
	93	1.39	1.37	5.64	5.62
	105	1.07	1.05	3.9	3.86
	125	0.75	0.80	2.82	2.76
Chromosorb 750	25	–	–	–	–
	50	–	4.26	–	–
	60	–	–	–	–
	70	–	2.17	–	–
	80	–	1.65	–	–
	93	1.54	1.25	–	–
	125	1.12	0.67	–	–
Chromosorb W AW	25	–	–	–	–
	50	–	6.24	–	–
	60	–	–	–	–
	70	–	3.07	–	–
	80	–	2.3	–	10.49
	93	–	1.73	–	6.97
	105	1.38	1.33	5.04	4.77
	125	0.95	1.01	2.81	4.13

tograph equipped with a flame-ionization detector connected to a 3380A reporting integrator. The columns were not pre-heated. The oven, detector and injector temperatures were either each 100°C, or 100, 250 and 150°C, respectively. The carrier gas (nitrogen) flow-rate was 30 ml/min.

Retention times t_{R_1} were measured before the stationary phases had reached their crystal to nematic transition temperatures and t_{R_2} were measured after the phases had been heated above these temperatures.

Retention times recorded below and above the crystal to nematic transition temperature are reported in Tables II–IV.

RESULTS AND DISCUSSION

When retention times are recorded before the column is heated above the crystal to nematic transition temperature, the retention time (t_{R_1}) decreased as the oven temperature was increased up to the crystal to nematic transition temperature. At the crystal to nematic transition temperature an abrupt increase in retention time was observed, followed by a linear decrease in retention time with further increase in oven temperature (Fig. 1a).

Retention times (t_{R_2}) were again observed after keeping the column at room temperature for 24 h and maintaining all the parameters the same as before. It was

TABLE V

RETENTION TIMES AND RELATIVE RETENTION VALUES OF COMPOUND NO. 1 ON SUPPORTS IN THE SOLID STATE AND NEMATIC STATE

Support	*State*	*Oven temperature (°C)*	*Retention time (min)*		*Relative retention*	*Retention time (min)*		*Relative retention*
			m-Xylene	*p-Xylene*		*m-Bromotoluene*	*p-Bromotoluene*	
Cromosorb G AW DMCS	Before conditioning the column	50	1.12	1.14	1.0178	4.19	4.51	1.076
		80	0.76	0.75	1.00	1.5	1.6	1.066
	After heating the column above crystal to nematic transition temperature	50	5.08	5.76	1.1338	–	–	–
		80	0.58	0.59	1.10	8.84	10.43	1.179
Anakrom ABS	Before conditioning the column	50	1.34	1.44	1.074	5.81	6.8	1.17
		80	0.72	0.75	1.0416	2.16	2.32	1.074
	After conditioning the column	50	8.74	10.25	1.172	–	–	–
		80	3.27	3.67	1.122	–	–	–

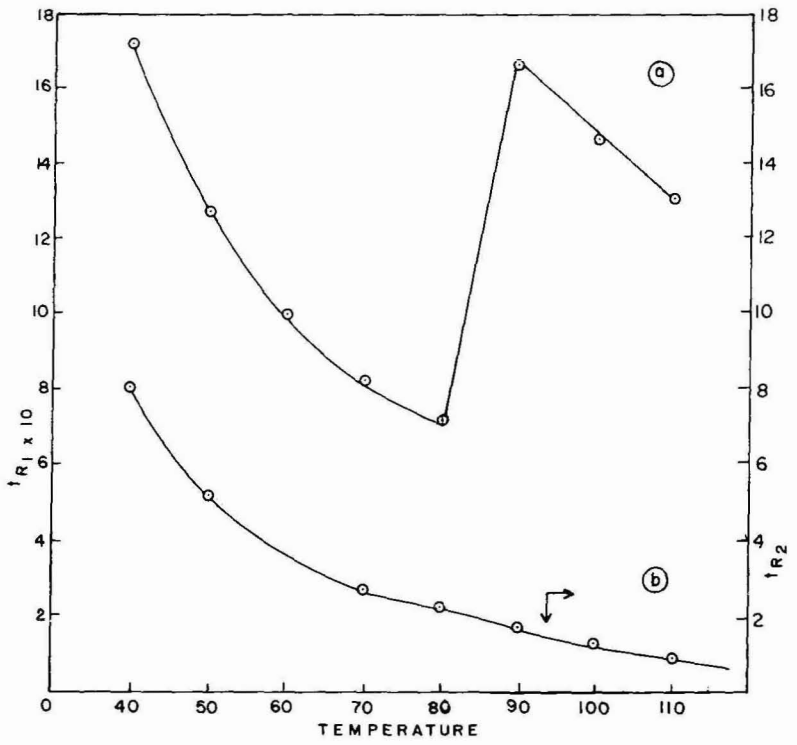

Fig. 1 Oven temperature (°C) *versus* retention time (min) for compound No. 1. For a and b, see text.

observed that the retention time decreased with increase in oven temperature and did not show any increase even at the crystal to nematic transition temperature (Fig. 1b).

A mixture of *m*- and *p*-xylene and *m*- and *p*-bromotoluene was analysed after keeping the columns for 3 months at room temperature (Table V); the gas chromatogram is shown in Fig. 2. No change in the pattern of retention time was observed (even after about 12 months); it was found to decrease linearly with increase in oven temperature and no increase in retention time was observed at the crystal to nematic transition temperature.

These liquid crystalline stationary phases were cooled at 0°C for 24 h in order to establish whether they are transformed into the crystalline state below room temperature. It was observed from the retention time data that they retain their supercooling nature even after cooling below room temperature and the retention time did not show sudden change at the crystal to nematic transition temperature.

The same patterns of retention time were observed when impregnation was effected using a low-boiling solvent (diethyl ether).

Study of different solid supports

In order to study the effect of the solid support, different packing materials [Chromosorb G AW DMCS (80–100 mesh), Chromosorb W AW (60–80 mesh), Chromosorb 750 (60–80 mesh) and Celite (80–120 mesh)] were employed for coating the liquid crystals.

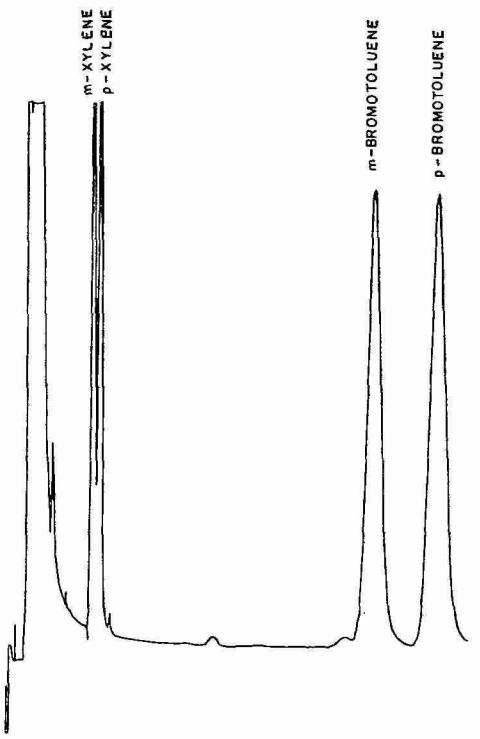

Fig. 2. Gas chromatogram of *m*- and *p*-xylene and *m*- and *p*-bromotoluene on column No. 1. Oven temperature, 70°C (20°C below the transition temperature); detector, 140°C.

Retention times were recorded below and above the crystal to nematic transition temperatures. Celite and Chromosorb W AW DMCS show absorption of solutes even before conditioning the columns, and retention times could be recorded both before and after conditioning of the columns above the crystal to nematic transition temperature.

However, Chromosorb 750 and Chromosorb W AW showed absorption of solutes only after conditioning the columns at 20°C above the crystal to nematic transition temperature and therefore retention times could be recorded only after conditioning the columns (Table IV).

Comparison of solubilities on mono- and disubstituted liquid crystalline phases

When solubility was measured for any sample molecule using a laterally monosubstituted liquid crystalline stationary phase, the retention time decreased linearly with increase in oven temperature. On the other hand, using a disubstituted liquid crystalline stationary phase the solubility of a sample molecule below the crystal to nematic transition temperature was poor and near this temperature it increased considerably and subsequently decreased with increase in temperature (Tables II and III).

It can therefore be inferred from the results that the laterally monosubstituted crystals exhibit supercooling properties even below room temperature for an indefinite period when they are coated on a solid support and do not attain their original

crystalline state. Moreover, they showed the same efficiency for isomer separation throughout the period.

This pattern has not been observed with laterally disubstituted liquid crystalline stationary phases having the same end groups. They are converted to the crystalline state as soon as they are cooled below their crystal to nematic transition temperature.

Applicability

As a result of their supercooling properties from ambient temperature, stationary phases of laterally monosubstituted liquid crystalline compounds are suitable for use in the analysis of low-boiling isomers such as xylenes to high-boiling isomers such as naphthalene and anthracene.

REFERENCES

1 K. P. Naikwadi, D. G. Panse, B. V. Bapat and B. B. Ghatge, *J. Chromatogr.*, 195 (1980) 309.
2 K. P. Naikwadi, D. G. Panse, B. V. Bapat and B. B. Ghatge, *J. Chromatogr.*, 206 (1981) 361.
3 S. Wasik and S. Chesler, *J. Chromatogr.*, 122 (1976) 451.
4 V. Hlozek and H. Gutwillinger, *Chromatographia*, 13 (1980) 234.
5 Z. Witkiewicz and S. Popiel, *J. Chromatogr.*, 154 (1978) 60.
6 Z. Witkiewicz, M. Pietrzyk and R. Daborwski, *J. Chromatogr.*, 177 (1979) 189.
7 M. S. Vigdergauz and R. V. Vigalok, *Mater. Nauchn. Konf. Inst. Org. Fiz. Khim. Akad. Nauk SSSR, 1969*, (1970) 166; *C.A.*, 78 (1973) 13180y.
8 G. M. Janini and M. T. Ubeid, *J. Chromatogr.*, 248 (1982) 217.
9 J. Rayss, L. Witkiewicz, A. Waksmundzki and R. Dobrowaski, *J. Chromatogr.*, 188 (1980) 107.
10 Z. P. Vetrova, N. T. Kavabnov and J. A. Jashin, *Chromatographia*, 10 (1977) 341.
11 D. G. Panse, B. V. Bapat and B. B. Ghatge, *Indian J. Chem.*, 21B (1982) 66.
12 P. P. Pawar, K. P. Naikwadi, S. M. Likhite, B. V. Bapat and B. B. Ghatge, *J. Chromatogr.*, 245 (1982) 57.

Journal of Chromatography, 264 (1983) 287–290
Elsevier Science Publishers B.V., Amsterdam — Printed in The Netherlands

CHROM. 15,845

Note

Supercooled liquid crystal gas chromatographic separation of the 2,4- and 2,5-xylyloxy isomers of gemfibrozil and xylenol

JEROME E. HAKY*, BOGUSLAWA LEJA and HORST G. SCHNEIDER
Chemistry Department, Warner-Lambert/Parke-Davis Pharmaceutical Research Division, Warner-Lambert Company, Ann Arbor, MI 48106 (U.S.A.)
(Received March 9th, 1983)

Gemfibrozil is the generic name for 2,2-dimethyl-5-(2,5-xylyloxy)-valeric acid, which has been demonstrated to be a safe and effective hypolipemic agent[1]. A potential contaminant in this drug is its 2,4-xylyloxy isomer, which would be the direct result of 2,4-xylenol contamination in the 2,5-xylenol from which the gemfibrozil was synthesized.

Gas–liquid chromatographic (GLC) determination of 2,4-xylyloxy isomer contamination in either gemfibrozil or 2,5-xylenol is difficult, owing to the close similarities in the physical properties of the isomeric compounds. GLC separation of 2,4-xylenol and 2,5-xylenol has been accomplished only through the utilization of highly specialized stationary phases, such as phthalates[2], sugar derivatives[3], and most recently, alkali-metal salts[4,5]. We report here the use of a popular commercially available liquid crystal stationary phase, N,N′-bis-(*p*-methoxybenzylidene)-α,α′-bi-*p*-toluidine (BMBT) for the efficient GLC separations of the easily prepared methyl esters of gemfibrozil and its 2,4-xylyloxy isomer and the benzyl ethers of 2,4-xylenol and 2,5-xylenol, both with sufficient resolution for the quantitative determination of 2,4-xylyloxy isomer contamination in either the drug or its 2,5-xylenol precursor.

EXPERIMENTAL

Materials

The liquid crystal stationary phase, 2.5% BMBT on 100–120 mesh Chromosorb W HP, was obtained from Alltech (Arlington Heights, IL, U.S.A.). The alkylating reagent dimethylformamide (DMF)–dimethylacetal (2 mequiv./ml in pyridine) was obtained from Pierce (Rockford, IL, U.S.A.) and the benzylating reagent benzyl bromide was obtained from Aldrich (Milwaukee, WI, U.S.A.).

Experimental and bulk samples of 2,4-xylenol and 2,5-xylenol were obtained from Aldrich, while samples of gemfibrozil and 2,2-dimethyl-5-(2,4-xylyloxy)valeric acid were synthesized in these laboratories using published procedures[6].

Derivatization reactions

Methyl esters of gemfibrozil and its 2,5-xylyloxy isomer. The sample to be analyzed (2 mg) was placed in a vial containing 250 μl of a solution of DMF–dimethyl-

0021-9673/83/$03.00

acetal in pyridine (2 mequiv./ml) and shaken until dissolved. This solution was used directly for GLC analysis.

Benzyl ethers of 2,4-xylenol and 2,5-xylenol. To 1 ml of methylene chloride containing 4 mg of the sample to be analyzed was added 1 ml of an aqueous solution which was 0.1 *M* in tetrabutylammonium hydrogen sulfate and 0.2 *M* in sodium hydroxide. Benzyl bromide (20 μl) was then added and the mixture was shaken for 20 min. Aliquots of the isolated methylene chloride phases were used directly for GLC analysis.

Apparatus and procedure

GLC analyses were performed on a Perkin-Elmer Model 910 gas chromatograph equipped with a flame ionization detector (FID) and a 6 ft. × 2 mm I.D. glass column packed with the BMBT stationary phase. Chromatograms were recorded and processed on a Varian Model 401 data system. Carrier gas (nitrogen) flow-rate was set at 10 ml/min, while hydrogen and air flow-rates were set at 30 and 300 ml/min, respectively. Solutions (5 μl for the gemfibrozil derivatives and 2 μl for the xylenol derivatives) were injected with a Hamilton 701N 10-μl syringe.

Routinely, samples of the gemfibrozil derivatives were analyzed at a column temperature of 135°C, while samples of the xylenol derivatives were analyzed at 160°C. In all cases, the column temperature was set by first heating the column to 200°C and then cooling to the operating temperature over a 10-min period.

Separation factors shown in Fig. 1 were calculated by the ratio of corrected retention times, using butane as an unretained substance for the determination of dead volumes.

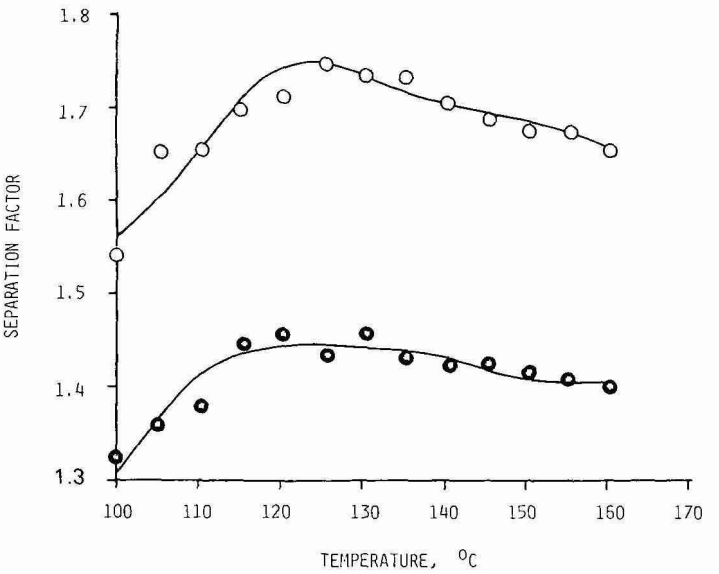

Fig. 1. Behavior of the separation factor with temperature on the BMBT column. ● = Gemfibrozil and 2,2-dimethyl-5-(2,4 xylyloxy)valeric acid methyl esters; ○ = 2,4-xylenol and 2,5-xylenol benzyl ethers.

RESULTS AND DISCUSSION

The liquid crystal stationary phase BMBT has been widely used for the GLC separation of positional isomers of a number of high-boiling compounds, including steroids[7], polychlorinated biphenyls[8], and 3–5-ring polycyclic aromatic hydrocarbons[9]. More recently, the ability of this stationary phase to remain in a supercooled liquid crystalline state below its normal solid–nematic transition temperature (181°C) has enabled it to be used at lower column temperatures for the analysis of more volatile 2-ring aromatic compounds, such as the isomers of dimethylnaphthalene[10,11]. It is this supercooling property, coupled with the proper choice of derivatizing reactions, which has now enabled BMBT to be used for the GLC separation and analysis of the single-ring aromatic compounds under study here.

Fig. 1 shows the behavior of the separation factors, α, between the 2,4- and 2,5-xylyloxy isomers of both the gemfibrozil methyl esters and the xylenol benzyl ethers, as the column is cooled in 5°C increments. For both sets of isomers, maximum separation occurs near the temperature corresponding to the supercooled nematic → solid phase transition for BMBT (*ca.* 120–125°C), which is consistent with previous

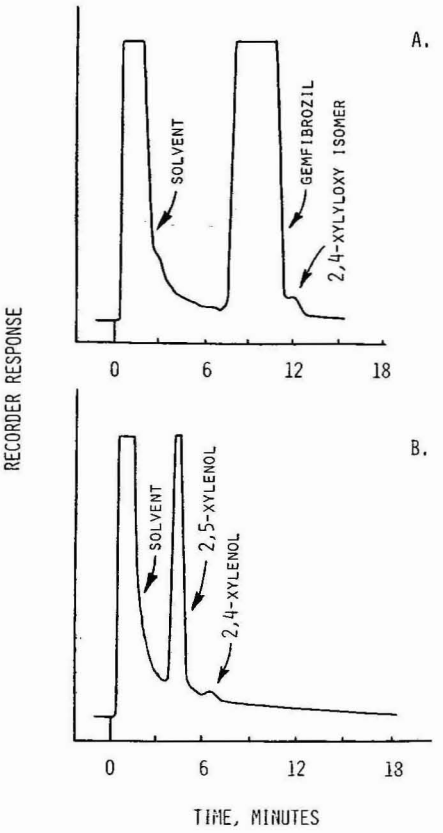

Fig. 2. Representative chromatograms from the GLC analysis of bulk lots. A, Gemfibrozil containing 0.3% 2,4-xylyloxy isomer contamination, column temperature = 135°C. B, 2,5-xylenol containing 0.7% 2,4-xylenol contamination, column temperature = 160°C.

studies of separations of dimethylnaphthalenes on the BMBT stationary phase[10,11]. At column temperatures below this phase transition, separation becomes poor and chromatographic peaks badly broaden, due to the loss of liquid crystalline order and selectivity in the stationary phase.

Separation of isomers on liquid crystal stationary phases has been ascribed to a geometric mechanism based on the retention of compounds in the order of their molecular length-to-breadth ratios[12]. The elution of the longer 2,4-xylyloxy isomers of gemfibrozil and xylenol subsequent to their corresponding 2,5-xylyloxy isomers on the BMBT column in this study is consistent with this mechanism. Moreover, the greater separation observed for the xylenol isomers than for the gemfibrozil isomers (Fig. 1) also follows this mechanism, since the flat, relatively rigid benzyl derivatives of the xylenol isomers would be expected to have greater differences in their average molecular length-to-breadth ratios than the flexible, branched isomers of the methyl ester of gemfibrozil. In any event, separation of either set of isomers is sufficient for the quantitative determination of 2,4-xylyloxy isomer present, although a lower column oven temperature is required to accomplish this determination in the analysis of gemfibrozil samples.

Representative chromatograms from the GLC analyses of bulk lots of both gemfibrozil and 2,5-xylenol on the BMBT column are shown in Fig. 2. Both show the presence of trace amounts (less than 1%) of 2,4-xylyloxy isomer contamination. Since FID detector response is virtually identical for isomeric compounds of this type[13], quantitation of the amount of the 2,4-xylyloxy isomer present is readily accomplished through area or height-percent calculations. The limit of detection for 2,4-xylyloxy isomer content by this procedure is at least 0.1% for either gemfibrozil or 2,5-xylenol.

CONCLUSIONS

In this study, utilization of the supercooled nematic thermal region of the stationary phase BMBT has allowed its use in the GLC determination of positional isomer contamination in bulk lots of a single-ring aromatic drug and its synthesis precursor. The utility of such a liquid crystal stationary phase in helping to define the isomeric purity of a bulk drug demonstrates a potential application for such stationary phases which has not been fully exploited. Investigations in these laboratories on similar applications are continuing.

REFERENCES

1 W. F. Bremner, J. L. Third, B. Clark, C. Corstophine and T. D. Lawrie, *Proc. Roy. Soc. Med., Suppl. 2*, 69 (1976) 83.
2 C. Landault and G. Guiochon, *Anal. Chem.*, 39 (1967) 713.
3 A. Ono, *Chromatographia*, 13 (1980) 574.
4 A. Bhattacharjee and A. N. Basu, *J. Chromatogr.*, 71 (1972) 534.
5 A. Bhattacharjee, D. K. Mukherjee and D. Guha, *J. Chromatogr.*, 247 (1982) 335.
6 P. L. Creger, G. W. Moersch and W. A. Neuklis, *Proc. Roy. Soc. Med., Suppl. 2*, 69 (1976) 3.
7 W. L. Zielinski. Jr., K. Johnston and G. M. Muschik, *Anal. Chem.*, 48 (1976) 907.
8 P. W. Albro, J. K. Haseman, T. A. Clemmer and B. J. Corbett, *J. Chromatogr.*, 136 (1977) 147.
9 G. M. Janini, K. Johnston and W. L. Zielinski, Jr., *Anal. Chem.*, 47 (1975) 670.
10 S. Wasik and S. Chesler, *J. Chromatogr.*, 122 (1976) 451..
11 J. E. Haky and G. M. Muschik, *J. Chromatogr.*, 238 (1982) 367.
12 H. Kelker, *Advan. Liquid. Cryst.*, 3 (1978) 237.
13 W. A. Dietz, *J. Gas Chromatogr.*, 5 (1967) 68.

Journal of Chromatography, 264 (1983) 291–296
Elsevier Science Publishers B.V., Amsterdam — Printed in The Netherlands

CHROM. 15,849

Note

Amino acid content of heparins

EDWARD A. JOHNSON*, PATRICK H. CORRAN and MARY PATERSON
National Institute for Biological Standards and Control, Holly Hill, Hampstead, London NW3 6RB (Great Britain)
(Received March 7th, 1983)

The configuration of "native" or "macromolecular" heparin, as released from (presumably) mast cell granules, has received attention over the past twenty years[1–6], but as yet its nature has not been settled. Whatever it may be, it is generally agreed that the heparin of commerce consists of unbranched single-chain fragments of the macromolecular form, which is not stable to commercial isolation procedures. These fragments are believed to derive from side-chains attached in some numbers to core molecules which have variously been thought to be polypeptide[3] or polysaccharide[4] chains. The side-chains have a molecular weight which is several times that of commercial heparin, so only a proportion of the molecules of the latter can retain anything of the side-chain-to-core linkage region; most are the product of mid-chain scission by an endoglycosidase[7]. As with other glycosaminoglycans the linkage region consists of a glucuronyl-galactosyl-galactosyl-xylosyl-O-serine sequence, of which the serine is regarded as part of the core. Recent work[6] concludes that the core is probably a peptidase-resistant poly(glycylserine). However, other amino acids have been persistently reported as being present in heparin hydrolysates[1,3,8], and Metcalfe *et al.*[9] have acknowledged that a number, chief among them aspartic and glutamic acids, appear to form part of the structure of larger proteoglycans constituting the native heparin of rat peritoneal mast cells. Since none of these amounted to more than a tenth of the serine or glycine present, Metcalfe *et al.* regarded the poly(glycylserine) model as largely valid.

In the course of collaborative work on the possible origin of small nuclear magnetic resonance signals from heparins, we were asked to check on the presence of amino acids in the samples. We found that, when using conventional amino acid analyser equipment, it was very difficult to be sure of the identity of ninhydrin-reacting compounds from heparin hydrolysates, and therefore investigated two more recent analytical procedures using high-performance liquid chromatography with pre-column derivatisation and fluorimetric detection[10,11]. The nature of the problem then became clear: with the higher resolution large numbers of peaks which could not be identified with known amino acids appeared on the chromatograms at all levels of intensity. It was reasonable to attribute them to basic breakdown products of glucosamine, since it had previously been reported that hexosamine yield, as observed on amino acid analyser traces, decreases with increase in the severity of hydrolysis conditions[8]. The interference so caused was sufficient to make it impossible

0021-9673/83/$03.00

to quantify, and in some cases even to detect with certainty, many amino acids, including the ubiquitous serine and glycine, even though two different procedures were available.

The greater part of the hexosamine was therefore destroyed before hydrolysis by reaction with nitrous acid, yielding, principally, anhydromannose residues from all except the N-acetylated glucosamines. This procedure yields much low-molecular-weight material, and to remove this the product was fractionated on Sephadex G-25; remaining peptide bound to the linkage region will be among the larger fragments. Hydrolysis of this material did in fact yield "cleaner" chromatograms on which identification of amino acids was usually unequivocal, though N-terminal amino acids and unprotected lysine would have been destroyed by the nitrous acid treatment. The proportions therefore were not necessarily those present in the heparin sample.

These procedures were applied to five samples of unbleached heparin, three porcine mucosal and one each porcine duodenal and bovine lung, and one sample each of bleached pharmacopoeial-quality porcine mucosal and bovine lung heparin.

EXPERIMENTAL

The porcine mucosal heparin samples were, in origin, as follows: (1) Evans Medical batch 630/2, unbleached; (2) Riker lot N4234; (3) Laboratori Derivati Organici "Fraction 8"; (4) Bioiberica lot F4. The porcine duodenal sample (5) was from Crinos Fraction F5. The bovine lung samples were: (6) Upjohn lot 730EH; (7) from a mixed glycosaminoglycan fraction, no reference, from Riker. Nos. 2, 3, 5 and 7 were more or less crude mixed products from which the heparins were isolated by fractional barium salt precipitation from aqueous solution using isopropanol[12] followed by precipitation as the potassium salts from strong potassium acetate solution[13]. Sample 1 was dissolved in 2 *M* sodium chloride solution and exhaustively dialysed to remove possible electrostatically bound peptide material, and samples 4 and 6, of pharmaceutical quality, were used as received. Sulphate-to-carboxylate ratios[14] ranged from 2.1 (sample 4) to 2.45 (sample 6), and in all samples glucosamine constituted 99% or more of the total hexosamine[15]. The detailed application of these purification and analytical procedures is discussed in ref. 16.

Deamination was carried out essentially as described by Shively and Conrad[17]. The heparin (200 mg) was dissolved in *ca.* 1 ml of water and mixed with *ca.* 5 ml of cold nitrous acid solution obtained by mixing equivalent volumes of chilled 0.5 *M* sulphuric acid and 0.5 *M* barium nitrite and centrifuging. After *ca.* 1 h at room temperature most of the excess of nitrogen oxides was removed by agitating under water pump vacuum, the product was precipitated with 2–3 volumes of ethanol, redissolved and reprecipitated with ethanol containing some sodium acetate, washed with ethanol and dried; the yield was *ca.* 130 mg.

Fractionation on Sephadex G-25 was carried out with 100-mg loads on a column (73 × 2.2 cm I.D.) with 0.1 *M* sodium chloride as eluent, flow-rate 30 ml/h. The detector was a Waters R403 differential refractometer. Four complex peaks eluted from each deamination product, of which the first two gave strong carbazole reactions for uronic acid. The first peak, K_{av} = 0–*ca.* 0.3, was collected for amino acid estimation. Desalting was performed using a column of Sephadex G-15, 37 × 1.4 cm I.D., with a Thorn-NPL type 243 polarimeter as detector.

Hydrolysis for amino acid determination was carried out in 4 *M* hydrochloric acid at 100°C for 16 h. The derivatisation and chromatographic procedures were essentially those of De Jong *et al.*[10] using 1-dimethylaminonaphthalene-5-sulphonyl chloride (Dns), and of Jones *et al.*[11] using *o*-phthaldialdehyde (OPTH). In both cases the column, 200 × 5 mm I.D., was packed with ODS-Hypersil (Shandon Southern). For the Dns procedure β-alanine was added to the sample before hydrolysis as an internal standard, and chromatography was run at ambient temperature. For the OPTH procedure α-aminooctanoic acid (Fluka) served as internal standard, solvent A was modified to tetrahydrofuran–0.05 *M* sodium acetate (pH 5.9) (1:99), solvent B remained methanol–sodium acetate (80:20), and the gradient was linear from 0% to 85% solvent B.

RESULTS AND DISCUSSION

The greater part of any tryptophan and cysteine present, and much of the methionine, are likely to have been destroyed during hydrolysis, though small peaks in the position of methionine were often observed. The tyrosine content was always insignificant. These amino acids are not listed in Table I.

Figs. 1 and 2 show that the reduction in interference by non-amino acid material after deamination is more pronounced with the OPTH system than with the Dns one, though still useful with the latter. Unfortunately, but not surprisingly, the elution sequence is rather similar with the two systems; a principal difference is that the basic arginine and histidine elute much earlier in the Dns sequence than in the OPTH one. With OPTH heparin hydrolysates yield an intense peak precisely in the arginine position (asterisked in Fig. 2), though after deamination its intensity is considerably, and disproportionately, reduced. In contrast, the Dns records show that arginine, which should elute immediately before serine, is substantially absent. Histidine estimation presents difficulties; in the Dns traces it is unidentifiable in the initial clutter of peaks, and with OPTH it is more or less obscured at the foot of the most intense of all the non-amino acid peaks, between serine and glycine. It is thus obscured in Fig. 2B, but other runs indicate that sample 7 does in fact contain a trace of histidine. With our OPTH system threonine was poorly resolved from glycine; it

TABLE I

AMINO ACID CONTENT OF HEPARIN SAMPLES

Sample No.	*Amino acid content (μmol/g)*												
	Asp	*Thr*	*Ser*	*Glu*	*Pro*	*Gly*	*Ala*	*Val*	*Ile*	*Leu*	*Phe*	*His*	*Lys*
1	1.5	2	20	2	1	4	1	0.5	0.5	1	0.5	tr*	tr
2	3	2	15	2	1	5	2	0.5	tr	0.5	tr	tr	tr
3	2	2	25	4	1.5	4	2	2	0.5	0.5	0.5	tr	tr
4	0.5	1	18	1	tr	2	0.5	0.5	tr	tr	tr	tr	tr
5	8	5	25	10	5	20	5	3	2	4	2	tr	5
6	1	1	1	1	tr	1	tr	tr	tr	tr	—	tr	tr
7	3	1	13	4	2	8	3	1.5	1	1.5	1	0.5	2

* tr = trace (*i.e.* less than 0.5).

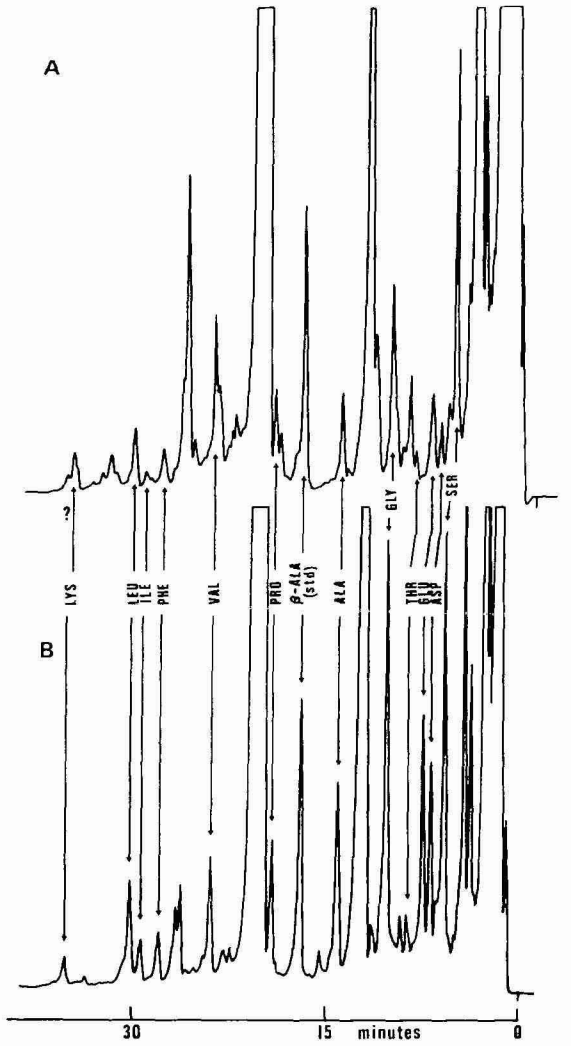

Fig. 1. Recorder traces (Dns procedure) of amino acids from sample 7. (A) Original sample. (B) First Sephadex G-25 fraction after deamination.

appears as a small spike on the tail of the glycine peak in Fig. 2B (and Fig. 2A). The two procedures are seen to be complementary.

None of the heparin samples contained more than 1% or so of peptide material, and no attempt is made to give values in Table I with precision. For some amino acids levels of less than 2 μmol/g may depend on somewhat subjective interpretations of recorder traces; sample 7 (Figs. 1 and 2) was richer than most in peptide material. The samples were all ultimately products of commercial processing, and they will all have undergone either treatment with strong alkalies (which cleave xylose-serine linkages[5]), autolysis, or treatment with proteolytic enzymes, or combinations of these, all resulting in the breakdown of peptide material whether covalently

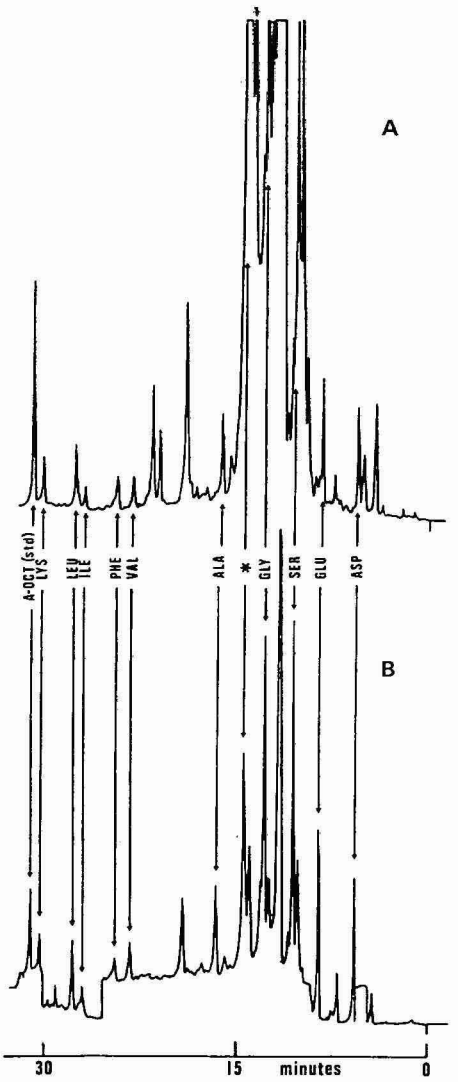

Fig. 2. As Fig. 1, OPTH procedure. For * see text.

bound or not. Some of the remaining bound serine might retain other linked amino acids, and it is to be expected that the amounts of these would bear some kind of inverse relation to their distance from the terminal serine in the chains. From the present work the order seems to be, with fair consistency, Ser > Gly > Glu > Asp > Thr = Ala, with Pro, Val, Leu, Lys, Ile and Phe almost always present as well. Contamination might be suspected, but the results on the two pharmaceutical-grade samples, 4 and 6, show that "bleaching" (with permanganate, peroxide or hypochlorite) is effective in removing all but traces of amino acids, except for serine and some glycine in sample 4. As far as can be judged, the deamination procedure does not much affect the relative proportions of amino acids, and the mass percentage in

the first fraction from Sephadex G-25 does not differ greatly from that in the original sample.

Some of these results are not readily interpretable. Nevertheless, it is quite difficult to reconcile the amino acid distributions found here —which are generally in good accord with those reported for similar samples by Lindahl *et al.*[1] nearly 20 years ago— with a poly(glycylserine) model, either in its simple form or with relatively minor variations as envisaged by Metcalfe *et al.*[9]. Samples such as we have examined, of various and largely unknown origins, may not be regarded as suitable material with which to develop ideas about the nature of the heparin "core", but nevertheless they are products of chain-shortening processes which would be unlikely to result in such radical rearrangement of the relative amino acid proportions. A structure which could yield such a result would consist of a chain, essentially of poly(glycylserine), linked by side-chains of other aminoacids to the "linkage region" serine (or glycylserine) —an indication of the problem rather than a serious speculation. It may be that the tissues from which commercial heparins are obtained contain heparin proteoglycans which differ from those of rat peritoneal mast cells or skin. Certainly it is easier to reconcile the rather consistent pattern of residual amino acids in commercial-type samples with the results of Serafini-Fracassini *et al.*[3] from ox liver capsule heparin, or even those of Oldberg *et al.*[18] from a heparan proteoglycan. Metcalfe *et al.*[9] were unable to estimate four amino acids because of hexosamine interference, and it may be that such difficulties have contributed to the variety of results reported.

ACKNOWLEDGEMENTS

We are most grateful to Dr. Prino (Crinos), Dr. De-Ambrosi (L.D.O.), Dr. Petracek (Riker), Dr. Buller (Upjohn) and to other manufacturers and colleagues for their generous provision of samples for this and related work.

REFERENCES

1 U. Lindahl, J. A. Cifonelli, B. Lindahl and L. Roden, *J. Biol. Chem.*, 240 (1965) 2817.
2 A. G. Lloyd, G. D. Bloom and E. A. Balasz, *Biochem. J.*, 103 (1967) 76P.
3 A. Serafini-Fracassini, J. J. Durward and L. Floreani, *Biochem. J.*, 112 (1969) 167.
4 A. A. Horner, *J. Biol. Chem.*, 246 (1971) 231.
5 R. W. Yurt, R. W. Leid, K. F. Austen and J. E. Silbert, *J. Biol. Chem.*, 252 (1977) 518.
6 H. C. Robinson, A. A. Horner, M. Höök, S. Ögren and U. Lindahl, *J. Biol. Chem.*, 253 (1978) 6687.
7 L. Jansson, S. Ögren and U. Lindahl, *Biochem. J.*, 145 (1975) 53.
8 C. C. Wang and L. B. Jaques, *Arzneim.-Forsch.*, 24 (1974) 1945.
9 D. D. Metcalfe, J. A. Smith, K. F. Austen and J. E. Silbert, *J. Biol. Chem.*, 255 (1980) 11753.
10 C. de Jong, G. J. Hughes, E. van Wieringen and K. J. Wilson, *J. Chromatogr.*, 241 (1982) 345.
11 B. N. Jones, S. Pääbo and S. Stein, *J. Liquid. Chromatogr.*, 4 (1981) 587.
12 S. Gardell, *Methods Carbohydr. Chem.*, 5 (1965) 9.
13 J. D. Scott, *Brit. Pat. 1,221,784 (1971).*
14 B. Casu and U. Gennaro, *Carbohydr. Res.*, 39 (1975) 168.
15 J. D. Navratil, E. Murgia and H. F. Walton, *Anal. Chem.*, 47 (1975) 122.
16 E. A. Johnson, *Pharmacol. Res. Commun.*, 14 (1982) 289.
17 J. E. Shively and H. E. Conrad, *Biochemistry*, 15 (1976) 3932.
18 Å. Aldberg, L. Kjellén and M. Höök, *J. Biol. Chem.*, 254 (1979) 8505.

Journal of Chromatography, 264 (1983) 297–303
Elsevier Science Publishers B.V., Amsterdam — Printed in the Netherlands

CHROM. 15,857

Note

Analysis of N-alkylphthalimides and N,N′-polymethylene-bis-phthalimides in industrial dye carrier formulations by gas chromatography-mass spectrometry

J. KOVAR, A. H. LAWRENCE*,* and D. MOCCIA
Laboratory and Scientific Services Division, Revenue Canada, Customs and Excise, Ottawa, Ontario K1A 0L5 (Canada)
(Received March 15th, 1983)

N-Alkylphthalimides (NAPs) (I) and N,N′-polymethylene-bis-phthalimides (NNPMBPs) (II) are valuable chemicals in many areas of industry. For example, NAPs are widely used as dye carriers for dyeing polyester/wool and polyester/cellulose triacetate fiber blends with disperse dyes[1]. In contrast to other dye carriers, these compounds are largely free from odour, non-toxic and biodegradable[2]. Similarly, N,N′-hexamethylene-bis-phthalimide was reported to improve the dyeability of polyester fibers[3].

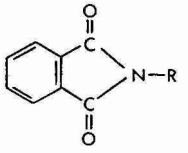

I

R = ethyl, isopropyl, *n*-butyl, *n*-pentyl, isopentyl

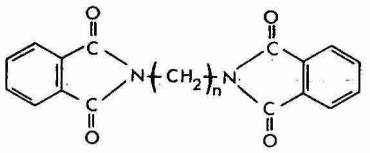

II

n = 2, 4, 6

The identification and determination of chemical components, including NAPs and NNPMBPs, in imported products is of importance for tariff classification purposes and is one of the major activities[4] of this laboratory. To this end, the usefulness of gas chromatography–mass spectrometry (GC–MS) for separating and identifying some of the NAPs and NNPMBPs used in dye-carrier formulations was investigated.

EXPERIMENTAL

Reagents and materials

Amines were obtained from Eastman (Rochester, NY, U.S.A.), Anachemia (Montreal, Canada) and Matheson Coleman and Bell (Norwood, OH, U.S.A.).

* Present address: Unsteady Aerodynamics Laboratory, National Research Council of Canada, National Aeronautical Establishment, Ottawa, Ontario K1A 0R6 Canada.

0021-9673/83/$03.00

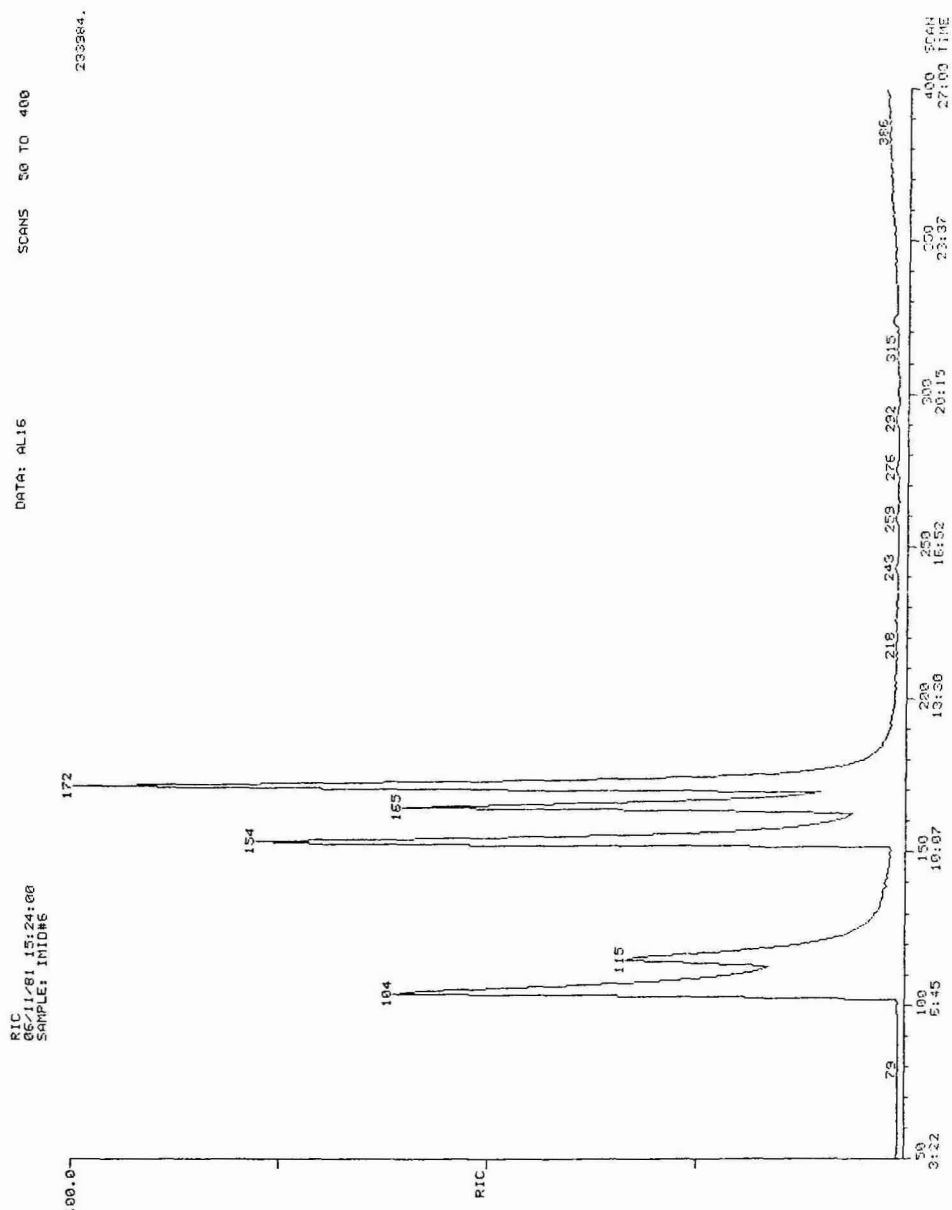

Fig. 1. Gas chromatographic separation of N-ethyl- (104), isopropyl- (115), *n*-butyl (154), isopentyl (165) and *n*-pentylphthalimide (172).

Phthalic anhydride and glacial acetic acid were obtained from Anachemia. All solvents used were analytical reagent grade.

Instrumentation and procedure

The gas chromatograph–mass spectrometer (Finnigan model 1020) was equipped with a jet separator, an electron impact source and a Nova 4 data system. The mass spectrometer was set up and tuned according to the manufacturer's instructions. The scanning rate was 4 sec/scan in the range 40–440 a.m.u. The GC instrument (Perkin-Elmer Sigma-3B) was fitted with a 3 ft. × 0.125 in. O.D. (WA–DMCS) stainless-steel column packed with 1.5% Dexsil 300®* on 60–80 mesh Chromosorb W. The oven temperature was kept at 100°C for 5 min then programmed to 350°C at 10°C/min. The injector temperature was maintained at 300°C and the carrier gas was helium, at 25 ml/min.

NAPs and NNPMBPs were prepared from phthalic anhydride and the corresponding amine according to the procedure described by Vanags[5,6]. NAPs and NNPMBBs were extracted from commercial dye carrier formulations with *n*-heptane. The completeness of the extraction was ascertained by the absence of the 1710–1780 cm^{-1} split carbonyl phthalimide band in the infrared (IR) spectrum of the extraction residue. IR spectra were recorded using a Digilab Model FTS-1C Fourier transform infrared spectrometer.

RESULTS AND DISCUSSION

Preliminary GC–MS analysis was performed using a synthetic mixture consisting of approximately equal amounts of N-ethyl-, isopropyl-, butyl-, pentyl- and isopentyl phthalimides (1.4% in toluene). The chromatogram resulting from the injection of 0.1 μl of the solution is shown in Fig. 1. A good separation was achieved with the Dexsil 300 column, selected for its stability at high temperatures. Fig. 2 shows the GC separation of three N,N′-polymethylene-bis-phthalimides with N-ethylphthalimide as reference (0.2-μl injection of a 0.7% toluene solution). The above results indicate that Dexsil 300 provides a versatile and suitable phase for the separation of the NAPs and NNPMBPs investigated.

The electron impact fragmentation pattern of NAPs and NNPMBPs has been previously reported[7,8]. Our mass spectra agree well with these published data and exhibit fragment ions typical of NAPs and NNPMBPs. The peak due to the cleavage of the C–C bond β with respect to the nitrogen was generally the most intense, *viz.* *m/e* 160 in N-ethyl-, butyl-, pentyl- and isopentylphthalimides, and in the polymethylene-bis-phthalimides; however, N-isopropylphthalimide exhibited a base peak at *m/e* 174. The expected fragment ions at *m/e* 146, 133, 130, 105 and 76 were also observed. In the case of N,N′-polytetramethylene-bis-phthalimide, a low-abundance ion at $m/e = 215$ (*i.e.* $M - 133$) was observed. The formation of the $[M - C_6H_4(CO)_2 + H]$ ion in the fragmentation pattern of NNPMBPs has been previously described[8].

Fig. 3 shows the trace obtained during the GC–MS analysis of a sample produced by solvent extraction of a commercial dye carrier formulation. Peak No. 134 consists of a major and a minor component. The selected ion monitoring technique

* Carborane–methylsilicone copolymer.

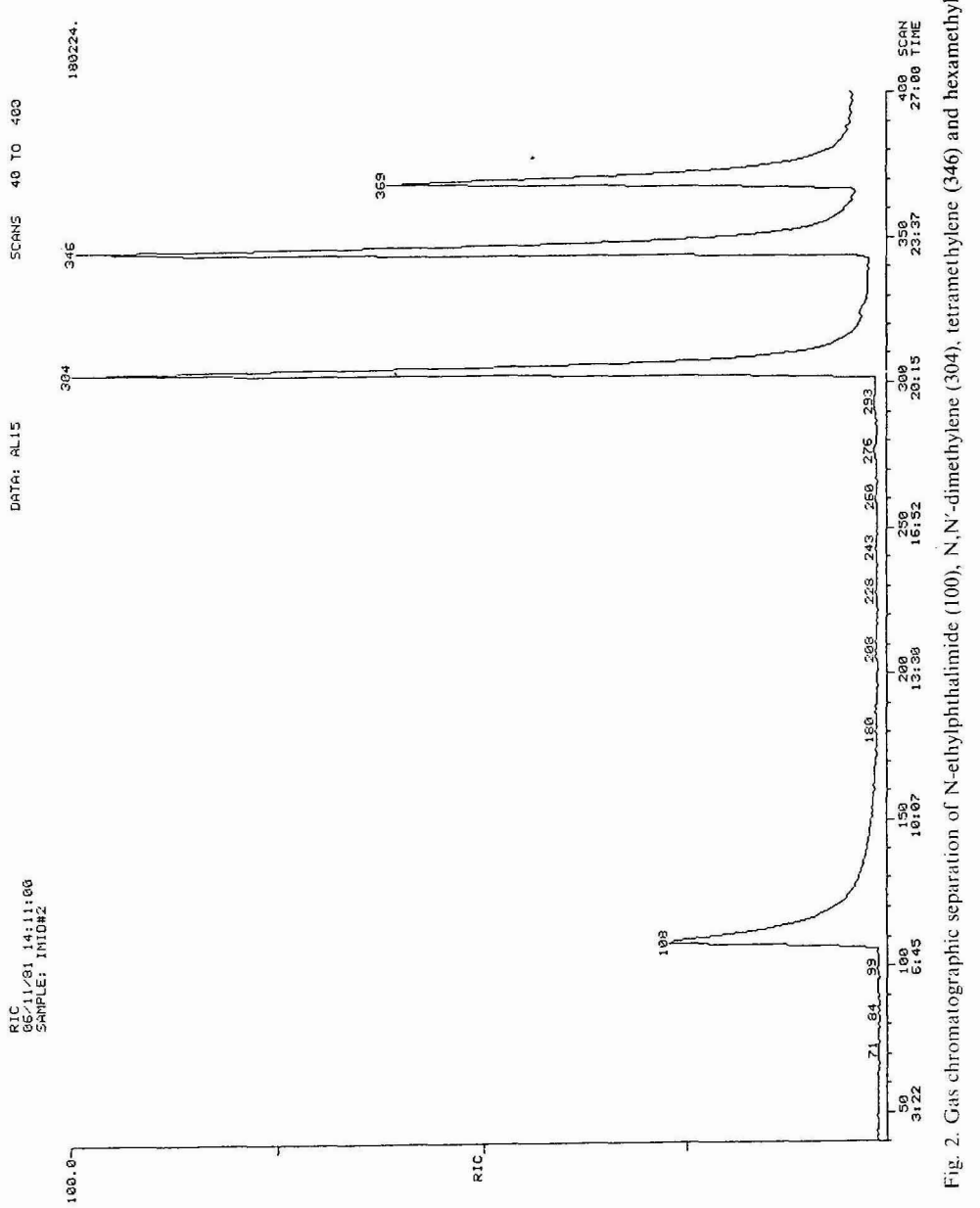

Fig. 2. Gas chromatographic separation of N-ethylphthalimide (100), N,N'-dimethylene (304), tetramethylene (346) and hexamethylene-bis-phthalimide (369).

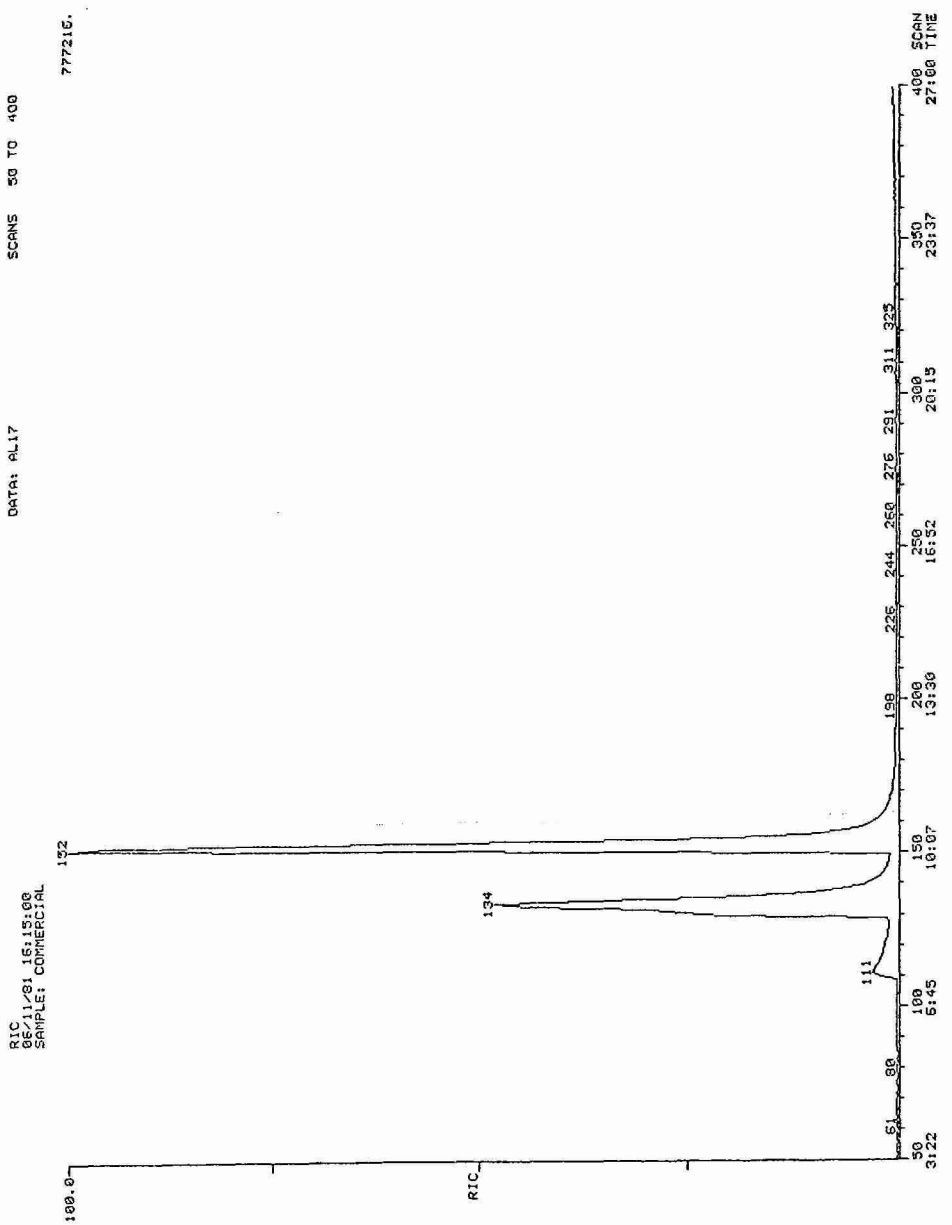

Fig. 3. Chromatogram of a NAP mixture obtained by solvent extraction of a commercial dye carrier formulation.

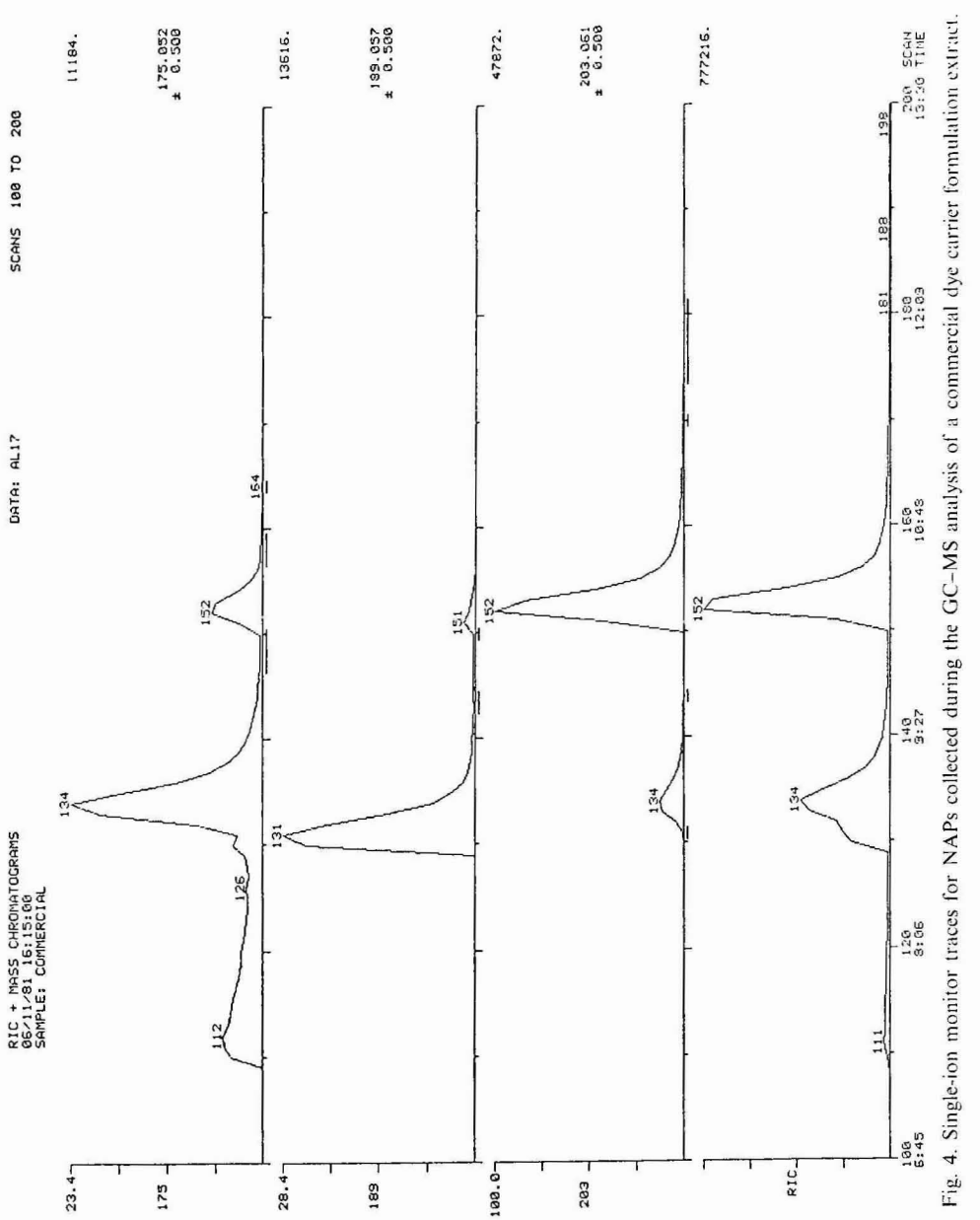

Fig. 4. Single-ion monitor traces for NAPs collected during the GC–MS analysis of a commercial dye carrier formulation extract.

provided the selectivity required for the specific identification of all the components in the mixture. The single ion monitor traces in Fig. 4 clearly indicate the presence of four components in the extract. The MS corresponding to peak no. 134 exhibited a molecular ion peak at *m/e* 203 (aliphatic side-chain with four carbon atoms) and a base peak at *m/e* 174 (*i.e.* $M - 29$) formed by β-cleavage of the C–C bond next to the nitrogen and loss of an ethyl group. Peak No. 134 was therefore identified as corresponding to N-*sec.*-butyl-phthalimide (III). The minor component at no. 131 gave a

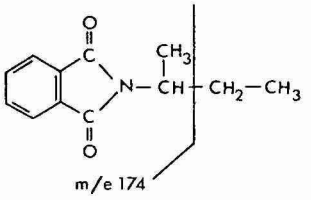

III

distinct mass spectrum consistent with the structure of N-*n*-propyl-phthalimide. Peaks 111 and 152 were identified as N-ethyl- and *n*-butylphthalimide, respectively, on the basis of comparison of their mass spectra with the spectra of authentic samples. No NNPMBPs were detected in the above commercial sample.

It is concluded that GC–MS is suitable as a rapid and specific technique (when the instrument is available) for the separation and identification of NAPs and NNPMBPs.

REFERENCES

1 W. Wolf, J. Eibl and K. Wojatschek, *Br. Pat.*, 1,193,948 (Cl. D 06p, 1970); *C.A.*, 73 (1970) 57097y.
2 F. H. Hassanein, *Can. Textile J.*, January (1972) 69.
3 J. R. Caldwell and R. Gilkey, *U.S. Pat.*, 3,386,795 (Cl. 8-100, 1968); *C.A.*, 69 (1968) 28539f.
4 A. H. Lawrence and D. Ducharme, *J. Chromatogr.*, 194 (1980) 434.
5 G. Vanags, *Acta Univ. Latviensis, Kim. Fakultat. Ser. 4*, No. 8 (1939) 405; *C.A.*, 34 (1940) 1982.
6 G. Vanags, *Ber.*, 75B (1942) 719.
7 R. T. Aplin and J. H. Jones, *J. Chem. Soc. C*, (1968) 1770.
8 P. A. Blanc, F. O. Gülaçar and A. Buchs, *Helv. Chim. Acta*, 62 (1979) 2230.

Journal of Chromatography, 264 (1983) 304–311
Elsevier Science Publishers B.V., Amsterdam — Printed in The Netherlands

CHROM. 15,834

Note

Gas chromatographic–mass spectrometric investigation of the volatile components of myrtle berries (*Myrtus communis* L.)

GIACOMO MAZZA
Istituto Sperimentale per l'Enologia, Sezione di Chimica Enologica, Via Pietro Micca 35, 14100 Asti (Italy)
(First received February 3rd, 1983; revised manuscript received March 7th, 1983)

Myrtus communis L., pertaining to the family of Myrtaceae, is an evergreen shrub typical of the Mediterranean area. It grows spontaneously in Spain, France, Tunisia, Algeria and Morocco. In Italy it enriches the Mediterranean scrub from Tuscan Maremma to Sicily. The essential oil, obtained from leaves and flowers, is used in perfumery but is also employed in cooking as an ingredient of sauces. Terpenes and terpene alcohols make up nearly the whole of the volatile compounds of the essential oil[1–4].

Myrtle berries, spherical in shape and dark red-to-violet in colour, are used in the formulation of bitters and Myrtle liqueurs.

The purpose of this work was to obtain a detailed picture of the volatile components of Myrtle berries, as no information is available in the recent literature. The investigation was carried out on berries from Sardinia, on alcoholic extracts obtained by cold infusion in aqueous alcoholic solutions of Myrtle berries of the same origin and on commercial samples of liqueurs.

EXPERIMENTAL

Crushed berries (25 g) were left in contact with 100 ml of methanol for 48 h. The methanol extract obtained after centrifugation was diluted to 500 ml in distilled water, 195 μg of 1-heptanol added as internal standard and the mixture continuously extracted with pentane–methylene chloride (60:40) for 8 h. The resulting extract was finally dried over Na_2SO_4 and concentrated. Liqueurs and alcoholic extracts were diluted to a 20% alcohol content before extracting them as above. The concentrations of the respective components were computed assuming equal responses for each with respect to 1-heptanol (standard).

Gas chromatography (GC) was performed using a Perkin-Elmer Sigma 3 gas chromatograph, with a 50 m × 0.2 mm fused silica capillary column coated with Carbowax 20M. Splitting ratio: 60:1. Temperature program: 5 min at 50°C then from 50°C to 180°C at 2°C/min. Carrier gas (helium) flow-rate: 1 ml/min.

Gas chromatography (GC)–mass spectrometry (MS) was carried out using a Hewlett-Packard 5992 B instrument equipped with a 50 m × 0.3 mm fused-silica capillary column, coated with Carbowax 20M. Splitless injection. Temperature program: 5 min at 50°C then from 50°C to 200°C at 3°C/min. Carrier gas (helium), flow-rate: 3 ml/min. Mass spectra were recorded at 70 eV.

0021-9673/83/$03.00

RESULTS AND DISCUSSION

A gas chromatogram of the volatile components from Myrtle berries (harvest 1982) obtained by extraction with pentane–methylene chloride (see Experimental) is shown in Fig. 1 (sample A). α-Pinene, limonene and 1,8-cineole make up 72% of the volatile fraction (percentages calculated without inclusion of the methyl esters pres-

TABLE I

IDENTIFICATION OF PEAKS IN FIG. 1

Peak No.	*Compound*	*Amount (mg/kg)*	*Mol.wt.*	*Peak No.*	*Compound*	*Amount (mg/kg)*	*Mol.wt.*
	Hydrocarbons				*Esters*		
5	α-Pinene	77.1	136	2	Methyl butyrate	0.1	102
7	β-Pinene	1.2	136	6	Butyl butyrate	0.1	144
8	*p*-Xylene	*	106	27	Dimethyl malonate	0.1	132
9	*m*-Xylene	*	106	32	Methyl benzoate	0.1	136
10	Δ^3-Carene	3.9	136	58	Methyl hexadecanoate	9.1	270
11	α-Phellandrene	0.6	136	62	Methyl octadecanoate	1.0	298
12	Myrcene	0.5	136		*Terpene esters*		
13	*o*-Xylene	*	106	29	Linalyl acetate	1.9	196
14	Limonene	18.4	136	38	α-Terpinyl acetate	2.7	196
16	*cis*-Ocimene	0.1	136	43	Neryl acetate	7.8	196
17	γ-Terpinene	3.6	136	47	Geranyl acetate	0.1	196
18	*trans*-Ocimene	0.3	136		*Phenols and phenol ethers*		
19	*p*-Cymene	5.7	134	36	Estragole	0.4	148
20	Terpinolene	1.3	136	46	Anethole	0.1	148
26	Unknown	*	57***	55	Phenol	1.1	94
30	β-Caryophyllene	1.0	204	56	Methyleugenol	2.3	178
35	α-Humulene	1.5	204		*Oxides*		
40	Unknown	0.7	204	15	1,8-Cineole	69.3	154
49	Unknown	0.1	204	23	Linalool oxide A	0.1	170
	Alcohols			25	Linalool oxide B	0.1	170
21	1-Hexanol	0.1	102		*Others*		
22	*cis*-3-Hexen-1-ol	0.1	100	1	Diethyl ketone	*	86
24	1-Heptanol	**		3	Ethyl isopropyl ketone	*	100
28	Linalool	6.0	154	4	Diisopropyl ketone	*	114
31	Terpinen-4-ol	2.2	154	41	Unknown	0.5	212
33	Unknown	0.1	154	57	Unknown	2.7	163***
34	*trans*-Pinocarveol	0.6	152	59	Unknown	0.7	152***
37	Unknown	1.8	152	60	Unknown	1.1	92***
39	α-Terpineol	8.3	154	61	Unknown	0.8	163***
42	*cis*-Piperitol	0.1	154	63	Unknown	0.9	43***
44	Myrtenol	0.1	152	64	Unknown	1.2	43***
45	Nerol	0.1	154	65	Unknown	7.9	43***
48	*trans*-Carveol	0.1	152	67	Dibutyl phthalate	*	278
50	*p*-Cymen-8-ol	0.3	150				
51	Geraniol	0.6	154				
52	Benzyl alcohol	0.3	108				
53	2-Phenylethanol	0.9	122				
54	3,7-Dimethyl-1,5-octadiene-3,7-diol	0.7	170				
66	Sesquiterpene alcohol	3.4	220				

* Compound extraneous to the berries.
** Internal standard.
*** Base mass peak.

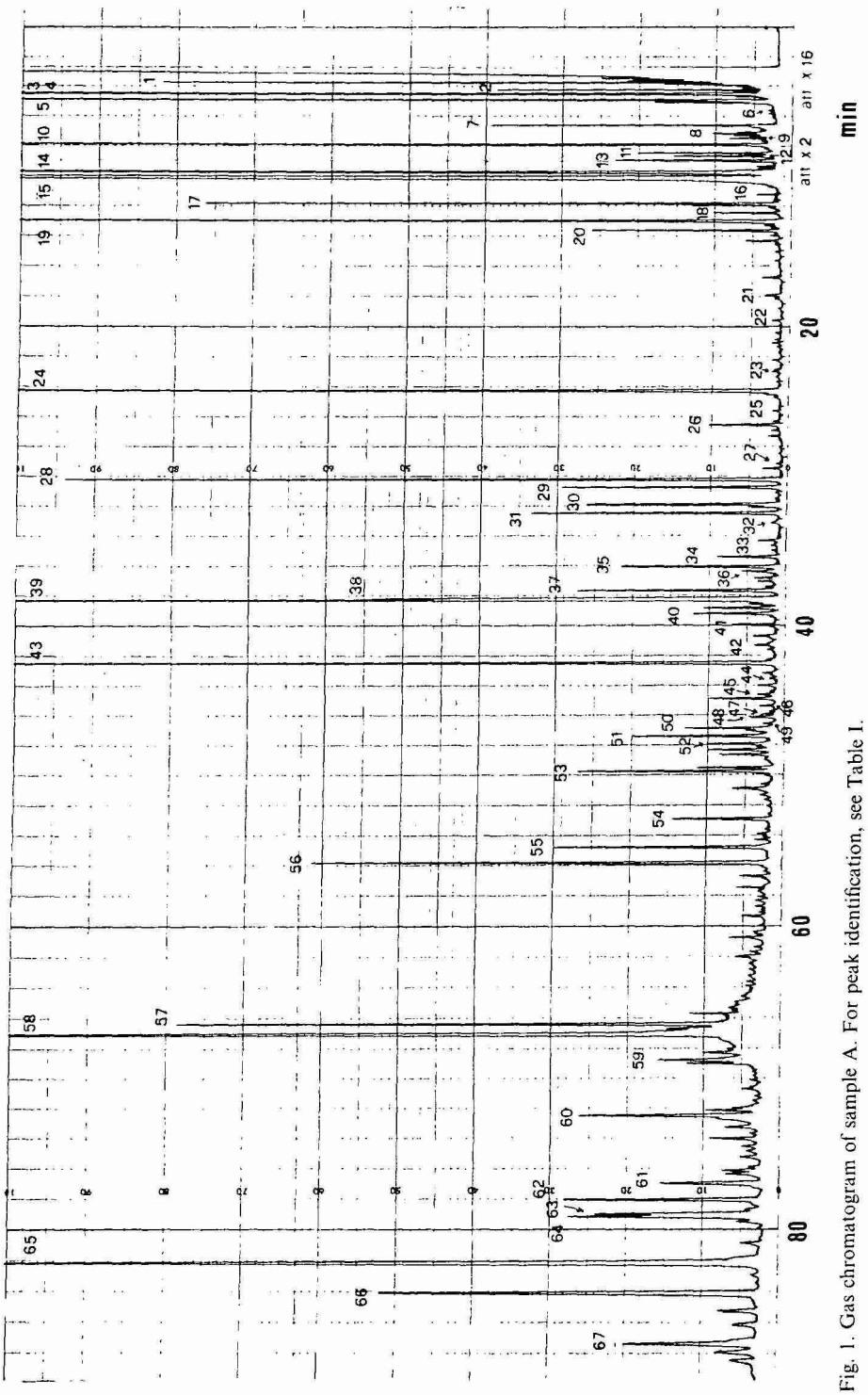

Fig. 1. Gas chromatogram of sample A. For peak identification, see Table I.

ent). Hydrocarbons form 51% of the volatile fraction. Eleven terpene hydrocarbons have been identified: the major ones are α-pinene, Δ^3-carene, limonene, γ-terpinene, *p*-cymene and terpinolene. Alcohols represent 11.1% of the volatile fraction, linalool and α-terpineol being the most abundant (57% of alcohol fraction), together with smaller amounts of terpinen-4-ol, *trans*-pinocarveol, *cis*-piperitol, *trans*-carveol and *p*-cymen-8-ol, which are not found in the essential oil from leaves and flowers[1–4]. The aromatic content of Myrtle berries differs from that of the latter essential oil also in

TABLE II

IDENTIFICATION OF PEAKS IN FIG. 2

Peak No.	*Compound*	*Mol.wt.*	*Peak No.*	*Compound*	*Mol.wt.*
1	Ethyl isobutyrate	116	37	Diethyl malonate	160
2	1,1-Diethoxy-2-methylpropane	146	38	Terpinen-4-ol	154
3	Diisopropyl ketone	114	39	Unknown terpene alcohol	154
4	α-Pinene	136	40	*trans*-Pinocarveol	152
5	Butyl acetate	116	41	Ethyl decanoate/α-Humulene	200–204
6	1,1-Diethoxy-2-methylbutane	160	42	Ethyl benzoate/Estragole	150–148
7	1,1-Diethoxy-3-methylbutane	160	43	Diethyl succinate	174
8	Isobutyl butyrate	144	44	α-Terpinyl acetate	196
9	β-Pinene	136	45	α-Terpineol	154
10	Δ^3-Carene	136	46	Unknown	85*
11	α-Phellandrene	136	47	Unknown	212
12	Myrcene	136	48	*cis*-Piperitol	154
13	Limonene	136	49	Neryl acetate	196
14	1,8-Cineole	154	50	Myrtenol	152
15	*cis*-Ocimene	136	51	Nerol	154
16	γ-Terpinene	136	52	Geranyl acetate	196
17	*trans*-Ocimene	136	53	Anethol	148
18	*p*-Cymene	134	54	*trans*-Carveol	152
19	Terpinolene	136	55	*p*-Cymen-8-ol	150
20	1,1,3-Triethoxypropane	176	56	Geraniol	154
21	3,7-Dimethyl-3-ethoxy-1,6-octadiene	182	57	Benzyl alcohol	108
22	Ethyl lactate	118	58	2-Phenylethanol	122
23	1-Hexanol	102	59	Unknown	76*
24	Unknown ethyl ether	182	60	3,7-Dimethyl-1,5-octadiene-3,7-diol	170
25	*trans*-3-Ethoxy-2(10)-pinene?	180	61	Methyleugenol	178
26	*cis*-3-Hexen-1-ol	100	62	Diethyl malate	190
27	4-Ethoxy-1-*p*-menthene	182	63	Unknown	236
28	*cis*-3-Ethoxy-1-*p*-menthene	182	64	Unknown	163*
29	Linalool oxide A	170	65	Ethyl hexadecanoate	284
30	Ethyl octanoate	172	66	Unknown	43*
31	8-Ethoxy-1-*p*-menthene	182	67	Unknown	163*
32	1-Heptanol	**	68	Unknown	43*
33	Linalool oxide B	170	68a	Ethyl octadecanoate	312
34	8-Ethoxy-*p*-cymene	178	69	Sesquiterpene alcohol	220
35	Linalool	154	70	Unknown	43*
36	Linalyl acetate	196	71	Dibutyl phthalate	278

* Base mass peak.

** Internal standard.

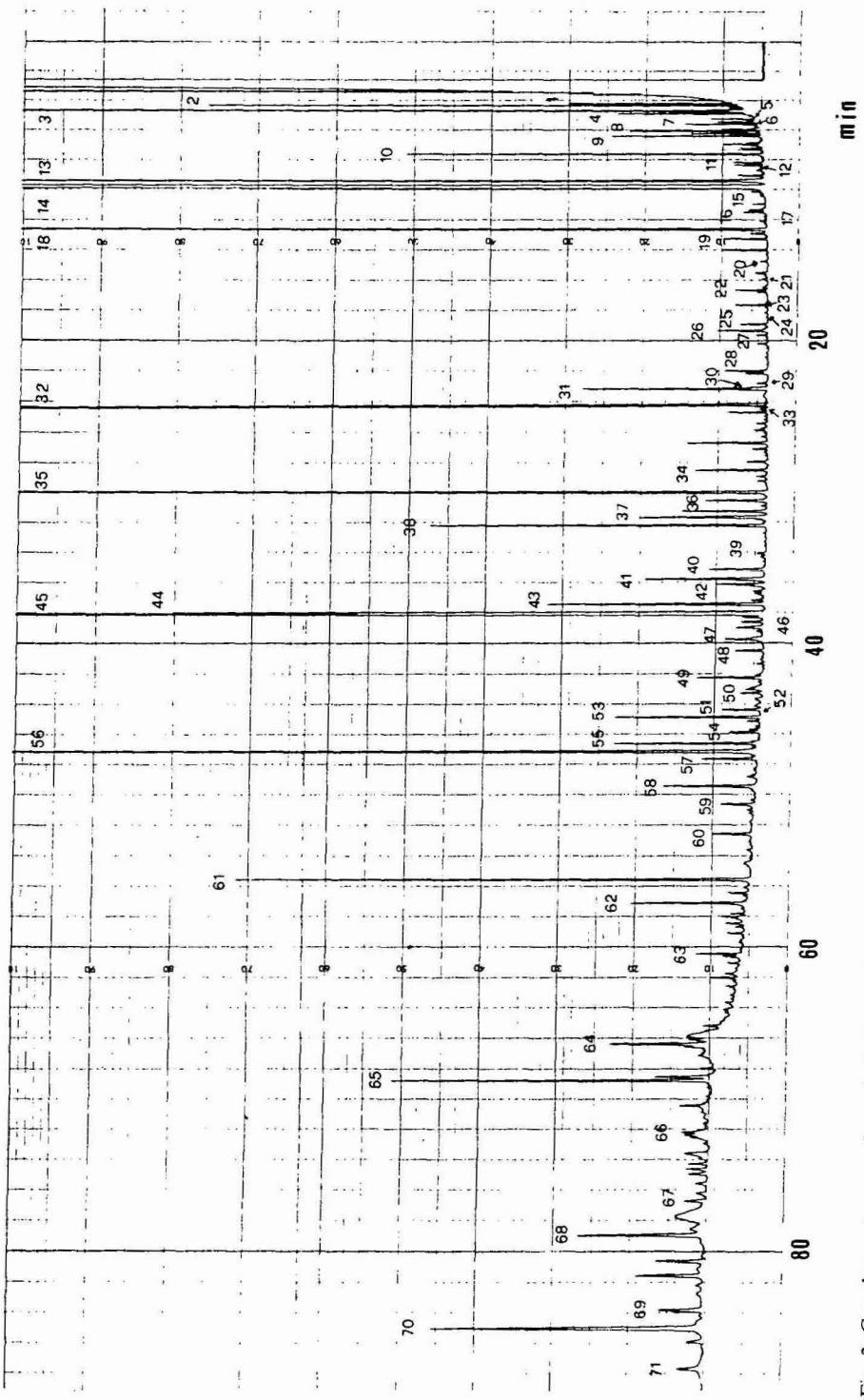

Fig. 2. Gas chromatogram of sample B. For peak identification, see Table II.

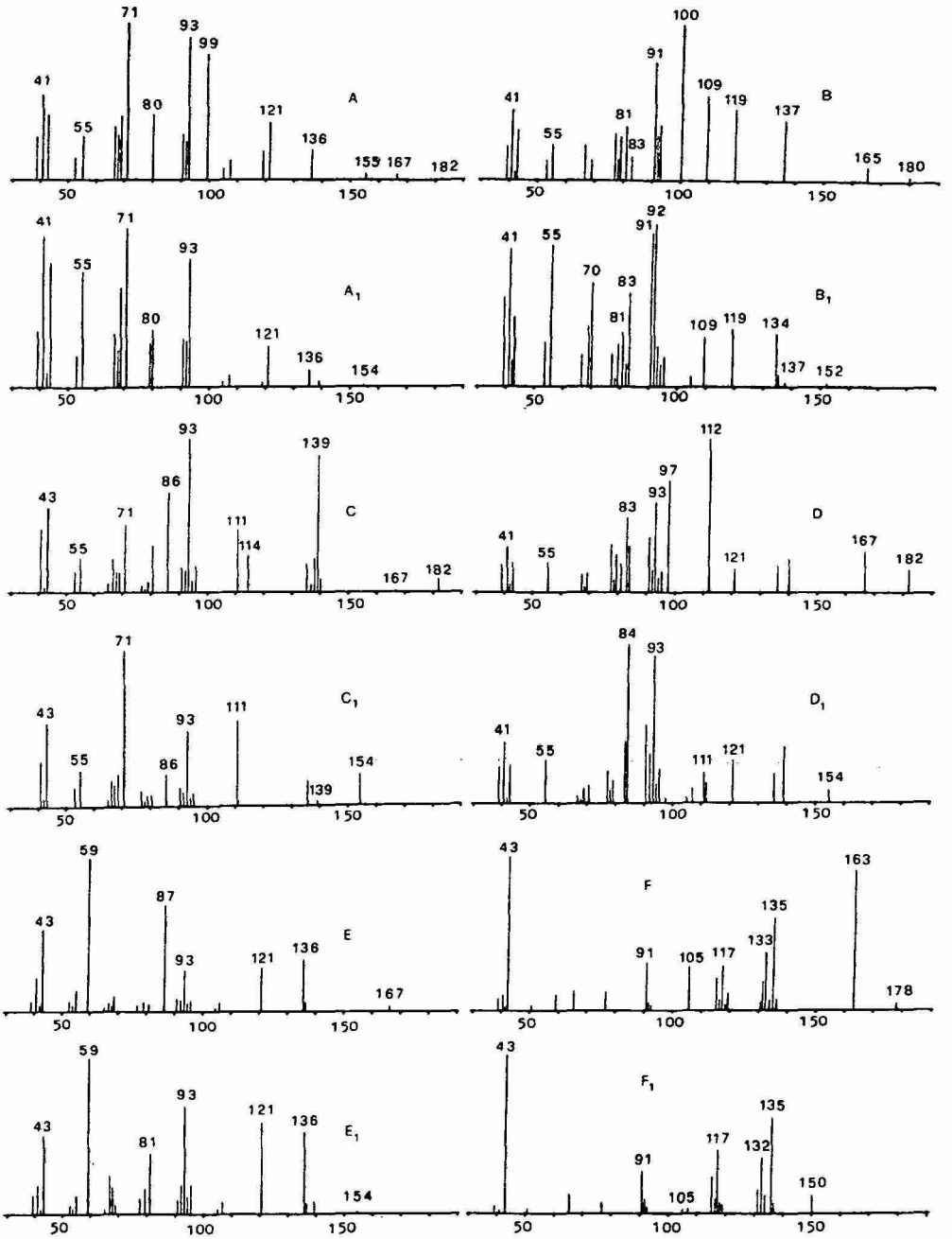

Fig. 3. Mass spectra of 3,7-dimethyl-3-ethoxy-1,6-octadiene (A), linalool (A_1), *trans*-3-ethoxy-2(10)-pinene? (B), *trans*-pinocarveol (B_1), 4-ethoxy-1-*p*-menthene (C), terpinen-4-ol (C_1), *cis*-3-ethoxy-1-*p*-menthene (D), *cis*-piperitol (D_1), 8-ethoxy-1-*p*-menthene (E), α-terpineol (E_1), 8-ethoxy-*p*-cymene (F) and *p*-cymen-8-ol (F_1).

respect to the small amount of myrtenol present and the lack of myrtenyl acetate, which are important and typical components of the essential oil. Terpene esters constitute 5.5% of the volatile fraction. Linalyl-, α-terpinyl-, neryl- and geranyl acetates have been identified. Also, significant amounts of phenol and methyleugenol have been found.

Fig. 2 shows a gas chromatogram of an extract (60% ethanol) obtained by cold infusion of Myrtle berries harvested in January 1981 and subjected to analysis 2 months after preparation (sample B). In this case, the profile is even more complex owing to the presence of acetals and ethers formed through equilibrium reactions dependent on the alcohol concentration and pH.

In sample B and C (liqueurs in 35% ethanol), six ethyl ethers have been identified, derived respectively from linalool (peak 21), *trans*-pinocarveol? (peak 25), terpinen-4-ol (peak 27), *cis*-piperitol (peak 28), α-terpineol (peak 31) and *p*-cymen-8-ol (peak 34). The mass spectra of these ethyl ethers (some of which are published for the first time) are compared with those of the parent terpene alcohols in Fig. 3. Possible fragmentation modes are shown in Fig. 4[5].

The earliest information about ethyl ethers of monoterpene alcohols is provided by the work of Taskinen and Nykänen (1974–1975)[6,7], who investigated the

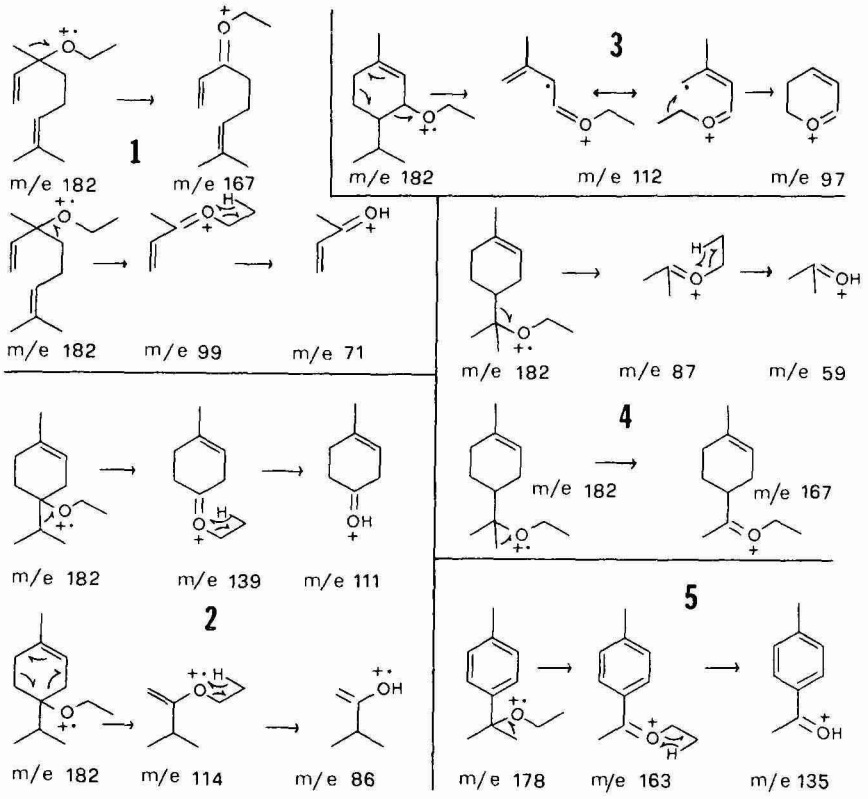

Fig. 4. Fragmentation pathways of 3,7-dimethyl-3-ethoxy-1,6-octadiene (scheme 1), 4-ethoxy-1-*p*-menthene (scheme 2), *cis*-3-ethoxy-1-*p*-menthene (scheme 3), 8-ethoxy-1-*p*-menthene (scheme 4) and 8-ethoxy-*p*-cymene (scheme 5).

composition of the essential oils of *Origanum majorana* L. and *Angelica archangelica* L., and that of distillates from the corresponding aqueous alcoholic infusions. These authors found various ethyl ethers, namely those of *cis*-piperitol and terpinen-4-ol, and described their most significant masses and respective fragmentation pathways. Subsequently, De Smedt and Liddle (1976)[8] identified linalyl ethyl ether (the mass spectrum of which was reported) in alcoholic extracts of Coriander and wild mint, and pointed out the possibility that analogous ethyl ethers can be formed from citronellol, nerol, α- and β-terpineol and geraniol.

After 2 months of ageing, the overall flavour profile of alcoholic extracts of Myrtle can undergo noticeable changes brought about by the formation of terpenyl ethyl ethers and other "artifacts" (acetals, esters).

REFERENCES

1 M. Vanhaelen and R. Vanhaelen-Fastré, *Planta Med.*, 39 (1980) 164.
2 L. Peyron, *Plant. Med. Phytother.*, 4 (1970) 279.
3 B. M. Lawrence, S. J. Terhune and J. W. Hogg, *Amer. Perfum. Cosmet.*, 85 (1970) 53.
4 K. P. Singh and G. N. Gupta, *Indian Perfumer*, 5 (1961) 23.
5 F. W. McLafferty, *Anal. Chem.*, 29 (1957) 1782.
6 J. Taskinen, *Acta Chem. Scand. Ser. B*, 28 (1974) 1121.
7 J. Taskinen and L. Nykänen, *Acta Chem. Scand., Ser. B*, 29 (1975) 757.
8 P. De Smedt and P. A. P. Liddle, *Ann. Falsif. Expert. Chim.*, 69 (1976) 865.

Journal of Chromatography, 264 (1983) 312 315
Elsevier Science Publishers B.V., Amsterdam — Printed in The Netherlands

CHROM. 15,826

Note

Sensitive method for the determination of methadone in small blood samples

HEBE B. GREIZERSTEIN* and IRIS G. McLAUGHLIN
Research Institute on Alcoholism, 1021 Main Street, Buffalo, NY 14203 (U.S.A.)
(Received March 4th, 1983)

Quantitation of low levels of methadone in small size samples required a sensitive and specific method of analysis. Methods for clinical application have been described for blood and urine samples using immunoassay techniques[1–4], gas chromatography[5–11] and combined gas chromatography–mass spectrometry[12–14]. These methods are not sensitive enough for determination of plasma concentrations in small volume blood samples. The sensitivity of those methods was in the 40–50 ng/ml range; however, they required sample sizes of 4–15 ml[5,7]. These techniques were not appropriate to study the methadone–ethanol interaction in experimental animals. This report presents a simple and accurate method of quantification using the addition of an internal standard, extraction with an organic solvent and gas–liquid chromatography (GLC) determination. The internal standard selected, 4-dimethylamino-1,2-diphenyl-3-methyl-2-butanol (chirald), is commercially available.

METHODS

Reagents

All solvents and chemicals used were reagent grade. Chirald (99%) was purchased from Aldrich and used as the internal standard. Methadone hydrochloride was supplied by Burt Mayfield of Mallinckrodt.

Apparatus

The chromatographic determinations were performed using a Perkin-Elmer Sigma I analyzer equipped with a flame ionization detector. The inlet and detector temperatures were 275°C each. The column used was a 3% OV-7 on Gas-Chrom Q (100–120 mesh), with a flow of 35 ml/min of nitrogen. The column was heated to an initial temperature of 220°C for 7 min and then programmed at 20°C/min to 300°C and held constant for 7 min.

Sensitivity and linearity

A standard solution of methadone hydrochloride in water was prepared in concentrations ranging between 1 and 10 μg/ml and containing 6.5 μg/ml chirald in methanol (internal standard). Aliquots (1 μl) of these solutions were injected into the chromatograph.

0021-9673/83/$03.00

Recovery

Blood was withdrawn from naive mice. To each sample 6.5 μl of 0.1 mg/ml chirald in methanol and methadone solution to obtain concentrations of 0.1–1 μg/ml were added. The samples were then extracted as described below. The recovery rates were calculated by comparison with methanol standards containing both drugs.

Extraction procedure

To 50 or 100 μl of blood in a Teflon-lined, screw-capped testtube 6.5 μl of 1 mg/ml chirald in methanol (internal standard) and 75 or 150 μl of phosphate buffer (pH 8.0) were added. The extraction was carried out by the addition of 3 ml heptane containing 1.5% isoamyl alcohol. The mixture was vortexed for 1 min and centrifuged on a clinical bench centrifuge for 15 min. The organic mixture was removed to a second testtube and evaporated to dryness under a gentle stream of nitrogen. The dried extract was reconstituted with 10 μl of methanol and vortexed, and 1-μl aliquots were injected twice into the gas chromatograph. Other solvents (ethyl acetate) and buffers (Tris) were tried, but the recovery rates were lower and more interferences were observed.

Blood and methadone analyses

Male BL6J mice (28–30 g in weight), purchased from Jackson Labs. (Bar Harbor, ME, U.S.A.) were fasted overnight. A dose of 20 mg/kg methadone hydrochloride in saline was administered i.p. to 20 mice. Groups of 5 animals each were sacrificed after 1, 2, 3 and 4 h, and four blood samples (2 × 50 μl; 2 × 100 μl) were collected from each mouse with micropipettes. The blood samples (50 or 100 μl) were immediately poured into glass tubes containing 75 or 150 μl of phosphate buffer (pH = 8.0) and 6.5 μl of 1 mg/ml chirald in methanol and extracted as previously described. Multiple blood samples were withdrawn from the same animal to test the reproducibility between samples of different volume and to determine whether a 50-μl was sufficient and as accurate as a 100-μl sample.

RESULTS

Sensitivity and linearity

The detection limit for methadone was 1 ng injected into the chromatograph. The response curve for methadone (1-μl injection) was found to be linear ($y = 0.121 + 0.123x$) in the range of 1–10 μg/ml. The correlation coefficient calculated for the regression line was 0.961.

Recovery

The recovery rate, calculated on the basis of the amount of methadone measured after extraction compared with standard methanol solutions, was 95.4 ± 0.51%. Using a sample size of 50 μl of blood, methadone was readily quantitated to 0.1 μg/ml.

Methadone blood levels in mice

A typical chromatogram of a blood sample from a mouse receiving 20 mg/kg methadone i.p. is shown in Fig. 1. The retention times for methadone and chirald

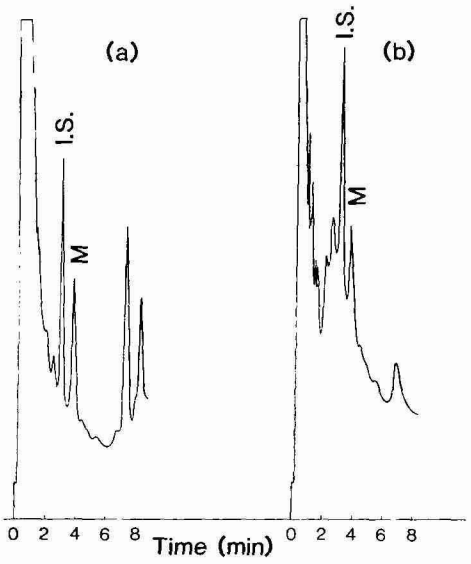

Fig. 1. Chromatogram of the extract of a blood sample taken from (a) naive mouse with added methadone (M) and (b) mouse injected with methadone. Chirald (I.S.) was added to both samples.

were 4.10 and 3.32 min, respectively. The chromatographic analysis was completed in 10 min, and although some peaks with shorter and longer retention times were present, there were no interferences with the analysis.

The concentration of methadone in the blood using 50- and 100-μl samples are shown in Table I. Comparison by Student's t-test between the two samples sizes for each time period did not show significant differences.

DISCUSSION

This report describes a rapid, sensitive and reproducible assay for methadone in blood samples. The small volume (50 μl) needed and the low limit of detection (0.1 μg/ml) allow for the determination of complete curves for methadone concentration in blood without significant risks to the animals.

In the present report, each mouse was sacrificed at each time period to ascertain the volume of blood needed and the reproducibility of the method. However, the

TABLE I

MEAN ± S.E.M. METHADONE CONCENTRATION (μg/ml)

Two samples from each mouse; five mice per time period.

Sample size (μl)	*Time (h)*			
	1	*2*	*3*	*4*
50	3.64 ± 0.09	3.48 ± 0.20	2.68 ± 0.22	2.25 ± 0.05
100	3.81 ± 0.13	3.56 ± 0.22	2.68 ± 0.23	2.32 ± 0.07

results show that it is possible to obtain serial blood samples (50 μl) from the tail tip of a mouse at hourly intervals to follow methadone concentration.

The peak blood levels of methadone occurred in 1 h or less and declined with time. The blood curve, although higher in values, follows the same pattern observed in rats receiving 5 mg/kg s.c. or 30 mg/kg p.o. for 4 weeks[15].

This method can also be used to quantitate methadone in clinical studies requiring high sensitivity and small sample size.

REFERENCES

1 D. L. Roerig, R. I. H. Wang, M. M. Mueller, D. L. Lewand and S. M. Adams, *Clin. Chem.*, 22 (1976) 1915.
2 J. Manning, J. H. Bidanest, S. Cohen and L. Lukash, *J. Forensic Sci.*, (1976) 112.
3 F. Bartos, G. D. Olsen, R. N. Leger and D. Bartos, *Chem. Pathol. Pharmacol.*, 16 (1977) 131.
4 J. S. F. Ling, J. G. Umans and C. E. Inturrisi, *J. Pharmacol. Exp. Ther.*, 217 (1981) 147.
5 C. E. Inturrisi and K. Verebely, *J. Chromatogr.*, 65 (1962) 361.
6 P. Hartvig and B. Näslund, *J. Chromatogr.*, 111 (1975) 347.
7 R. K. Lynn, R. M. Leger, W. P. Gordon, G. D. Olsen and N. Gerber, *J. Chromatogr.*, 131 (1977) 329.
8 N. C. Jain, D. M. Chinn, T. C. Sneath and R. D. Budd, *J. Anal. Toxicol.*, 1 (1977) 192.
9 B. C. Thompson and Y. H. Caplan, *J. Anal. Toxicol.*, 1 (1977) 66.
10 P. Jacob, J. F. Rigod, S. M. Pond and N. L. Benowitz, *J. Anal. Toxicol.*, 5 (1981) 292.
11 M. J. Kreek, *NY State J. Med.*, 23 (1973) 2773.
12 H. R. Sullivan, F. J. Marshall, R. E. McMahon, E. Anggard, L. M. Gunne and J. H. Hohnstrand, *Biomed. Mass Spectrom.*, 2 (1975) 197.
13 D. L. Hachey, M. J. Kreek and D. H. Mattson, *J. Pharm. Sci.*, 66 (1977) 1579.
14 G. I. Kang and F. S. Abbott, *J. Chromatogr.*, 231 (1982) 311.
15 M. J. Kreek, *Pharmacol. Biochem. Behav.*, 11 (Suppl.) (1979) 7.

Journal of Chromatography, 264 (1983) 316–320
Elsevier Science Publishers B.V., Amsterdam — Printed in The Netherlands

CHROM. 15,890

Note

Determination of piperine in pepper *(Piper nigrum)* using high-performance liquid chromatography

MALINIE RATHNAWATHIE and K. A. BUCKLE*
School of Food Technology, University of New South Wales, P.O. Box 1, Kensington, N.S.W. 2033 (Australia)
(Received March 31st, 1983)

Pepper (*Piper nigrum* L), a major spice in world trade, is valued for its pungent taste and aroma. The pungent principles of pepper have been the subject of many investigations since the early 19th century. The knowledge of the chemistry of pepper dates back to 1820, when the most abundant alkaloid piperine was isolated[1]. Piperine or 1-piperoylpiperidine ($C_{17}H_{19}NO_3$), the pungent principle, together with other pungent substances present in small quantities such as chavicine, piperidine and piperettine are responsible for the sharp biting taste and pungency. In addition, pigments, resins, sugars and fixed oils may also be found in the non-volatile ether extract. Since piperine is universally accepted as the predominant pungent principle in pepper, the quality of pepper and also of the oleoresin is dependent largely on the piperine content and thus methods for estimating piperine are becoming more important[1–3].

Methods available for analysis of piperine include Kjeldahl nitrogen determination[4], adaptation of the chromotrophic acid test for formaldehyde[5], colorimetric methods using nitric acid[6], sulphuric acid and aromatic aldehyde[7], phosphoric acid[8] and based on alkaline hydrolysis[9], reaction with *p*-nitrophenyl diazonium fluoborate[10], volumetric analysis[11], spectrophotometric analysis[12,13] and high-performance liquid chromatography (HPLC)[14–17].

Graham[7] and Labruyere[9] have reviewed the available methods and pointed out their merits and demerits. The Kjeldahl and UV-spectrophotometric methods have been widely and frequently practised. The Kjeldahl method, however, measures other nitrogenous compounds and always gives high values[12,13,16,18,19]. The UV-spectrophotometric method has been developed for the direct measurement of piperine and is very specific and reliable under controlled conditions[12,13,16,18,19]. Recently HPLC was selected as a rapid, sensitive and specific method for the quantitative determination of piperine, because of its ease of operation and proven ability to detect and separate the small quantities of non-volatile, UV-active components[14–17].

In this study we have used a reversed-phase μBondapak CN column and a mobile phase of methanol–water to develop a method for the rapid analysis of piperine in pepper and non-volatile ether extracts. The piperine levels were compared with those obtained using a UV method.

0021-9673/83/$03.00

EXPERIMENTAL

Samples and chemicals

An authentic sample of piperine was purchased from Sigma (St. Louis, U.S.A.).

Black, green and white pepper samples of the Kuching variety, harvested at different maturities were obtained from the Minor Export Crops Research Station, Matale, Sri-Lanka.

All chemicals were of analytical-reagent grade. Water was double distilled in glass.

HPLC conditions

The equipment used was manufactured by Waters Assoc. (Milford, MA, U.S.A.) and consisted of a Model M 6000A solvent delivery pump and Model 440 absorbance UV detector set at 280 nm, a stainless-steel μBondapak CN column (30 cm × 3.9 mm I.D.). The mobile phase was methanol (Waters Assoc., chromatographic grade) and water which had been filtered through a Sartorius filter (0.45 μm pore size, SM 11106) and degassed under vacuum. A flow-rate of 2 ml/min, attenuation of 0.5 a.u.f.s. and a chart speed of 1 cm/min were used. Samples (10 μl) were injected directly after filtration.

Some experiments were carried out using a Waters Model 480 variable-wavelength UV detector set at 345 nm using the same separation conditions as above except that attenuation was 2.0 a.u.f.s. and sample size 5 μl.

Extraction

Pepper samples were ground to a fine powder in a coffee grinder and extracted (5.00 g) with diethyl ether in a Soxhlet apparatus for 20 h. The solvent ether was removed by vacuum distillation and the extract heated to constant weight at 100°C.

Spectrophotometric procedure

The method developed by Fagen *et al.*[12], was used. A well-mixed sample of non-volatile ether extract of pepper (0.25 g) was dissolved in 100 ml chloroform and an aliquot (0.5 ml) further diluted to 100 ml. The flasks were covered with aluminium foil to protect the samples from photoisomerisation. The absorbance at 345 nm was measured immediately using chloroform as a blank and the proportion of piperine in the non-volatile ether extract calculated with reference to a calibration curve over the range from 0.2 mg to 1.2 mg piperine in 100 ml chloroform.

HPLC procedure

A well-mixed sample of non-volatile ether extract of pepper (10 mg) was dissolved in 20 ml methanol and filtered through a Sartorius membrane filter (0.45 μm pore size, SM 11806) before injection. The four mobile phases which were tested with the pure piperine and pepper samples were (i) double distilled water, (ii) methanol–water (50:50), (iii) methanol–water (80:20), and (iv) methanol. Methanol–water (50:50) was used in subsequent experiments.

Pure piperine (10–50 mg) was dissolved in 100 ml methanol and aliquots (10 μl) injected into the HPLC. Calibration graphs were plotted with peak height against

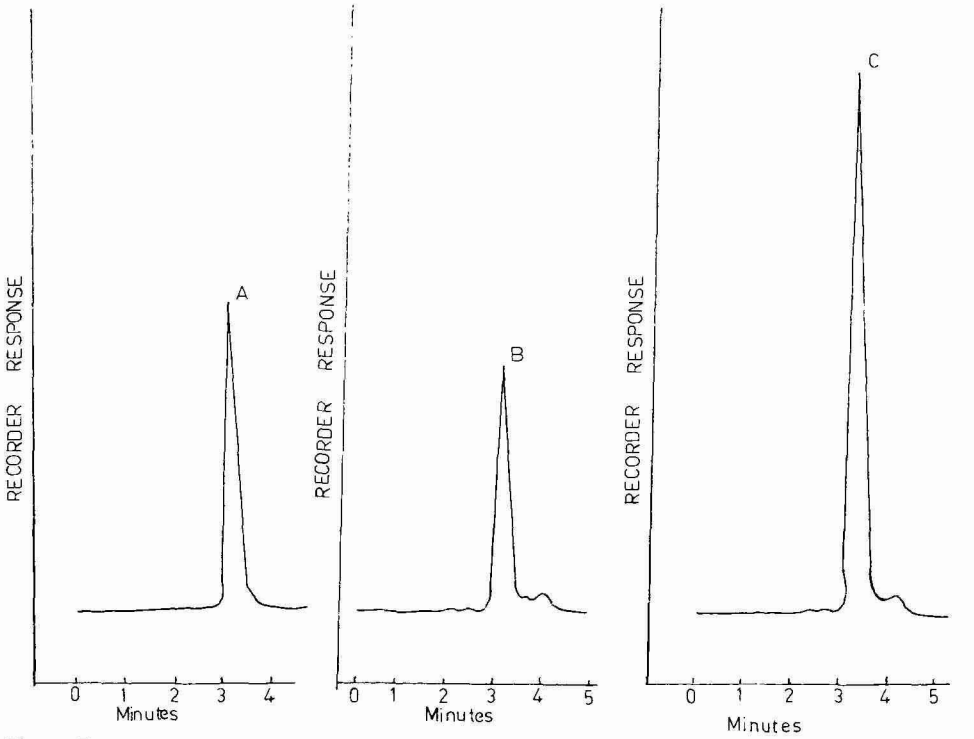

Fig. 1. Typical HPLC chromatograms of piperine (A); pepper extract (B) and pepper extract spiked with piperine (C), detected at 280 nm.

TABLE I

PIPERINE LEVELS IN NON-VOLATILE ETHER EXTRACT OF PEPPER

Values in %.

Sample	*Age of berries (months)*	*Spectrophotometric method*	*HPLC method**
Black pepper	2	35.4	32.4
	3	47.2	44.1
	4	50.5	49.7
	5	49.5	47.6
	6	47.9	44.1
Green pepper	4	53.6	53.1
	4½	55.2	54.2
	5	51.6	49.7
	5½	50.6	48.3
White pepper	5	47.2	44.1
	5½	45.7	43.5
	6	42.6	41.4

* Detection at 280 nm.

TABLE II

RECOVERY OF PIPERINE ADDED TO NON-VOLATILE ETHER EXTRACT BY SPECTROPHOTOM RIC AND HPLC METHODS

Samples	*Spectrophotometric method*			*HPLC method at 280 nm*			*HPLC method at 345 nm*		
	Added (mg)	*Found (mg)*	*Recovery (%)*	*Added (mg)*	*Found (mg)*	*Recovery (%)*	*Added (mg)*	*Found (mg)*	*Recov (%)*
Black pepper	5.00	4.60	92.0	4.75	4.75	100.0	6.30	6.26	99.4
	10.00	9.60	96.0	7.85	7.79	99.2	9.15	9.03	98.7
Green pepper	5.00	4.80	96.0	4.75	4.69	98.7	4.35	4.33	99.5
	10.00	9.80	98.0	7.85	7.87	100.4	8.50	8.47	99.7
White pepper	5.00	4.80	96.0	4.75	4.82	101.6	5.15	5.14	99.8
	10.00	9.40	94.0	7.85	7.78	99.1	8.97	8.95	99.8

piperine concentration detected at both 280 and 345 nm. Linear relationships were found over the range 10 to 40 mg piperine/100 ml methanol.

RESULTS AND DISCUSSION

Fig. 1 shows the chromatograms of pure piperine, a pepper sample and a pepper sample spiked with piperine and using the selected mobile phase and piperine detection at 280 nm. At a flow-rate of 2.0 ml/min piperine was eluted after 3 min; considerably faster than HPLC separations reported previously[15–17] and also using a simple and cheap mobile phase.

Results of spectrophotometric and HPLC (280 nm) methods of analysis of piperine are given in Table I. Although the difference in piperine levels determined by both methods is small, the spectrophotometric method always gave slightly higher results than did the HPLC method. Interference by other nitrogenous components such as piperettine may be the reason for the higher values with the UV method.

The recovery of piperine by both methods shown in Table II demonstrates that the present HPLC procedure gives a higher and less variable recovery for all samples tested, as well as rapid and inexpensive separation. Of considerable interest is the increased sensitivity of the HPLC method when detection at 345 nm is used compared to detection at 280 nm. The method was found to be nearly 8 times as sensitive when HPLC separation was coupled with detection at 345 nm. Thus availability of a variable-wavelength detector further improves the value of the HPLC method described when compared with the traditional UV-spectrophotometric methods.

Further work will establish the variability of piperine levels in several pepper varieties at different stages of maturation, processing and storage.

REFERENCES

1 J. W. Purseglove, E. G. Brown, C. L. Green and S. R. J. Robbins, *Spices*, Vol. 1, Longman, New York, 1981, Ch. 2, p. 50.

2 E. S. Nambudiri, Y. S. Lewis, N. Krishnamurthy and A. G. Mathew, *Flav. Ind.*, 1 (1970) 97.
3 R. O. B. Wijesekera, U. M. Senanayake and A. L. Jayewardene, *Flav. Ind.*, 3 (1972) 133.
4 *Official Methods of Analysis*, Association of Official Analytical Chemists, Washington, DC, 13th ed, 1980.
5 L. A. Lee, *Anal. Chem.*, 29 (1956) 1621.
6 H. D. Graham, *J. Pharm. Sci.*, 54 (1965) 319.
7 H. D. Graham, *J. Food Sci.*, 30 (1965) 644.
8 H. D. Graham, *J. Food Sci.*, 30 (1965) 651.
9 B. Labruyere, *J. Agr. Food Chem.*, 14 (1966) 469.
10 R. S. Kap, *Korean J. Food Sci. Technol.*, 6 (1974) 56.
11 M. L. Shankaranarayana, S. Nagalakshmi and C. P. Natarajan, *Flav. Ind.*, 1 (1970) 173.
12 H. J. Fagen, E. P. Kolen and R. P. Hussong, *J. Agr. Food Chem.*, 3 (1955) 860.
13 C. Genest, D. M. Smith and D. G. Chapman, *J. Agr. Food Chem.*, 11 (1963) 508.
14 R. De Cleyn and M. Verzele, *Chromatographia*, 5 (1972) 346.
15 R. De Cleyn and M. Verzele, *Chromatographia*, 8 (1975) 342.
16 W. G. Galetto, D. E. Walger and S. M. Levy, *J. Ass. Offic. Anal. Chem.*, 59 (1976) 951.
17 M. Verzele, P. Mussche and S. A. Qureshi, *J. Chromatogr.*, 172 (1979) 493.
18 F. Tausig, J. I. Suzuki and R. E. Morse, *Food Technol.*, 10 (1956) 151.
19 T. N. R. Rao, C. T. Dwarakanath and D. S. Johar, *J. Proc. Inst. Chem.*, 32 (1960) 125.

Journal of Chromatography, 264 (1983) 321–328
Elsevier Science Publishers B.V., Amsterdam — Printed in The Netherlands

CHROM. 15,831

Note

Simple separation of adenine and adenosyl-sulfur compounds by high-performance liquid chromatography

BOE-GWUN CHUN, WOON KI PAIK and SANGDUK KIM*
Fels Research Institute, Temple University School of Medicine, Philadelphia, PA 19140 (U.S.A.)
(Received March 2nd, 1983)

Much information has been accumulated concerning the role of S-adenosyl-L-methionine (SAM) in transmethylation, transsulfuration and aminopropylation reaction[1–3]. Its demethylated product, S-adenosyl-L-homocysteine (SAH), is one of the most potent inhibitors for various transmethylation reactions[4] and spermine synthetases[5]. These two compounds, SAM and SAH, are key intermediates in the regeneration of methionine methyl group[6] as well as in the transfer of the sulfur atom from methionine to cysteine[7]. 5′-Deoxy-5′-methylthioadenosine (MTA), a cleavage product of S-adenosyl-(5′)-3-methylthiopropylamine (decarboxy-SAM), which is the intermediate for polyamine synthesis, acts as a product inhibitor for the reaction[8,9], and inhibitor for some of transmethylases[10]. These two reaction products, SAH and MTA, subsequently give rise to the formation of adenine, a strong competitive inhibitor of MTA phosphorylase[11]. Therefore, the above mentioned inter-related metabolic pathway suggests that the simultaneous and quantitative determination of the metabolites in tissues should greatly enhance the study for their biological functions.

Numerous methods for determination of SAM metabolites have been described[11–26], including some that utilize high-performance liquid chromatography (HPLC)[11–16]. Although the reported HPLC methods are capable of resolving a few SAM metabolites, the simultaneous separation of various metabolites of SAM is impossible; poor resolution between adenine and MTA and/or MTA and SAH has been a drawback. In the present paper, we describe a simple improved method for simultaneous and quantitative measurement of adenine, MTA, SAH and decarboxy-SAM in addition to SAM.

MATERIALS AND METHODS

Apparatus

A Partisil-10/SCX (25 × 0.46 cm) I.D. column was obtained from Whatman. A solvent-delivery system, a Model 660 solvent programmer equipped with Model 45 single-piston pump and Model 6000A dual-piston pump, a Model U6K Universal Injector and a Model 440 dual absorbance detector were from Waters Assoc. The chromatographic runs were recorded on an Omniscribe recorder from Houston Instrument.

0021-9673/83/$03.00

Materials

Adenine, SAM and MTA were purchased from Sigma. SAH was from Calbiochem Decarboxy-SAM was generously provided by Dr. Vincenzo Zappia through Dr. Patrizia Galletti of the University of Naples (Italy). Acetonitrile was a HPLC grade preparation from Fisher Scientific. Other chemicals were analytical grade. Dowex 50W-X8 (200–400 mesh) was from Bio-Rad Labs. Male Sprague-Dawley rats (weighing *ca.* 200 g) were obtained from Charles River Breeding Labs.

Tissue extraction

All extraction steps were done at 0–4°C. After decapitation of rats, tissues were rapidly removed, rinsed in cold saline and blotted on filter paper. About 1 g of freshly excised tissue was homogenized with 1.5 *M* perchloric acid (1:4, w/v). After centrifugation, the deproteinized supernatant was chromatographed using a column of Dowex 50 (H^+) (resin bed, 4 × 0.5 cm) previously equilibrated with 0.1 *M* hydrochloric acid to remove contaminating compounds, and the desired metabolites of SAM were collected with 10 ml of 6 *M* hydrochloric acid. The 6 *M* hydrochloric acid eluate was mixed with 20 μl of thiodiglycol prior to evaporation and then dried under reduced pressure at 33–35°C with Buchi Rotovapor. Samples were routinely stored at −20°C

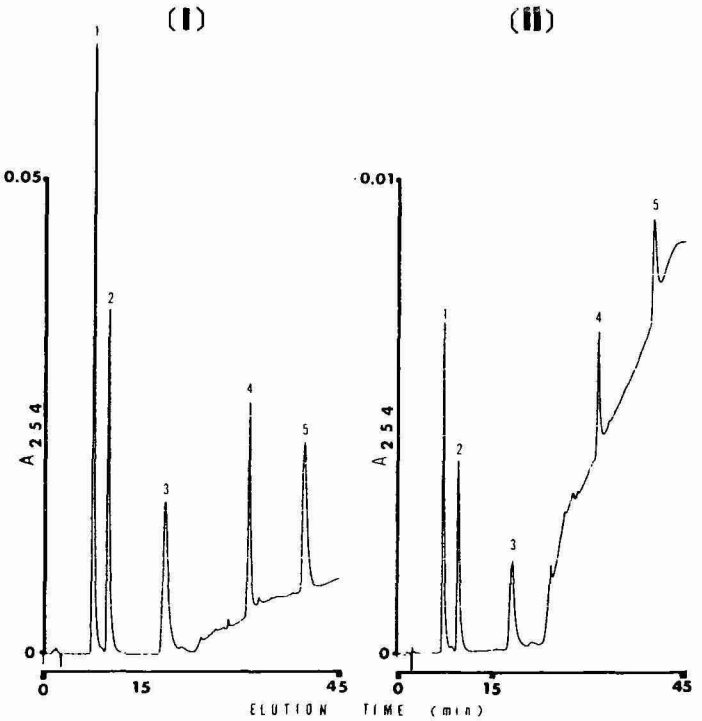

Fig. 1. Analytical HPLC elution patterns of adenine and adenosyl-sulfur compounds. The biphasic chromatographic elution was employed as described in Materials and Methods: [I], 1.25 nmoles of each compound with 0.1 a.u.f.s.; [II], 125 pmoles of each compound with 0.02 a.u.f.s. Peaks: 1 = MTA; 2 = adenine; 3 = SAH; 4 = SAM; 5 = decarboxy-SAM.

overnight. Just before HPLC analysis, this dried sample was redissolved in 1 ml of deionized water (final sample pH 3.0–3.4).

HPLC separation

The acid-soluble extracts of tissues were analyzed at room temperature for adenine and adenosyl-sulfur compounds using a Whatman Partisil-10 strong cation-exchange HPLC column. The flow-rate was 1.2 ml/min. Two elution buffers were utilized: buffer A, 15% (v/v) acetonitrile in 0.01 *M* ammonium formate, pH 2.6; buffer B, 15% (v/v) acetonitrile in 1.0 *M* ammonium formate, pH 4.3.

Prior to sample application, the column was equilibrated with buffer A. Following sample (10 μl) injection, the separation of SAM metabolites was effected by an isocratic elution with buffer A for initial 15 min followed by a linear 30-min gradient to 30% buffer B. There was a lag of *ca.* 7.5 min between the change to gradient elution buffer and the initial appearance of buffer B absorbance on the chromatogram (Fig. 1). The effluent was monitored by absorbance at 254 nm.

Calibration curves and recovery

SAM was purified by HPLC and found to be 84.2% pure using the molar absorbance as 15,000 $mole^{-1}$ cm^{-1} (ref. 2). Purities of other commercial standard compounds were analyzed individually by HPLC. Each compound exhibited more than 97% of UV-absorbing material as a single peak. All calibration curves were consistently linear over a range from 125 pmoles to 5 nmoles with less than 5% variation between identical samples (Fig. 2).

Recovery of each compound was determined as follows: 50 nmoles of each standard were added to a set of the original perchloric acid tissue homogenates, which served as the internal standards. Absorbance of each added standard peaks were then corrected by subtracting the absorbance due to the endogenous origin which was obtained from the another set of tissue preparations without added standards. The percentage recovery of added standards were then calculated on the basis of added amount of each compound. Usually 1/100 of the extract, which is equivalent to 500 pmoles of the added standard, was applied to HPLC.

Quantitation

The amount of each compound per gram of wet tissue was first estimated directly from the calibration curve based on the peak heights, and the values were corrected according to the recovery percent of each standard.

RESULTS AND DISCUSSION

Separation of MTA, adenine and SAH

Although HPLC method is frequently used to quantitate various nucleosides and their analogues, the available methods do not adequately resolve MTA, adenine and SAH, all of which are present in most biological samples. As an initial experiment, we used 0.01 *M* ammonium formate buffer, pH 3.3 (not containing acetonitrile) at a flow-rate of 2.5 ml/min as the mobile phase, and found that adenine, MTA and SAH essentially coeluted under these conditions (not shown). However, by decreasing the PH and flow-rate of the mobile phase to pH 2.6 and 1.2 ml/min, re-

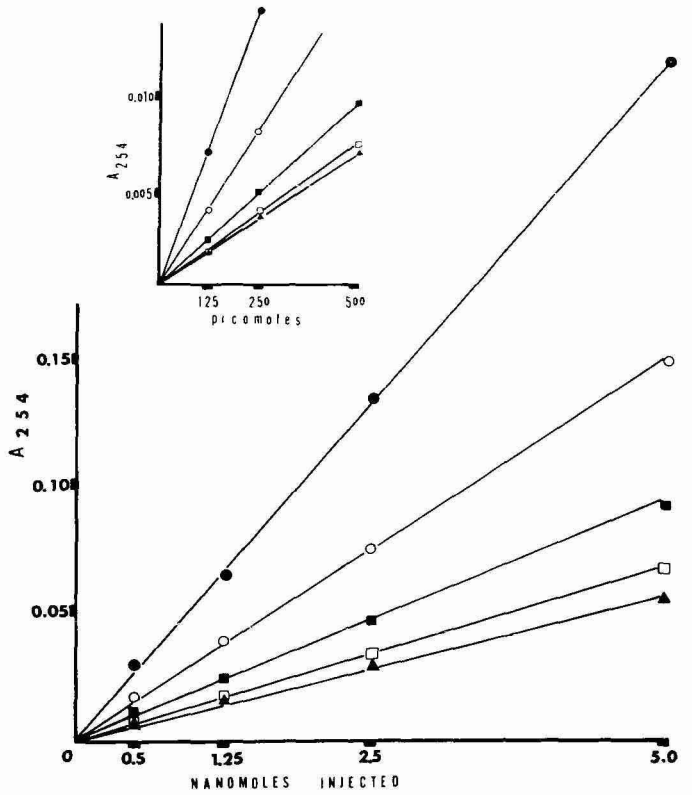

Fig. 2. Calibration curves of standard compounds. The chromatographic conditions were the same as Fig. 1. ● = MTA; ○ = adenine; ■ = SAM; □ = SAH; ▲ = decarboxy-Sam.

spectively, the SAH peak was clearly separated from those of adenine and MTA, although the latter two compounds were not effectively resolved (Fig. 3 [I]). However, on addition of acetonitrile to this low-pH mobile phase at 15% concentration, complete separation of all three peaks was achieved (Fig. 3 [II]). The use of this acetonitrile containing buffer, not only decreased the capacity factor (compare capacity factors, k', in Fig. 3 [I] and [II] for each compound)[27], but also increased the absorbance of SAH *ca.* 1.3-fold (A_{254} = 0.076 *vs.* 0.102). The apparent reason for the better resolution when acetonitrile is present in the elution buffer is that the retention times of the compounds on cation-exchange HPLC are proportionately decreased in a manner dependent on acetonitrile concentration due to the hydrophobicity of the solute[28].

Sensitivity of the improved HPLC method

Compared with the previously reported HPLC methods for the separation of SAM and its metabolites[12–16], the present method has the advantages of higher sensitivity and better resolution efficiency as illustrated in k' values in Table I and Fig. 1. We estimate that for each compound the limit of detection using this technique is somewhat less than 100 pmoles per 10-μl injection (Fig. 1 [II]). All the standard

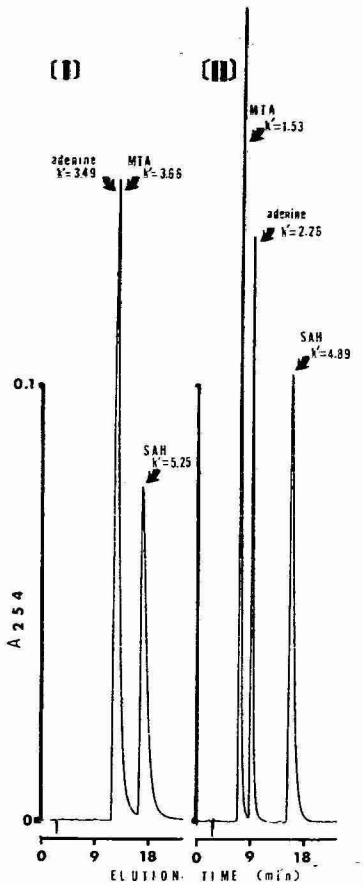

Fig. 3. Isocratic separation of MTA, adenine and SAH by HPLC. The standard mixture (10 μl) containing MTA (4 nmoles), adenine (4 nmoles) and SAH (8 nmoles) was applied on HPLC using a flow-rate of 1.2 ml/min at 850 p.s.i. and 0.2 a.u.f.s. at ambient temperature. The mobile phases applied were: [I], 10 m*M* ammonium formate buffer, pH 2.6; and [II], buffer A (a 5:1 mixture of the above ammonium formate buffer and acetonitrile).

TABLE I

CAPACITY FACTORS OF ADENINE AND ADENOSYL-SULFUR COMPOUNDS

Compounds	*Capacity factor (k')**
5'-Methylthioadenosine (MTA)	1.53 ± 0.02
Adenine	2.26 ± 0.03
S-Adenosyl-L-homocysteine (SAH)	4.89 ± 0.06
S-Adenosyl-L-methionine (SAM)	9.76 ± 0.05
S-Adenosyl-(5')-3-methylthiopropylamine (decarboxy-SAM)	12.37 ± 0.11

* The capacity factors were calculated according to the equation in ref. 27 from the retention time of distilled water, and indicate mean ± standard error of three independent determinations.

TABLE II

TISSUE CONTENTS OF ADENINE AND ADENOSYL-SULFUR COMPOUNDS IN NORMAL RATS

Compounds	*Concentration (nmoles/g wet weight)**		
	Liver	*Heart*	*Brain*
MTA	<0.05	ND**	ND
Adenine	32.8	98.2	110.9
SAH	18.0 (45.5)*** (43.8)§	5.48 (3.9)§	3.34 (3.4)§
SAM	59.0 (66.3)*** (57.5)§ (72.7)§§	27.1 (38.5)§ (65.2)§§	20.6 (25.4)§ (27.6)§§
Decarboxy-SAM	1.98	ND	ND

* Values were corrected by recovery factors of each compounds as follows; 57.6% for MTA, 85.1% for adenine, 40% for SAH, 98.7% for SAM and 91.0% for decarboxy-SAM.

** Not detectable.

*** Ref. 15, Table 2.

§ Ref. 30, Table 2.

§§ Ref. 31, Table 1.

curves are linear for concentration up to 5 nmoles (Fig. 2). The sensitivity of the present method is comparable to that of the isotope-dilution technique[21,22].

Extraction of SAM and its metabolites from tissues

In establishing optimal conditions for the quantitative measurement of SAM and its metabolites in tissues, recovery of these compounds in the steps prior to the HPLC analysis is an extremely important factor for the accurate quantitation. Preliminary experiments using a Dowex 50 (H^+) column to remove undesirable compounds from the tissue extract by successive washings of the column with 0.1 *M* hydrochloric acid and 1.8 *M* hydrochloric acid[12] indicated considerable loss of MTA, adenine and SAH in the 1.8 *M* hydrochloric acid wash. Therefore, the column was washed with 50 ml of 0.1 *M* hydrochloric acid followed by only 15 ml of 1.0 *M* hydrochloric acid, and finally the compounds of interest eluted with 10 ml of 6 *M* hydrochloric acid. Although the 1.0 *M* hydrochloric acid wash still contained small amounts of MTA and adenine, massive loss of the compounds can be prevented using the washing procedure described. Thiodiglycol (20 μl) was added to the 6 *M* hydrochloric acid eluate before concentrating it, since the addition of this compound is known to suppress hydrolysis of SAH[22] which might be occurring during the subsequent steps. With these precautions, the recoveries of MTA and SAH were found to be 57.6% and 40%, respectively, while that of adenine was 85.1%. On the other hand, the recoveries of SAM (98.7%) and decarboxy-SAM (91.0%) were quite satisfactory. These recovery values were used to calculate the tissue concentrations of each compounds after HPLC analysis.

Application of the method to estimate the concentration of SAM and its derivatives in tissues

The present improved HPLC method was used for quantitative simultaneous

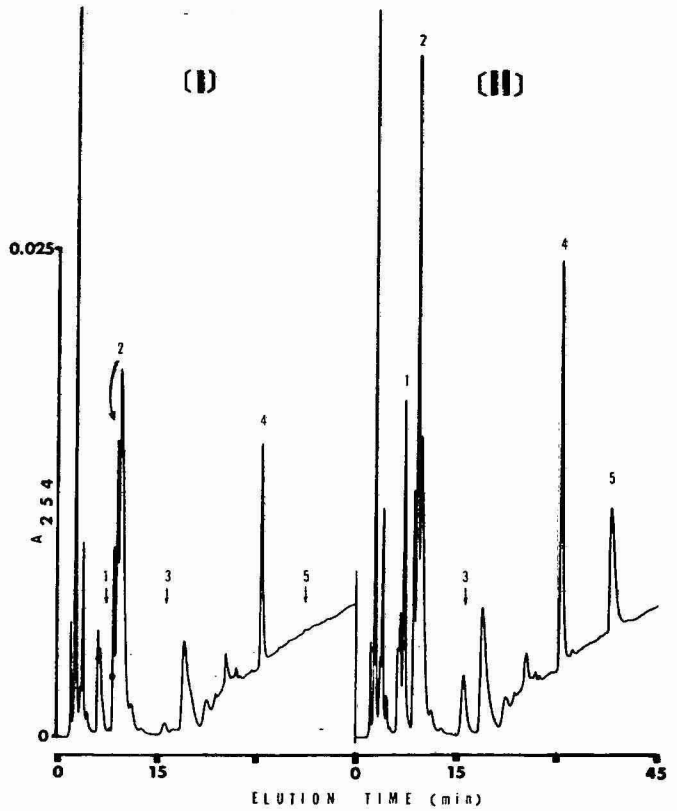

Fig. 4. Separation of adenine and adenosyl-sulfur compounds in rat liver. The chromatographic conditions were the same as Fig. 1 with sensitivity of 0.05 a.u.f.s.: [I], the extract equivalent to 8 mg of wet liver; [II], the above plus internal standards equivalent to 0.5 nmole of each compounds. Peak numbers as in Fig. 1.

estimation of adenine and adenosyl-sulfur compounds in rat tissues (Table II and Fig. 4). Although the data generally show slightly lower values than those reported by others[15,30,31], this is most likely due to higher efficiency of resolution with our method. The full separation of five compounds takes only 45 min.

For separation of one or two of these five compounds (SAM, SAH, adenine, MTA and decarboxy-SAM), the elution pattern can be adjusted in order to save time and elution buffer. For instance, the separation of SAM and decarboxy-SAM can be achieved by using a linear-gradient elution without the initial isocratic elution.

The first chromatographic method[20] ensuring reliable quantitation of SAM and SAH in tissues was based on the separation and purification by several chromatographic columns and subsequent estimation of the ribose moiety by the orcinol reaction. However, Eloranta[29] recently pointed out that even the improved method[15,17] was not suitable for the simultaneous analysis of SAM and SAH in routine analysis. Moreover, there had been no method available until now for the simultaneous quantitation of adenine and biologically important adenosyl-sulfur compounds.

We can conclude from the present study that, although various compounds which are present in the tissue samples prepared by Dowex 50 (H+) column interfere with HPLC separation of adenine and adenosyl-sulfur compounds, the described cation-exchange HPLC method is a highly sensitive and reproducible method for the simultaneous and quantitative determination of the major SAM metabolites.

ACKNOWLEDGEMENTS

This work was supported by Research grants AM09602 from the National Institute of Arthritis, Diabetes, and Digestive and Kidney Diseases, CA12226 and CA12227 from the National Cancer Institute, and BNS-8119666 from National Science Foundation. We are grateful to Dr. David E. Jensen for helpful discussion and enthusiasm during the course of this study, and also Prabhakar D. Lotlikar for allowing us to use his HPLC instrument.

REFERENCES

1 G. L. Cantoni, *J. Biol. Chem.*, 204 (1953) 403.
2 F. Schlenk, in S. K. Shapiro and F. Schlenk (Editors), *Transmethylation and Methionine Biosynthesis*, The University of Chicago Press, Chicago, IL, 1965, pp. 48–65.
3 E. Usdin, R. T. Borchardt and C. R. Creveling, in *Transmethylation*, Elsevier/North-Holland, New York, 1979.
4 J. D. Mann and S. E. Mudd, *J. Biol. Chem.*, 238 (1963) 381.
5 H. Hibasami and A. E. Pegg, *Biochem. Biophys. Res. Commun.*, 81 (1978) 1398.
6 J. Knappe and T. Schmidt, *Biochem. Biophys. Res. Commun.*, 71 (1976) 1110.
7 V. Zappia, F. Salvatore, M. Porcelli and G. Cacciapuoti, in V. Zappia, E. Usdin and F. Salvatore (Editors), *Biochemical and Pharmacological Roles of Adenosylmethionine and the Central Nervous System*, Pergamon Press, Oxford, 1979, pp. 1–16.
8 C. W. Tabor and H. Tabor, *Ann. Rev. Biochem.*, 45 (1976) 285.
9 H. Hibasami, R. T. Borchardt, S. Y. Chen, J. K. Coward and A. E. Pegg, *Biochem. J.*, 187 (1980) 419.
10 V. Zappia, R. Zydek-Cwick and F. Schlenk, *J. Biol. Chem.*, 244 (1969) 4499.
11 J. Seidenfeld, J. Wilson and H. G. Williams-Ashman, *Biochem. Biophys. Res. Commun.*, 95 (1980) 1861.
12 V. Zappia, P. Galletti, M. Porcelli, C. Manna and F. Della-Ragione, *J. Chromatogr.*, 189 (1980) 399.
13 P. A. Crooks, R. N. Dreyer and J. K. Coward, *Biochemistry*, 18 (1979) 2601.
14 N. M. Kredish and M. S. Hershfield, *Proc. Nat. Acad. Sci., U.S.*, 76 (1979) 2450.
15 J. Hoffman, *Anal. Biochem.*, 68 (1975) 522.
16 T. P. Zimmerman, R. D. Deeprose, G. Wolberg and G. S. Duncan, *Biochem. Biophys. Res. Commun.*, 91 (1979) 997.
17 R. A. Schatz, C. R. Vunnan and O. Z. Sellinger, *Life Sci.*, 20 (1977) 375.
18 B. E. Chabannes, J. N. Bidard, N. Sarda and L. A. Cronenberger, *J. Chromatogr.*, 170 (1979) 430.
19 R. J. Baldessarini and I. J. Kopin, *Anal. Biochem.*, 6 (1963) 289.
20 M. K. Gaitonde and G. E. Gaull, *Biochem. J.*, 102 (1967) 959.
21 F. Salvatore, R. Utili, V. Zappia and S. K. Shapiro, *Anal. Biochem.*, 41 (1971) 16.
22 K. M. Taylor and P. K. Randall, *J. Pharmacol. Exp. Ther.*, 194 (1975) 303.
23 J. D. Finkelstein and B. Harris, *Arch. Biochem. Biophys.*, 171 (1975) 282.
24 J. E. Poulton and V. S. Butt, *Arch. Biochem. Biophys.*, 172 (1976) 135.
25 T. O. Eloranta, E. O. Kayander and A. M. Raina, *Biochem. J.*, 160 (1976) 287.
26 V. Zappia, P. Galletti, A. Oliva and A. deSantis, *Anal. Biochem.*, 79 (1977) 535.
27 L. R. Snyder, in E. Heftmann (Editor), *Chromatography: A Laboratory Handbook of Chromatographic and Electrophoretic Methods*, Van Nostrand Reinhold, Princeton, NJ, 3rd ed., 1975, pp. 46–76.
28 P. J. M. Van Haastert, *J. Chromatogr.*, 210 (1981) 241.
29 T. O. Eloranta, in V. Zappia, E. Usdin and F. Salvatore (Editors), *Biochemical and Pharmacological Roles of Adenosylmethionine and the Central Nervous System*, Pergamon Press, Oxford, 1979, pp. 25–35.
30 T. O. Eloranta, *Biochem. J.*, 166 (1977) 521.
31 R. J. Baldessarini, *Int. Rev. Neurobiol.*, 18 (1975) 41.

Journal of Chromatography, 264 (1983) 329–335
Elsevier Science Publishers B.V., Amsterdam — Printed in the Netherlands

CHROM. 15,859

Note

Separation and analysis of 2-(5-cyanotetrazolato)pentaamminecobalt-(III) and related cobalt(III) complexes by capillary tube isotachophoresis

JOHN M. LAVOIE* and PAUL S. BACK
Mound Facility, Monsanto Research Corporation, P.O. Box 32, Miamisburg, OH 45342 (U.S.A.)
(First received February 10th, 1983; revised manuscript received March 14th, 1983)

The perchlorate salt of 2-(5-cyanotetrazolato)pentaamminecobalt(III), designated CP, is a relatively new explosive which is much less sensitive to accidental initiation than other primary explosives such as lead azide, yet it can rapidly grow to detonation when properly confined[1]. The main impurities in CP explosive after it is synthesized are (5-carbamoyltetrazolato)pentaamminecobalt(III) perchlorate and (5-amidinotetrazolato)tetraamminecobalt(III) perchlorate (Fig. 1). Many common separation and analysis approaches, *i.e.*, gas chromatography (GC), electron ionization and chemical ionization mass spectrometry (EI-MS, CI-MS) and GC–MS, are not feasible due to the very nature of these species being ions of unprecedented polarity and negligible vapor pressure. Analysis approaches based on thin-layer chromatography (TLC) have met with some success, but complete resolution of the complexes was not achieved[2]. Quantitative estimation of the amide by IR measurements at 1675 cm^{-1} are complicated/hindered by the presence of a broad band in the same region arising from a deformation vibration of the NH_3 ligands[2,3]. Modern liquid chromatographic approaches which are currently being explored are hindered by the limited solubility, and great differences in concentration are a source of problems due to limitations imposed by sample capacity of ion-exchange resins. Furthermore, a reproducible high-performance liquid chromatographic (HPLC) method suitable for routine analysis has yet to be found[4].

Since most of the above procedures have not proven to date to be as straightforward or fruitful as desired, we investigated the possibility of using isotachophoresis (ITP) for the analysis of CP. The ITP technique has been described previously[5,6] and recently in extensive reviews[7,8].

EXPERIMENTAL

The LKB 2127 Tachophor® isotachoelectrophoresis equipment was used to separate cations in a PTFE capillary tube, length 61 cm, 0.5 mm I.D., thermostated at 20°C. The leading electrolyte was 10 m*M* K^+ with $\approx$10 m*M* acetate as counter ion at pH 5.5. The terminating electrolyte was 10 m*M* Tris. Separations required about 20 min at a current of 150 μA. Separated zones were detected by their UV absorption at 254 nm. A recorder-paper speed of at least 10 cm/min was required for accurate measurement of the records.

0021-9673/83/$03.00

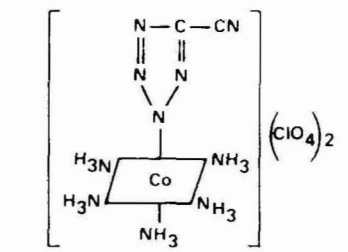

A. CP

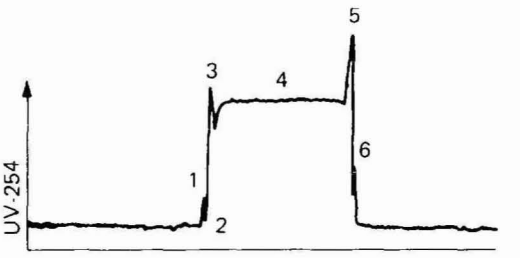

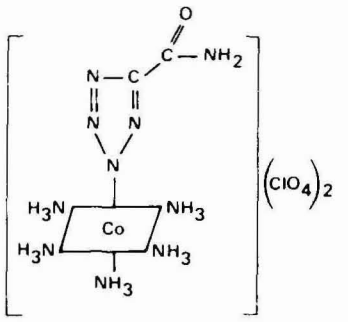

B. Amide

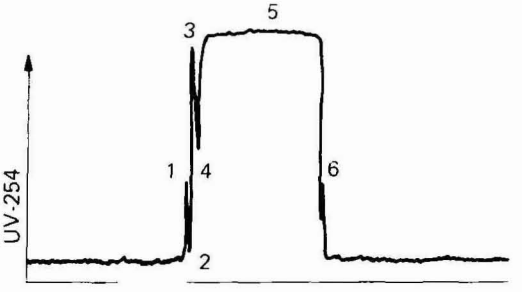

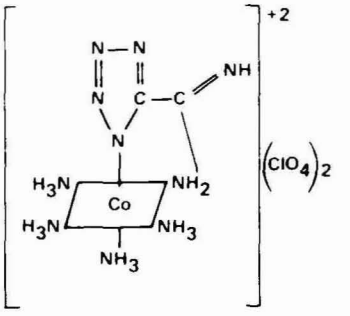

C. Amidine.

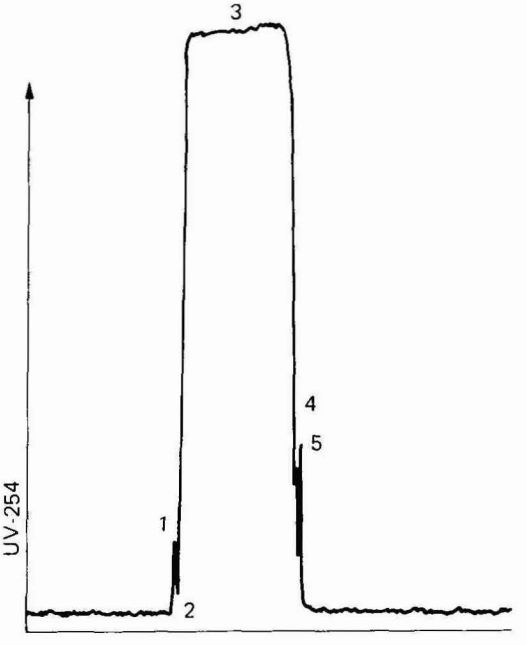

Fig. 1. Isotachopherograms resulting from injections (3 μl) of 7.5 nanomoles of CP/EL58633 (A), amide complex/EL-43182 (B) and amidine complex/EL52685 (C). Zones identified: 1 = electrolyte contaminant; 2 = non-UV-absorbing unknown; 3 = amidine; 4 = CP; 5 = amide; 6 = UV-absorbing unknown.

RESULTS AND DISCUSSION

Isotachopherograms resulting from separate injections with samples (3 μl injection) of CP, amide and amidine containing about 7.5 nmole each are shown in Fig. 1. The assignment of contaminants will be discussed below. The absorbance observed at 254 nm for each major zone was consistent with extinction coefficients obtained from the UV spectra of authentic standards. In the instance of UV absorbing species, the area under the peak records, after transform from a transmittance scale to an absorbance scale, is linearly related to the amount of material. A typical calibration curve over the 0.1–2.0 nmole concentration range of CP is depicted in Fig. 2. These data clearly demonstrate the direct proportionality of zone areas to CP concentration which is essentially linear over the concentration range studied.

In Fig. 3 the separation of an equal molar mixture of CP and its two major contaminants is shown. The resolution of the cations appears satisfactory. Three methods were employed to investigate the purity and identity of the indicated zones. (1) Molar extinction coefficients obtained from the UV–visible spectra of authentic standards and absorbance ratios of respective ITP zones were compared at both 254 and 280 nm in Table I. It should be noted that zone concentration cannot be determined directly, therefore, only observed absorbance ratios under identical conditions are compared to extinction data. (2) Thermal step heights, a relative index of

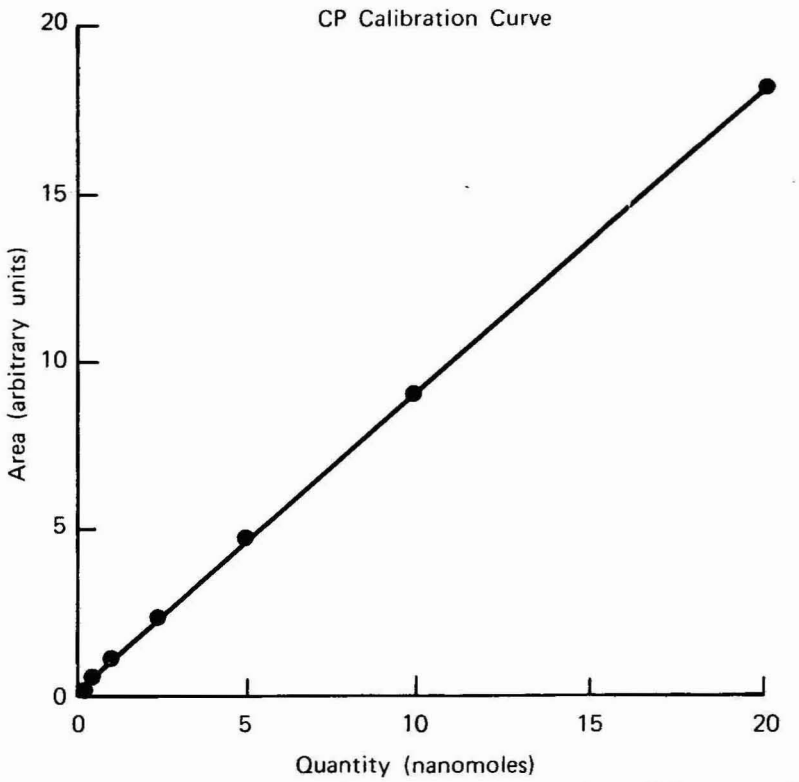

Fig. 2. The direct proportionality of zone areas to concentration, which was essentially linear over the concentration range studied, is shown by a typical calibration curve.

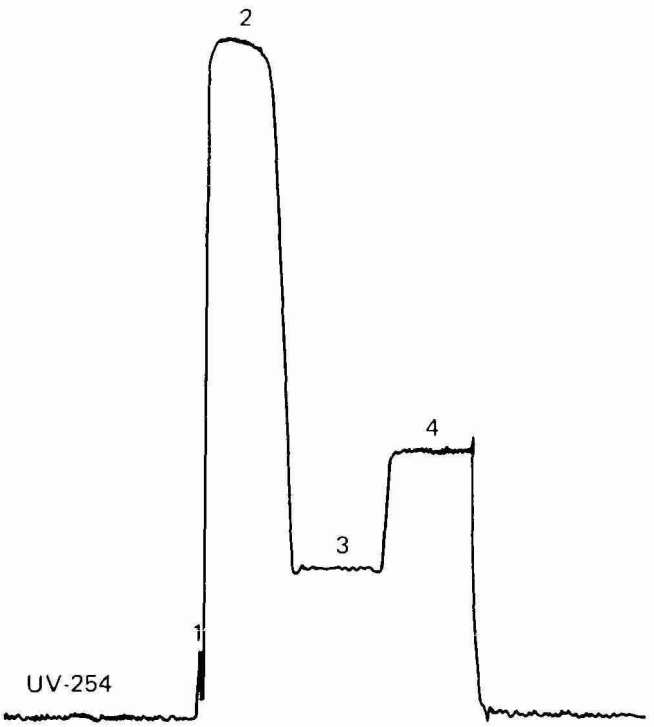

Fig. 3. Isotachopherogram of an equal molar mixture of amidine (2), CP (3) and amide (4). Zone 1 is due to an electrolyte contaminant.

the mobility for each species producing a zone, were compared to step heights obtained from analysis of purified standards under identical conditions. These relative step heights are somewhat analogous to relative retention indexes employed for similar purposes in chromatographic analytical procedures. Table II lists the values observed under the condition of these experiments. Values have been normalized relative to potassium where the step height of sodium is 100 arbitrary units. Under our experimental conditions a minimum of 10 units difference in step height was required for complete separation. It should be pointed out that step heights could not be determined precisely for very small UV zones observed because of the lower sensi-

TABLE I

COMPARISON OF ZONE ABSORBANCES AT 254 AND 280 nm TO EXTINCTION DATA FROM UV SPECTRA OF AUTHENTIC STANDARDS

Compound	*UV molar extinction*		*ITP zone absorbance*	
	E_{254}	E_{280}	A_{254}	A_{280}
CP	510	30	0.080	0.0056
Amide	920	60	0.16	0.011
Amidine	3800	1100	0.71	0.22

TABLE II

THERMAL STEP HEIGHTS AT 150 μA

Values normalized relative to potassium so that the step height of sodium is 100 arbitrary units. A minimum of 10 units difference in step height is required for complete separation under the experimental conditions employed.

Ion	*Thermal step height*
K^+	0
Na^+	100
$Amidine^{2+}$	105
Co^{2+}	114
CP^{2+}	117
$Amide^{2+}$	131
$Tris^{2+}$	358

tivity of the thermoionic detector. (3) A third confirmation test was the chemical modification of samples by spiking with authentic standards followed by reanalysis. This approach demonstrated in Fig. 4 was particularly useful for very small UV zones where precise step height determination was not possible. The assignments of small UV zones in Fig. 1 were made in a similar fashion.

Taking advantage of the high sensitivity and resolving power of the Tachophor combined with the wide dynamic range of the method, the purity of CP Lot EL58633 was calculated from the relative areas of the resulting zones shown in Fig. 5. The precision of the ITP method has also been calculated from a standard calibration curve, Fig. 2, where eight different concentrations were measured three times each. The relative standard deviation was 0.0004. Samples giving areas below 0.1 units ought to be rerun at double volume to give a more reliable result. ITP analysis of CP

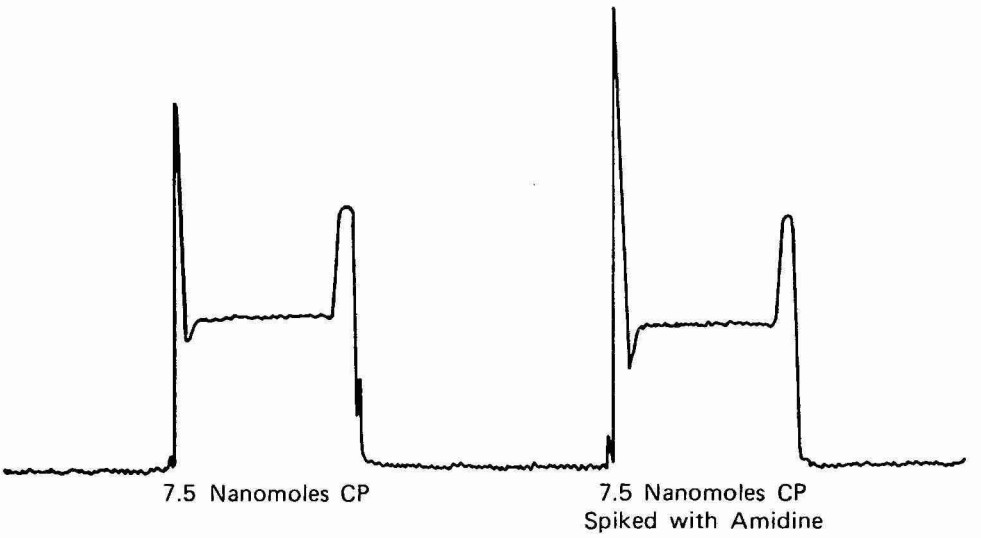

Fig. 4. Effect of spiking with amidine on isotachopherogram.

Fig. 5. Isotachopherogram resulting from a 7.5 nanomole injection of CP Lot EL58633. Zones: 1 = electrolyte contaminant; 2 = non-UV-absorbing unknown; 3 = amidine (0.5 ± 0.02%); 4 = CP (95.6 ± 0.3%); 5 = amide (3.9 ± 0.04%); 6 = UV-absorbing unknown. Percentages were calculated from relative areas, with uncertainties at the 95% confidence level based on three replicates.

should contain as a minimum about 10 pmole. Below this level the coefficient of variation is more than 1.0%. Using of an internal standard should improve the reproducibility because a significant source of error can be traced to the reproducibility of making microliter injections.

CONCLUSIONS

These results demonstrate that ITP can provide useful qualitative and quantitative data on charged cobalt(III) complexes and their salts. Its advantages are that it resolves several ions in one experiment, that it is sensitive to picomole amounts, that both large and small amounts of different compounds can be measured simultaneously, that it is relatively quick (3 runs per hour), and little or no sample pretreatment is required.

It is concluded from the present experiments with ITP that qualitative and quantitative analysis of charged complexes and their salts by electrophoretic methods offers a viable tool for studies of such materials with advantages over more commonly employed analytical methodology for many applications. Areas of direct applicability include: quality control/quality assurance (QC/QA), stability/compatibility studies, purification both prior to further analysis work, *i.e.*, spectroscopic study and as a preparation step as well as utility in certain physical chemical studies. Work in this laboratory has already begun in all of the above areas. The recent development of a high resolution capillary adaptation of conventional zone electrophoretic techniques[9] should also offer new expanded possibilities in these and other areas as refinements and interest develop.

REFERENCES

1 W. B. Leslie, R. W. Dietzel and J. Q. Searcy, *A New Explosive for Low Voltage Detonator Application*, Office of Naval Research Technical Report ACR-221, Sandia Lab., Albuquerque, NM, 1976; *C.A.*, 91 (1979) 177491r.

2 H. S. Schuldt, *CP Compatibility/Reliability, Report SAND-77-1420*, Sandia Lab., Albuquerque, NM, 1977, available from Sandia Lab.

3 A. Attalla. *DDT Project Semiannual Report. Report SAND 81-0937*. Sandia Lab.. Albuquerque. NM. 1981; available from National Technical Information Service (NTIS), U.S. Department of Commerce, Springfield, VA.
4 K. Bullock, Monsanto Research Corporation, Dayton, personal communication.
5 A. J. P. Martin and F. M. Everaerts, *Proc. R. Soc. London, Ser. A*, 316 (1970) 493.
6 F. M. Everaerts and Th. P. E. M. Verheggen, *J. Chromatogr.*, 53 (1970) 315–328.
7 F. M. Everaerts, J. L. Beckers and P. E. M. Verheggen, *Isotachophoresis — Theory, Instrumentation and Applications*, Elsevier, Amsterdam, New York, 1976.
8 Y. Shiogai and T. Yagi, *Amer. Lab.*, (10) 1980 101.
9 J. W. Jorgenson and K. D. Lukacs, *Anal. Chem.*, 53 (1981) 1298–1302.

Journal of Chromatography, 264 (1983) 336–338
Elsevier Science Publishers B.V., Amsterdam — Printed in The Netherlands

CHROM. 15,483

Note

Thin-layer chromatographic–mass spectrometric identification of 11-nor-Δ^9-tetrahydrocannabinol-9-carboxylic acid*

G. R. NAKAMURA*, W. J. STALL, V. A. FOLEN and R. G. MASTERS
United States Army Crime Investigation Laboratory, Pacific APO, San Francisco, CA 96343 (U.S.A.)
(Received March 8th, 1983)

Kaistha and Tadrus[1] previously described a procedure for thin-layer chromatographic (TLC) detection of 11-nor-Δ^9-tetrahydrocannabinol-9-carboxylic acid (Δ^9-THC-COOH), a major metabolite of tetrahydrocannabinol (THC). An enzyme multiplied immunoassay technique (EMIT) was employed to confirm the presence of Δ^9-THC-COOH. For forensic purposes, we adapted this TLC method for the clean-up of urinary extracts as an important step in isolating the metabolite. The elution of the TLC spot corresponding in R_F and Fast Blue B stain color to Δ^9-THC-COOH provided an extract for gas chromatographic (GC)–mass spectrometric (MS) determination with a low background reading.

EXPERIMENTAL

The hydrolysis and extraction procedures for Δ^9-THC-COOH are essentially those of Kaistha and Tadrus[1]. The cyclohexane–ethyl acetate extract of hydrolyzed urine was passed through a bed of anhydrous sodium sulfate in the cone of Whatman I filter-paper to provide a cleaner residue upon evaporation.

TLC was performed on a silica gel G plate, Analtech Uniplate, 250 μm thick, irrigated with chloroform–methanol–ammonia (70:30:2). The R_F for 11-nor-Δ^8-tetrahydrocannabinol-9-carboxylic acid (Δ^8-THC-COOH) and Δ^9-THC-COOH is approximately 0.25 under these conditions. The spot for these compounds, after staining with Fast Blue B, was scraped off the plate onto a weighing paper and transferred to a small tube, approximately 12 × 75 mm, to which *ca.* 2 ml methanol were added. The tube was agitated on a Vortex mixer and then centrifuged to clear. The supernatant was transferred by means of a Pasteur pipet to another tube, approximately 10 × 75 mm, and evaporated to dryness under nitrogen.

The resulting residue was methylated according to Whiting and Manders[2] by treating it with 70 μl aqueous 25% tetramethylammonium hydroxide–dimethylsulfoxide (1:20). The tube was agitated and allowed to stand for 2 min. Approximately 5 μl of 1-iodomethane were added to the mixture, agitated and allowed to stand for 5 min. The mixture was acidified with 0.2 ml 0.1 *M* hydrochloric acid and then agitated with 1.0 ml hexane for 1 min. The upper layer was passed through *ca.* 1 cm

* This article represents the opinions of the authors and does not necessarily reflect the views of the Department of the Army or the Department of Defense.

0021-9673/83/$03.00

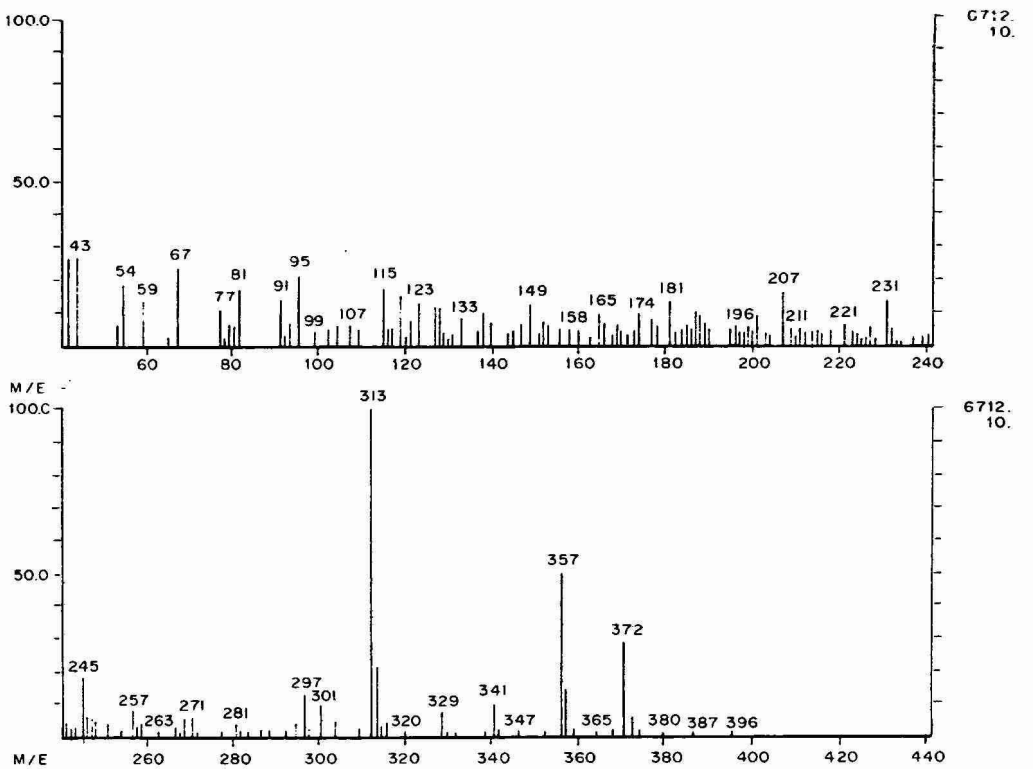

Fig. 1. Electron impact mass spectrum of the methylated derivative of 11-nor-Δ^9-tetrahydrocannabinol-9-carboxylic acid extracted from urine of a suspected marihuana user.

of sodium sulfate packed over glass wool in a Pasteur pipet and collected in a tube approximately 75 × 10 mm. The acidified mixture was extracted again with hexane, the upper layer was filtered and the extracts were combined. The residue was dissolved in 20 μl of methanol and 5 μl of the resulting solution were injected into a Model 1020 Finnegan GC–MS instrument. A 6 ft. × 1/4 in. column packed with OV-17 on Chromosorb W HP (80–1100 mesh) was used in GC and the oven temperature was programmed from 220 to 270°C at 10°C/min. The retention time for Δ^9-THC-COOH was in the range of 5–6 min under these conditions.

RESULTS AND DISCUSSION

In our hands, the clean-up procedure using TLC afforded an extractive residue devoid of much of the impurities normally transferred through a solvent double extraction system[2] to the final residue. The mass spectrum of Δ^9-THC-COOH, shown in Fig. 1, was obtained from the extract of a urine specimen of a suspected user, and is to be compared with that of standard Δ^9-THC-COOH shown in Fig. 2. The spectrum of Fig. 1 exhibits a fragmentation pattern which is consistent with that of Fig. 2, particularly in respect of the peaks at m/z 313, 357 and 372 and in the order of relative intensity. Although the TLC R_F values of Δ^8-THC-COOH and Δ^9-THC-COOH are similar, the mass spectra of the two compounds are decidedly different. The spectrum of Δ^8-THC-COOH shows a base peak at m/z 372 while Δ^9-

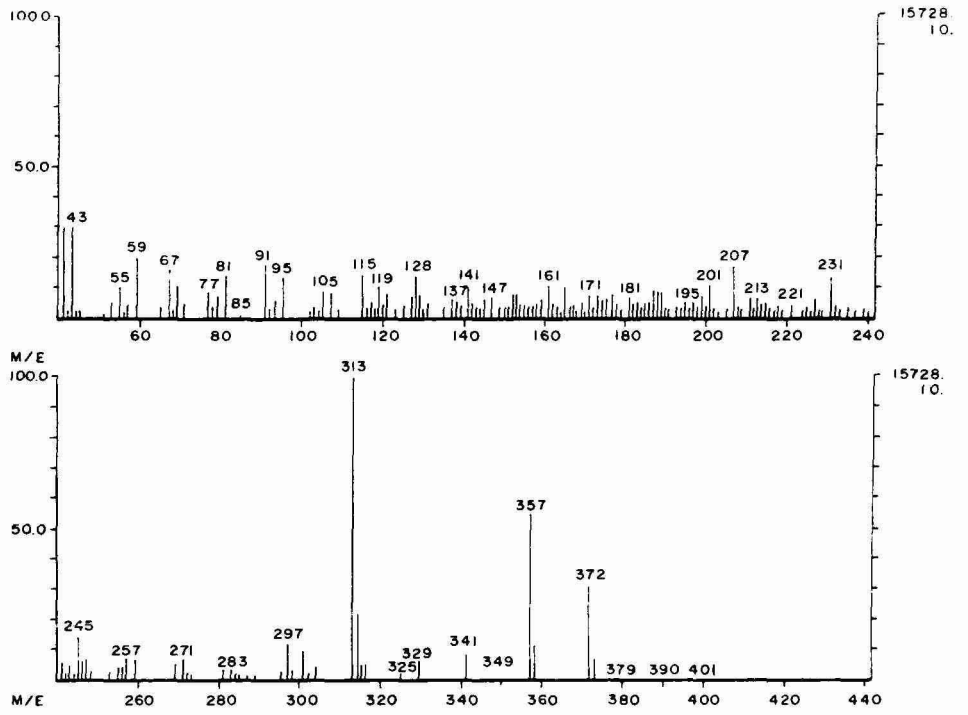

Fig. 2. Electron impact mass spectrum of the methylated derivative of standard 11-nor-Δ^9-tetrahydrocannabinol-9-carboxylic acid.

THC-COOH exhibits a base peak at *m/z* 313. This difference indicates the need to obtain a mass spectrum of the sample to differentiate the two isomers.

As indicated by Whiting and Manders[2], once the dry extract containing Δ^9-THC-COOH is methylated, the rest of the analysis should be completed on the same day to preclude a possible degradation of the derivatized compound. An inert gas should be used to evaporate to dryness solvent extracts containing the methylated cannabinoid since air tends to degrade the derivative. The TLC procedure *per se* provides a screening procedure for excluding negative specimens, especially when multiple samples are being processed. The "positive" spot can be eluted with methanol and the extract is analyzed by mass spectrometry. For forensic purposes, an MS determination affords an unequivocal identification of Δ^9-THC-COOH.

ACKNOWLEDGEMENTS

We are indebted to Robert C. Sanders, III for his assistance in the photographic presentation of mass spectra and to Armed Forces Institute of Pathology, Washington, DC, U.S.A. for their gift of standard 11-nor-Δ^9-tetrahydrocannabinol-9-carboxylic acid.

REFERENCES

1 K. K. Kaistha and R. Tadrus, *J. Chromatogr.*, 237 (1982) 528–533.
2 J. D. Whiting and W. W. Manders, *J. Anal. Toxicol.*, 6 (1982) 49–52.

PUBLICATION SCHEDULE FOR 1983

Journal of Chromatography (incorporating *Chromatographic Reviews*) and *Journal of Chromatography, Biomedical Applications*

MONTH	D 1982	J	F	M	A	M	J	J	A	
Journal of Chromatography	252 253/1 253/2	254 255 256/1	256/2 256/3 257/1	257/2 258 259/1	259/2 259/3 260/1	260/2 261/1 261/2	261/3 262 263	264/1 264/2 264/3 265/1	265/2 266	The publication schedule for further issues will be published later.
Chromatographic Reviews					271/1		271/2		271/3	
Biomedical Applications		272/1	272/2	273/1	273/2	274	275/1	275/2	276/1	

INFORMATION FOR AUTHORS

(Detailed *Instructions to Authors* were published in Vol. 244, No. 2, pp. 401-404. A free reprint can be obtained by application to the publisher.)

Types of Contributions. The following types of papers are published in the *Journal of Chromatography* and the section on *Biomedical Applications:* Regular research papers (Full-length papers), Short communications and Notes. Short communications are preliminary announcements of important new developments and will, whenever possible, be published with maximum speed. Notes are usually descriptions of short investigations and reflect the same quality of research as Full-length papers, but should preferably not exceed four printed pages. For review articles, see page 2 of cover under Submission of Papers.

Submission. Every paper must be accompanied by a letter from the senior author, stating that he is submitting the paper for publication in the *Journal of Chromatography.* Please do not send a letter signed by the director of the institute or the professor unless he is one of the authors.

Manuscripts. Manuscripts should be typed in double spacing on consecutively numbered pages of uniform size. The manuscript should be preceded by a sheet of manuscript paper carrying the title of the paper and the name and full postal address of the person to whom the proofs are to be sent. Authors of papers in French or German are requested to supply an English translation of the title of the paper. As a rule, papers should be divided into sections, headed by a caption (*e.g.,* Summary, Introduction, Experimental, Results, Discussion, etc.). All illustrations, photographs, tables, etc., should be on separate sheets.

Introduction. Every paper must have a concise introduction mentioning what has been done before on the topic described, and stating clearly what is new in the paper now submitted.

Summary. Full-length papers and Review articles should have a summary of 50-100 words which clearly and briefly indicates what is new, different and significant. In the case of French or German articles an additional summary in English, headed by an English translation of the title, should also be provided. (Short communications and Notes are published without a summary.)

Illustrations. The figures should be submitted in a form suitable for reproduction, drawn in Indian ink on drawing or tracing paper. Each illustration should have a legend, all the *legends* being typed (with double spacing) together on a *separate sheet.* If structures are given in the text, the original drawings should be supplied. Coloured illustrations are reproduced at the author's expense, the cost being determined by the number of pages and by the number of colours needed. The written permission of the author and publisher must be obtained for the use of any figure already published. Its source must be indicated in the legend.

References. References should be numbered in the order in which they are cited in the text, and listed in numerical sequence on a separate sheet at the end of the article. Please check a recent issue for the layout of the reference list. Abbreviations for the titles of journals should follow the system used by *Chemical Abstracts.* Articles not yet published should be given as "in press", "submitted for publication", "in preparation" or "personal communication".

Proofs. One set of proofs will be sent to the author to be carefully checked for printer's errors. Corrections must be restricted to instances in which the proof is at variance with the manuscript. "Extra corrections" will be inserted at the author's expense.

Reprints. Fifty reprints of Full-length papers, Short communications and Notes will be supplied free of charge. Additional reprints can be ordered by the authors. An order form containing price quotations will be sent to the authors together with the proofs of their article.

News. News releases of new products and developments, and information leaflets of meetings should be addressed to: The Editor of the News Section, Journal of Chromatography/Journal of Chromatography, Biomedical Applications, Elsevier Science Publishers B.V., P.O. Box 330, 1000 AH Amsterdam, The Netherlands.

Advertisements. Advertisement rates are available from the publisher on request. The Editors of the journal accept no responsibility for the contents of the advertisements.